

## **IARC Technical Report # 5**

# **Report of the NABOS/CABOS 2007 Expedition Activities in the Arctic Ocean**

*With support from*  
**National Science Foundation  
National Oceanic and Atmospheric Administration  
Japan Agency for Marine-Earth Science and Technology**



## TABLE OF CONTENTS

PREFACE ( <i>L.Hinzman, I.Polyakov, IARC L.Timokhov, AARI</i> ).....	7
<b>I. NABOS-07 EXPEDITION IN THE EURASIAN BASIN ABOARD THE R/V VICTOR BUYNITSKIY (SEPTEMBER - OCTOBER 2007)</b>	9
I.1. INTRODUCTION ( <i>I.Polyakov IARC, I.Dmitrenko, IFM-GEOMAR</i> ).....	10
I.2. RESEARCH VESSEL ( <i>I.Polyakov, IARC</i> ) .....	10
I.3. CRUISE TRACK ( <i>I.Polyakov, IARC</i> ).....	13
I.4. SCIENTIFIC PARTY ( <i>I.Dmitrenko, IFM-GEOMAR, and S. Kirillov, AARI</i> ).....	14
I.5. ICE CONDITIONS ( <i>.N.Koldunov, MPI</i> ).....	14
I.6. OBSERVATIONS ( <i>V.Ivanov, I.Polyakov, IARC, (I.Dmitrenko, IFM-GEOMAR and S.Kirillov, AARI)</i> )....	16
I.6.1. METEOROLOGICAL OBSERVATIONS ( <i>P.Minnett, UM</i> ).....	19
I.6.1.1. Objectives.....	19
I.6.1.2. Cruise Narrative.....	19
I.6.1.3. Instruments .....	20
I.6.1.4. Data Summary.....	22
I.6.2. OBSERVATIONS OF AIR-SEA INTERACTIONS ( <i>I.Repina, IAF</i> ).....	24
I.6.2.1. Introduction.....	24
I.6.2.2. Instruments .....	24
I.6.2.3. Measurements.....	26
I.6.3. OCEANOGRAPHIC OBSERVATIONS.....	29
I.6.3.1. Background Information ( <i>I.Polyakov, IARC, and D.Walsh, NRL</i> ).....	29
I.6.3.2. Routine CTD Measurements and Water Sampling.....	31
I.6.3.2.1 Objectives ( <i>I.Polyakov, V.Ivanov, IARC</i> ).....	31
I.6.3.2.2. Methods ( <i>I.Dmitrenko, IARC, and S.Kirillov, AARI</i> ).....	31
I.6.3.2.3. Equipment ( <i>R.Chadwell, IARC</i> ).....	34
I.6.3.2.4 Data Processing ( <i>I. Polyakov, IARC</i> )	35
I.6.3.2.5 Preliminary Results ( <i>I.Dmitrenko, V.Ivanov, IARC, and S.Kirillov, L.Timokhov, AARI</i> )	36
I.6.3.3. Mooring Observations.....	40
I.6.3.3.1. Objectives ( <i>I.Polyakov, I.Dmitrenko, IARC</i> ).....	41
I.6.3.3.2. Mooring Design and Equipment ( <i>R.Chadwell, IARC</i> )	41
I.6.3.3.3. Mooring Deployments ( <i>R.Chadwell, IARC</i> ).	42
I.6.3.3.4. Mooring Recovery ( <i>R.Chadwell, IARC</i> ).....	49
I.6.3.3.5. Preliminary Results ( <i>V.Ivanov, I.Polyakov, IARC, I.Dmitrenko, IFM-GEOMAR, S.Kirillov, L.Timokhov, AARI</i> ).....	51
I.6.4. TURBULENCE MEASUREMENTS ( <i>P.J. Wiles, B.I. Powel, UW</i> )....	58
I.6.4.1. Equipment Setup.	58
I.6.4.2. Data Results.....	59
I.6.4.3. Summary.....	70
I.6.5. HYDROCHEMICAL OBSERVATIONS ( <i>S. Torres-Valdes, NOSC and E. Dobrotina, AARI</i> ).....	70
I.6.5.1. Background: AARI .....	70
I.6.5.2. Sampling and Analysis: AARI .....	70
I.6.5.3. Background: NOCS .....	71
I.6.5.4. Sampling and Analysis: NOCS	71
I.6.5.5 Samples Analyzed on Board.....	72
I.6.6. BIOLOGICAL OBSERVATIONS ( <i>C. Bouchard, L. Fortier, M.-È. Garneau, C. Lalande, C. Lovejoy, J.-É. Tremblay, LU</i> ).....	77
I.6.6.1. Arctic Cod ( <i>Boreogadus saida</i> ) Ecology ( <i>C. Bouchard, L. Fortier</i> ).....	77
I.6.6.1.1.Objectives.....	77
I.6.6.1.2. Methods	78

I.6.6.1.3. Preliminary Results	78
I.6.6.2. Vertical Export Flux of Biogenic Matter ( <i>C. Lalande, L. Fortier</i> )	79
I.6.6.2.1. Objectives	79
I.6.6.2.2. Methods	79
I.6.6.2.3. Preliminary Results	80
I.6.6.3. Nutrient Concentrations ( <i>C. Lalande, J.-É. Tremblay</i> )	80
I.6.6.3.1. Objectives	80
I.6.6.3.2. Methods	80
I.6.6.4. Microbial Ecology ( <i>M.-È. Garneau, C. Lovejoy</i> )	80
I.6.6.4.1. Objectives	80
I.6.6.4.2. Methodology	81
I.6.6.4.3. Future Work.....	81
I.6.7. BIOGEOCHEMICAL STUDIES: CONTRIBUTION FROM THE SIBERIAN SHELF STUDY	83
PROJECT ( <i>I. Semiletov, N. Shakhova, IARCO. Dudarev, A. Salyuk, .I. Pipko, .N. Savelieva, POC</i> <i>I. Repina, IAF, O. Gustaffson, USS, Bart van Dongen, SEAES, M. Elmquist, USS, and A. Charkin,</i> <i>D. Kosmach, E. Spivak, POI</i> )	
I.6.7.1. Introduction	83
I.6.7.2. Expedition Itinerary	84
I.6.7.3. Methods and Measurements	85
I.6.7.3.1. Methane (and non-Methane Hydrocarbons) Dissolved in Water	85
I.6.7.3.2. Carbonate System Parameters	86
I.6.7.3.3 CO <sub>2</sub> and CH <sub>4</sub> Fluxes	86
I.6.7.3.4 Methane in the Air	87
I.6.7.3.5. Freshwater Components	87
I.6.7.3.6. C and H Isotope Signatures of CH <sub>4</sub>	87
I.6.7.3.7. Establishing a New Methodical Approach to Monitoring Environmental Changes over the East Siberian Shelf	88
I.6.7.3.8. Other Measurements	88
I.6.7.4. Preliminary Look at the Data	89
I.6.7.4.1 Methane in the Water	89
I.6.7.4.2. Carbonate System.	90
I.6.7.5 Preliminary Conclusions	93
<b>II. CABOS-07 Expedition to the Beaufort Sea aboard the Canadian Coast Guard Icebreaker <i>Louis</i></b>	<b>95</b>
<b><i>S. St-Laurent (September 2007)</i></b>	
II.1. INTRODUCTORY NOTE.....	96
II.2. RESEARCH VESSEL.....	97
II.3. MOORING RECOVERY AND DEPLOYMENT.....	97
II.3.1. Chronology of the Mooring Recovery ( <i>M. Dempsey, OM</i> )	97
II.3.2. Chronology of the Mooring Deployment ( <i>M. Dempsey, OM</i> )	99
II.4. MOORING DESCRIPTION.....	99
II.5. A PRELIMINARY LOOK AT MOORING DATA.....	100
REFERENCES	104
Acknowledgements.....	106
APPENDIX: NABOS-07 Station List ( <i>I.A. Dmitrenko, S.A. Kirillov</i> ).	107

## **GLOSSARY:**

**AARI:** Arctic and Antarctic Research Institute, St.Petersburg, Russia

**IAF:** Institute of Atmospheric Physics, Russian Academy of Science, Moscow, Russia

**IARC:** International Arctic Research Center, University of Alaska Fairbanks, Alaska, USA

**IFM-GEOMAR:** Leibniz Institute of Marine Sciences, University of Kiel, Germany

**IOS:** Institute of Ocean Sciences, BC, Canada

**LU:** Laval University, Quebec City, Quebec, Canada

**MPI-M:** Max Plank Institute, University of Hamburg, Germany

**NOCS:** National Oceanographic Center, Southampton, UK

**NRL:** Naval Research Laboratory, Washington DC, USA

**OM:** Oceanetic Measurement Ltd., Sidney, BC, Canada

**POI:** V.I.II'ichov Oceanographic Institute, Far Eastern Branch of the Russian Academy of Sciences

**RSHU:** Russian State Hydrometeorological University, St.Petersburg, Russia

**SEAES:** School of Earth, Atmospheric and Environmental Sciences, University of Manchester, UK

**UM:** Rosenstiel School of Marine and Atmospheric Science, University of Miami, USA

**USS:** Department of Applied Environmental Science, Stockholm University, Stockholm , Sweden

**UW:** University of Wales, Bangor, UK



## PREFACE

It was a tough year, but scientifically very successful. This season was particularly difficult due to problems with chartering the nuclear icebreaker *Yamal* which forced us to find a replacement vessel at very short notice. Our researchers were able to charter the small ice-class research vessel *Viktor Buynitsky* from Murmansk RosHydroMet and the expedition was still a huge success, but that achievement is mainly due to the unceasing and near-heroic efforts of the research team. On the research vessel (RV) *Viktor Buynitsky*, the expedition was able to proceed into the Laptev, East Siberian, and Barents seas due to the anomalous ice-free conditions. The team successfully recovered two deep-water moorings and deployed five moorings, thus providing long-term stationary observations at key locations of the Arctic Ocean. The oceanographic cross-sections and extensive biochemistry and turbulence observations complemented mooring-based measurements.

These observations showed that the exceptional warming which entered the Eurasian Basin in 1999 progressed from Fram Strait along the Barents and Laptev slopes and was captured by conductivity/temperature/depth (CTD) cross-section in the East Siberian Sea, approaching Alaska's backyard. Observations during this cruise also documented strong warming of the very uppermost layer in the eastern Eurasian and Makarov basins. The magnitude of this warming is unprecedented in the history of regional instrumental observations. The unique strength and spatial distribution of this warm surface anomaly suggests the important role of oceanic heat in shaping this summer's substantially reduced Arctic Ocean ice cover. The intrusion of warm Atlantic water, combined with the on-going reduction of the sea-ice cover, will have major impacts on the unique Arctic fauna and ecosystems and human inhabitants.

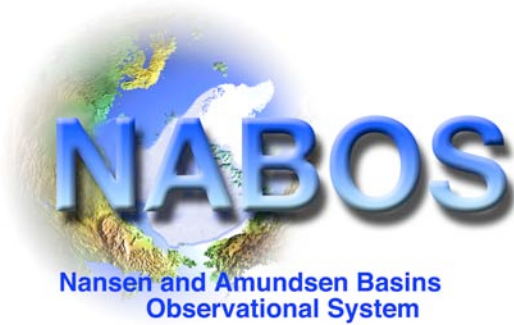
NABOS has been an unqualified success, and in this time of rapid environmental and political change presents a critically important scientific and political route to developing the understanding of the Arctic that is so important to the global community. Our program has become an important element of the IPY by enhancing international cooperation, resulting in shared research infrastructure, updated databases, and fostering of synergy and interdisciplinary dialog.

Larry Hinzman  
IARC Director

Igor Polyakov  
USA Principal Investigator

Leo Timokhov  
Russian Principal Investigator





## **SECTION I**

**NABOS-07 Expedition  
in the Eurasian Basin aboard  
the RV *Viktor Buynitsky*  
(September-October 2007)**

## **I.1. INTRODUCTION** (*I.Polyakov, IARC, and I.Dmitrenko, IFM-GEOMAR*)

NABOS (Nansen and Amundsen Basins Observational System) is a long-term program intended to provide a quantitative observationally-based assessment of circulation, water mass transformations, and transformation mechanisms along the principal pathways transporting water from the Nordic Seas into the central Arctic Basin. The scope of the field problem clearly calls for international cooperation/coordination, a task commensurate with the capabilities and scope of an international center. NABOS is currently conducted jointly by the IARC, IOS, AARI, NPI, LU in cooperation with the University of Washington (International Arctic Buoy Project), AWI and a consortium of UK universities.

The primary monitoring tool of the NABOS program is the series of moorings placed at carefully chosen locations around the Arctic Ocean. Time series obtained from these moorings allow separation of synoptic-scale signals (e.g., eddies, shelf waves) from longer-term climatic signals. Located along the major pathways of water, heat, and salt transport, such moorings capture climatically important changes in oceanic conditions. The NABOS moorings operate for one year at a time, with replacement every year.

This section of the report describes field research during the NABOS-07 oceanographic cruise aboard the research vessel (RV) *Viktor Buynitsky* in September-October 2007. The overarching goal of the 2007 field program was to characterize the oceanographic and ice conditions over the continental margins of the Eurasian and Makarov basins, while at the same time deploying and recovering moorings.

## **I.2. RESEARCH VESSEL** (*I.Polyakov, IARC*)

The Russian RV *Viktor Buynitsky* (**Figure I.2.1**) was chartered by the University of Alaska Fairbanks to carry out oceanographic research over the continental slope of the Siberian Arctic shelf. The ship is operated by the Murmansk RosHydroMet Administration located in Murmansk, Russia. RV *Viktor Buynitsky* is a small ice-class research vessel, constructed for work in the conditions of the high-latitude marginal seas. The vessel was built in Turku, Finland in 1986. The RV's main technical characteristics are presented in **Table I.2.1**. The ship is navigated from the bridge (**Figure I.2.1**). In addition to freshwater storage, fresh water is provided from a distillation apparatus; this system can produce a maximum of 5 tons of water per day. Safety equipment includes two 20-person life boats and four 10-person inflatable life rafts (total capacity 80 persons). The fuel consumption rate is shown in **Table I.2.1**. The ship is equipped with one deck crane on the bow and two loading booms on the stern; the crane can lift 3 tons, and each loading boom can lift up to 1 ton. Note that the crane was not capable of loading our equipment from the dock, and a dock crane was essential. One loading boom was out of order.



**Figure I.2.1.** RV *Viktor Buynitsky* on the NABOS-07 cruise in the northern Barents, Laptev, and East Siberian seas.

**Table I.2.1:** The main technical characteristics of RV *Viktor Buynitsky*

Displacement	693 t
Draft	3.6 m
Breadth	10.00 m
Length	49.9 m
Main engine	One Wärtsilä-Diesel engine. Diesel develops 985KW
Built	1986, Finland, Turku
Propellers	One
Hold	One, 149 m <sup>3</sup>
Fuel	MGO
Fuel/water storage	112.3 m <sup>3</sup> and 95.4 m <sup>3</sup>
Speed	Full: 11 knots (loaded); cruising speed: 12.6 knots in calm open water.
Fuel consumption	3.5 tons at 10.5 knots speed
Crew and passengers	21 and 25



**Figure I.2.2:** (Left) LEBUS double-drum oceanographic winch and (right) HAWBOLDT C15-40 horizontal capstan on the deck (photo by Robert Chadwell, IARC).



**Figure I.2.3:** HAWBOLDT C15-40 horizontal capstan and A-frame installed on RV *Viktor Buynitsky* (photo by Robert Chadwell, IARC).

A LEBUS double-drum electric oceanographic winch (**Figure I.2.2**) manufactured by LEBUS Engineering International Ltd., England was additionally deployed on the deck of the ship in order to deploy the conductivity/temperature/depth (CTD) profiler, biological nets, and trawl, and to deploy/recover the moorings. Winch electric motor power is 7.3 KW. Each drum capacity is 3500 m of 0.3-inch cable. The left drum is used only for mooring recovery. The right drum with spooling mechanism contains the 3000 m long mechanical cable that carries the CTD probe, nets, and trawl.

A HAWBOLDT C15-40 horizontal capstan manufactured by HAWBOLDT Industries Ltd., Canada in 1989 (**Figure I.2.2**) was installed near the LEBUS winch. The capstan is equipped with an 11.2 KW two-speed Toshiba electric motor, and is used for mooring deployment/recovery. The horizontal drum diameter is 40". An A-frame manufactured by Kimek, Norway in 2007 was also used on the cruise (**Figure I.2.3**).

### I.3. CRUISE TRACK (*I.Polyakov, IARC*)

RV *Viktor Buynitsky* left Murmansk, Russia on September 7<sup>th</sup> 2007 sailing towards Kirkenes, Norway where scientific equipment was uploaded, A-frame and winches were installed, and the scientific party was taken aboard. The research area was over the Eurasian Basin and its adjacent continental margin (**Figure I.3.1**). CTD profiles were carried out along several transects across the continental slope in the western, central, and eastern Laptev and East Siberian seas and along one transect approximately oriented along the continental slope. The survey and mooring deployments within the Russian Exclusive Economic Zone (REEZ) were authorized by the Russian Ministry for Education and Science. On the way to the research area the ship passed through the Barents and northern Kara seas and entered the Laptev Sea through Vilkitskiy Strait on September 16, 2007. During this leg, two moorings (M1 and M3) were recovered and five moorings (M1, M3, M8, M9, and M10) were deployed. Because we could not reach the ice-covered area north of Severnaya Zemlya, moorings in that area were left in the water for recovery next year. Having completed the major goals of the cruise in the Laptev and East Siberian seas on October 2, the ship sailed towards the northern Barents Sea with the plan to recover two moorings and deploy five moorings and carry out a CTD survey off Svalbard. However, strong northern winds moved ice southward, covering the area of our moorings with ice and precluding any work from RV *Viktor Buynitsky* in this area. On October 11, the ship left the Svalbard area sailing towards Kirkenes (**Figure I.3.1**) where winches and A-frame were removed and scientific equipment was offloaded. The RV *Viktor Buynitsky* then left for Murmansk and returned to port on October 17<sup>th</sup>, 2007, concluding the cruise.

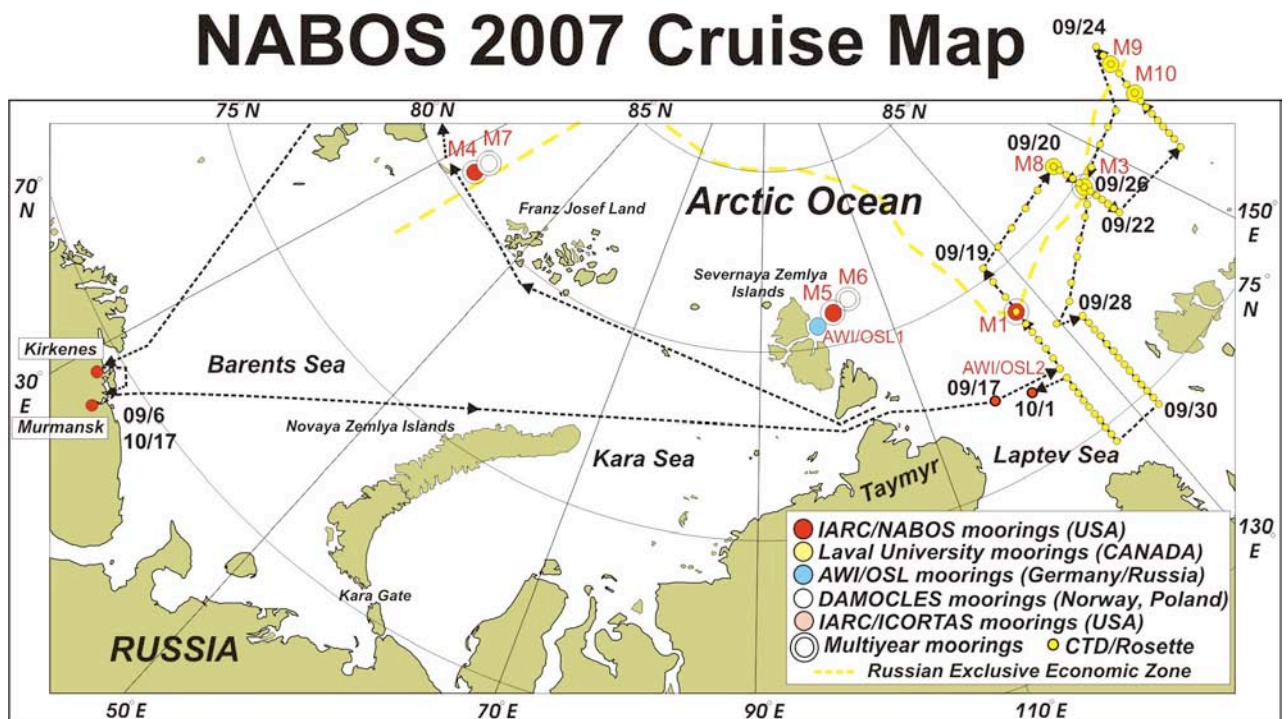


**Figure I.3.1:** NABOS-07 cruise track, 09/07/2007-10/17/2007.

#### **I.4. SCIENTIFIC PARTY** (*I.Dmitrenko, IFM-GEOMAR, and S. Kirillov, AARI*)

<b>#</b>	<b>Name</b>	<b>Position</b>	<b>Affiliation</b>	<b>Country of affiliation</b>
1	Beliveau, Ian	Technician	Oceanetic Measurements, Inc.	Canada
2	Blondeau, Sylvain	Technician	Laval University	Canada
3	Bodrova, Elizaveta	MS Student	St.Petersburg State University	Russia
4	Bouchard, Caroline	PhD Student	Laval University	Canada
5	Chadwell, Robert	Technician	University of Alaska Fairbanks	USA
6	Charkin, Alexander	PhD Student	Pacific Oceanographic Institute	Russia
7	Chernyavskaya, Ekaterina	PhD Student	Arctic and Antarctic Research Inst.	Russia
8	Dmitrenko, Igor	Chief Scientist	University of Alaska Fairbanks	USA
9	Dobrotina, Elena	Scientist	Arctic and Antarctic Research Inst.	Russia
10	Doxaran, David	Scientist	Université Pierre et Marie Curie	France
11	Garneau, Marie-Ève	PhD Student	Laval University	Canada
12	Ivanov, Vladimir	Scientist	University of Alaska Fairbanks	USA
13	Kirillov, Sergey	Co-Chief Sc.	Arctic and Antarctic Research Inst.	Russia
14	Koldunov, Nikolay	PhD Student	Hamburg University	Germany
15	Kosmach, Denis	PhD Student	Pacific Oceanographic Institute	Russia
16	Lalande, Catherine	Scientist	Laval University	Canada
17	Makhotin, Mihail	PhD Student	Arctic and Antarctic Research Inst.	Russia
18	Minnett, Peter	Scientist	University of Miami	USA
19	Powell, Benjamin Ian	Technician	University of Wales	UK
20	Repina, Irina	Scientist	Institute of Atmospheric Physics	Russia
21	Salyuk, Anatoly	Scientist	Pacific Oceanographic Institute	Russia
22	Semiletov, Igor	Scientist	University of Alaska Fairbanks	USA
23	Smirnov, Alexandr	Scientist	Institute of Atmospheric Physics	Russia
24	Spivak, Eduard	PhD Student	Pacific Oceanographic Institute	Russia
25	Syromyatina, Margarita	Adm.assisttant	St. Petersburg State University	Russia
26	Torres-Valdes, Sinhue	Scientist	National Oceanography Centre	UK
27	Waddington, Ian	Technician	National Oceanography Centre	UK
28	Wiles, Philip John	Scientist	University of Wales	UK
29	Yurek, John	Technician	University of Alaska Fairbanks	USA

#### **I.5. ICE CONDITIONS** (*N.Koldunov, MPI-M*)

The 2007 ice conditions in the Laptev and East Siberian seas were exceptional. The sea-ice concentration in the Arctic reached its historical minimum for the entire period of instrumental observations. An anomalous pressure pattern over the Arctic could be the primary cause of this substantial ice reduction. Strong high pressure systems over the Arctic Ocean and low pressure systems over Siberia caused offshore winds which brought warm continental air and pushed ice from the coast of Siberia to the central Arctic Ocean. In addition, melting was enhanced by cloud-free conditions under the high-pressure area.

Because of these unusual ice conditions and because a low-ice-class ship was used for observations, requiring us to avoid heavy ice, we made few ice observations. Our observations covered periods during which an ice breaker escorted us through Vilkitsky Strait on the way to the Laptev Sea and back, and were made during daylight from the bridge. Sea-ice concentration and ice type were recorded. We used a 15' time interval which allowed us to make at least one measurement per satellite image pixel.

Satellite observations of sea-ice concentration were received from the Institute of Oceanography, Hamburg University (Institut für Meereskunde der Universität Hamburg) on a daily basis. Ice concentrations were calculated with the ARTIST (Arctic Radiation and Turbulence Interaction

Study) sea ice (ASI) concentration algorithm using AMSR-E 89 GHz brightness temperatures [Spreen, 2007].

A comparison of visual observations and satellite data is shown in **Figure I.5.1**. Satellite data tend to overestimate sea-ice concentration on the way to the Laptev Sea and underestimate it on the way back. This lack of agreement could be related either to the time lag between a satellite pass and a visual observation or to errors in the algorithm.

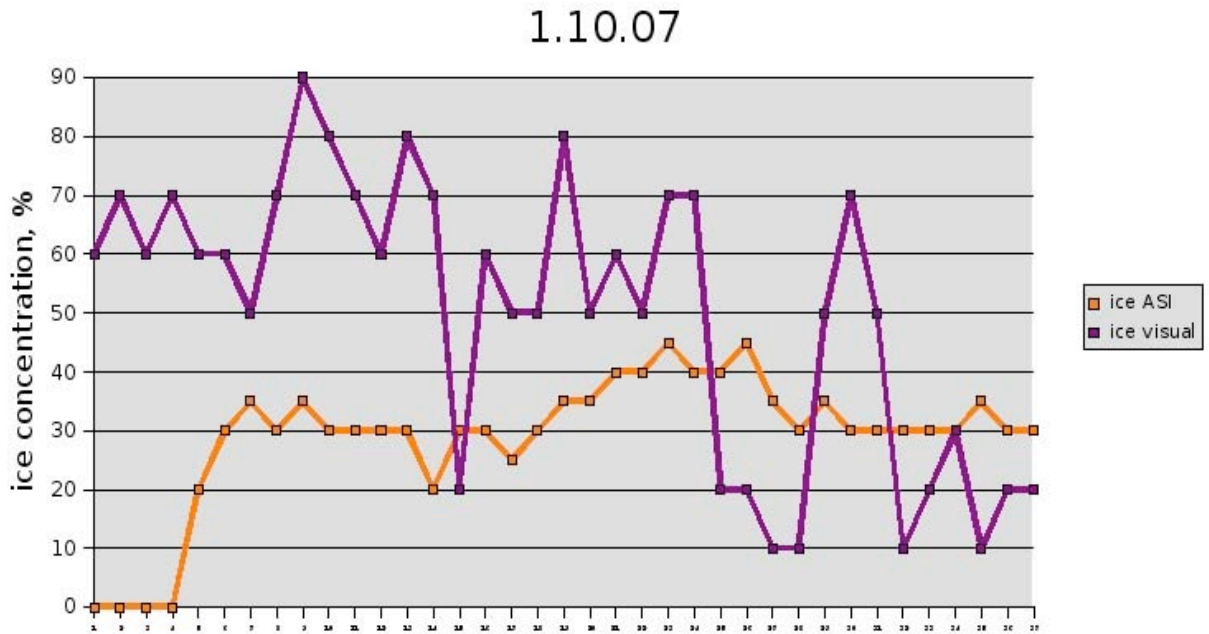
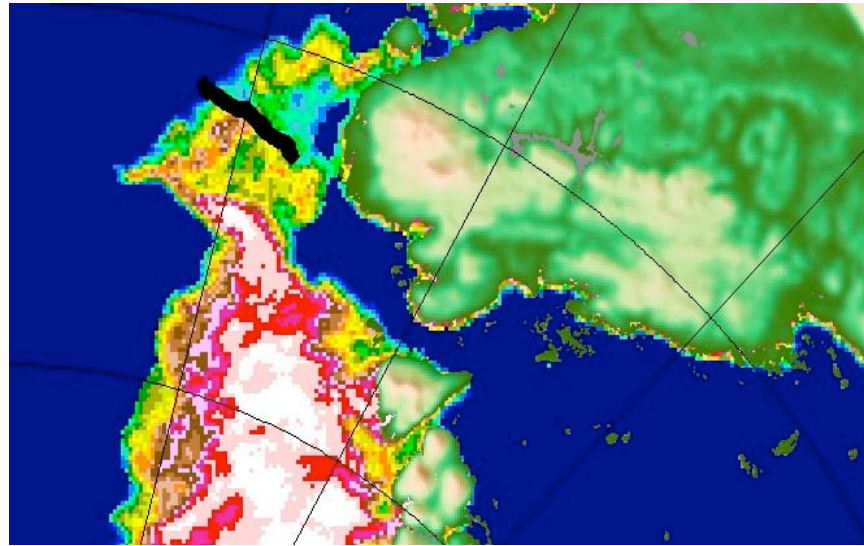


**Figure I.5.1. Top:** Sea-ice concentration in Vilkitsky Strait for 17.09.2007 according to satellite data. Black dots are the points of visual observations. **Bottom:** Comparison of satellite data (orange line) and visual observations (magenta line) for 17.09.2007.

## I.6. OBSERVATIONS (*I.Dmitrenko, IFM-GEOMAR, V.Ivanov, IARC, and S. Kirillov, AARI*)

The NABOS-07 program included routine CTD and XCTD observations, water sampling, recovery and deployment of oceanographic moorings, and turbulence, hydrochemical, geochemical, ice, and meteorological observations. The operational map of the NABOS-07 *R/V Victor Buynitskiy* cruise is shown in **Figure I.6.1.**; measurements made during the cruise are listed in **Table I.6.1**

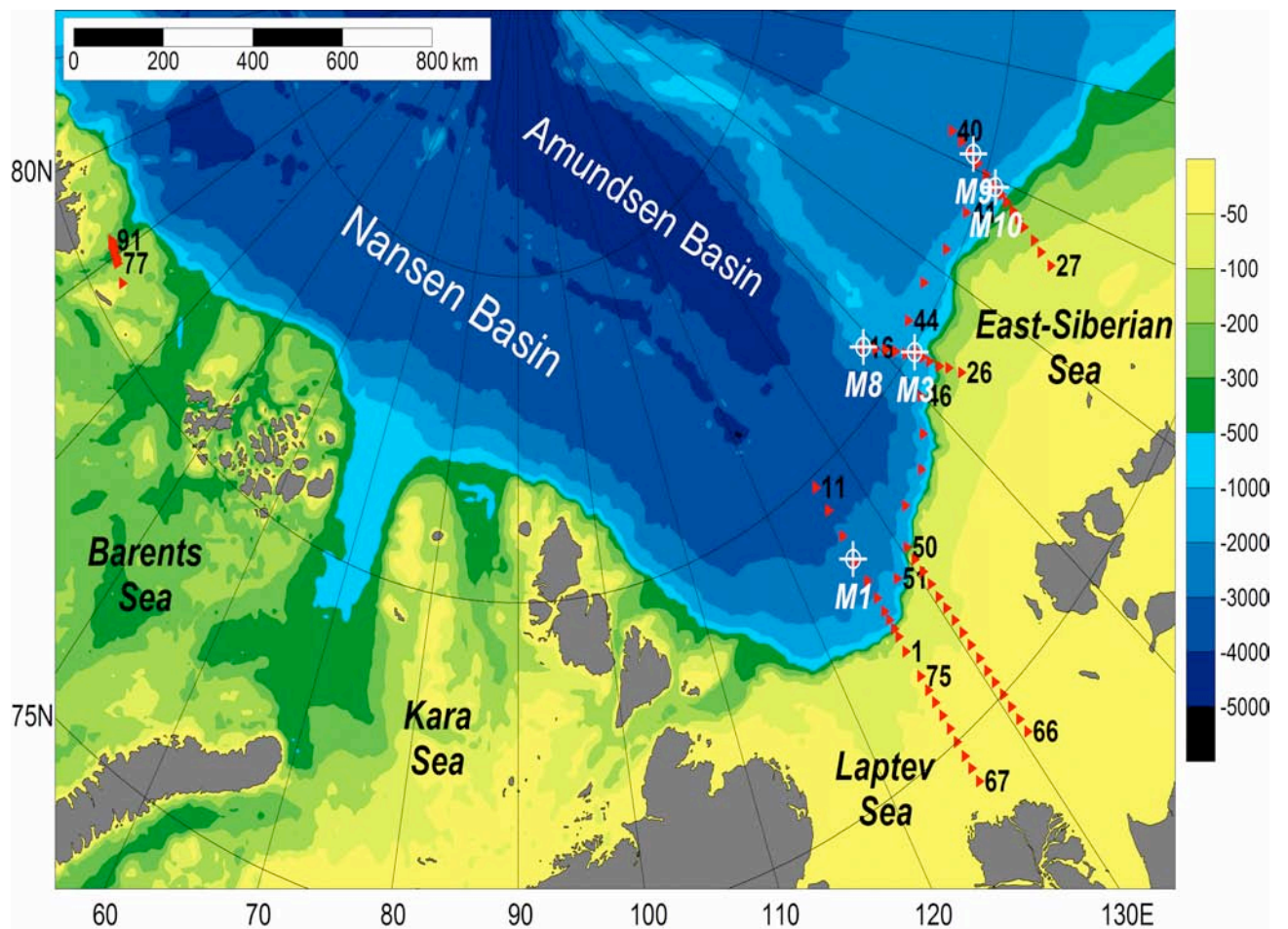


**Figure I.6.1:** Map of NABOS-07 operations: red triangles show CTD and XCTD stations, black numbers show station numbers, white crosses show NABOS moorings

**Table I.6.1:** Observations during the NABOS-07 cruise of the R/V *Victor Buynitskiy*

Station #	Date Dd/mm	Time GMT	Lat	Lon	Depth m	CTD	Rosette	XCTD	XBT	Moor. Dep.	Moor. Rec.	Turbulence
VB0107	17/09	18:35	76 43.9'	125 53.7'	69	X	X					X
VB0207	17/09	21:50	77 00.8'	125 59.7'	93	X	X					X
VB0307	17/09	23:45	77 70.0'	125 59.5'	925	X	X					X
VB0407	18/09	02:17	77 20.0'	126 00.0'	1278	X	X					X
VB0507	18/09	05:07	77 30.1'	125 59.8'	1500	X	X					X
VB0607	18/09	09:15	77 45.0'	125 59.1'	>2km	X	X					X
VB0707	18/09	13:30	78 04.8'	125 58.9'	>2km	X	X					X
VB0807	18/09	18:22	78 28.0'	125 43.8'	>2km	X	X			X	X	X
VB0907	19/09	09:30	78 55.0'	125 58.9'	>2km	X	X					X
VB1007	19/09	14:33	79 25.0'	126 00.1'	>2km	X	X					X
VB1107	19/09	18:51	79 50.1'	125 59.5'	>2km	X	X					X
VB1207	19/09	23:32	80 01.1'	128 20.4'	>2km			X				
VB1307	20/09	02:23	80 12.4'	130 47.3'	>2km			X				
VB1407	20/09	05:15	80 24.0'	133 23.0'	>2km			X				
VB1507	20/09	08:08	80 35.3'	136 01.0'	>2km			X				
VB1607	20/09	11:10	80 47.1'	138 42.5'	2050	X	X			X		X
VB1707	20/09	19:53	80 35.5'	139 36.4'	>2km	X	X					X
VB1807	20/09	23:08	80 25.2'	140 19.3'	1700	X	X					X
VB1907	21/09	02:00	80 15.1'	140 58.9'	1614	X	X					X
VB2007	21/09	05:00	80 05.0'	141 34.3'	>2km	X	X					X
VB2107	21/09	08:00	79 56.2'	142 18.7'	1347	X	X				X	X
VB2207	21/09	14:20	79 47.0'	142 30.2'	1200	X	X					X
VB2307	21/09	17:35	79 37.2'	142 41.2'	3112	X	X					X
VB2407	21/09	20:58	79 25.0'	143 00.5'	563	X	X					X
VB2507	21/09	23:38	79 15.1'	143 30.6'	214	X	X					X
VB2607	22/09	02:22	79 00.1'	144 00.8'	100	X	X					X
VB2707	22/09	17:55	78 17.0'	155 43.1'	78	X	X					
VB2807	22/09	20:40	78 32.1'	156 16.6'	85	X	X					
VB2907	22/09	22:55	78 45.0'	156 50.0'	128	X	X					
VB3007	23/09	01:25	79 00.1'	157 24.0'	155	X	X					
VB3107	23/09	03:16	79 09.1'	157 47.1'	160	X	X					
VB3207	23/09	04:45	79 19.0'	158 10.6'	225	X	X					
VB3307	23/09	06:10	79 28.1'	158 35.1'	348	X	X					X
VB3407	23/09	08:33	79 36.9'	158 59.2'	950	X	X					X
VB3507	23/09	11:34	79 46.0'	159 24.4'	1511	X	X			X		X
VB3607	23/09	19:20	80 00.1'	159 59.3'	>1km	X	X					X
VB3707	23/09	23:10	80 13.6'	160 37.5'	>2km	X	X					
VB3807	24/09	01:58	80 27.0'	161 14.6'	>2km	X	X			X		X
VB3907	24/09	14:50	80 39.9'	161 52.7'	>1km	X	X					X
VB4007	24/09	18:20	80 52.8'	162 28.8'	>2km	X	X					X
VB4107	25/09	04:04	80 10.0'	156 00.4'	1000	X	X					

Station #	Date Dd/mm	Time GMT	Lat	Lon	Depth m	CTD	Rosette	XCT	XB	Moor. Dep.	Moor. Rec.	Turbu lence
VB4207	25/09	09:28	80 16.2'	152 00.6'	1680	X	X					
VB4307	25/09	15:14	80 24.1'	148 00.7'	1800	X	X					X
VB4407	25/09	22:18	80 18.8'	144 01.4'	1500	X	X					X
VB4507	26/09	06:10	79 56.6'	142 24.9'	>1km	X	X			X		X
VB4607	27/09	02:10	79 25.0'	139 50.9'	>1km	X	X					
VB4707	27/09	08:35	79 00.3'	137 40.6'	>1km	X	X					X
VB4807	27/09	14:00	78 39.9'	135 31.0'	1500	X	X					X
VB4907	27/09	19:37	78 29.2'	132 25.8'	2050	X	X					
VB5007	28/09	01:00	77 60.0'	130 29.6'	>1km	X	X					X
VB5107	28/09	05:40	77 44.4'	128 20.0'	>1km	X	X					X
VB5207	28/09	10:00	77 45.0'	130 30.0'	1500	X	X					X
VB5307	28/09	12:50	77 30.0'	130 30.5'	72	X	X					X
VB5407	28/09	15:00	77 15.0'	130 30.8'	67	X	X					X
VB5507	28/09	17:20	76 59.9'	130 27.8'	60	X	X			X		X
VB5607	28/09	20:00	76 45.2'	130 29.7'	62	X	X					X
VB5707	28/09	23:30	76 30.1'	130 30.0'	58	X	X					X
VB5807	29/09	00:45	76 15.1'	130 30.3'	53	X	X			X		X
VB5907	29/09	03:07	76 00.0'	130 30.3'	51	X	X					
VB6007	29/09	04:45	75 44.9'	130 30.1'	48	X	X					
VB6107	29/09	06:30	75 30.0'	131 29.9'	53	X	X					
VB6207	29/09	08:38	75 15.1'	130 30.2'	43	X	X					X
VB6307	29/09	10:56	75 00.1'	130 30.5'	39	X	X					X
VB6407	29/09	13:12	74 45.0'	130 30.5'	30	X	X					X
VB6507	29/09	15:31	74 30.1'	130 30.1'	26	X	X					X
VB6607	29/09	17:28	74 15.1'	130 30.1'	27	X	X					X
VB6707	30/09	02:20	74 15.1'	127 00.2'	29	X	X					
VB6807	30/09	04:10	74 30.1'	125 59.9'	40	X	X					X
VB6907	30/09	06:09	74 45.0'	125 59.9'	26	X	X					X
VB7007	30/09	08:23	75 00.2'	125 59.7'	36	X	X					
VB7107	30/09	10:20	75 15.1'	126 00.1'	40	X	X					X
VB7207	30/09	12:45	75 30.1'	126 00.1'	40	X	X					X
VB7307	30/09	14:40	75 45.0'	126 00.1'	45	X	X					X
VB7407	30/09	17:11	76 00.0'	125 59.9'	48	X	X					X
VB7507	30/09	19:24	76 15.0'	125 59.6'	51	X	X					X
VB7607	07/10	11:20	80 33.5'	032 37.4'	91				X			
VB7707	07/10	13:07	80 38.2'	030 44.6'	199			X				
VB7807	07/10	13:24	80 38.6'	030 26.0'	225			X				
VB7907	07/10	13:30	80 39.1'	030 19.3'	264				X			
VB8007	07/10	13:34	80 39.2'	030 15.0'	294			X				
VB8107	07/10	13:42	80 39.3'	030 06.1'	346				X			
VB8207	07/10	13:52	80 39.5'	029 57.4'	312			X				
VB8307	07/10	14:13	80 40.4'	029 31.4'	369				X			
VB8407	07/10	14:30	80 41.1'	029 12.4'	494			X				

VB8507	07/10	14:36	80 41.3'	029 05.6'	557				X			
VB8607	07/10	14:50	80 41.5'	028 51.4'	541			X				
VB8707	07/10	14:56	80 41.5'	028 45.3'	446				X			
VB8807	07/10	15:00	80 41.5'	028 41.2'	426			X				
VB8907	07/10	15:05	80 42.0'	028 36.1'	346				X			
VB9007	07/10	15:08	80 42.1'	028 32.5'	154				X			
VB9107	07/10	15:11	80 42.0'	028 29.4'	79				X			

## I.6.1. METEOROLOGICAL OBSERVATIONS (P.Minnett, UM)

### I.6.1.1 Objectives

The objective of this project is to study the cloud radiative forcing at the surface of the Arctic Ocean.

### I.6.1.2 Cruise narrative

Meteorological observations were carried out throughout the entire cruise track shown in **Figure I.6.1.1**. The ship sailed from Kirkenes, Norway, on the evening of September 10, 2007, and headed northeast across the Barents Sea, passing to the north of Novaya Zemlya into the Kara Sea, and through the Vilkitskiy Strait, with an icebreaker escort, into the Laptev Sea. The first station was occupied on the evening of September 17, 2007. Operations in the Laptev and East Siberian seas continued until September 30, 2007. Passage back through the Vilkitskiy Strait was again with icebreaker escort. The ship docked in Longyearbyen, Svalbard, on October 9 to refuel, and sailed the following day for a transit to Kirkenes, arriving on the morning of October 14, 2007.

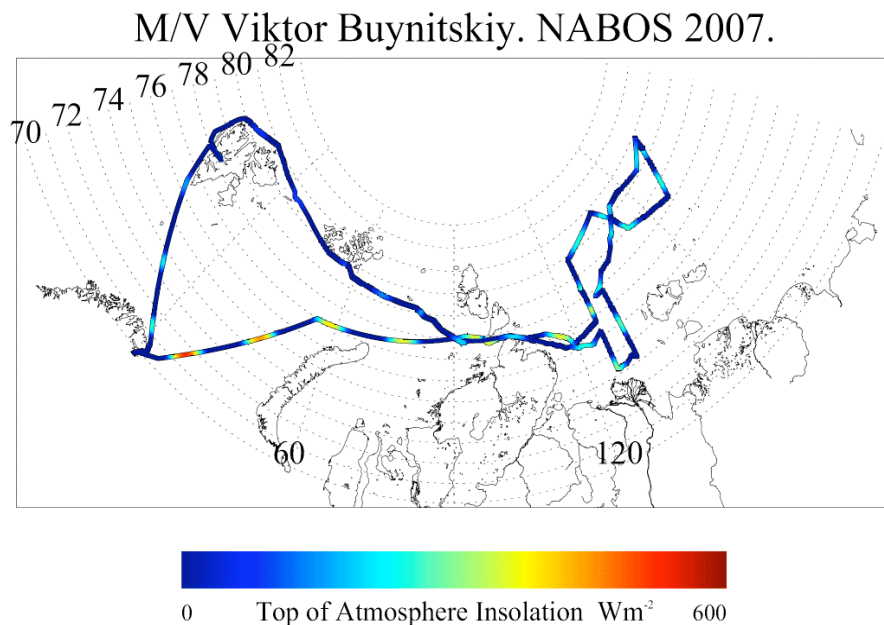


**Figure I.6.1.1.** Track of the NABOS 2007 cruise, colored by the calculated top-of-atmosphere insolation.

### I.6.1.3. Instruments

The instruments installed on the R/V *Viktor Buynitskiy* are listed in **Table I.6.1.1** with the variables they measure.

**Table I.6.1.1.** Measured and derived variables and sensors

Variable	Ship-based Sensor
Cloud type and cover	All-sky camera
Insolation (SW↓)	Gimbaled Eppley pyrometer
Incident thermal radiation (LW↓)	Gimbaled Eppley pyrgeometer
Atmospheric humidity profiles	Radiosondes
Atmospheric temperature profiles	Radiosondes
Columnar water vapor	Microwave radiometer
Cloud liquid water content	Microwave radiometer
Air Temperature	Thermistor*
Relative humidity	Vaisala “Humicap” *
Wind speed	R. M. Young anemometer*
Wind direction	R. M. Young anemometer*
Barometric pressure	Digital barometer*
*Part of Coastal Environmental System’s “Weatherpak”	

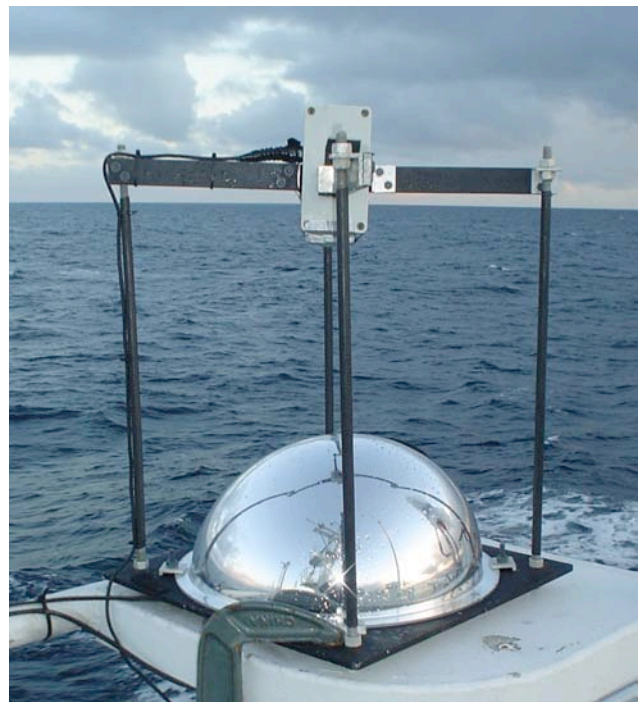
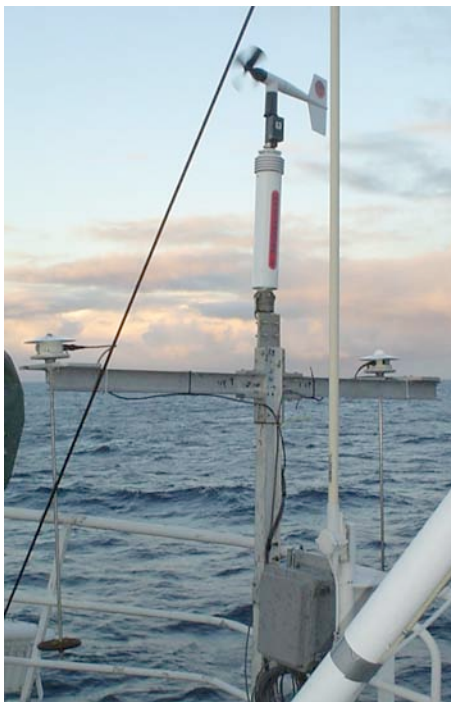


**Figure I.6.1.2a.** (Left) Weather station mounted above the bridge of the M/V *Viktor Buynitskiy*.

**Figure I.6.1.2b.** (Right) The all-sky camera mounted on the bridge top of the M/V *Viktor Buynitskiy*.

### ***Meteorology and incident radiation***

A meteorological station (a Coastal Environmental System's Weatherpak) was set up on the forward, starboard railing above the bridge. (**Figure I.6.1.2a**).

### ***All-sky camera***

An all-sky camera system was mounted above the bridge where a view of the dome of the sky was available with as little obstruction as possible (**Figure I.6.1.2b**).

### ***Microwave radiometer***

A Radiometrics WVR 1100 was mounted on the starboard railing above the bridge where it had a clear view of the atmosphere from zenith to horizon. This instrument measures atmospheric brightness temperatures at zenith at 23 and 31 GHz from which precipitable water and cloud liquid water content are derived in real time.

**Table I.6.1.2.** Radiosonde log.

NABOS 2007 Viktor Buynitskiy

Radiosonde log

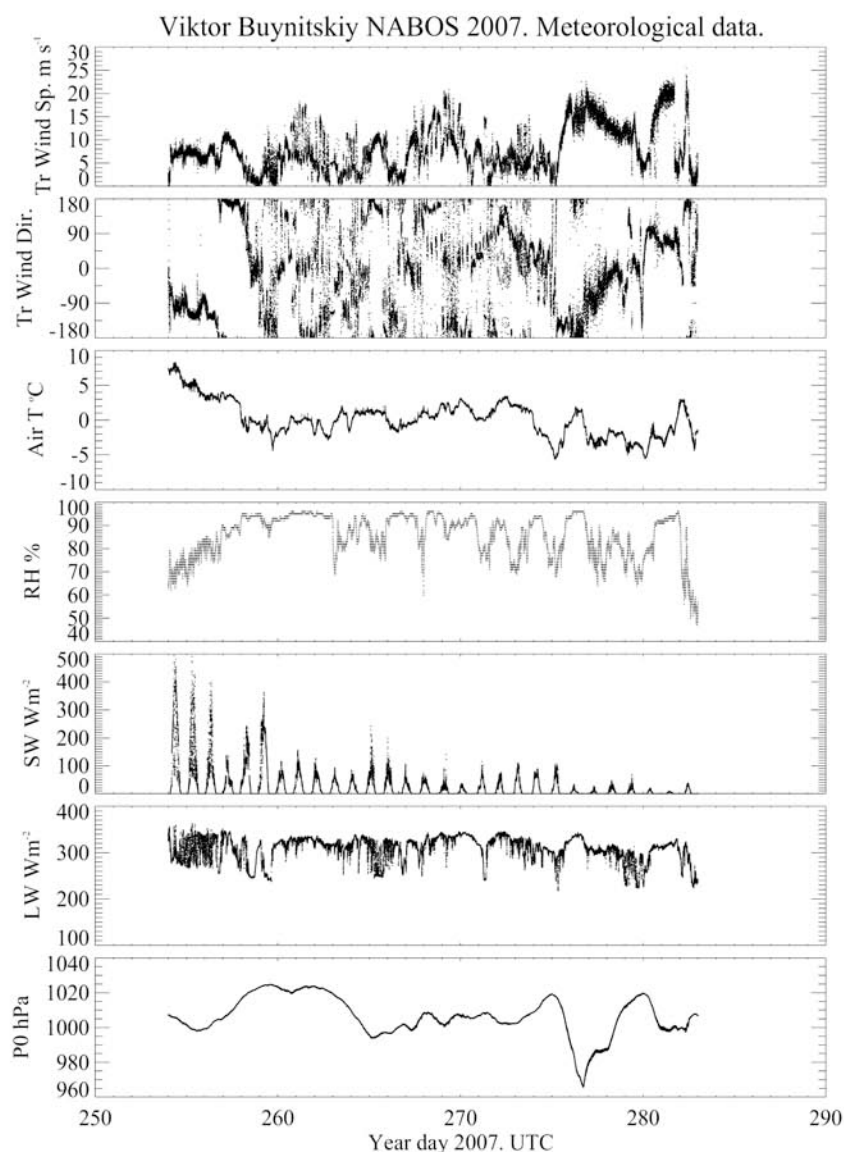
Date	Time	s/n	Lat N	Lon E	Po	Tair	RH	Duration	Max height	Pmin	Comments
UTC					hPa	oC	%	minutes	km	hPa	
9/13/2007	7:49	B1724672	77.05	57.75	1001.0	3.1	82.0	96.00	22.417	37.7	
9/14/2007	7:13	B1824079	77.60	76.70	1007.5	3.4	85.0	120.00	24.450	27.2	
9/15/2007	6:36	B1824073	77.94	96.65	1019.1	-1.5	93.0	46.50	9.141	288.0	
9/16/2007	5:29	A2813102	77.69	98.90	1024.1	-1.2	91.0	95.33	21.782	41.3	Clear skies. Following I/B Taymyr through Vilkitskiy St
9/17/2007	6:41	B1724669	76.73	118.32	1021.8	-1.2	93.0	120.00	24.076	28.9	Overcast. Following I/B Taymyr through Vilkitskiy Str
9/18/2007	6:19	A2813127	77.50	126.00	1022.4	-0.3	95.0	120.00	23.102	33.4	Overcast. In Laptev Sea
9/19/2007	9:47	A2813130	78.92	125.99	1022.6	-1.1	95.0	95.67	21.062	45.9	Overcast. In Laptev Sea. Fog at launch.
9/20/2007	7:22	B1824072	80.51	134.60	1017.2	-0.1	91.0	120.00	24.254	27.8	Overcast. In Laptev Sea. Very calm conditions
9/21/2007	5:21	A2813131	80.08	141.57	1006.5	1.1	94.0	111.50	23.581	30.8	Overcast. In Laptev Sea. Fog at launch.
9/22/2007	5:47	B1824071	78.88	146.13	994.0	1.1	77.0	106.33	23.460	31.2	
9/23/2007	6:01	B1724674	79.40	158.41	996.8	-0.9	94.0	104.00	22.337	37.1	Foggy
9/25/2007	5:03	B1824108	80.32	156.01	1008.7	0.9	95.0	120.00	23.991	28.4	Foggy
9/26/2007	6:27	A3213085	79.95	142.41	1002.5	2.2	85.0	103.00	22.624	35.0	
9/28/2007	6:11	B1824105	77.75	128.33	1008.3	-0.1	57.0	94.00	22.517	35.3	Skies partially clear
9/29/2007	5:14	B1824103	75.75	130.52	1002.6	2.7	90.0	103.33	22.569	34.8	
9/30/2007	9:39	A4023636	75.15	126.00	1005.1	1.4	90.0	90.22	21.900	38.4	
10/1/2007	5:19	A4023637	76.07	120.40	1010.7	-2.1	95.0	77.17	18.276	67.5	Overcast. Light snow. Following I/B Rossiya through Vi
10/2/2007	5:12	A4023639	77.71	105.45	1018.0	-5.5	69.0	91.17	21.934	38.0	
10/6/2007	8:00	B1814565	79.83	55.63	1014.5	-3.4	80.0	83.33	17.268	78.8	
10/7/2007	5:41	A4023635	80.40	38.39	1018.2	-4.9	80.0	73.83	17.791	73.9	
10/11/2007	6:57	B1724670	76.84	14.68	1004.1	-0.7	56.0	92.17	22.826	32.9	Off the west coast of Svalbard. Clear overhead
10/12/2007	10:57	B1824074	73.53	24.05	1006.6	2.4	72.0	76.83	16.087	98.0	Northern Barents Sea, following gale. Overcast
10/13/2007	7:22	A2813132	71.58	28.96	1015.8	4.7	80.0	58.67	13.474	146.5	Light showers. StCu overhead

### Radiosondes

Radiosondes (weather balloons) were launched from the bridge deck on the leeward side of the ship. Launches were made each day except when weather conditions were too poor to allow safe access to the decks. The system's receiver was installed in the cabin, and the antenna mounted on an aft railing above the bridge. The sondes reached a height of about 20km, well into the stratosphere, and radioed measurements of atmospheric pressure ( $P_0$ , hPa), temperature ( $T_{air}$ , °C), and relative humidity (RH, %).

#### I.6.1.4. Data Summary

All of the instruments worked well and provided a near-continuous data record throughout the cruise.



Peter J. Minnett, RSMAS-MPO, Mon Dec 17 23:18:48 2007 e:\VB07\Wpak\True\_Winds\NABOS\_2007\_All\_met.true\_wind.ps

**Figure I.6.1.3.** Meteorological variables measured by the instrumentation above the bridge (see **Figure I.6.1.2a**).

### *Meteorological measurements*

The time series of the meteorological variables measured above the bridge are shown in **Figure I.6.1.3**. The wind speed and direction are corrected for ship motion in an approximate fashion, because a time series of the headings from the gyrocompass is not available. While the ship is underway its course is a good approximation to its heading, but when on station it has been assumed the ship was drifting to port. The maneuvers as the ship came onto and left stations cannot be properly taken into account. There has been no correction for the flow distortion around the ship.

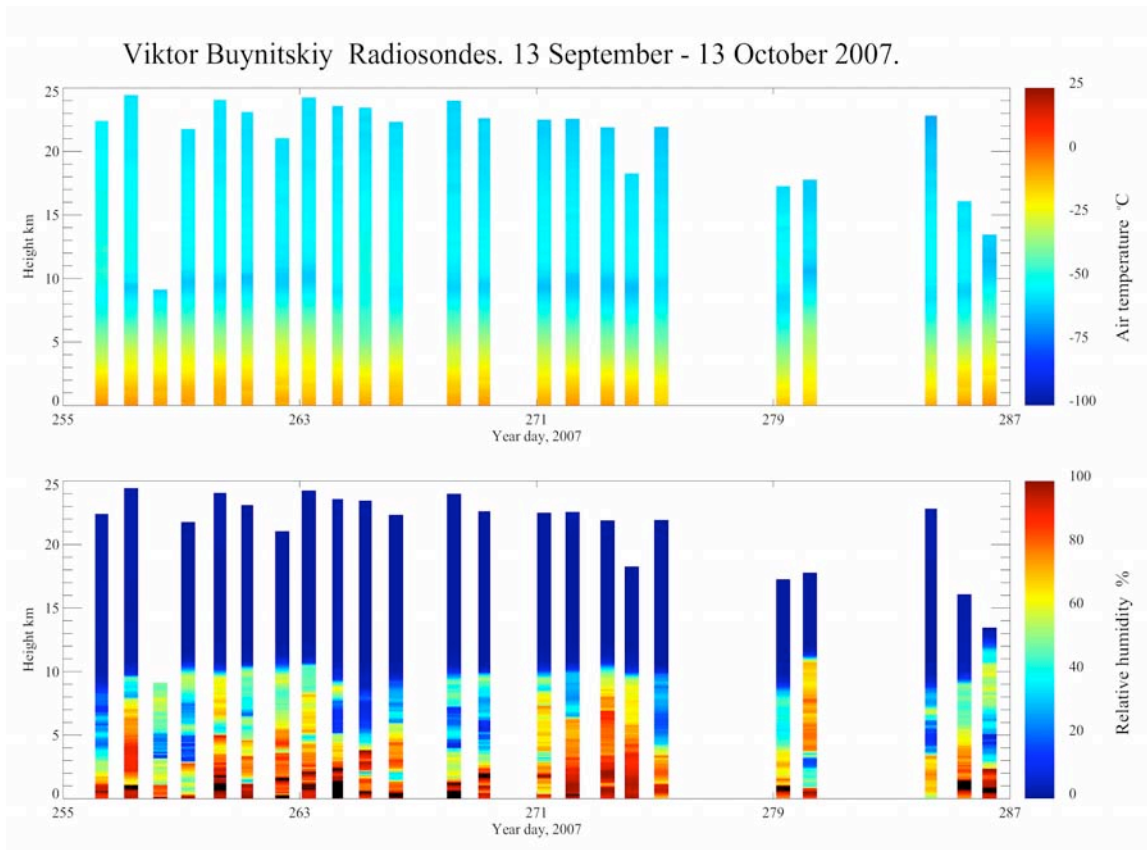


**Figure I.6.1.4.** Profiles of temperature and humidity measured from radiosondes during the NABOS 2007 cruise.

### *Radiosondes*

A total of 23 radiosondes were launched during the cruise. The details of the profiles are given in **Table I.6.1.2**, and the atmospheric profiles are shown in **Figure I.6.1.4**.

### *Microwave radiometer*

The time series of the atmospheric water vapor amounts and cloud liquid water for the duration of the cruise are shown in **Figure I.6.1.5**.

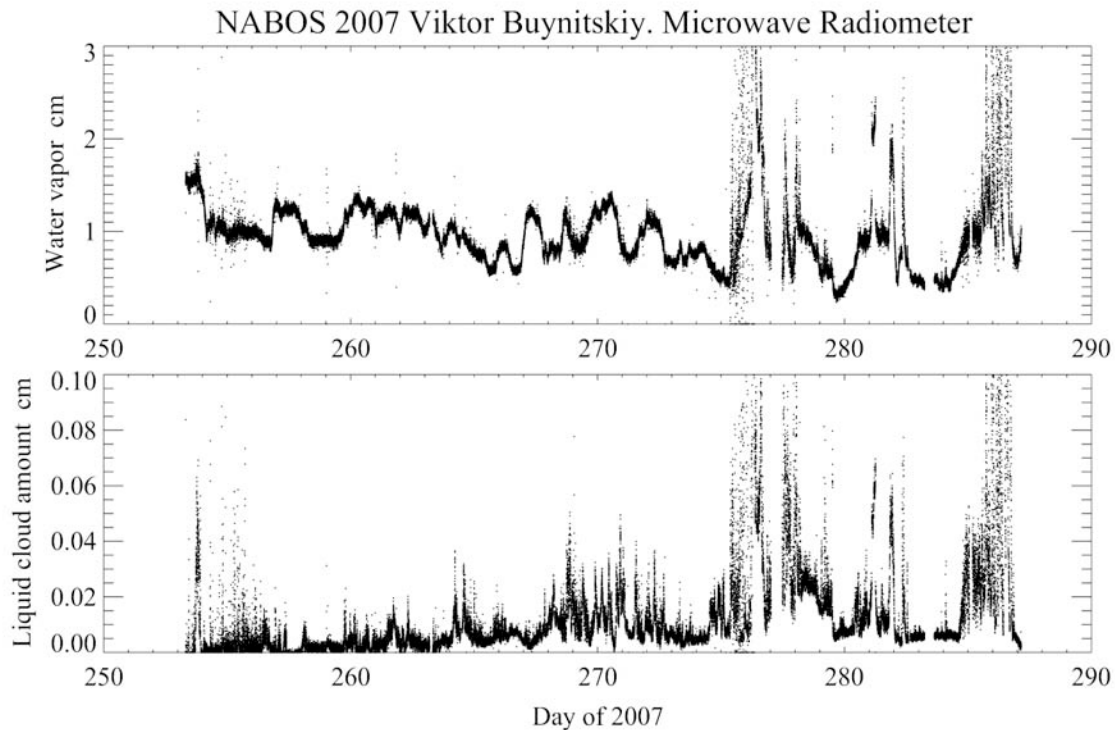


**Figure I.6.1.5.** Time series of the microwave measurements of atmospheric water vapor and cloud liquid water amounts, derived using a statistical retrieval.

## **I.6.2. OBSERVATIONS OF AIR-ICE INTERACTION (*I.Repina, IAF*)**

### **I.6.2.1. Introduction**

The following objectives defined the design of our experiments and the choice of instrumentation:

- •To analyze air-ice-ocean energy exchange using measurements of turbulent fluxes (latent and sensible heat fluxes, momentum fluxes) in the near-surface layer of the atmosphere.
- •To define the exchange coefficients in aerodynamic bulk formulas, the surface roughness parameter as a function of surface type, and meteorological conditions.

A suite of observations was carried out during the cruise:

- Direct measurements of temperature, horizontal and vertical components of wind speed, and humidity above sea surfaces under various conditions. The data were used for calculation of turbulent fluxes, as well as surface roughness parameters and atmospheric stability. The measurements were carried out when the ship was moving;
- measurements of sea-surface temperature in the infrared (IR) and microwave range;
- standard meteorological measurements.

### **I.6.2.2. Instruments**

To carry out the measurements described above, the following equipment was used:

- A USA-1 Sonic thermo-anemometer (METEK Co) that measures fluctuations of three components of wind speed and temperature fluctuations at frequency of 10-50 Hz.
- A WINDSONIC I Sonic anemometer (GILL Co) that measures fluctuations of two components of wind speed at a frequency of 5 Hz.
- A HMP-233 Vaisala high-frequency hygrometer to measure relative humidity and air temperature.
- An Eppley pyranometer for measurements of downwelling solar radiation.
- A YSI MODEL 30M unit for CTD measurements in the upper ocean layer.
- A microwave radiometer, 8 cm wave length. The unit was designed to measure accurate skin temperatures of the sea surface.
- An IR radiometer to measure skin temperatures of the sea surface.
- A VANTAGE PRO2 Weather Station. This is a self-contained system that measures air temperature and humidity, wind speed and direction, surface air pressure, and shortwave ( $\lambda \sim 0.3\text{-}3\mu\text{m}$ ) incident radiation.
- An inclinometer and three axis accelerometers and rate gyros to measure ship motions in three dimensions.
- A GARMIN GPS 17-HVS navigator to measure the ship's position.
- A video camera (web cam) for visual control of sea-surface conditions. The images were recorded by a laptop computer for subsequent analysis.

When the ship was moving, equipment for measuring air turbulence was installed on the bow to optimally reduce the dynamical and thermal ship-body effects. Under storm conditions the measurements were carried out from the deck above the bridge at a height of 10 m. (**Figure I.6.2.1**) The sensor locations are listed in **Table I.6.2.1**. The signals from turbulence sensors and motion sensors were sent to a PC-based data acquisition system that included Labview (National Instruments). The system samples at 10 Hz. After high-frequency noises and low-frequency trends were filtered out, ship-motion correction is applied to the wind velocity data. After these corrections, 10' eddy fluxes and statistics as well as row turbulence data were recorded.

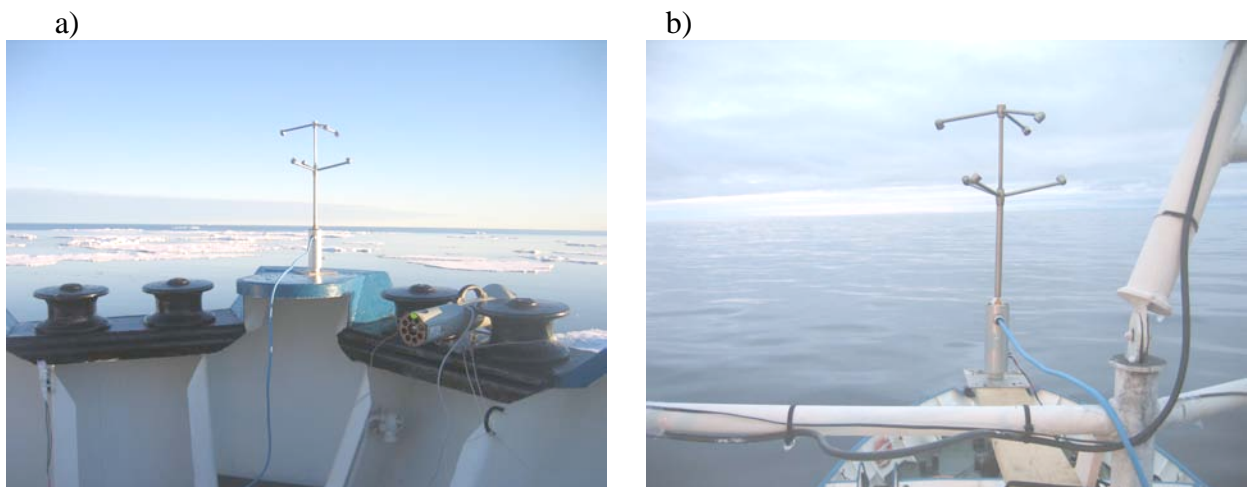


**Figure 1.6.2.1.** Turbulence-measurement devices installed on the bow (a) and on the deck above the bridge (b).

**Table I.6.2.1.** Instruments installed on the *Viktor Buynitskiy* for the NABOS 2007 cruise.

Instrument	Location
Weather station	At the top of the 2-m foremast on front face of deck above bridge
Microwave radiometer with video camera	On the deck above bridge under an angle $30^0$ to the surface
USA-1 Sonic anemometer	On the bow and deck above bridge
WindSonic	On the bow and deck above bridge
HMP-233	On the bow and deck above bridge
IR thermometer	Deployed by hand from the foredeck
Pyranometer	Above bridge
GPS	Antenna on front face of deck above bridge

For calculating turbulent fluxes an eddy-covariance (or eddy-correlation) technique was used [Edson *et al.*, 1998]. The roughness parameter was calculated following Grachev *et al.* [1998]. The technique of skin temperature calibration and calculation from microwave measurements is from Cherny and Raizer [1998].

### I.6.2.3. Measurements

The onboard measurements were carried out along icebreaker routes. Based on the measurement data the sensible and latent heat fluxes, momentum fluxes, and surface roughness parameter were calculated. During measurements unstable and neutral stratification dominated (**Figure I.6.2.2**). The variability of sensible heat fluxes during all measurement periods is presented in **Figure I.6.2.3**. Most-frequently observed positive values of fluxes which came up several tens  $W m^{-2}$ . This connected with positive sea surface temperature anomaly. Compared to last year's energy exchange conditions in the Laptev Sea, we measured less heat flux variability due to sea surface homogeneity in the observational region. During storm conditions in the Kara Sea an intensive energy exchange was observed. The greatest flux variability was measured in Vilkitskii Strait under ice conditions.

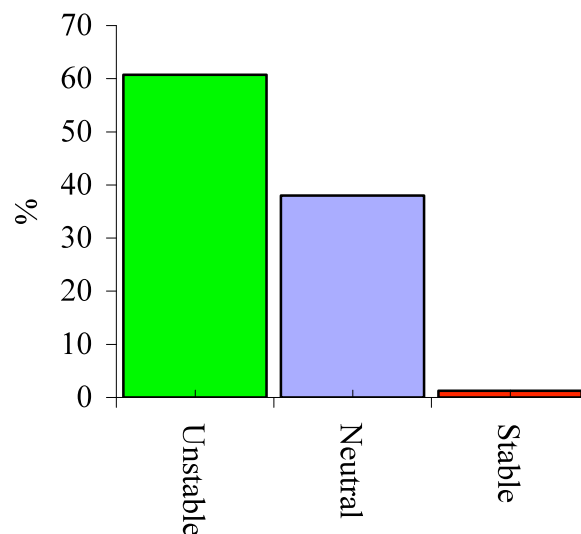


**Figure 1.6.2.2:** The relative occurrence of stability parameter from the measurements.

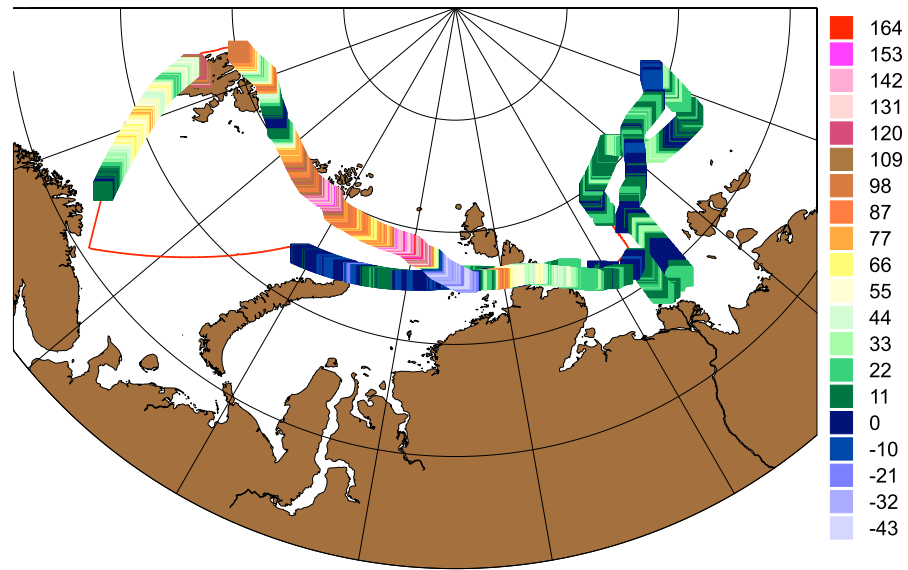


**Figure I.6.2.3:** Sensible heat flux ( $\text{W m}^{-2}$ ) variation along the NABOS-07 cruise track.

Direct measurements of sea-surface temperature in ice-covered areas are labor-intensive. The application of contact methods is not always possible, and when measuring inhomogeneous surfaces (e.g. a combination of ice floes and openings) large errors result [Cherry and Raizer, 1998]. We made an attempt to restore the surface temperature using remote microwave and IR radiometric measurements. Sea-surface conditions were recorded by video during all measurements. The surface skin temperatures derived from MW measurements along the ship's track are shown in **Figure I.6.2.4** and the resulting air-sea temperature differences are shown in **Figure I.6.2.5**.

Positive sea surface skin temperature anomalies were observed in the Laptev Sea. The relative occurrence of a range of air-sea temperature differences during the cruise is presented in **Figure I.6.2.6**. The predominately positive air-sea temperature difference (sea surface temperature warmer than air temperature) explains the positive turbulence exchange values.

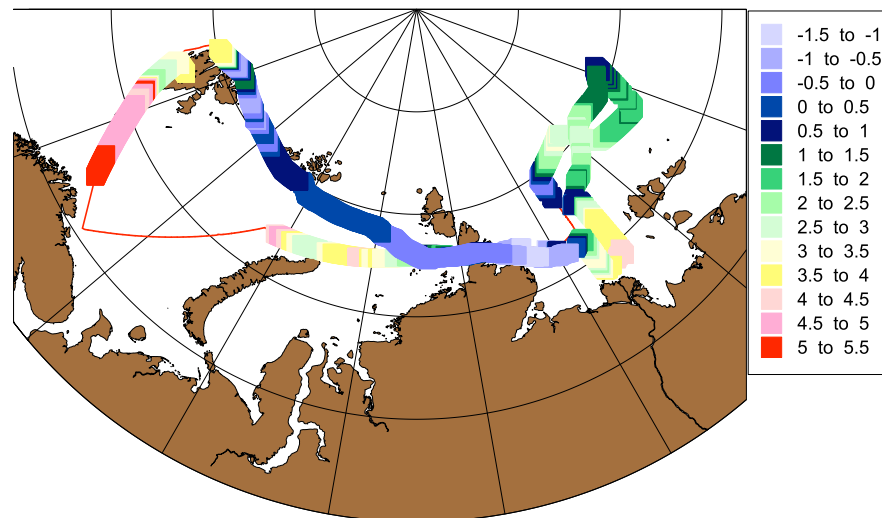


**Figure I.6.2.4:** Sea surface skin temperature along the ship's track.

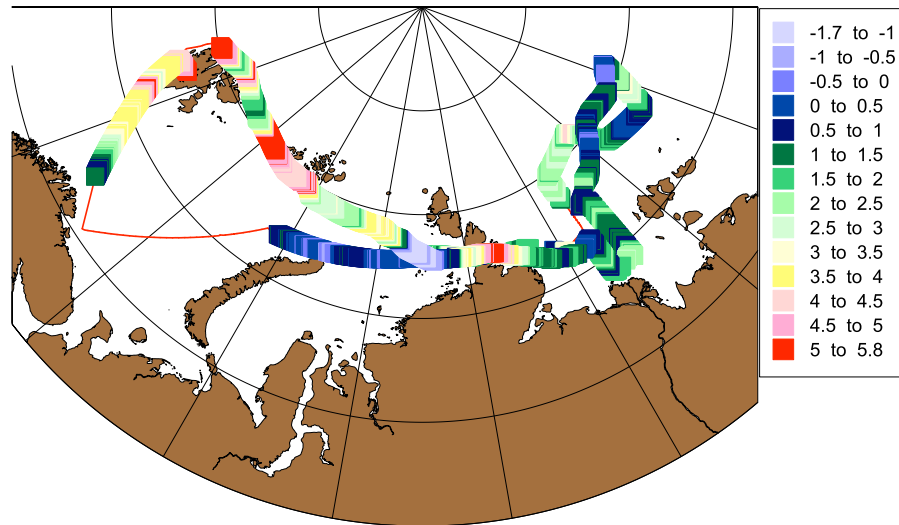


**Figure I.6.2.5:** Air-sea temperature difference along the ship's track; sea surface temperature minus air temperature.

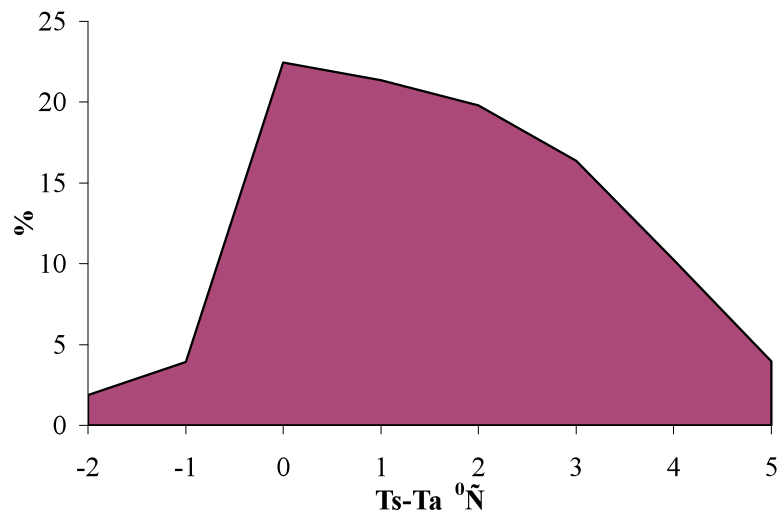


**Figure I.6.2.6:** The relative occurrence of a range of air-sea temperature differences during NABOS-07 cruise; sea surface temperature ( $T_s$ ) minus air temperature ( $T_a$ ).

The coefficient of aerodynamic drag of the underlying surface  $C_D$  and the related roughness parameter  $z_0$  are the most important aerodynamic surface characteristics, but direct measurements of these values above the sea surface, especially in high wind conditions, are rare [French *et al.*, 2007]. Our results are based on measurements obtained in the Laptev and Kara seas at wind speeds between 1 and 25 m/s. The drag coefficient was computed directly from the friction velocity and mean wind velocity measurements. For wind speeds between 4 and 20 m/s,  $C_D$  increases roughly linearly with wind speed (Figure I.6.2.7). Additional variability in  $C_D$  is due to wave age and swell. The effect of wave age is to increase the drag in fetch- or duration-limited conditions. We observed a reduction of sea surface drag coefficient in high wind conditions, in agreement with model calculations [Kudryavtsev, 2006]. This is probably connected to the sea drop effect. Unstable stratification results in an increased drag coefficient.

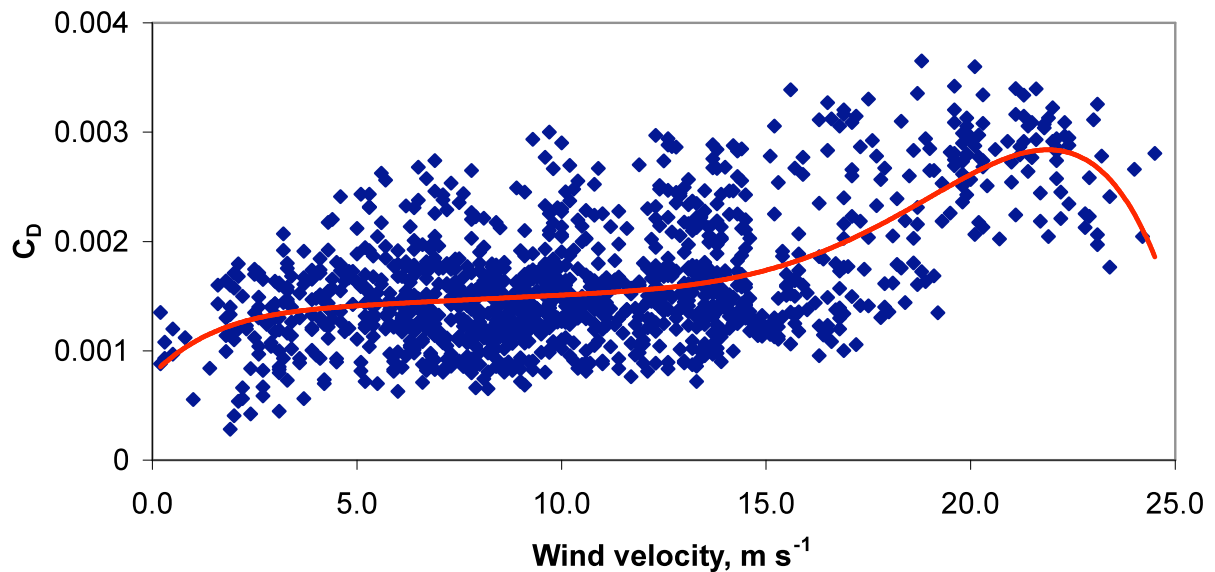


**Figure I.6.2.7:** Relationship between the drag coefficient ( $C_D$ ) and wind velocity, calculated using data obtained from the shipboard measurements.

### I.6.3. OCEANOGRAPHIC OBSERVATIONS

#### I.6.3.1. Background information (*I.Polyakov, IARC, and D.Walsh, PTWC*)

Observations made from ice-buoys, manned drifting stations, and satellites show that near-freezing surface waters, driven by surface winds and ice drift, exhibit a trans-polar drift from the Siberian Arctic toward Fram Strait [*Rigor et al.*, 2002]. In the eastern part of the Eurasian Basin this flow merges with several branches coming from marginal arctic seas (the East Siberian and Laptev Sea branches, and further west the Barents Sea branch). The basic features of the circulation in the Nansen and Amundsen basins are shown by blue arrows in **Figure I.6.3.1**. Nansen was the first to identify Atlantic Water (AW) in the Arctic Ocean during his drift on board the Fram in 1893-1896. Later observations provide evidence that the AW spreads cyclonically around the Arctic Basin, and is its major source of heat [*Timofeev*, 1960; *Coachman and Barnes*, 1963]. *Aagaard* [1989] used moored current measurements and hypothesized that major subsurface water transports occur in the form of narrow near-slope cyclonic boundary currents (**Figure I.6.3.1**, red arrows). Two major inflows supply the polar basins with AW - the Fram Strait AW branch and the Barents Sea AW branch [*Rudels et al.*, 1994].

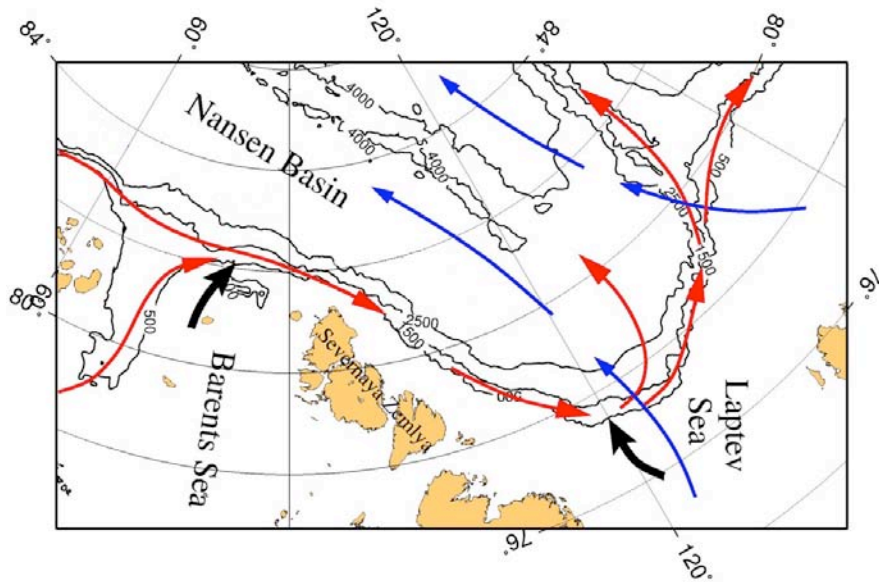


**Figure I.6.3.1:** Water mass circulation patterns in the Nansen Basin and adjacent arctic seas. Surface and subsurface circulation shown by blue and red arrows respectively.

The Fram Strait AW branch enters the Nansen Basin through Fram Strait and follows the slope until it encounters the Barents Sea AW branch north of the Kara Sea, an area characterized by strong water-mass mixing and thermohaline interleaving. The two merged branches follow the Eurasian Basin bathymetry in a cyclonic sense, forming a narrow, topographically-trapped boundary current which flows at about 5 cm/s [Woodgate *et al.*, 2001]. Near the Lomonosov Ridge the flow bifurcates, with part turning north and following the Lomonosov Ridge and another part entering the Canadian Basin [Woodgate *et al.*, 2001]. Jones [2001] stress that the circulation in the deep waters (>1700m) has not been well determined.

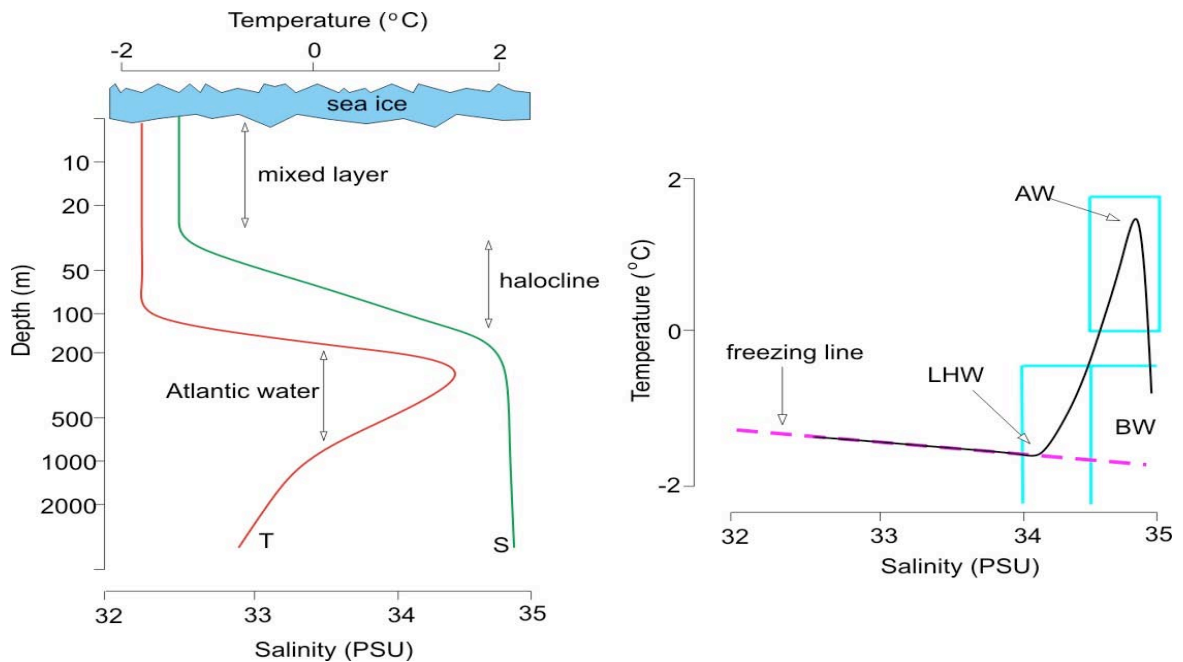


**Figure I.6.3.2:** Low Halocline Water (LHW), Atlantic Water (AW), and Bottom Water (BW) on the typical vertical temperature and salinity distribution and T-S curve in the research area.

The area of the northern Laptev Sea and adjacent Eurasian Basin has complex water-mass characteristics [Pfirman *et al.*, 1994; Schauer *et al.*, 1997; Schauer *et al.*, 2002]. AW originating in Fram Strait are found between 150 and 800 m depth in this region (**Figure I.6.3.2**, left panel). Lower Halocline Water (LHW) lies at the base of the permanent halocline, occupying the region of T-S space defined by temperature  $<-1.0$  °C and  $34.0 < S < 34.5$  psu [Woodgate *et al.*, 2001]. Below the AW layer we find the the Bottom Water (BW) with temperatures potentially as low as  $-0.95$ °C. The locations of these water masses in the T-S plane are shown in **Figure I.6.3.2**, right panel.

Little is known about temporal variability of thermohaline structure in the Eurasian Basin. An early attempt to quantify interannual variability of water-mass structure in this region is due to Quadfasel *et al.* [1993], who compared measurements from cruises in different years, finding significant year-to-year variability in the core temperature of the AW layer. However, because Quadfasel *et al.* compared measurements taken in different years and at different locations in the Nansen Basin, it is difficult to determine the extent to which their conclusions were influenced by aliasing of spatial and temporal variability, especially as the AW layer is known to cool dramatically as it flows through the Nansen Basin [Polyakov *et al.*, 2003]; quantifying interannual variability in this region is substantially complicated by the large spatial gradients in the area. Processes which affect fresh-water content (e.g., freezing, melting, and riverine inflow) are of first-order importance to Arctic Ocean dynamics [Aagaard, 1989]. Large amounts of ice form in winter on the wide continental shelves on the periphery of the Arctic Ocean, in some cases producing dense, briny waters which flow off the shelves and significantly influence the T-S structure in the interior.

### **I.6.3.2. Routine CTD measurements and water sampling**

#### **I.6.3.2.1. Objectives** (*I.Polyakov, IARC and I.Dmitrenko, IFM-GEOMAR*)

The major objectives of the 2007 field experiments were to:

- document progression of the strong warming found in the AW core during our previous expedition that appears to be approaching Alaska's backyard;
- quantify changes in the structure and spatial variability of the main water masses over the continental shelf of the Barents, Laptev, and East Siberian seas and adjoining Eurasian Basin in 2007; and
- enhance understanding of the mechanisms by which AW is transformed across and along the continental slope of the Eurasian Basin.

The hydrographic survey also provides important background information for processing the long-term mooring data.

#### **I.6.3.2.2. Methods** (*V.Ivanov, I.Polyakov, IARC*)

Over a 21-day period 73 CTD, 10 XCTD, and 8 XBT casts were made. Locations and sampling times for the CTD, XCTD and XBT casts are listed in **Table I.6.1** above, and the locations are also depicted in **Figures I.6.3.3a** and **1.6.3.3b**.

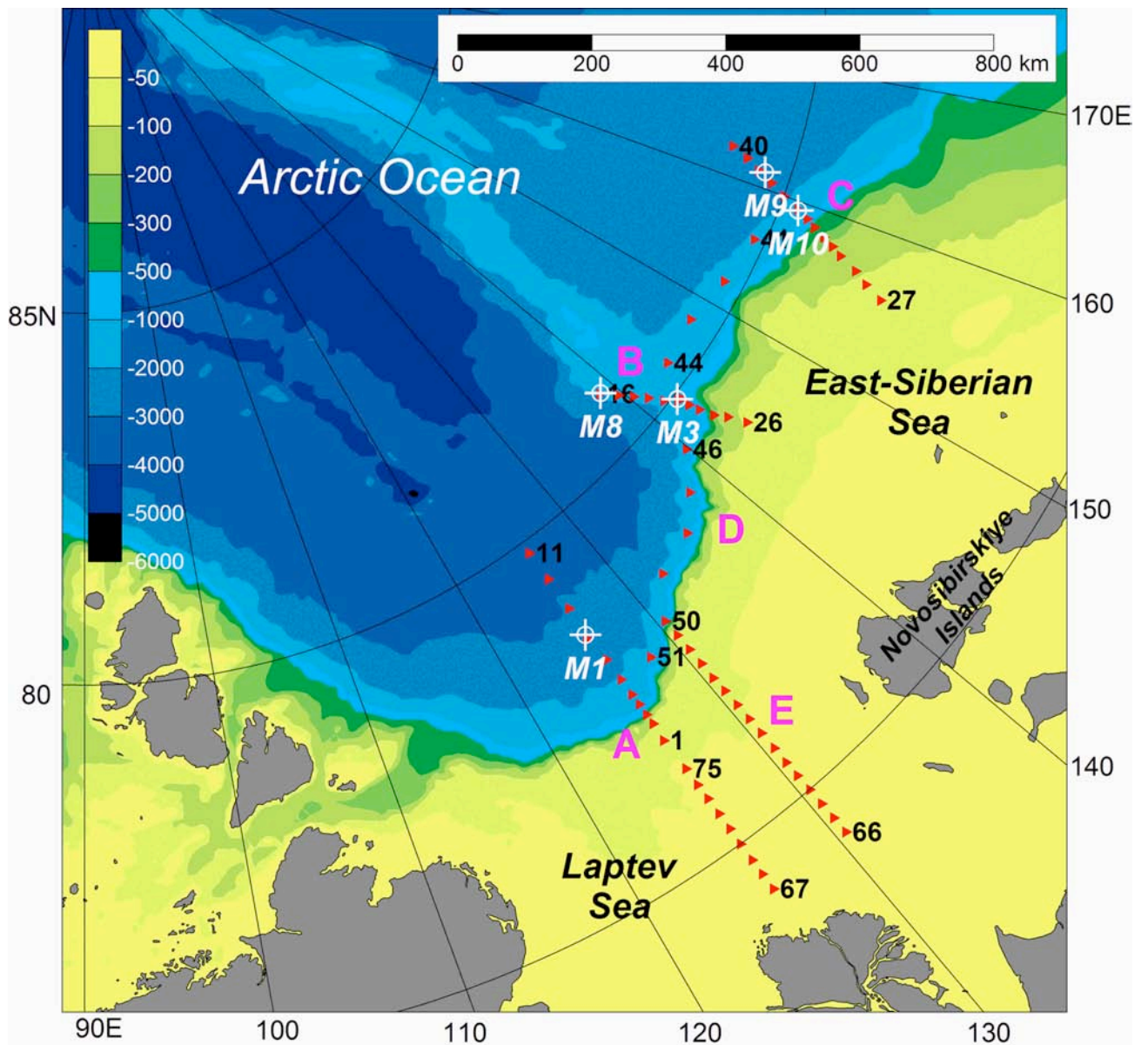


**Figure I.6.3.3a:** Scheme of CTD sections and mooring sites in the Laptev and the East Siberian seas during the NABOS-07 cruise. Red triangles represent CTD stations; white crosses denote mooring sites. Station numbers are in black.

Cross-section A crosses the REEZ and the Laptev Sea continental slope all the way from the shallow shelf to the Arctic Ocean deep interior. The northern part of this section (stations VB0107–VB1107; **Table 1.6.1**) was sampled at the very beginning of the observations program, from September 17–19, along with recovery/redeployment of the M1E/M1F mooring. The measurements in the shallow southern part of this section (stations VB6707–VB7507) were carried out at the very end of the observations program, from September 29–30.

Cross-section B (September 20–22, stations VB16–VB26) crossed the eastern Laptev Sea continental slope northward of the Novosibirskiy Islands where mooring M8A was deployed on September 20 near station VB1607, and mooring M3C was recovered on September 21 near station VB2107. M3D was deployed on September 26 at almost the same position as the earlier-recovered mooring M3C.

Cross-section C (stations VB2707-VB4007) crossed the East Siberian Sea shelf directly to the east of the Novosibirskiye Islands. Two new moorings were deployed on this cross-section; M10A on September 23, close to station VB3507, and M9A on September 24, close to station VB3807.

Along-slope section D approximately followed the 1500 m isobath. This section was carried out from east to west from September 25 to September 28 (stations VB4107–VB5107).

Cross-section E included CTD stations VB5007–VB6607 and covered the shallow shelf of the Laptev Sea, 100 miles to the east of section A.

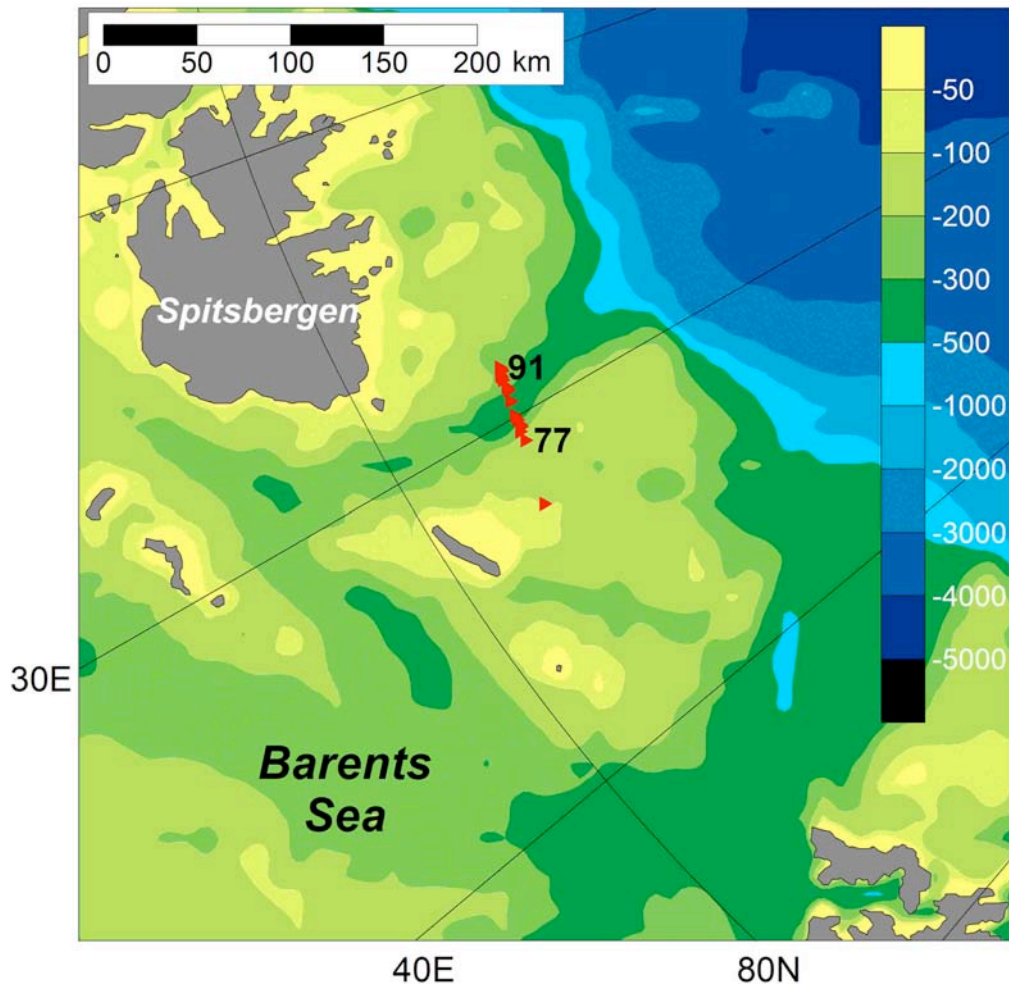


**Figure I.6.3.3b:** Scheme of the XCTD section in the Barents Sea during the NABOS-07 cruise. Red triangles represent CTD stations. Station numbers are denoted by black digits.

XCTD-XBT section E in the Barents Sea included stations VB7707–VB9107. This high-resolution section crossed the submarine canyon which cuts the northern slope of the Barents Sea, serving as a conduit for AW entering the canyon from the north.

CTD casts were limited to the upper 1000 m. Continuous CTD profiles were recorded on the downcast. Water sampling was carried out using five-liter Niskin bottles at most stations (**Table I.6.1**). Sampling depth levels are shown in Appendix 1. The CTD winch and A-frame were located on the fore deck of the vessel (**Figure I.2.3**). During CTD sounding the propellers were left running to keep the ship in the correct position relative to the wind.

### I.6.3.2.3. Equipment (*R. Chadwell, IARC*)

Continuous CTD profiles were made using a SEACAT Profiler SBE19plus. This system continuously measures conductivity, temperature, and pressure at 0.25 m intervals in the vertical. The Seacat is calibrated yearly. The technical description of sensors, according to the specifications of Sea-Bird Electronics, Inc., is presented in **Table I.6.3.1**. The full information can be downloaded from [http://www.seabird.com/products/spec\\_sheets/19plusdata.htm](http://www.seabird.com/products/spec_sheets/19plusdata.htm).

**Table I.6.3.1:** SEACAT Profiler SBE19plus technical information.

Sensors	Measurement Range	Initial Accuracy	Typical Stability (per month)	Resolution
Conductivity (S/m)	0 – 9	0.0005	0.0003	0.00005 (most oceanic waters) 0.00007 (high salinity waters) 0.00001 (fresh waters)
Temperature (°C)	-5 to +35	0.005	0.0002	0.0001
Pressure	3500 m	0.1% of full scale range	0.004% of full scale range	0.002% of full scale range
Oxygen	120% of Surface Saturation	2% Sat	2%	
Fluorometer				

Some vertical temperature and salinity profiles were carried out by the XCTD profiling systems manufactured by Lockheed Martin Co. The technical descriptions of XCTD and XBT sensors, according to the specifications of Lockheed Martin Co., are presented in **Tables I.6.3.2** and **I.6.3.3**, respectively.

**Table I.6.3.2:** Lockheed Martin Sippican XCTD technical information.

Sensors	Measurement range	Initial Accuracy	Response time	Resolution
Conductivity (mS/cm)	0 – 70	0.03	40 ms	0.017
Temperature (°C)	-2 to +35	0.02	100 ms	0.01
Pressure	1000 m	2%	-	17 cm

**Table I.6.3.3:** Lockheed Martin Sippican XBT technical information.

Sensors	Initial Accuracy
Temperature (°C)	0.1
Pressure	2%

#### I.6.3.2.4. Data processing (*I.Polyakov, IARC*)

For data collection and processing, we used the SBE SEASOFT software package for Windows. Observation data included pressure, water temperature, conductivity, oxygen, and fluorescence. Derived variables, as they were recorded in the output file, are presented in **Table I.6.3.4**.

**Table I.6.3.4** List of parameters in the output file

PR	pressure [db]
TEMP	temperature [deg C]
SALNTY	salinity [psu]
Density	Density [sigma-t Kg/m3] [Sigma_t]
V0	Voltage 0
V1	Voltage 1
V2	Voltage 2
V3	Voltage 3
Fluor	fluorescence Wetlab ECO-AFL/FL
OxC	Oxygen Current Beckman/YSI [uA]
OxSat	Oxygen Saturation [ml/l]
OxT	Oxygen Temperature Beckman/YSI [deg C]
Ox	Oxygen Beckman/YSI [ml/l].

These data were processed in several steps. At the first step we used the standard SBE software package which includes filtering, aligning, cell thermal mass module, loop editing, and 0.5m bin averaging. The resulting temperature and salinity profiles were edited using a matlab package kindly provided by Seth Danielson (Institute of Marine Studies/University of Alaska Fairbanks). This package allows manual editing of temperature and salinity spikes using linear interpolation. We found that the 0.5m bin averaging made by the SBE standard package produces very reasonable temperature output with only a few spikes left. Salinity profiles from shallow-water stations were also clean; however, deep-water profiles were much noisier and some cleaning of records was necessary. Typically, most noise was concentrated in the 100-300m layer. Unfortunately, several stations provided very noisy data throughout the entire water column. Stations 6, 14, and 46 were particularly noisy. Relatively minor errors were due to rolling of the ship (as expressed by wave-like structure in both temperature and salinity and clearly defined by vertical speed of the instrument). After corrections were made, the data were re-formatted to match data formatting standards adopted by IARC archives.

Comparison of salinities obtained by the SBE19plus and via salinometer (provided by our UK colleagues) is shown in **Figure I.6.3.4**. We found a good match between the data derived from these two different types of measurements. However, there are several outliers above the black line which are due to insufficient vertical resolution of the SBE19plus measurements (i.e. salinometer values were within one grid step). There is one outlier below the black line for which we do not have a reasonable explanation. Note, however, that the CTD-based salinity profile looks reasonable, and it matches the other two points provided by salinometer very well.

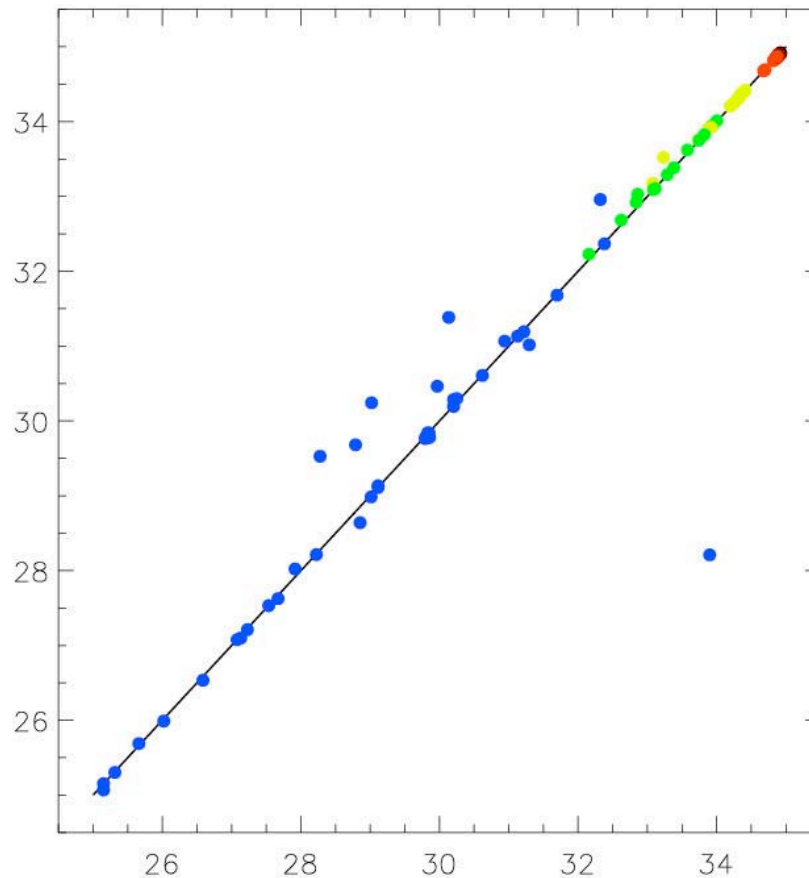


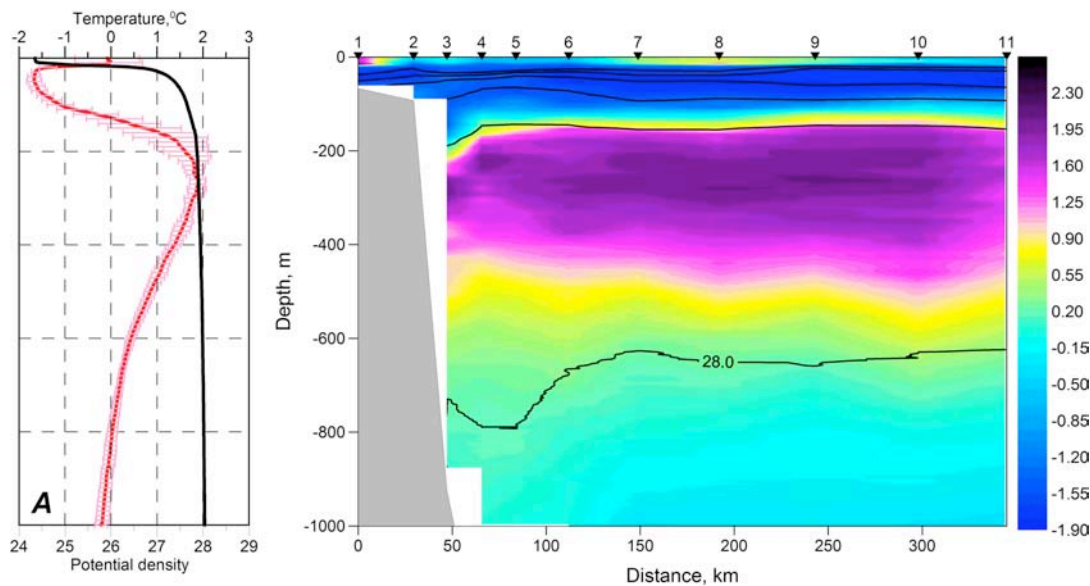
**Figure I.6.3.4.** Comparison of salinities obtained by SBE19plus (vertical) and via salinometer (horizontal). Blue color indicates points obtained in the upper (<20m) ocean layer, green points indicate observations made in the 20-75m layer, yellow points indicate measurements in the 75-300m layer, and red points indicate deep water (>300m) measurements.

#### **I.6.3.2.5. Preliminary Results** (*V.Ivanov, I.Polyakov, IARC, and S.Kirillov, L.Timokhov, AARI*)

Vertical distributions of thermohaline parameters in sections A, B, and C are shown in **Figures I.6.3.5** and **I.6.3.6**. Four distinctive water layers are distinguished in these plots. Low salinity water at temperatures close to the freezing point is found in a thin surface layer. The mean thickness of this layer can be estimated by the depth of the subsurface temperature maximum. This depth varies by about 10-15 m, reaching its maximum depth in section B. The highest temperature in the surface layer is also observed in section B. Salinity in the surface layer decreases by about 10 psu from section A to section C. Below the subsurface temperature maximum, temperature rapidly decreases, reaching minimum values at a depth of 42-53 m. In sections A and B, the depths and the values of subsurface temperature minima are very close, 48-52 m and  $-1.67/-1.65^{\circ}\text{C}$ , respectively. After passing through the minimum the temperature starts to increase, reaching maximum in the AW core. The depth of the AW warm core increases from 210 m in section A to 330 m in section C. Temperature maxima of sections A and C are  $2.18^{\circ}\text{C}$  and  $1.12^{\circ}\text{C}$ , respectively, differing by almost  $1^{\circ}\text{C}$ . Water salinity steadily increases from the surface through the temperature minimum layer and the AW. Within the AW layer, the local salinity maximum differs between section A (34.91 psu) and section B (34.88 psu). In both sections, the salinity maximum is  $\sim 150$  m deeper than is the corresponding temperature maximum that occurs at 350 m in section A and 485 m in section B. In section C a local salinity maximum in the AW is not distinguished. The lower AW boundary,

traditionally defined by the zero-degree isotherm, is located near 800 m. The major difference between the 2007 September vertical thermohaline structure and the ‘benchmark’ vertical thermohaline structure in the studied area can be seen by comparing **Figure I.6.3.2** (right panel) and **Figure I.6.3.7**. This difference is primarily concentrated in the upper part of the water column, where in the absence of ice cover anomalous water heating occurred in 2007. On average, this heating increased the surface temperature maximum by 3.5°C. This level of anomaly is huge, and we definitely expect a strong impact of this stored heat on ice. One obvious impact is that freezing had not even begun in September 2007, whereas at the same time in a "normal" year this area would be ice-covered and temperature would be close to the freezing point. Further analysis is necessary to quantify the impact of this upper ocean heat on ice.

The cross-slope distribution of thermohaline properties allows some details to be added to the described structure of water masses. Two branches of AW are well defined in section A salinity plots. The Fram Strait branch of AW is distinguished by maximum salinity, exceeding 34.92 psu at stations 7, 8, and 9 at a depth of 350-400 m. The highest measured temperature ( $>2^{\circ}\text{C}$ ) was also observed at the same stations but in shallower water. The core of the Barents Sea branch of AW is distinguished by its salinity minimum (34.86 psu) between 600 and 800 m depths at stations 4 and 5. A sharp salinity/density front separates this water mass from saltier water further offshore, indicating the existence of strong baroclinic flow associated with the Barents Sea AW. An isolated patch of low-salinity water centered around the 700 m depth at station 9 may be the evidence of meandering and eddy-formation in this flow. In sections B and C there are no visible signs of the two AW branches of salinity distribution; one possible reason is that the offshore portion of Fram Strait AW follows the bottom topography along the Lomonosov Ridge, leaving the continental slope somewhere before section B.



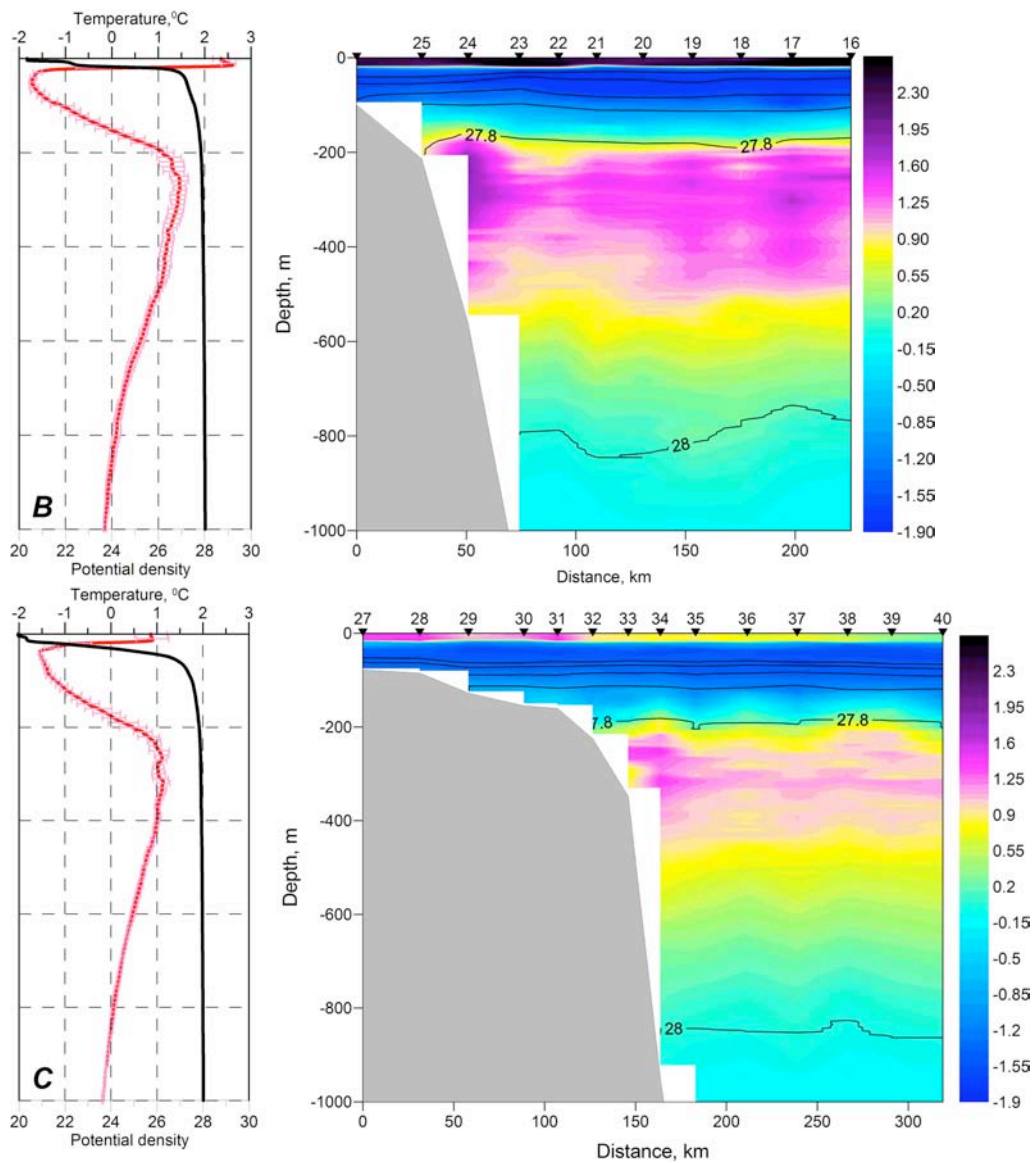


**Figure I.6.3.5** Vertical distribution of water temperature, °C and potential density in cross-slope sections A, B, and C. Left panels: horizontally-averaged profiles of temperature with standard deviation (red shadow) and horizontally averaged profiles of potential density (black). Right panels: temperature distribution (color) and potential density distribution (black lines) in the section plain.

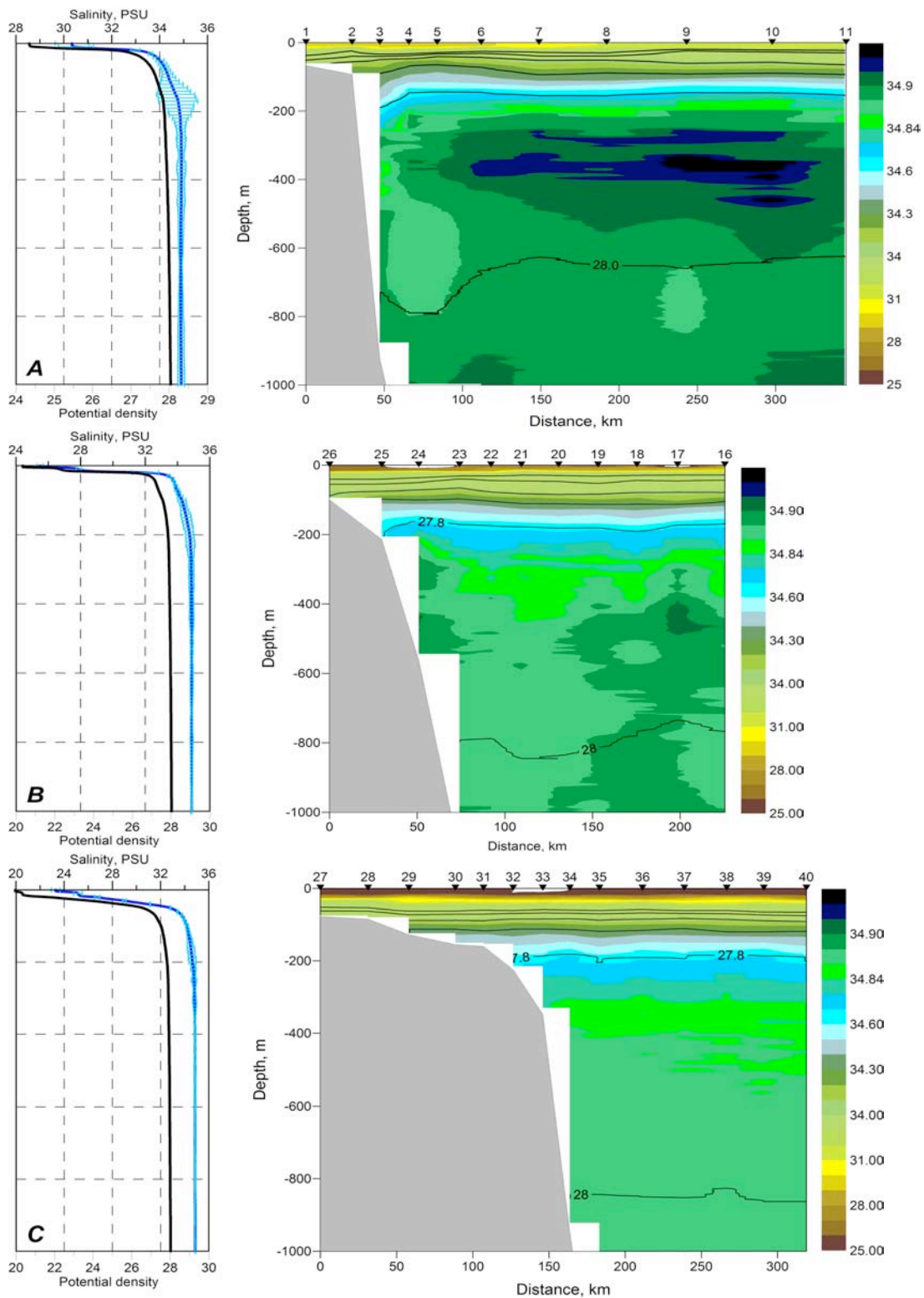


**Figure I.6.3.6** Vertical distribution of water salinity, psu, and potential density in cross-slope sections A, B and C. Left panels: horizontally-averaged profiles of salinity with standard deviation (blue shadow) and horizontally averaged profiles of potential density (black). Right panels: salinity distribution (color) and potential density distribution (black lines) in the section plane.

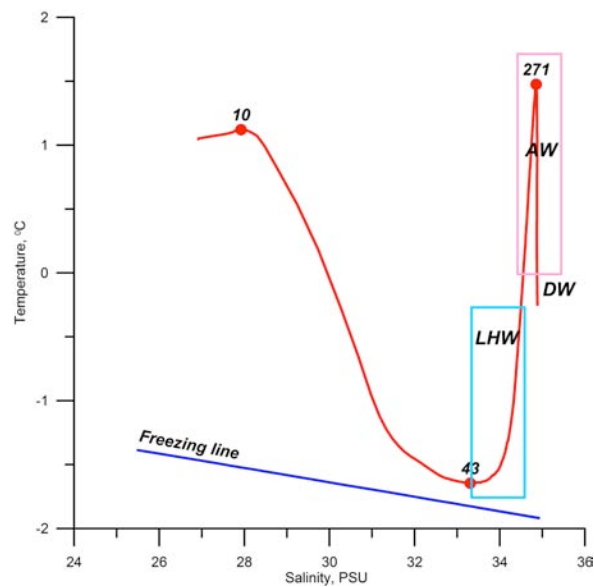


**Figure I.6.3.7.** Temperature-salinity (TS) diagram calculated using temperature and salinity profiles averaged over sections A, B, and C.

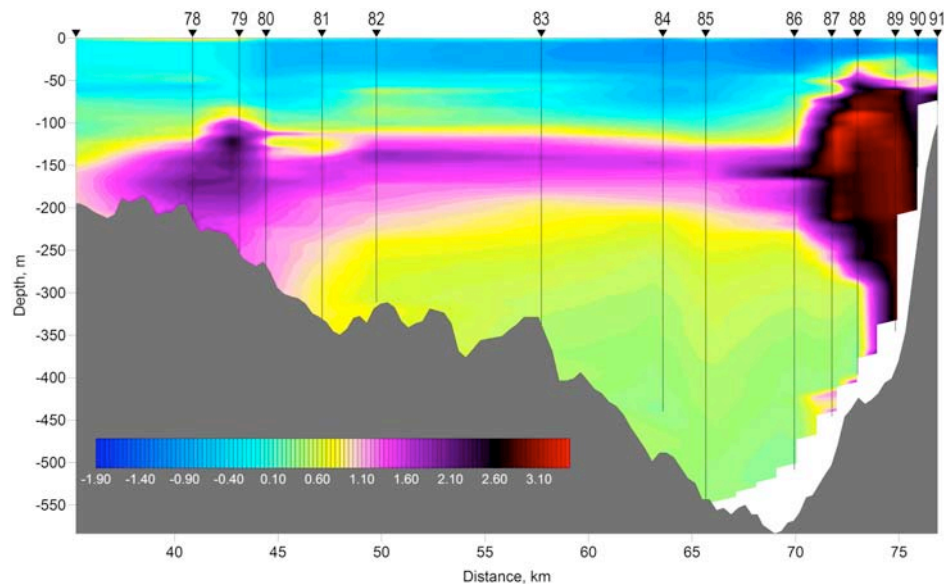


**Figure I.6.3.8.** Vertical distribution of water temperature across the submarine canyon in the northern Barents Sea (see **Figure I.6.3.3**)

The detailed structure of AW flow in the northern Barents Sea is depicted in **Figure I.6.3.8**. High spatial resolution of this survey together with detailed echo sounder-based bathymetry allowed accurate mapping of the AW core at the western (right) and the eastern (left) flanks of the canyon. AW enters the canyon from the north along the western slope. The spatial scale of the AW core is only about 5 km, which is close to the baroclinic Rossby radius. AW makes a loop within the canyon and moves back to the north along the eastern slope. Similar circulation patterns are also observed in Franz-Victoria and St. Anna canyons further to the east [Ivanov, 2002].

### I.6.3.3. Moorings observations

#### I.6.3.3.1. Objectives (*I.Polyakov, IARC and I.Dmitrenko, IFM-GEOMAR*)

The overall purpose of these mooring observations was to provide observationally-based information on temporal variability of water circulation and water mass transformation on the continental slope of the Laptev Sea. The major objectives were:

- to quantify the structure and temporal variability of the main water masses over the continental shelf of the Laptev Sea; and
- to obtain detailed information about AW layer dynamics and seasonal variations.

#### I.6.3.3.2. Mooring design and equipment (*R.Chadwell, IARC*)

Mooring design and oceanographic equipment are presented in **Figure I.6.3.9**. The modified avalanche beacons were removed from the mooring design at the beginning of the 2005 field season, because they would be needed only for a through-ice recovery and we are not equipped for through-ice recoveries, and because this equipment sometimes became entangled during deployments and recoveries.

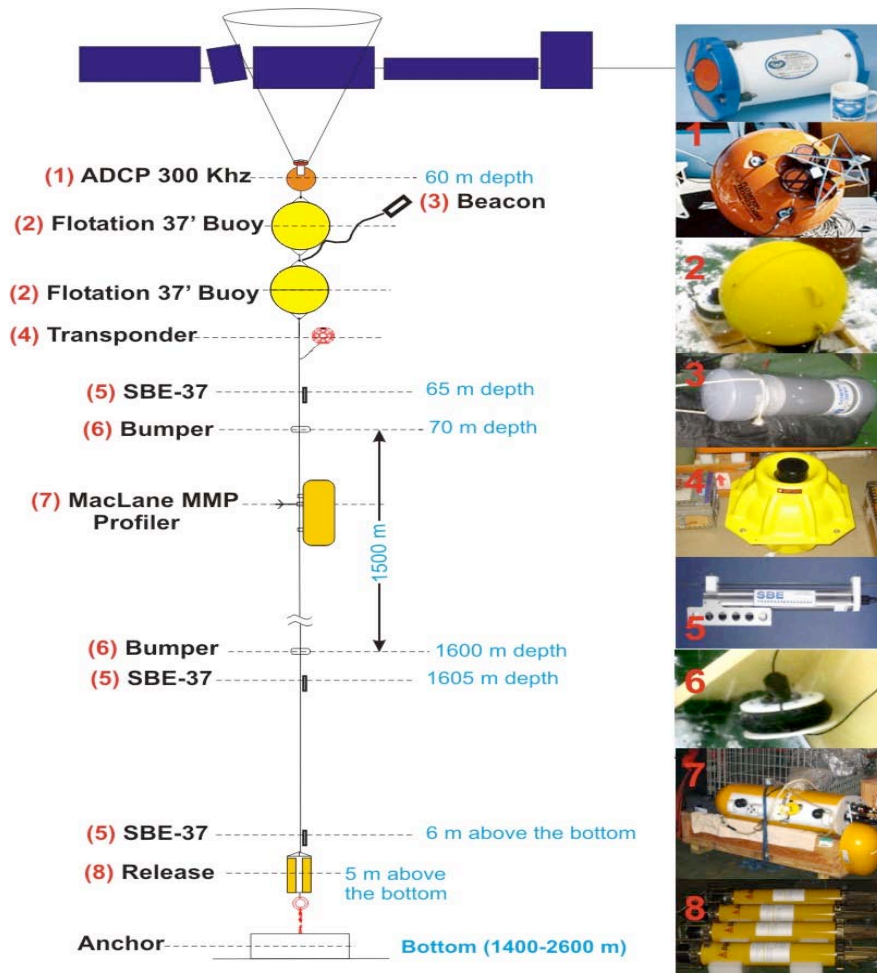


**Figure I.6.3.9.** NABOS moorings basic design and equipment.

The McLane Moored Profiler (MMP) (**Figure I.6.3.10**) designed and manufactured by McLane Research Laboratories, Inc. is the main component of NABOS moorings. The full technical information and description is available at <http://www.mclanelabs.com>.

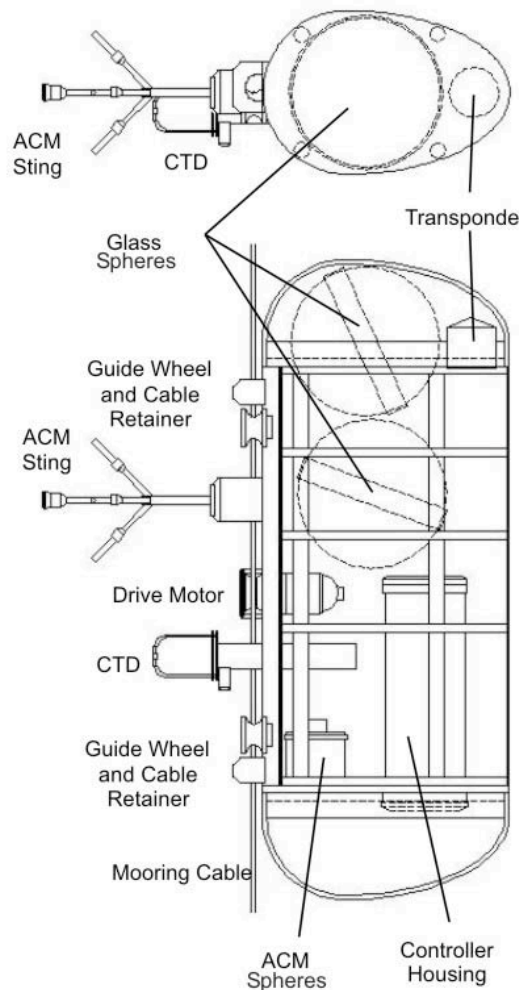


**Figure I.6.3.10.** Sketch of McLane Moored Profiler© of McLane Research Laboratories, Inc.

### I.6.3.3.3. Mooring deployments (*R. Chadwell, IARC*)

At the beginning of the 2007 field season the mooring team was tasked with an unprecedented twelve mooring deployments. Originally, the two moorings in the vicinity of Svalbard were to be serviced from a German research vessel, but that vessel suffered a propulsion failure and those two moorings were re-tasked to the NABOS group. The mooring group had ten moorings to deploy in the Laptev Sea area. Unfortunately, the larger ship-of-opportunity was not available and the expedition used a smaller vessel with less cargo capability and limited ability to work in ice-covered areas.

As a result, it was decided to attempt a two-leg operation; first, five mooring deployments in the Laptev Sea, then a return to port to load and prepare for an additional five deployments near Svalbard. It became apparent as soon as the charter agreement was completed that moorings M5B and M6A near the Severnaya Zemlya islands would be inaccessible due to ice cover.

The team was prepared, with borrowed equipment, to drag for several moorings and redeploy at least one mooring for a German institution; however, another vessel equipped properly for dragging successfully recovered the German moorings.

The *Viktor Buynitsky* departed Norway prepared for five mooring deployments on the first leg. The situation was dynamic and the future of the second leg was uncertain because of ice conditions and because the availability of an icebreaker escort in the straits connecting the Laptev and Kara seas was unknown.

After successfully completing two mooring recoveries and five mooring deployments in the Laptev Sea, a late-season ice convoy allowed the expedition the opportunity to steer directly for Svalbard where our gear had been staged for the second leg. While en route to Longyearbyen, it was decided to attempt a recovery of moorings M4B and M7A near Svalbard, and then prepare the moorings for re-deployment along with another three ICORTAS moorings after the Svalbard port call. Unfortunately, the expedition encountered ice approximately sixty nautical miles south of the mooring locations and therefore proceeded directly to port. The intention was to re-evaluate the remote sensing data regarding ice cover over the area of operations and make another attempt at servicing the two existing moorings and deploying the three new ICORTAS moorings.

It was determined that an attempt to reach the area was not practical due to ice cover; therefore, all science operations were cancelled and the vessel proceeded directly back to Kirkenes, Norway for demobilization and a final return to its homeport of Murmansk, Russia.

The 2007 field season resources were greatly enhanced by an abundance of equipment provided by the ICORTAS group. Mooring gear items such as releases were plentiful, on deck, and ready for redeployments, significantly reducing turnaround times and required man hours.

One mooring “anchor last” deployment was made, but the wire catenary was so problematic that the team decided to conduct all future deployments in the traditional (for NABOS) “anchor first” method.

### Mooring M1F, As Deployed 2007

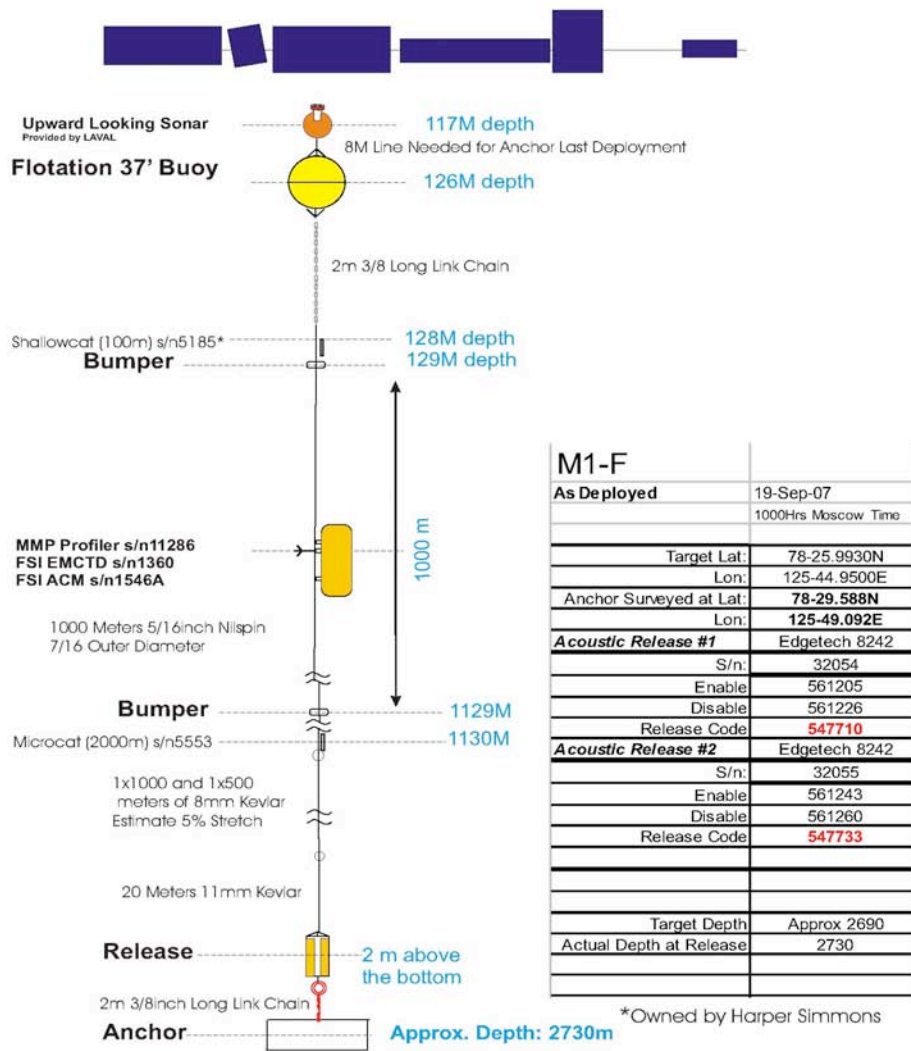


Figure I.6.3.11. NABOS-07 M1F mooring design and equipment.

Table I.6.3.5: M1F as deployed

Equipment	Serial #	Parameters	Last Calibration	Sampling Rate	Estimated Depth	Comments
ULS	Owned by Laval U.	Ice Keels	Unspecified	Unspecified	117M	Owned by LU
Shallowcat 37SM CTD (100m)	5183	Conductivity Temperature Pressure	2007	15 Minutes	128M	Owned by H.Simmons
MMP Profiler	11286	Sensor Platform	N/A	One profile per day	129M-1129M	
FSI EMCTD	1360	Pressure Conductivity Temperature	2007	"	"	
FSI ACM	1546A	Current	2007	"	"	
Microcat	5553	Conductivity Temperature Pressure	2007	15 Minutes	10130	

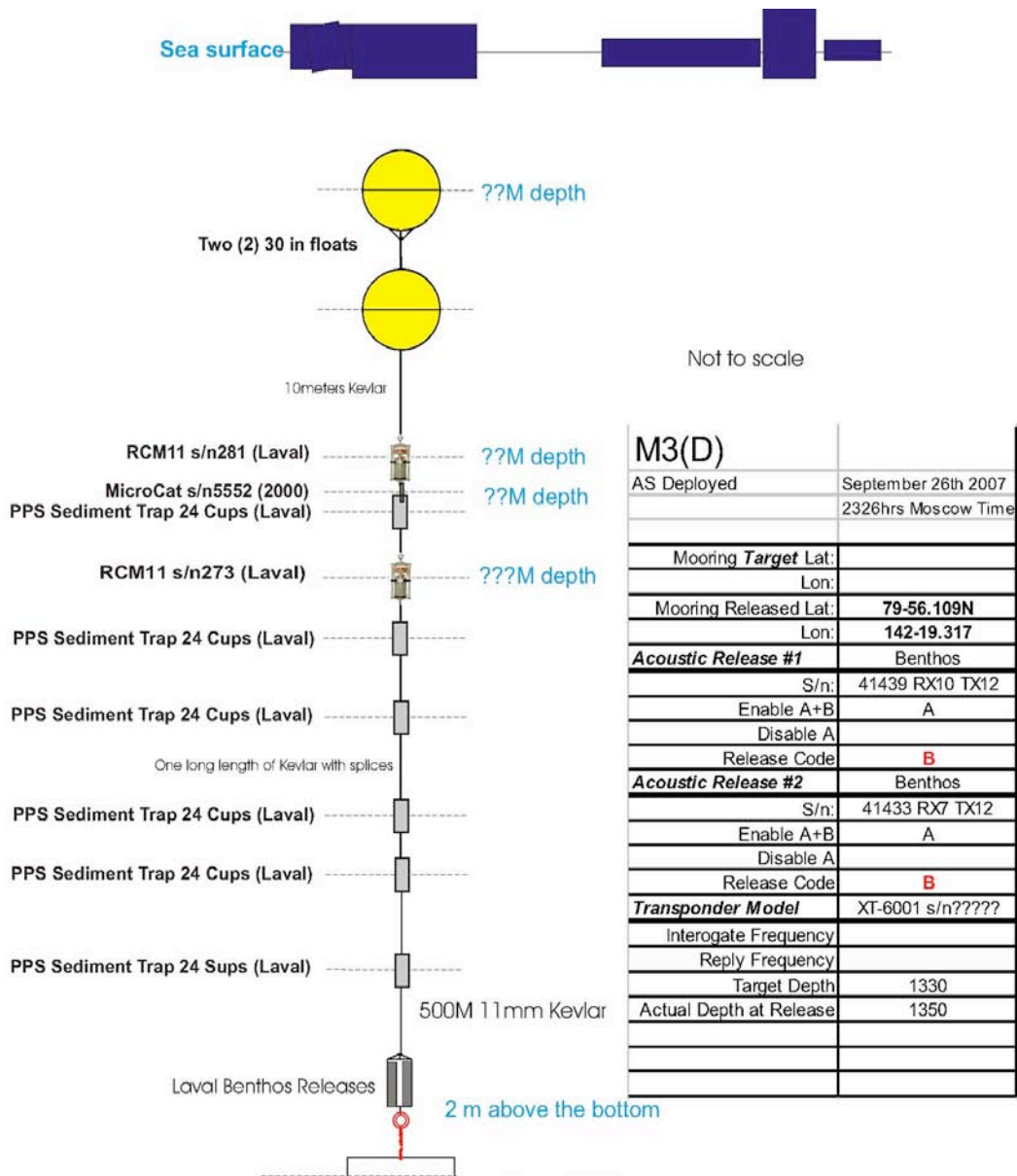


Figure I.6.3.12: NABOS-07 M3D mooring design and equipment.

Table I.6.3.6: M3D as deployed

Equipment	Serial #	Parameters	Last Calibration	Sampling Rate	Estimated Depth	Comments
RCM11	281	Current Temperature Conductivity Pressure Turbidity O2	N/A	1 Hour	Unspecified	Owned LU
Microcat 37SM CTD (2000m)	5552	Conductivity Temperature Pressure	2007	15 Minutes	Unspecified	Owned by UAF-IARC
PPS Sediment Trap	Unspecified	Sediment 24 Cups	N/A	N/A	Unspecified	Owned by LU

RCM11	273	Current Temperature Conductivity Pressure Turbidity O2	N/A	1 Hour	Unspecified	Owned by LU
PPS,Sediment Trap	Unspecified	Sediment 24 Cups	N/A	N/A	Unspecified	Owned by LU
PPS,Sediment Trap	Unspecified	Sediment 24 Cups	N/A	N/A	Unspecified	Owned by LU
PPS,Sediment Trap	Unspecified	Sediment 24 Cups	N/A	N/A	Unspecified	Owned by LU
PPS,Sediment Trap	Unspecified	Sediment 24 Cups	N/A	N/A	Unspecified	Owned by LU
PPS,Sediment Trap	Unspecified	Sediment 24 Cups	N/A	N/A	Unspecified	Owned by LU

**Mooring M8(A) As Deployed 2007  
Laval University**



M8A and M9A are essentially the same

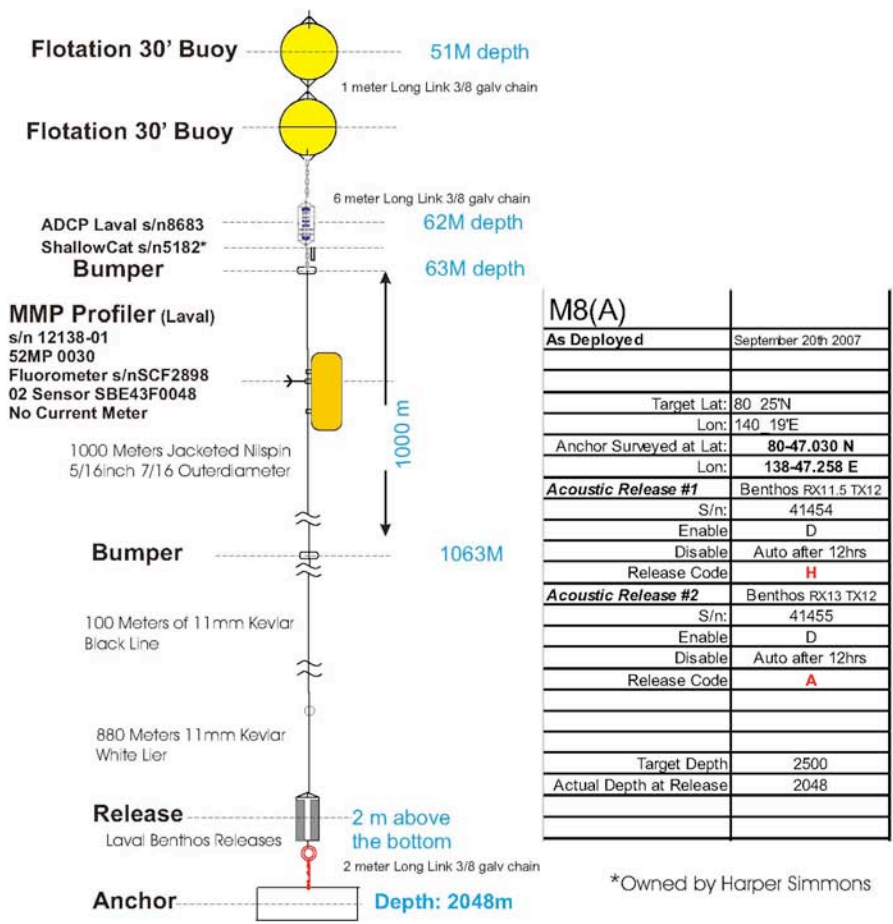


**Figure I.6.3.13: NABOS-07 M8A mooring design and equipment.**

**Table I.6.3.7: M8A as deployed**

Equipment	Serial #	Parameters	Last Calibration	Sampling Rate	Estimated Depth	Comments
ADCP	8683	Current	N/A	15 Minutes	61M	Owned by LU
ShallowCat	5182	Conductivity Temperature Depth	2006	15 Minutes	62M	Owned by H.Simmons
MMP Profiler	12138-01	Sensor Platform	N/A	One profile per day	63M-1063M	Owned by LU
Seabird 52MP	0030	Pressure Conductivity Temperature	2007	“	“	“
Fluorometer	SCF2898	Fluorescence	Unspecified	“	“	“
O2 SBE43F	0048	Oxygen		“	“	“

**Mooring M9(A) As Deployed 2007  
Laval University**



M8A and M9A are essentially the same

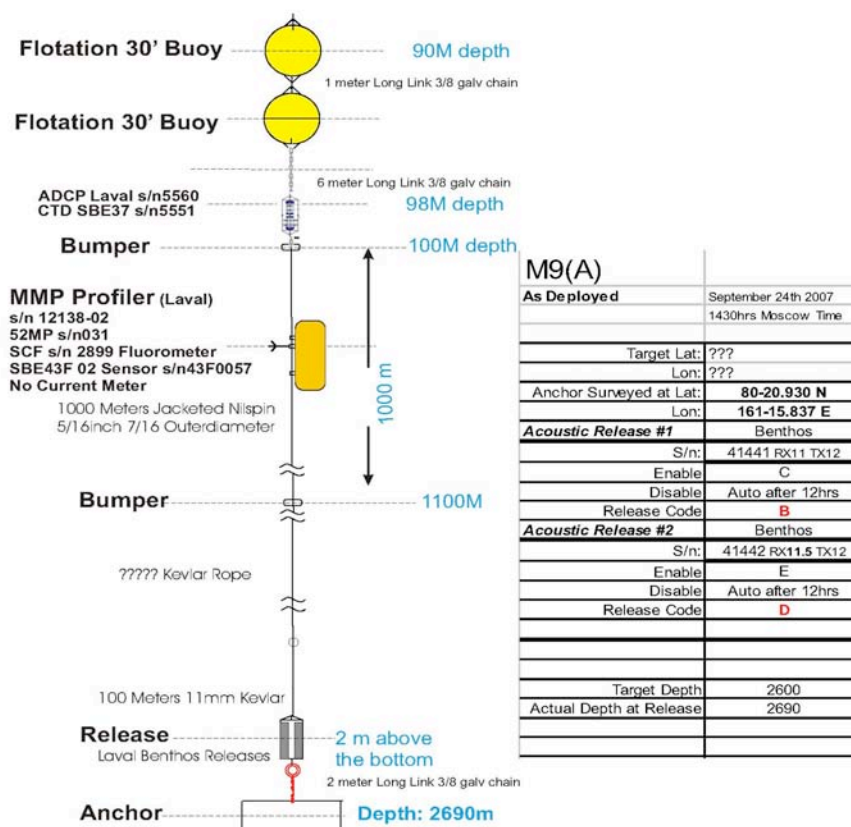


**Figure I.6.3.14. NABOS-07 M9A mooring design and equipment**

**Table I.6.3.8: M9A as deployed**

Equipment	Serial #	Parameters	Last Calibration	Sampling Rate	Estimated Depth	Comments
ADCP	5560	Current	N/A	15 Minutes	98M	Owned by LU
Microcat	5551	Conductivity Temperature Depth	2007	15 Minutes	99M	Owned by UAF-IARC
MMP Profiler	12138-02	Sensor Platform	N/A	One profile per day	100-1100M	Owned by LU
Seabird 52MP	0030	Pressure Conductivity Temperature	2007	“	“	“
Fluorometer	SCF2899	Fluorescence	Unspecified	“	“	“
O2 SBE43F	0057	Oxygen		“	“	“

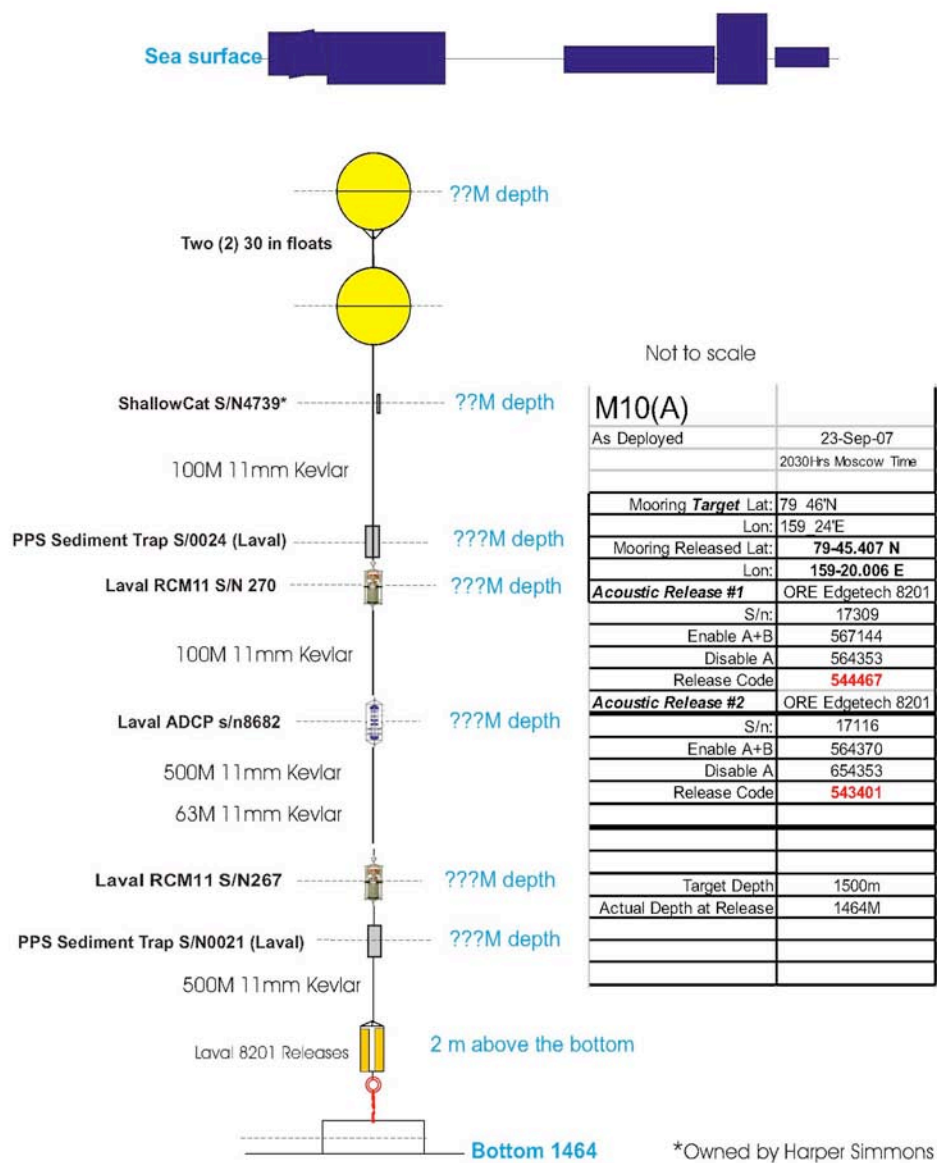


**Figure I.6.3.15. NABOS-07 M10a mooring design and equipment.**

**Table I.6.3.9: M10A as deployed**

Equipment	Serial #	Parameters	Last Calibration	Sampling Rate	Estimated Depth	Comments
Shallowcat	4739	Conductivity Temperature Depth	2006	15 Minutes	Unspecified	Owned by H.Simmons.
PPS,Sediment Trap	0024		N/A	Unspecified	Unspecified	Ownded by LU.
RCM11	270	Current Temperature Conductivity Pressure Turbidity O2	N/A	15 Minutes		Owned by LU
ADCP	8682	Current	N/A	15 Minutes	Unspecified	Owned by LU
RCM11	270	Current Temperature Conductivity Pressure Turbidity O2	N/A	15 Minutes		Owned by LU
PPS,Sediment Trap	0024		N/A	Unspecified	Unspecified	Ownded by LU

#### **I.6.3.3.4. Mooring recovery (*R..Chadwell, IARC*)**

The mooring team was originally tasked with the recovery of only four moorings; however, after the propulsion system of the German research vessel was damaged, the servicing of the two Svalbard moorings was re-tasked to the NABOS group for a total of six recoveries. For reasons mentioned above only two moorings were recovered and turned around, M1E and M3C. Moorings M5 and M6 located near the Severnaya Zemlya Islands were inaccessible due to ice cover. Moorings M4 and M7 had been scheduled for the second leg, but their recoveries also had to be postponed until 2008.

During two of the mooring recoveries we experienced problems with releases. The first problem was determined to be a small node on the machined parts of the release mechanism. The second anomaly was communications-related; it was determined that the releases operated properly but local acoustic conditions prevented the confirming reply sent from the mooring from being received by the deck unit.

To summarize, moorings M1 and M3 were recovered, serviced, and redeployed. The remaining moorings could not be reached due to ice cover and must be recovered in the 2008 field season because the release batteries will reach the end of their service life.

**Table I.6.3.10: Mooring M1E as recovered**

Equipment	Serial #	Parameters	Data	Sampling Rate	Actual Depth (db)	Time of Observations
ADCP	5560	Current	Yes	30 min	64	9/1/06 – 9/18/07
Microcat 37SM CTD (100m)	4975	Conductivity Temperature Pressure	Partial	15 min	65	9/1/06 – 11/15/06
MMP Profiler	12040	Sensor Platform	Partial	One profile per day	70 - 900	9/2/06 – 10/10/06
Seabird 52MP	0017	Pressure Conductivity Temperature	“	“	“	“
FSI ACM	1838	Current	“	“	“	“

**Table I.6.3.11: Mooring M3C as recovered**

Equipment	Serial #	Parameters	Data	Sampling Rate	Actual Depth (db)	Time of Observations
PPS Sediment Trap	687	Sediment	Yes	N/A	180	Sep 2006 – Aug 2007
Microcat 37SM CTD (2000m)	2308	Conductivity Temperature Pressure	Yes	15 min	170	8/29/06 – 8/21/07
ADCP	2226	Current	Yes	30 min	180	8/29/06 – 8/21/07
Microcat 37SM CTD (2000m)	3049	Conductivity Temperature NO Pressure	Yes	15 min	280	8/29/06 – 8/21/07
RCM11	270	Current Temperature Conductivity Pressure Turbidity O2	Yes	1 hour	280	8/28/06 – 8/21/07
SAMI	49	Temperature, CO <sub>2</sub>	Yes	1 hour	285 m	8/28/06 - 9/2/07
Microcat 37SM CTD (2000)	4976	Conductivity Temperature Pressure	Yes	15 min	780	8/28/06 – 8/21/07
RCM11	267	Current Temperature Conductivity Pressure Turbidity O2	Yes	1 hour	856	8/28/06 – 8/21/07
PPS Sediment Trap	0021	Sediment	Yes	N/A	850	Sep 2006 – Aug 2007

**I.6.3.3.5. Preliminary Results** (V.Ivanov, I.Polyakov, IARC, I.Dmitrenko, IFM-GEOMAR,, and S.Kirillov, L.Timokhov, AARI)

**M1e mooring**

The MMP profiler performed full casts only until October 10, 2006; after this date the instrument sat motionless at the lower bumper. Temperature, salinity, and orthogonal current components, recorded during one month of measurements, are presented in **Figures I.6.3.16** and **I.6.3.17**. AW (~2°C in the core) occupied the 100 to 800 m depth range, indicating that the warming event that started in February 2003 was still in progress. The salinity distribution in the 500-800 m layer reflects the measurement of relatively low salinity water between September 17 and October 7. During this time interval the AW temperature was also lower than either before or after. Comparing this record with the cross-slope salinity distribution in section A (see **Figure I.6.3.6**) we may assume that the instrument has recorded the meander of the Barents Sea AW flow, which is distinguished by lower salinity. Stronger currents measured in the deep water between September 15 and September 30 are consistent with this possible explanation.

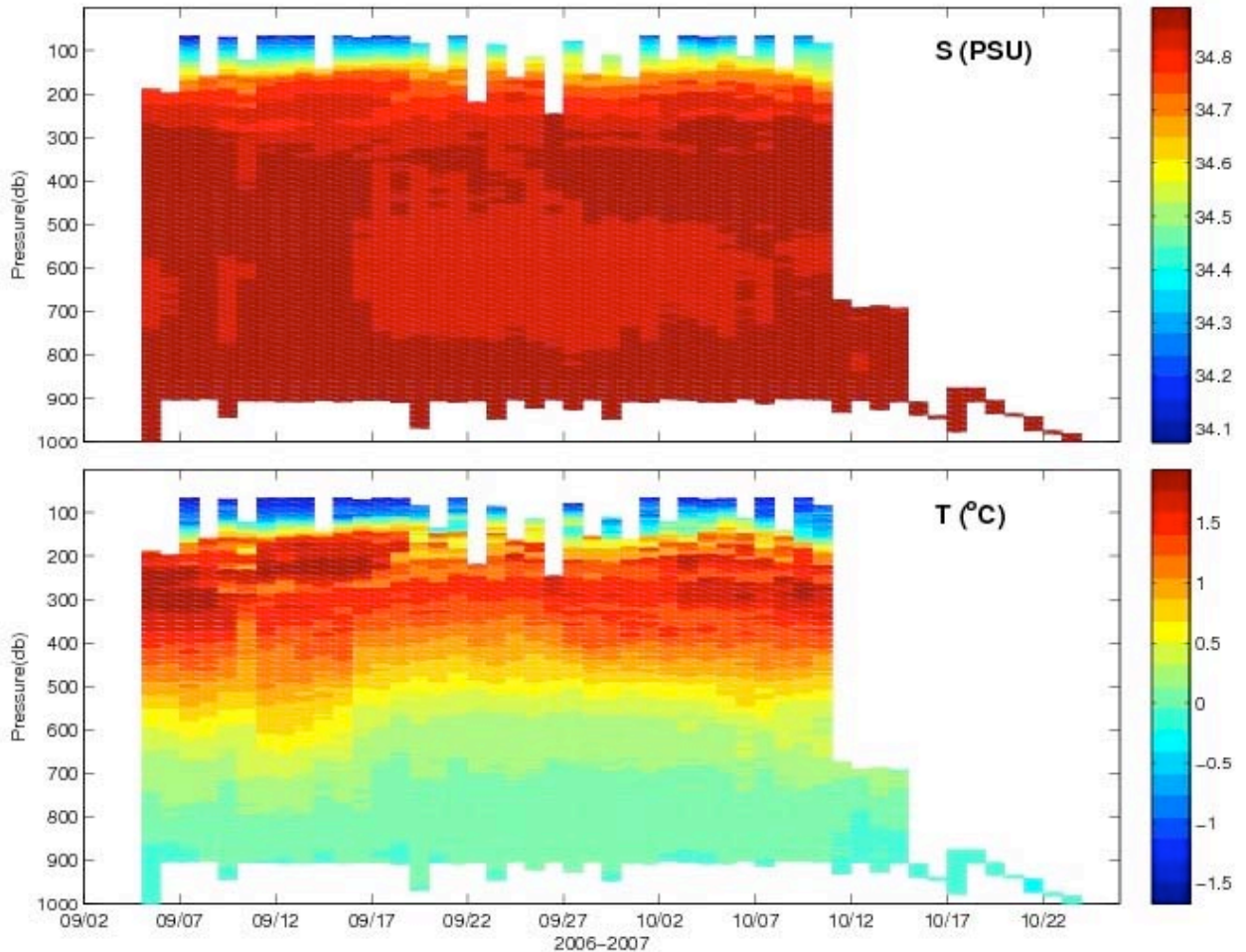


**Figure I.6.3.16.** Water salinity (S) and temperature (T) from the M1E MMP in September and October 2006

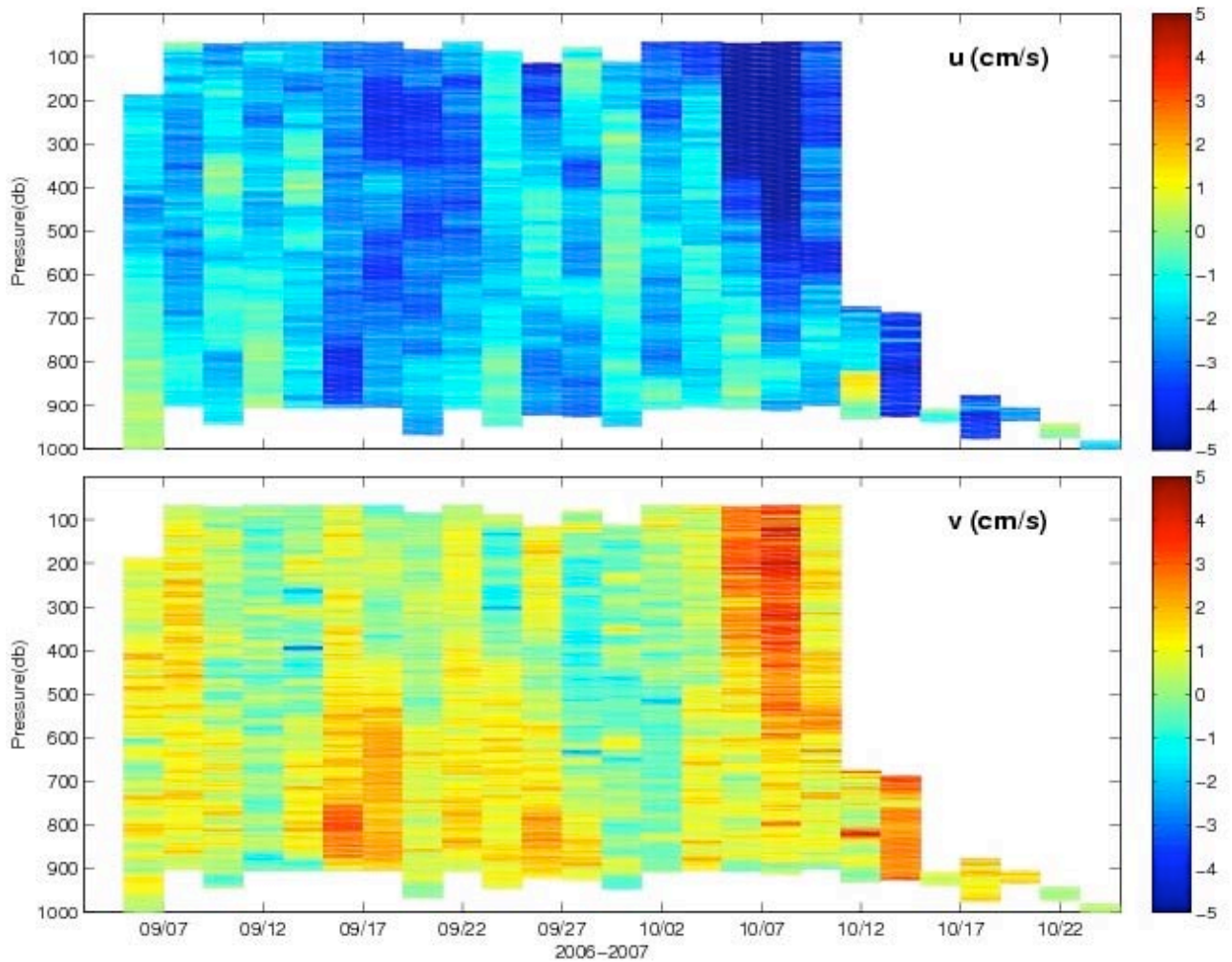


**Figure I.6.3.17.** Current components (u) and velocity (v) from the M1E MMP in September and October 2006

Current measurements by the upward-looking acoustic Doppler current profiler (ADCP) (**Figure I.6.3.18**) demonstrate a mosaic pattern of currents in the upper 50 m. Maximum current speed is about 10 cm/s. Short episodes during which current velocity exceeded 25 cm/s at the beginning and end of the record are not considered reliable and require additional examination. Current direction varies around the compass, showing no obviously prevalent direction.

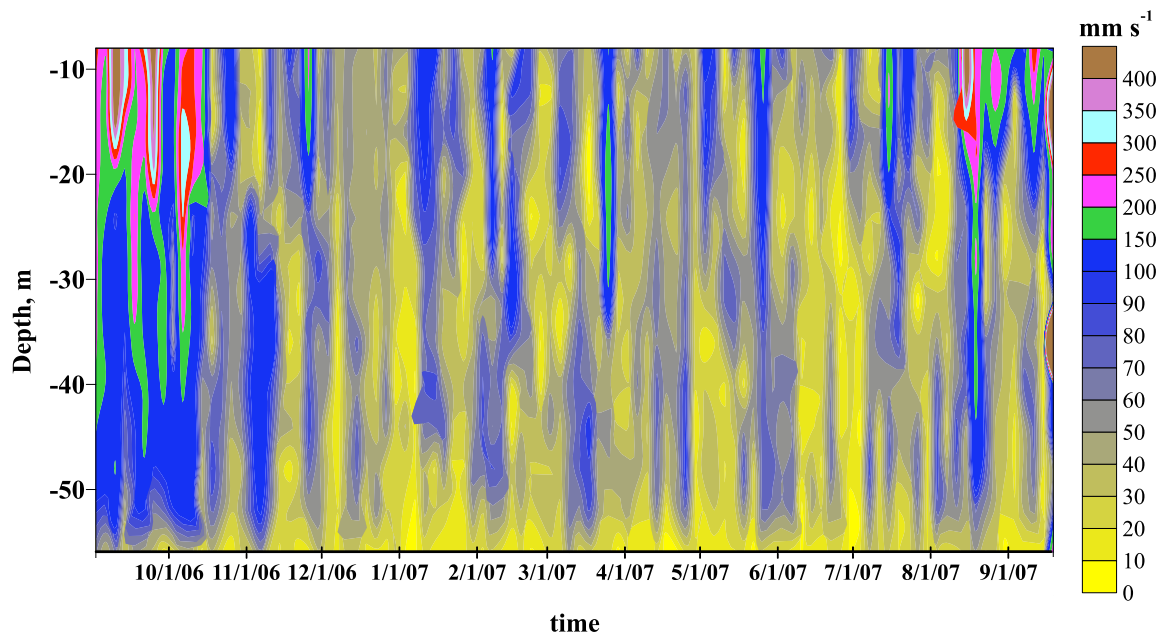


**Figure I.6.3.18a.** Current velocity measured by upward-looking ADCP deployed at 64 db

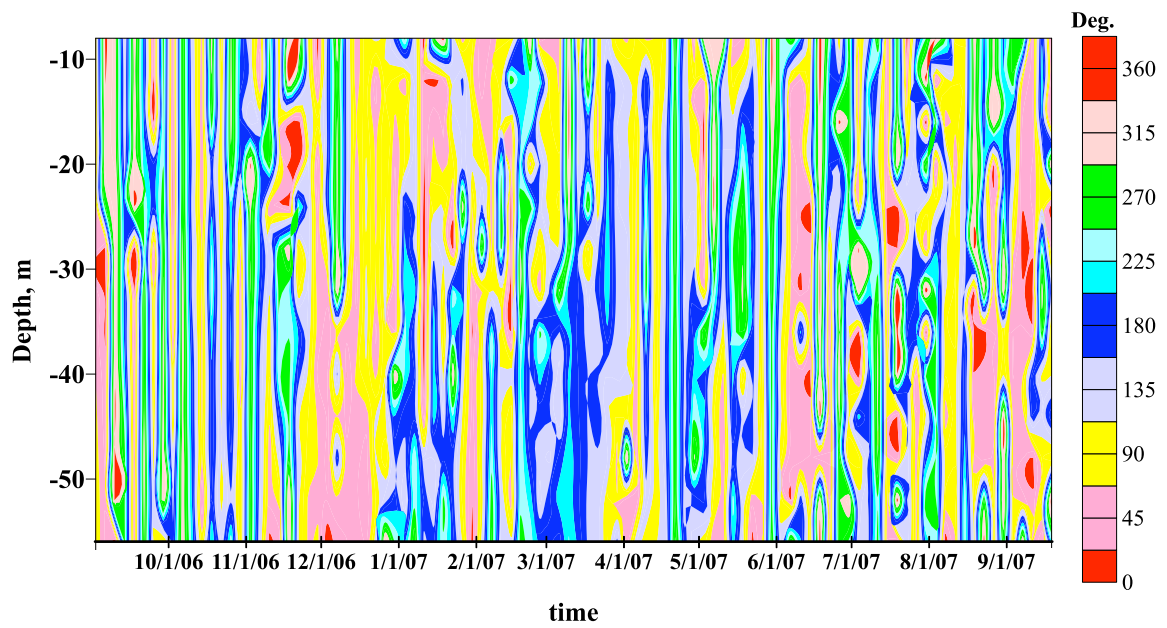


**Figure I.6.3.18b.** Current direction measured by upward-looking ADCP deployed at 64 db

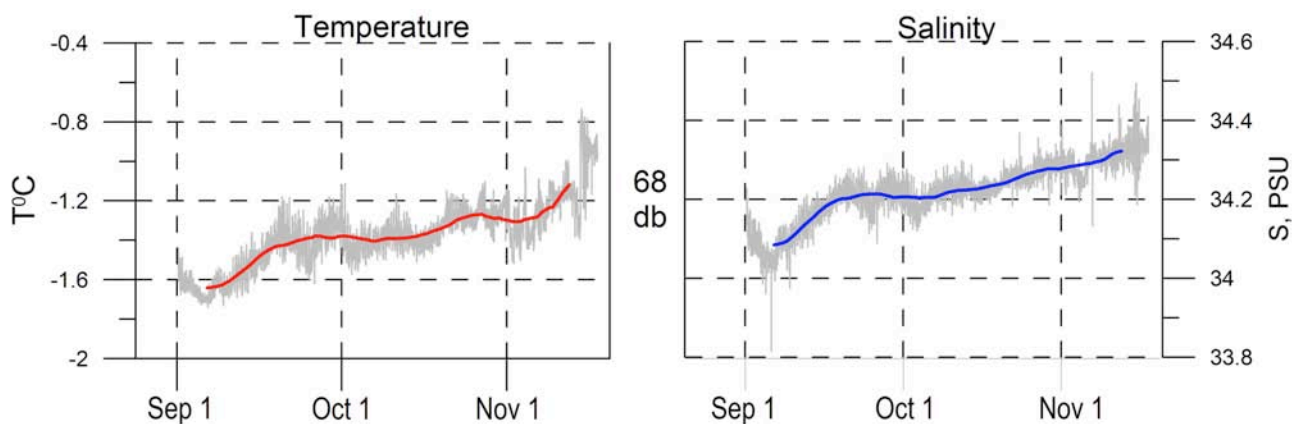


**Figure I.6.3.19.** Temperature ( $^{\circ}\text{C}$ ) and salinity (PSU) derived from 15-min records from the uppermost position of the SBE-37 deployed at 65 db. 10-day running means are shown by red and blue lines.

Halocline-depth (68 db) 2.5-month-long measurements demonstrate sustained warming and salinification of halocline water. Unfortunately the record obtained by this instrument is very short because the instrument was flooded, so comparison with the previous year's records might be helpful for understanding what is behind the observed trend.

### ***M3c mooring***

Temperature and salinity (**Figure I.6.3.20**) and current velocity time series at this mooring are now the longest continuous records obtained during NABOS operation. They cover a time span of three years, from September 2004 to September 2007. The most striking result captured by SBE-37s at 170 and 280 db during the recent year is a temporary 'disappearance' of AW, which continued for about one month and was reflected in an abrupt drop of water temperature by about about  $2^{\circ}\text{C}$ , and in a drop of salinity by about 0.2 psu. During this event, the temperature in the AW core declined below zero; this allows us to formally discuss a temporary 'disappearance' of the AW layer, because this layer is often defined as the 'intermediate water mass with positive temperature' [e.g. *Nikiforov and Shpaiher*, 1980]. A temperature drop of  $\sim 0.25^{\circ}\text{C}$  was also recorded by the deepest instrument at 780 db. However, this temperature change happened about 1.5 month later than the change in the upper part of the water column. Therefore, the question of whether the origin of recorded changes in the upper and lower parts of the water column was the same remains unresolved.

Time series of current velocity are available from the upward-looking ADCP, placed at 180 db (**Figure I.6.3.21**), and two RCM11s (**Figure I.6.3.22**). Observed cooling/freshening events were generally accompanied by deceleration of current and increase of the current directional variance.

During this year's deployment the RCM11s were also equipped with dissolved oxygen (DO) and turbidity sensors. The records obtained by these sensors are shown in **Figure I.6.3.23**. The cooling/freshening event is marked by increased DO concentration at both depths. At the deeper instrument the DO increase, which started almost in phase with the increase at the upper instrument, was not followed by a DO decrease. As a result, in the deeper water the difference in the DO concentration between the start and the end of the record is about  $10\ \mu\text{mol/L}$ . At the upper instrument the DO concentration returned to the initial values by the end of the deployment. The amplitude of DO variation is at the threshold of device accuracy (see web manual available at: [http://www.oceantech.co.kr/eng/2\\_product/brochure/aanderaa/B128%20Oxygen%20Optode%203830.pdf](http://www.oceantech.co.kr/eng/2_product/brochure/aanderaa/B128%20Oxygen%20Optode%203830.pdf)). Hence, this result has to be accepted with caution.

Turbidity records (**Figure I.6.3.23**) show localized peaks, separated by prolonged intervals during which turbidity was nearly constant. The first peak measured by the deeper instrument

corresponds to the timing of the cooling/freshening/oxygenation event. However, the accuracy of the entire turbidity record is in doubt and additional examination is required.

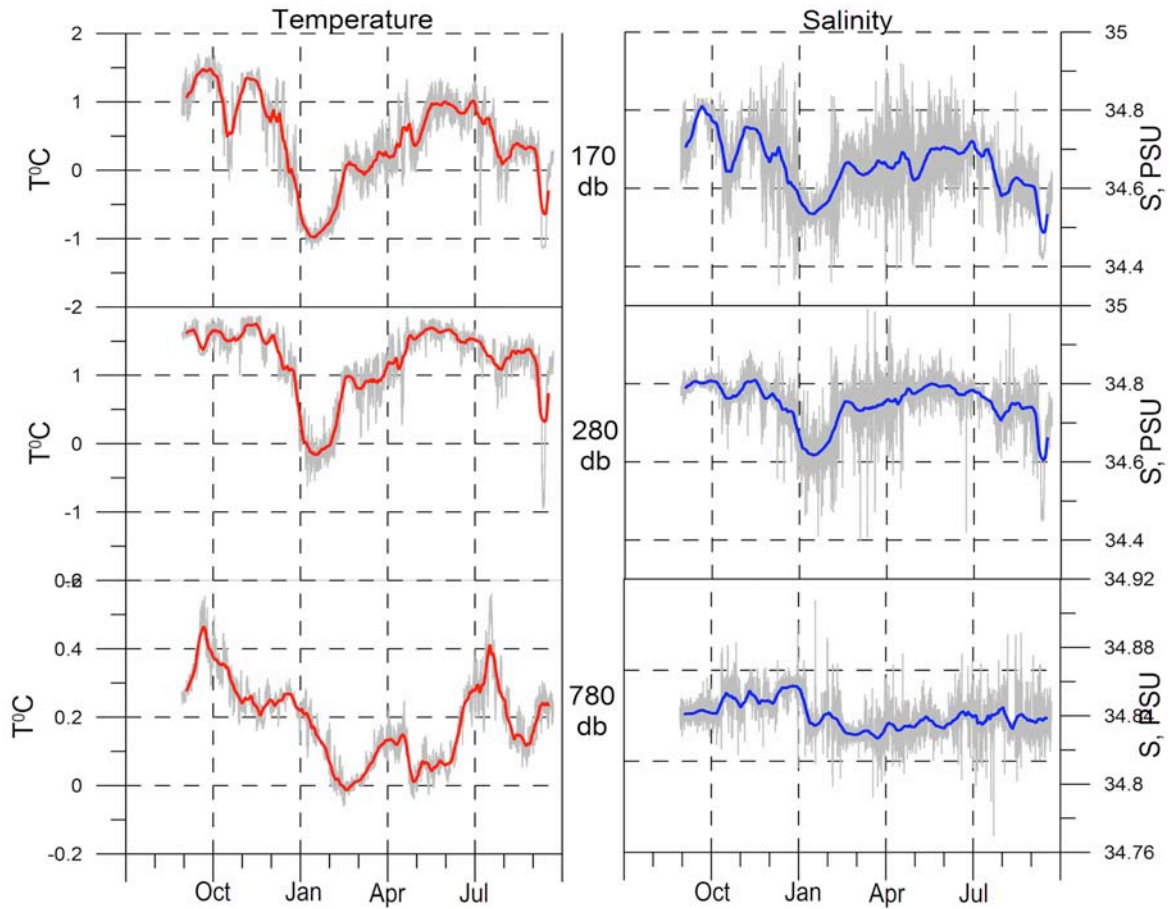


**Figure I.6.3.20.** Temperature (°C), and salinity (psu) derived from 15-min records from the three SBE-37s. One-month running averages are shown by red and blue lines.

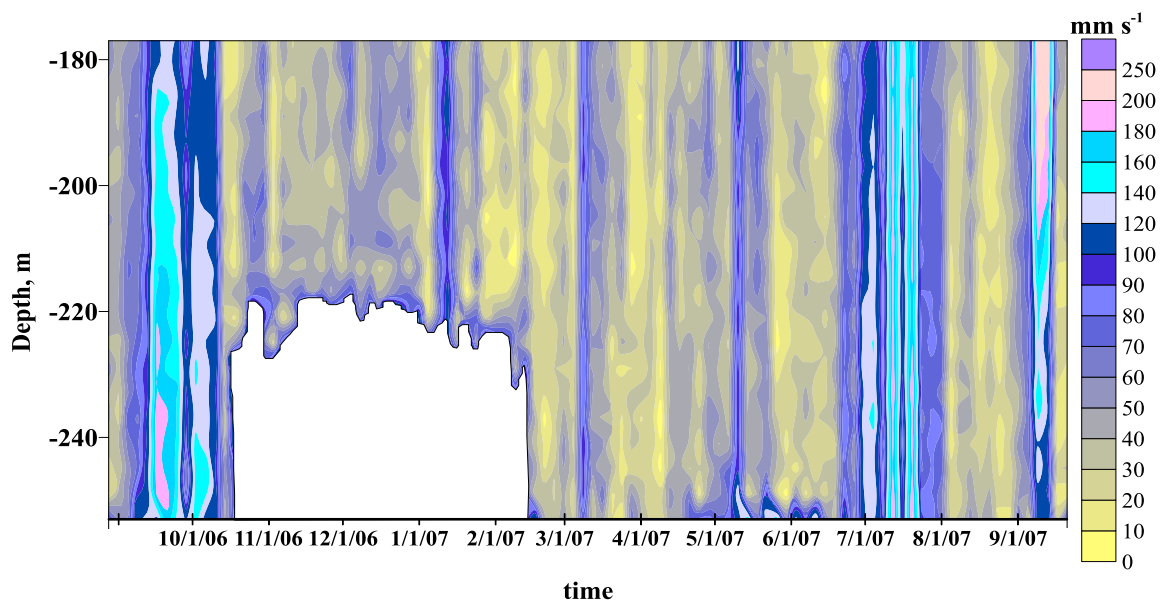


**Figure I.6.3.21a.** Current velocity measured by downward-looking ADCP at 180 m.

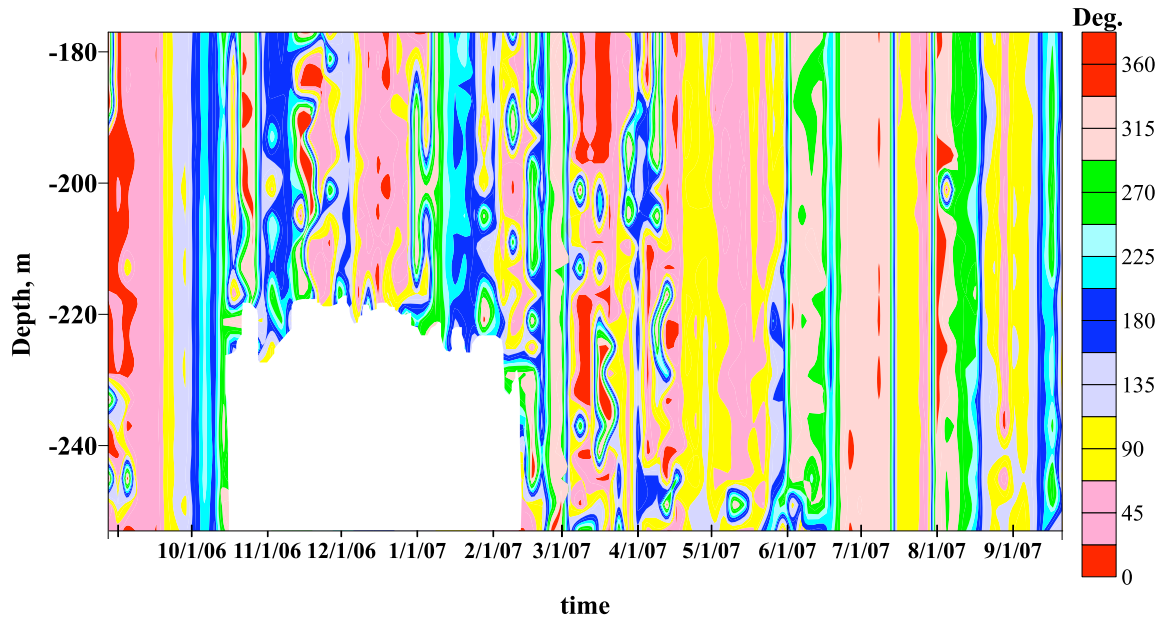


**Figure I.6.3.21b.** Current direction measured by downward-looking ADCP at 180 m.

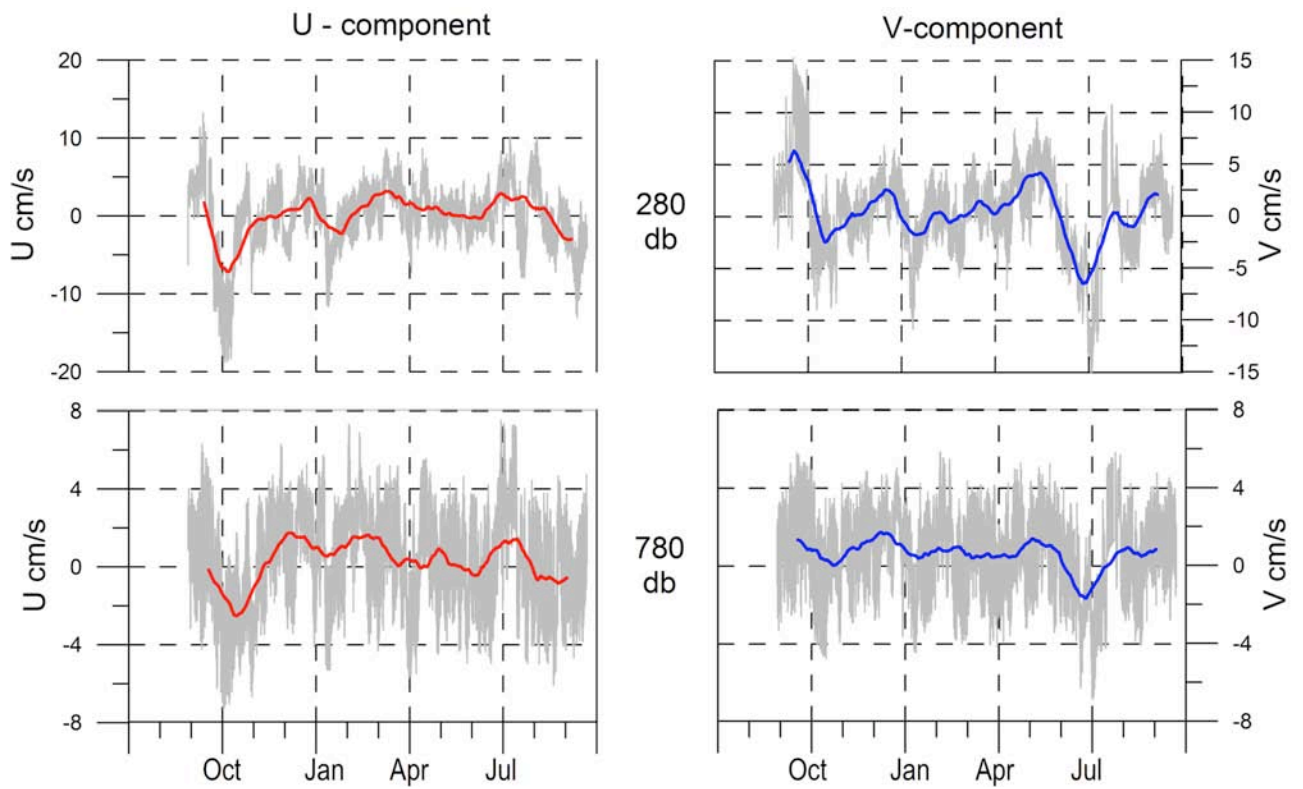


**Figure I.6.3.22.** Zonal (U) and meridional (V) current velocity components (cm/s) derived from 1-hourly records from two RCM11s. One-month running averages are shown by red and blue lines.

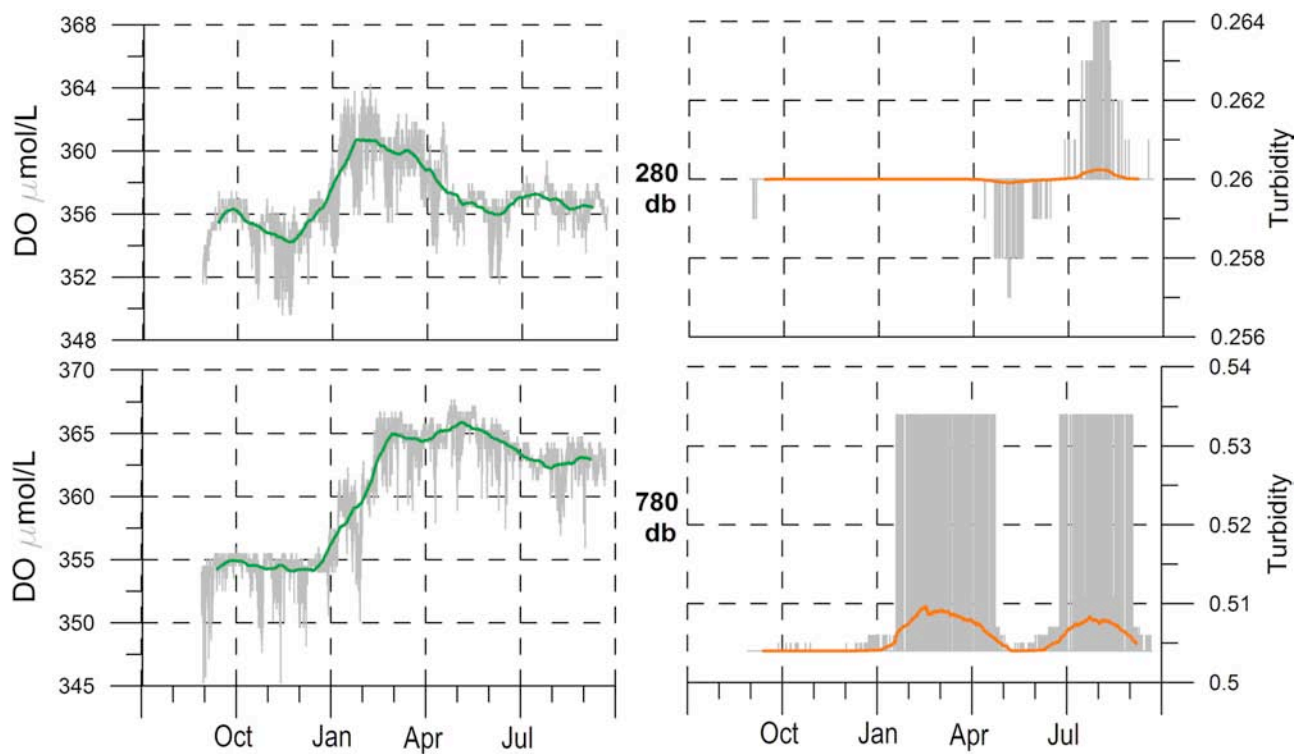


**Figure I.6.3.23.** Dissolved oxygen (DO) concentration ( $\mu\text{mol/L}$ ) and turbidity derived from 1-hourly records at two RCM1s. One-month running averages are shown by green and orange lines.

Continuous 3-year-long temperature records from around the AW core are presented in **Figure I.6.3.24**. This record shows strong seasonality in the water temperature with generally lower temperature in winter and higher temperature in summer. This seasonality could not be attributed to the local seasonal variability related to cooling/heating and ice formation/melting because the depth of winter convection in this region is limited to the upper  $\sim 30\text{-}40$  m layer [e.g. *Nikiforov and Shpaikher*, 1980]. It is also not related to riverine water impact because, in contrast to what was observed, river water input modifies ocean water properties towards warmer and fresher conditions during summer and saltier and colder conditions during winter.

At this stage, the obtained records allow us to state that (i) a strong seasonality reaches the AW core, and (ii) this seasonality has a remote origin. We can speculate about three possible sources of the observed seasonality. The first source may be the Barents Sea branch of AW (BSBW). At the mouth of St. Anna Trough this water is characterized by negative temperature, and salinity  $\approx 34.82$  psu [*Schauer et al.*, 2002]. After entering the Nansen Basin, BSBW propagates close to the slope, pushing the Fram Strait AW (FSAW) offslope. In the Laptev Sea the BSBW normally occupies the depth range of 400-800 m (see section I.6.3.5.2) and stays close to the slope. Fresh events, possibly linked to this water, were recorded at the M1e mooring (see **Figure I.6.3.16**) and at the cross-slope section along  $126^\circ\text{E}$  (see **Figure I.6.3.6a**). However, the observed periodicity of cooling/warming events, illustrated in **Figure I.6.3.24**, does not fit well with the expected sporadic occurrence of BSBW intrusions into the FSAW layer. It is unlikely that such intrusions occur on a regular seasonal basis, particularly taking into consideration the complicated interaction between BSBW and FSAW inflow in the northern Kara Sea [see *Dmitrenko et al.*, 2008, JGR in press, and *Dmitrenko et al.*, 2008, submitted to DSR]. A second possible source of this seasonality takes into consideration a recently-discovered strong seasonal signal in FSAW northeast of Spitsbergen [*Ivanov et al.*, submitted to DSR]. This signal is thought to propagate far along the Siberian continental margin,

changing its amplitude and phase due to heat exchange with the ambient water and varying flow speed [Ivanov *et al.*, 2008]. This explanation is weak, however; the minimum FSAW temperature recorded near Spitsbergen was well above zero ( $\approx 2^\circ\text{C}$ ). Hence, FSAW mixing with the surrounding water, or with BSBW, which is slightly below zero, is unlikely to result in the large temperature decreases observed at M3. In addition, the pattern of cooling/warming events depicted in **Figure I.6.3.24** is not symmetrical; rather, abrupt cooling events occur, separated by longer warming periods. Therefore, we suggest a third source of seasonality, which takes into account dense water formation inside flaw polynyas over the northwestern Laptev Sea shelf  $\sim 1000$  km upstream of M3 [Rudels *et al.*, 2000; Ivanov and Golovin, 2007]. A shelf polynya forms in this region every winter [Zakharov, 1996; Bareiss and Gorgen, 2005]. Dense (cold and fresh, relative to FSAW) water from this shelf is able to reach the AW warm core at 250-300 m depth [Ivanov and Golovin, 2007]. Thus, abrupt cooling and freshening in the AW core may be attributed to the downstream advection of shelf-origin dense water intrusions. Whether one of these scenarios is correct, or whether we witness the combined influence of different mechanisms is an open question, requiring further analysis and modeling.

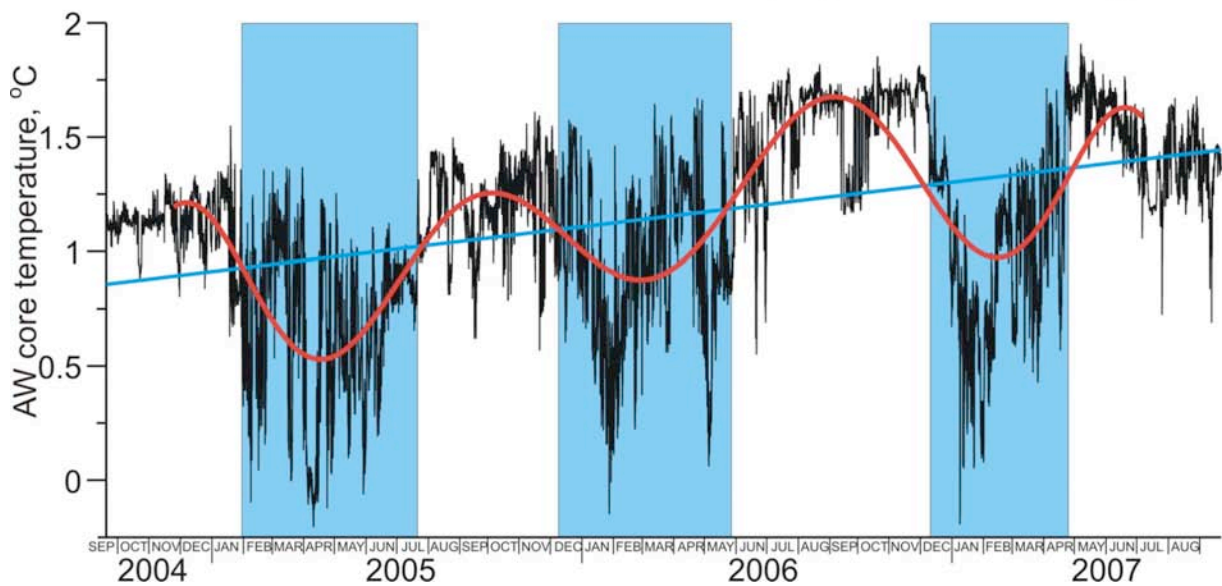


**Figure I.6.3.24.** Water temperature close to the AW warm core ( $\sim 250$  m) derived from hourly measurements for 3 years. Blue rectangles highlight seasonal minima. Blue line shows linear trend. Red line is a polynomial fit.

## I.6.4. TURBULENCE MEASUREMENTS (P.J. Wiles, P.E. Powel, UW)

### I.6.4.1 Equipment setup

A VMP500 was operated by Ben Powell and Philip Wiles from the aft deck of the RV *Viktor Buynitsky*. The probe was used in a tethered free-fall mode, i.e. although the probe was connected to the ship via a cable, when the probe was freefalling enough cable was spooled into the water to prevent the probe from being affected by ship motion. Before probe deployment, the vessel was stopped and the propeller was disengaged (so that it was not turning). The VMP500 was then

dropped from the starboard side, The vessel was oriented such that the wind was blowing from the starboard side. The resulting drift of the ship towards the port side (at ~1 knot) was used to prevent the turbulence probe (and cable) from going under the vessel into the area around the stationary propeller.

The profiler had 2 shear probes, 2 fast-response thermistors, and 1 fast-response conductivity meter mounted on the nose cone. Originally a short (~7cm) nose cone was used; however, this was replaced with a longer 15cm nose cone when the probe was operated in shallow water and occasionally hit the seabed. The shear probe was changed before profile 016 because it was producing erroneous readings. Seabird temperature (SBE3) and salinity (SBE4) sensors were attached to the body at the lower end of the profiler. Turbulence profiles were measured on as many stations as possible. Around the mooring sites, an attempt was made to intensify profiles to produce a pseudo-12.4-hour tidal cycle of turbulence measurements.

#### **I.6.4.2. Data Results**

The profiler successfully measured 115 profiles – to our knowledge, the first successfully-measured microstructure shear profiles in the Laptev and Eastern Siberian seas. The temperature and salinity structure measured by the seabird sensors showed discrete steps in the deeper shelf seas. The absence of significant turbulence indicates that these steps are a result of double diffusion. Although turbulent kinetic energy dissipation rates ( $\varepsilon$ ) derived from the shear probes in the deep water column show very low energy levels (at or below the noise floor of the instrument), significant levels of turbulence were observed in the shallower shelf seas, probably caused by the tides. Elevated turbulence levels were also observed in a surface thin (~15 m), warm, fresh layer and around the shelf break. Interpretations of turbulence in low-energy regions must be made with caution, as the fundamental assumptions used to convert the shear probe signal to  $\varepsilon$  become invalid. This caveat also applies to the calculation of vertical diffusivity estimates, as they are derived from the  $\varepsilon$  values. The data are split into 4 groups (along sections A,B,C, and E), as shown in **Figure I.6.3.3a**. Each section will be described going from west to east.

#### **SECTION A**

##### *Top 100m of section A profiles.*

The western section A shows a shallow (~15m), relatively warm (+2°C) and fresh (28 psu) tongue of fresh water originating from the coast (**Figure I.6.4.1**) up to almost 77° latitude. There are enhanced levels of turbulence dissipation on the shelf near the sea bed ( $5 \times 10^{-5} \text{ W m}^{-3}$ ), probably generated by the tide. There is also increased turbulence at the shelf break probably generated by the internal tide, and near the surface in the deeper water (around  $2 \times 10^{-4} \text{ W m}^{-3}$ ). The Cox-Osborn relation was used to estimate values of the vertical diffusion parameter  $K_z$  [Osborn, 1980]. The indicated enhanced diffusion occurred near the bed over the shelf (**Figure I.6.4.2**) and in the thin surface tongue of water.

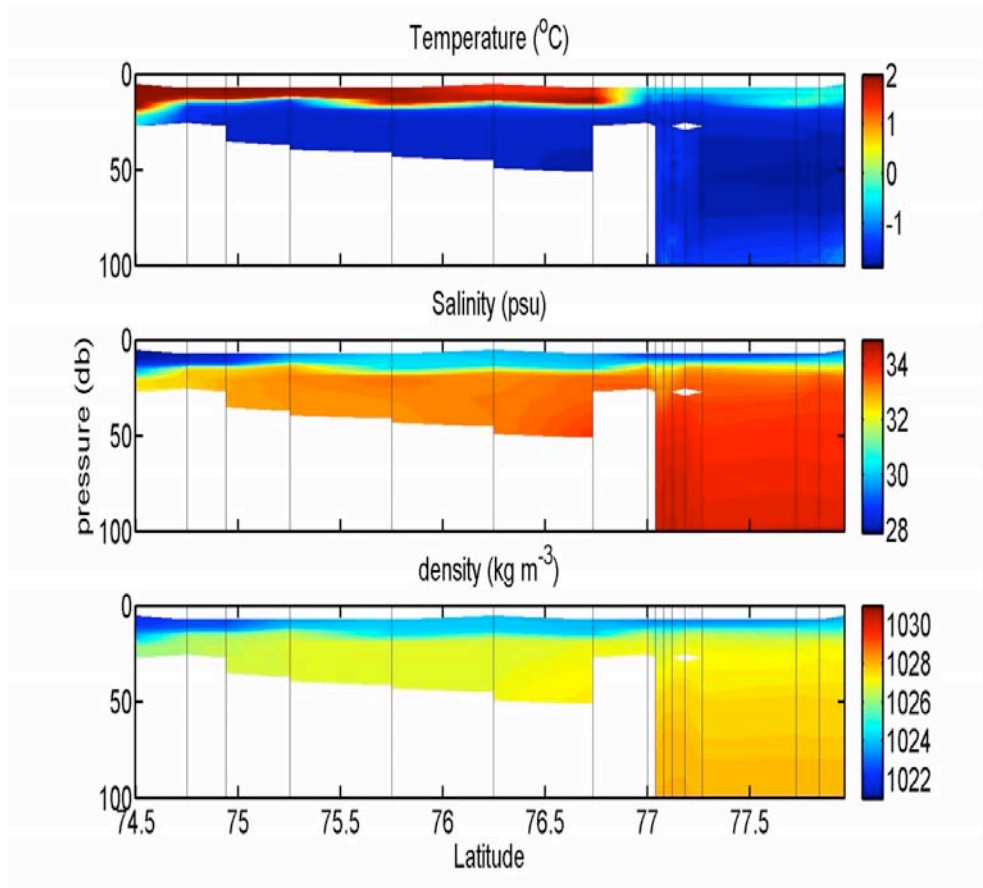


**Figure I.6.4.1.** Thermohaline properties from the shallow part of section A. The three panels indicate temperature, salinity, and density. The station numbers are shown in **Figure I.6.4.3**.

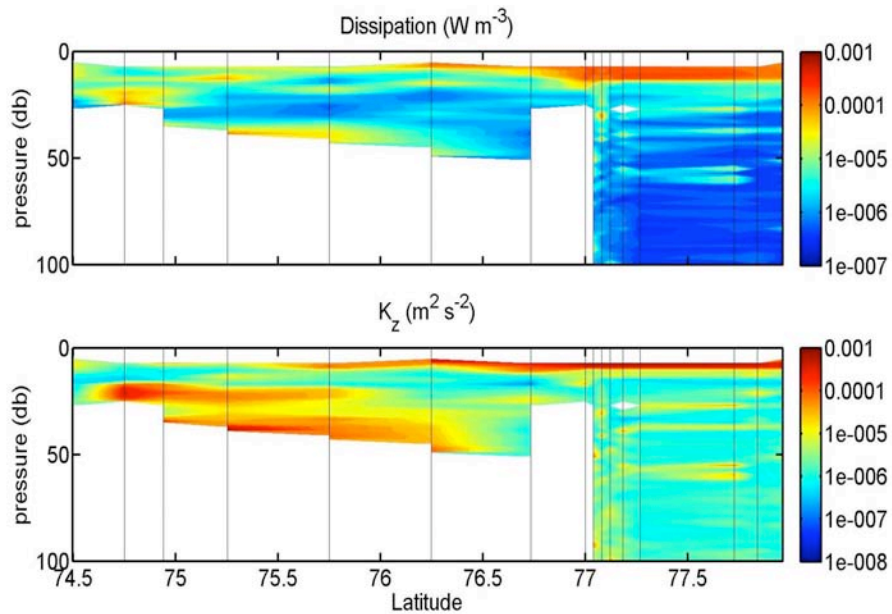


**Figure I.6.4.2** Turbulent kinetic energy dissipation rates ( $\varepsilon$ ) and calculated eddy diffusivities ( $K_z$ ) focused on the shallow part of the westernmost section A.

*Full-depth section A profiles*

Beneath the thin tongue of surface water mentioned above, the temperature remains cold ( $-2^{\circ}\text{C}$ ) and at a salinity  $<34\text{psu}$  down to a depth of  $\sim 120\text{m}$ . Below this, a signature of warm ( $+2^{\circ}\text{C}$ ) and saltier ( $>34\text{psu}$ ) AW is seen, with a temperature maximum at  $\approx 250\text{m}$  depth (**Figure I.6.4.3**). The slope of the isopycnals near the shelf break indicates that a geostrophically-adjusted shelf jet is located there. Turbulent kinetic energy dissipation rates of  $\varepsilon = 3 \times 10^{-7} \text{ W m}^{-3}$  were consistently seen in the deeper water off the shelf; this is the noise floor of the instrument. Closer to the shelf,  $\varepsilon$  increased to  $\sim 2 \times 10^{-7} \text{ W m}^{-3}$  (**Figure I.6.4.4**). Vertical diffusivities measured in deeper water were also at the noise floor of the instrument; however, diffusivity increased close to the shelf break.

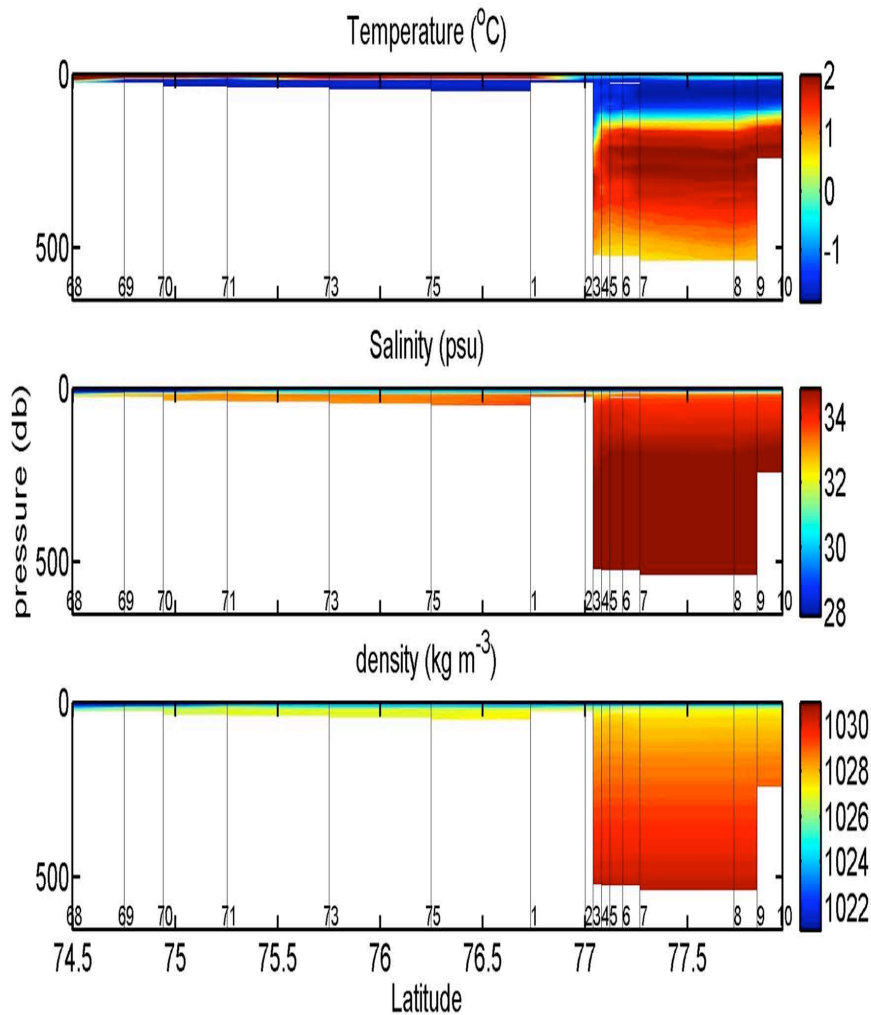


**Figure I.6.4.3.** As in **Figure I.6.4.1**, but showing the full depth of the profiles.

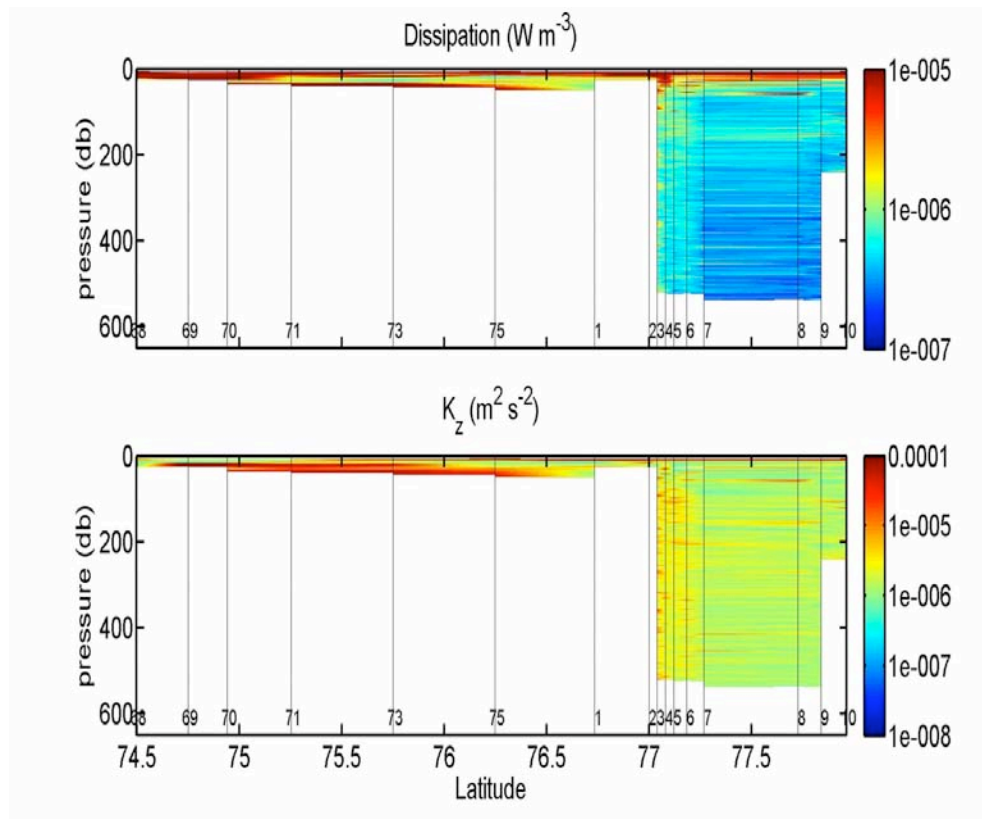


**Figure I.6.4.4.** As in **Figure I.6.4.2**, but showing the full depth of the profiles.

## **SECTION E**

### *Top 100m of section E profiles:*

The southern section E was predominantly conducted on the shelf. A strong influence of terrestrial water was observed near the coast, where water was measured to be nearly 3 °C and 27 psu. The signal of warm, fresh water continued out past 77° latitude (**Figure I.6.4.5**). Levels of  $\varepsilon$  on the shelf ranged from  $1 \times 10^{-6} \text{ W m}^{-3}$  in mid-water to  $3 \times 10^{-5} \text{ W m}^{-3}$  near the seabed. Higher levels of  $\varepsilon$  were observed near the surface above the shelf break (**Figure I.6.4.6**). Values of  $K_z$  were greater than  $1 \times 10^{-3} \text{ m}^2 \text{ s}^{-2}$  near the bed, but lower near the surface.

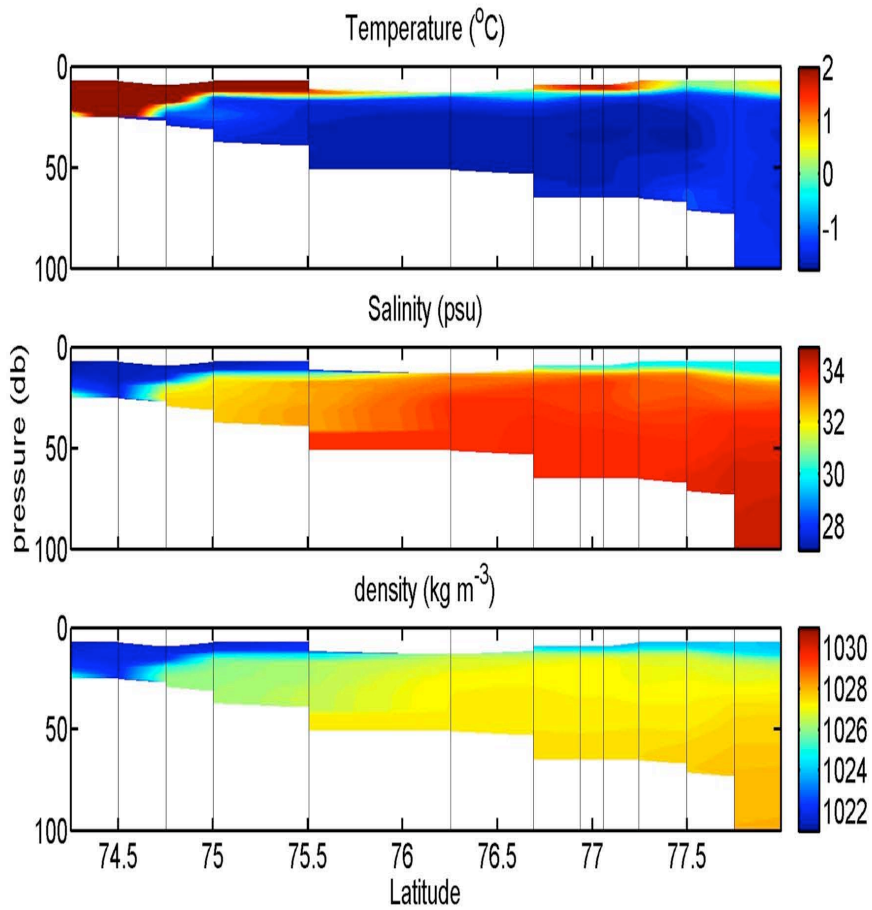


**Figure I.6.4.5.** Thermohaline properties of section E, focusing on the top 100 m. The station numbers are shown in **Figure I.6.4.7**.

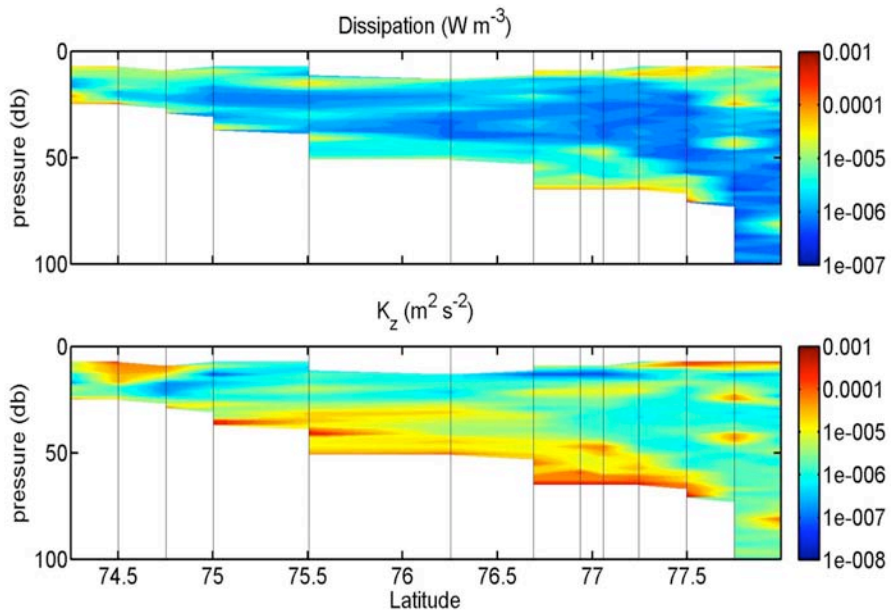


**Figure I.6.4.6** Turbulence measurements of section E, focusing on the top 100 m.

*Full section E profiles:*

The full profiles of temperature and salinity in southern section E (**Figure I.6.4.7**) again indicate that a geostrophically-adjusted flow is evident at the shelf edge. The levels of turbulence (**Figure I.6.4.8**) at the shelf edge are also larger ( $\sim 1 \times 10^{-6} \text{ W m}^{-3}$ ) than in the interior of the arctic (see above).

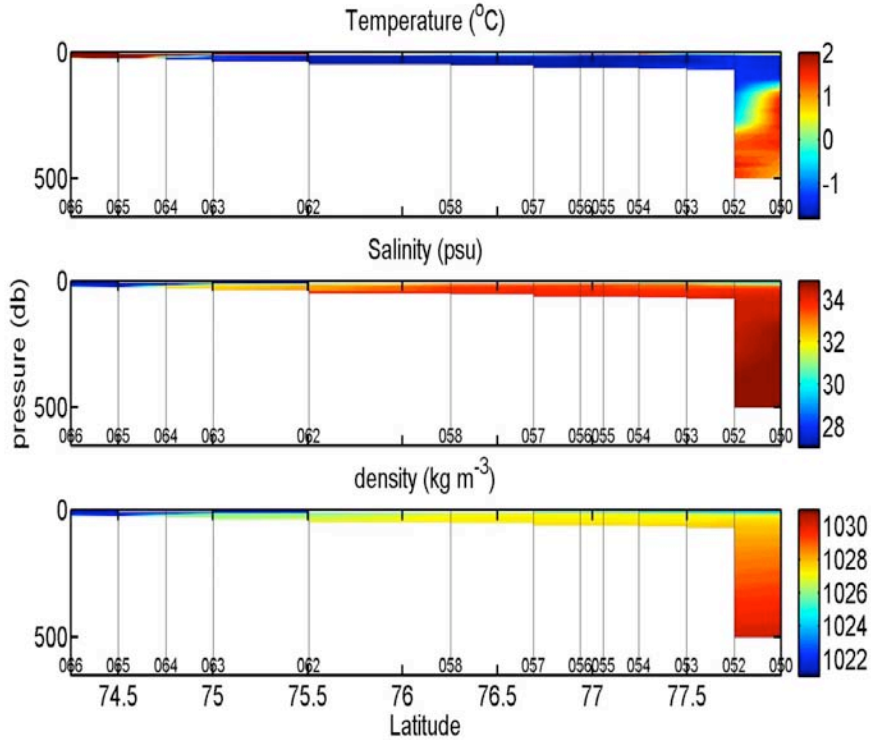


**Figure I.6.4.7.** Thermohaline properties of the southern section E. As in **Figure I.6.4.5.**, but showing the full profile depth.

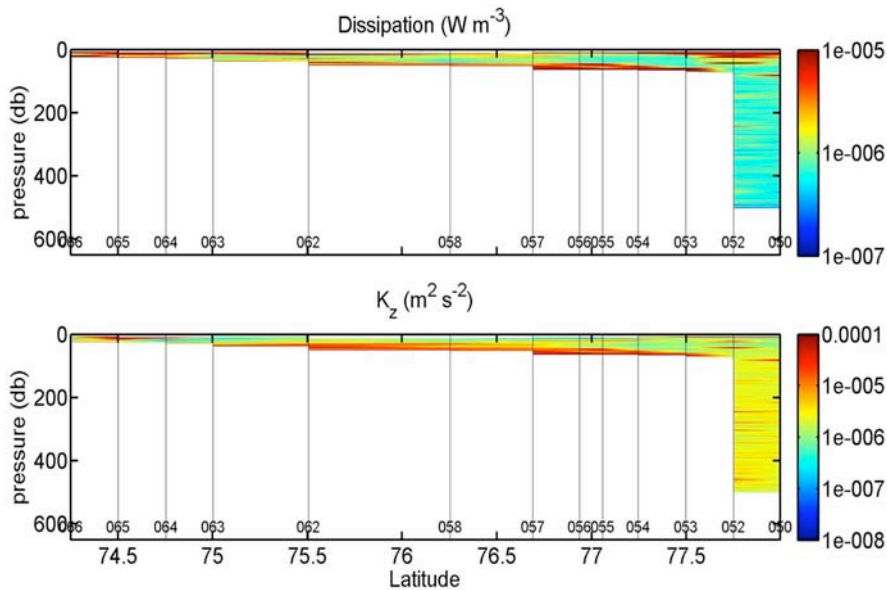


**Figure I.6.4.8.** Turbulence measurements of section E. As in **Figure I.6.4.6**, but showing the full profile depth.

## SECTION B

### Top 100m of northern section B profiles:

The northern section B was located close to the Lomonosov Ridge, and was mainly conducted in deeper water. Due to rough weather around station 19, surface estimates of turbulence were unreliable. A surface layer of warm and fresh water was evident, ranging from 2.4 °C and 27 psu at the southern end of the transect to 3 °C and 29 psu at the northern end of the transect (**Figure I.6.4.9**). Surface layer estimates of  $\varepsilon$  were mostly around the instrument's noise level, except for an occasional patch (**Figure I.6.4.10**). Therefore, estimates of  $K_z$  were also unreliable.

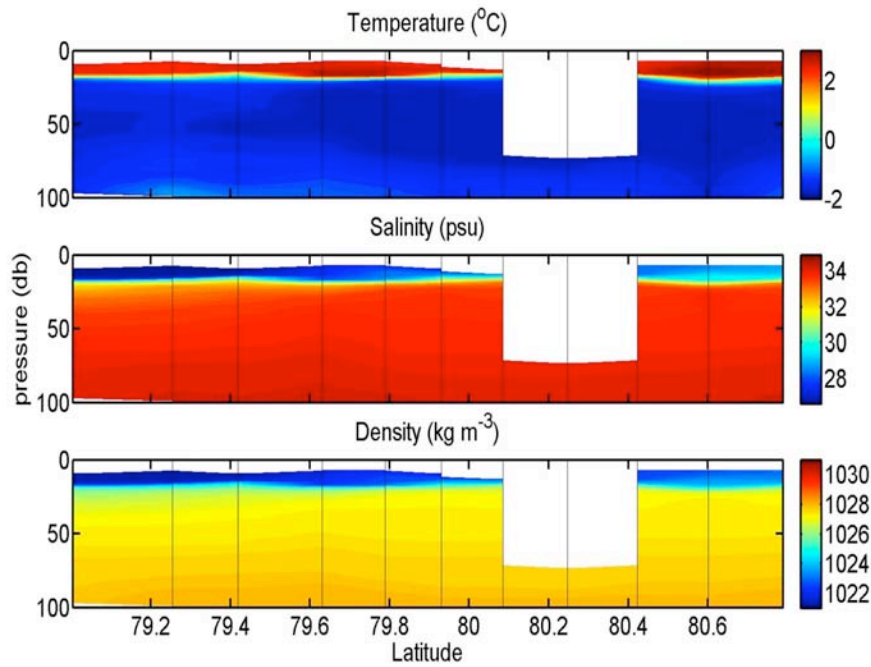


**Figure I.6.4.9.** Thermohaline properties of the upper 100m of section B.

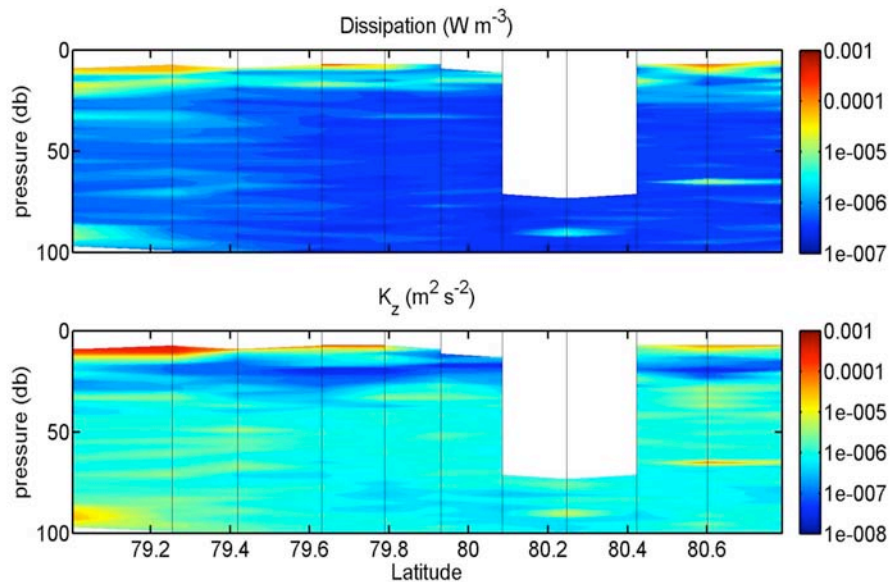


**Figure I.6.4.10.** Turbulence properties of the upper 100m of section B.

*Full section B profiles:*

The deeper profiles from the northern section B show that the AW has cooled to  $1.5^{\circ}\text{C}$  (**Figure I.6.4.11**). Turbulence levels away from the shelf (**Figure I.6.4.12**) are mostly around the noise level ( $2 \times 10^{-7}$ ); however, closer to the shelf elevated levels of turbulence ( $>5 \times 10^{-6}$ ) were observed. Relatively high levels of turbulence were observed at the seabed and up onto the shelf ( $1 \times 10^{-3}$ ), again probably driven by the tide.

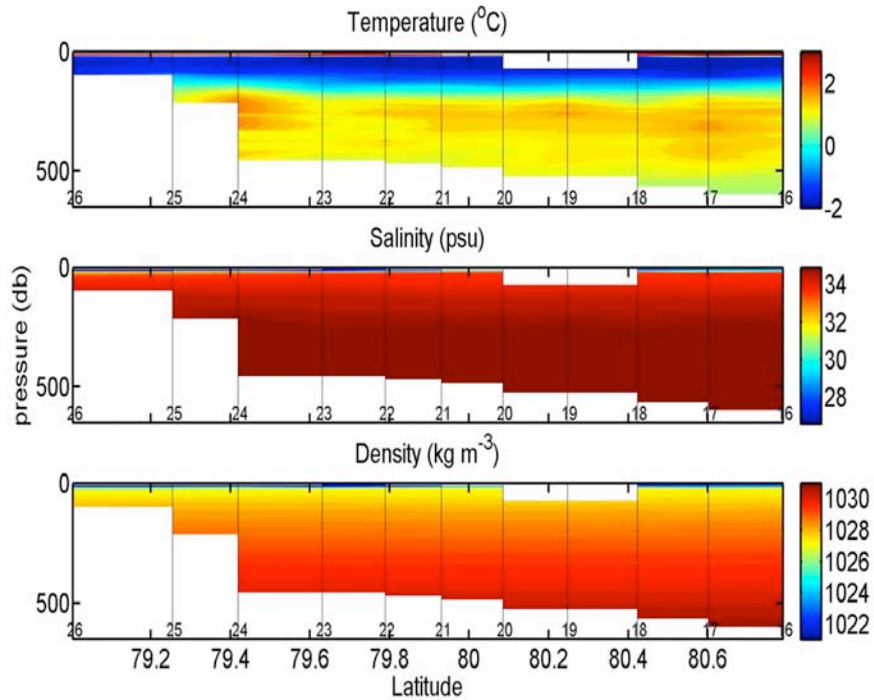


**Figure I.6.4.11** Thermohaline properties, section B. As in **Figure I.6.4.9.**, but full profile depth is shown.

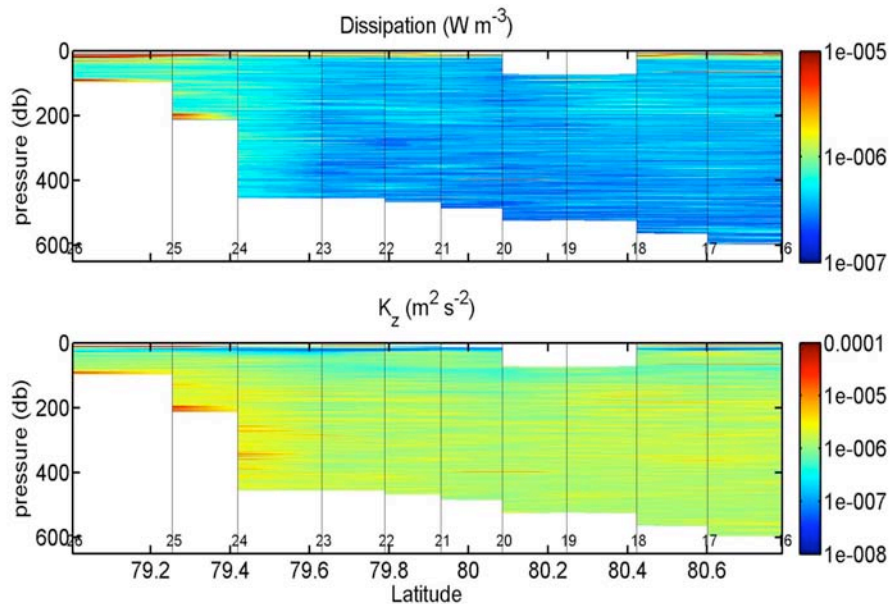


**Figure I.6.4.12.** Turbulence in section B. As in **Figure I.6.4.10**, but showing the full profile depth.

**SECTION C**

*Top 100m of section C profiles:*

The warm and fresh surface layer was still found in the eastern section C. The near-surface water temperature was 0.8°C and the surface salinity dropped to 25 psu (**Figure I.6.4.13**). Laterally, the water properties were almost homogeneous. Enhanced levels of  $\varepsilon$  were observed in the warm, fresh surface layer ( $3 \times 10^{-6}$ ), but were within the noise level of the instrument at lower depths (**Figure I.6.4.14**).

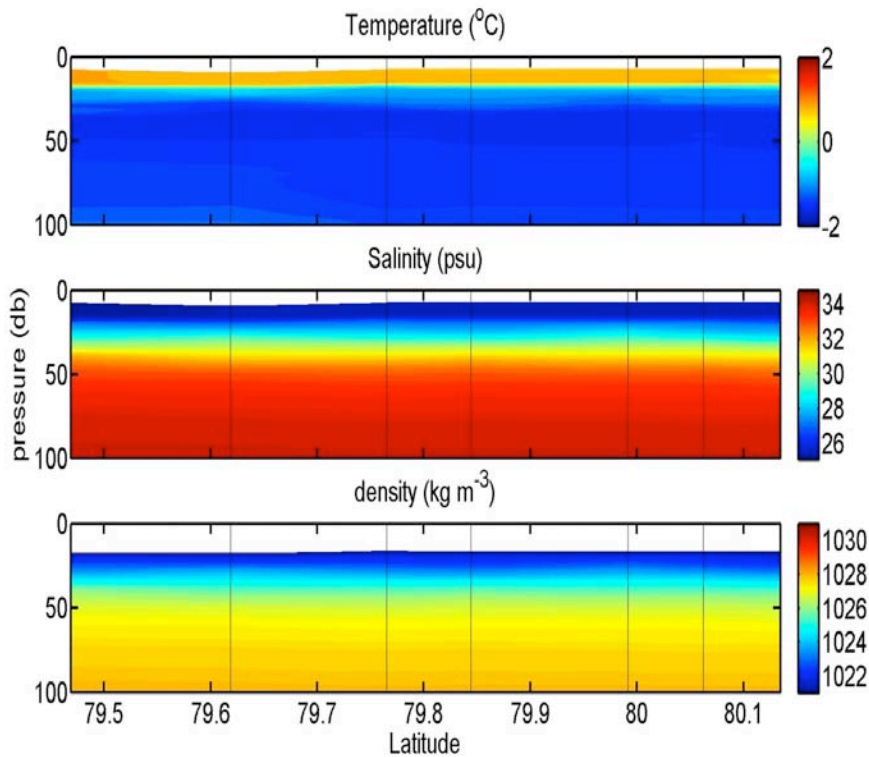


**Figure I.6.4.13.** Thermohaline properties of section C, measured in the top 100m of the water column. Note the changed salinity scale, from 25 to 35.

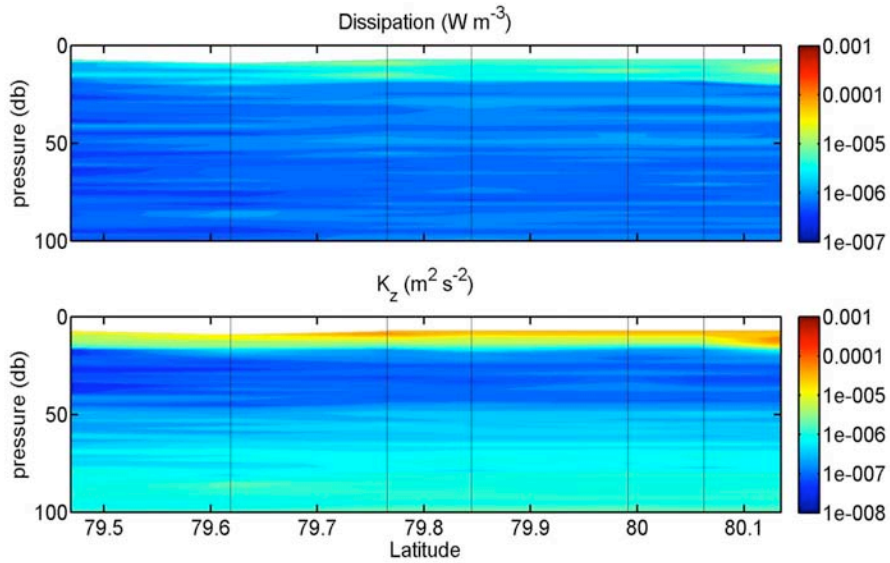


**Figure I.6.4.14.** Turbulence measurements in section C, focused on the top 100m of the water column.

*Full eastern section C profiles:*

The AW beneath the surface cold layer was at a temperature of  $\sim 1.1$  °C. Discrete steps in temperature were observed from stations 35 to 40 (e.g. see **Figure I.6.4.17**). The lack of significant turbulence indicates that these steps were caused by double diffusion.

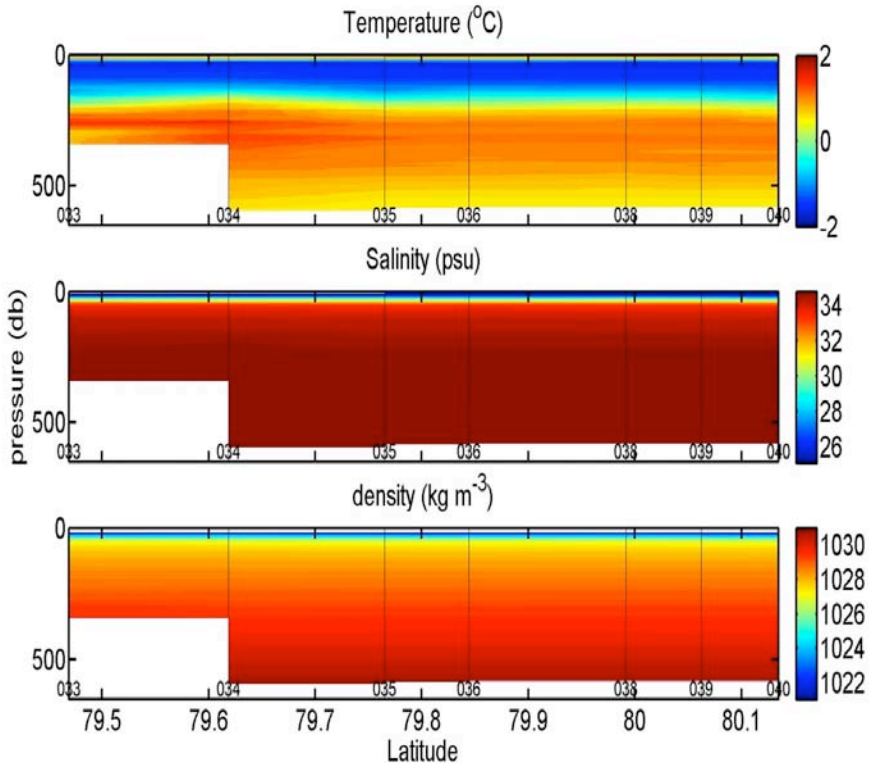


**Figure I.6.4.15.** Temperature, salinity, and density at section C. As in **Figure I.6.4.13** except the full profile depth is shown. Note the changed salinity scale, from 25 to 35.

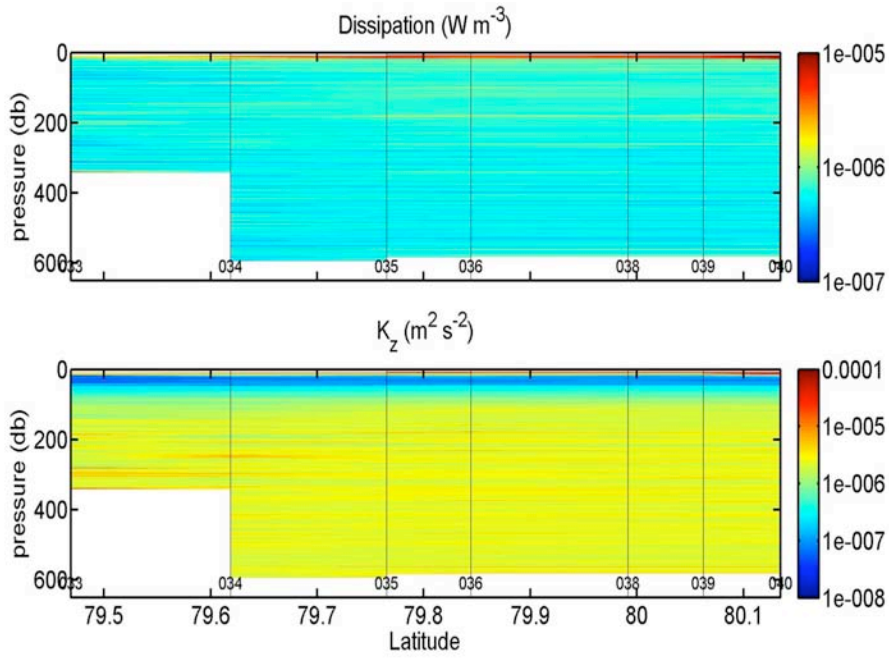


**Figure I.6.4.16.** Turbulence properties of section C. As in **Figure I.6.4.14**, except the full profile depth is shown.

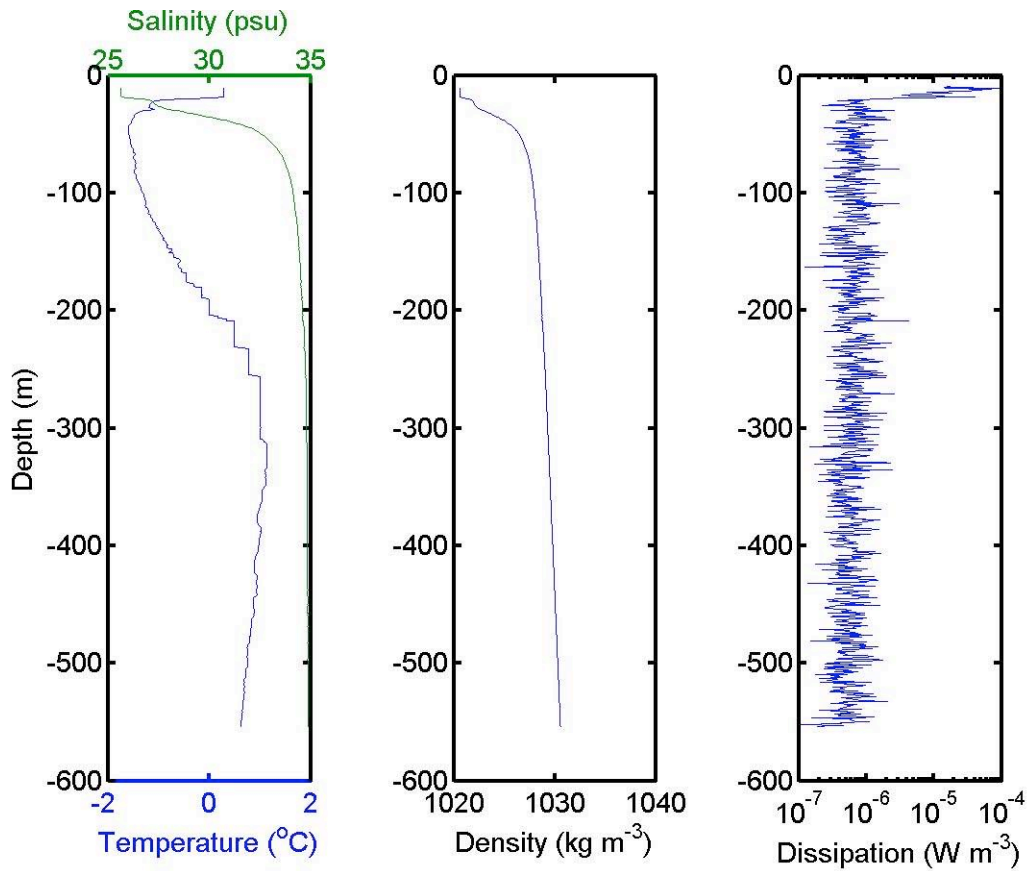


**Figure I.6.4.17.** Profile of temperature, salinity, density, and  $\epsilon$  at station 40, showing evidence of double diffusion from 180 to 300 m depth.

### **I.6.4.3 Summary**

Using a VMP500, 115 profiles were taken in the Laptev and Eastern Siberian seas. These are the first measurements of their type, and they shed light on processes in the regions. It appears that turbulence driven by tides and/or wind is not entirely responsible for transfer of heat from the deep AW to the atmosphere, except perhaps at the shelf edge where the internal tide seems to cause turbulence. This enhanced turbulence at the shelf edge may also play an important role in determining how hyper-saline water formed by brine rejection when sea-ice forms on the shelf interacts with the arctic as a whole.

The thin (~15m) surface layer was evident in all the profiles, and valuable surface data were produced. However the properties of this surface layer changed over space. Near the coast, the surface layer of southern section E was warm (+3°C) and fresh (~27psu). However, in the eastern section C, water temperature was below +1°C and much fresher (~25 psu). The temperature of the deeper AW also cooled as the profiles were measured from west to east.

By using the turbulence estimates and gradients of temperature and salinity, it is possible to decide whether we captured the main mixing events as the deep AW moves from west to east. There is a strong likelihood that in low-turbulence environments, double diffusion is the mechanism responsible for a significant amount of heat and salt flux.

### **I.6.5. HYDROCHEMICAL OBSERVATIONS** (*S. Torres-Valdés, NOCS and E. Dobrotina, AARI*)

#### **I.6.5.1 Background: AARI**

The Russian arctic seas play an important role in climate. Therefore, sustained monitoring of water masses of these seas, in particular the Laptev Sea, is important. A basic component of such monitoring is documenting hydrochemical distributions, which, together with temperature and salinity data, allow the position and sources of water masses to be specified. Hydrochemical data are also important for understanding marine ecosystem functioning. For instance, DO provides a glimpse into the existence of living organisms and reflects the intensity of oxidizing processes. Dissolved inorganic nutrients (phosphates, nitrates, nitrites, ammonium, and silicates) are the mineral bases of primary production. Thus, analysis of the basic hydrochemical distributions - DO and nutrients - is traditionally the main task of AARI's hydrochemists. The hydrochemical conditions of the Laptev Sea are formed under influence of the AW, river runoff, and fresh water from sea-ice melting. The ideal tracer for identifying the sources of fresh water is the isotope of oxygen,  $\delta^{18}\text{O}$ . Therefore we also collected samples for determination of  $\delta^{18}\text{O}$ , which will be subsequently analysed in IFM-GEOMAR, Kiel, Germany.

#### **I.6.5.2 Sampling and analysis: AARI**

**Nutrients**; 50 mL plastic bottles were used for sampling. Samples were frozen at -20°C immediately after sampling for storage and kept frozen during subsequent transport back to St. Petersburg for analysis at the OSL analytical facilities.

**$\delta^{18}\text{O}$** ; Water samples were collected in 100 mL glass bottles after rinsing each bottle three times with sampled water. A small air gap was left and the bottles were then closed with screw caps. All samples were stored and transported to the Kiel, Germany for later analysis.

### **I.6.5.3 Background: NOCS**

Participation of the National Oceanography Centre, Southampton (NOCS) on the NABOS 2007 expedition to the Arctic Ocean is part of the NERC (UK)-funded Arctic Synoptic Basin-wide Oceanography (ASBO) Consortium Programme, led by Dr. Seymour Laxon of University College London (UCL) and Dr. Sheldon Bacon (NOCS). The ASBO programme includes the participation of UCL, NOCS, Bangor University, University of Reading, British Antarctic Survey (BAS) and the Scottish Association for Marine Science (SAMS).

#### *ASBO Rationale*

The Arctic Ocean has experienced abrupt changes in the last few decades; the extent of ice coverage during the 2007 summer minimum reached the lowest values on record <sup>1</sup>. Modelling studies suggest this trend will continue and it is predicted that the sea ice extent over the Arctic will decrease to extreme minimum values by the year 2040 [Holland *et al.*, 2006]. Furthermore, it has been suggested that the Arctic Ocean is in transition to a warmer state [Polyakov *et al.*, 2005]. Currently-occurring and predicted changes are likely to impact the physical structure of the Arctic Ocean (e.g., fresh water storage and transport, heat fluxes, and water exchange with the adjacent oceans) with further implications such as modification of the thermohaline circulation. ASBO therefore aims to understand these changes and their likely impact on the Arctic and North Atlantic oceans by quantifying *i*) the current fresh water (both solid and liquid) and salt content of the Arctic Ocean, *ii*) the heat and freshwater exchanges between the Arctic shelves and deep basins, *iii*) freshwater exchange between Arctic sea ice and the surface and halocline layers, and by determining *i*) the origin of changes in Arctic Ocean and North Atlantic salinity structure and *ii*) the extent to which the thermohaline structure of the Arctic Ocean and its evolution is properly represented in Global Climate Models. Dissolved inorganic nutrients, Barium,  $\delta^{18}\text{O}$ , salinity, and temperature are important variables that can be used as tracers in order to identify the different water masses present in the Arctic Ocean. Therefore, our sampling program is focused on collecting samples for the analysis/determination of these variables.

### **I.6.5.4. Sampling and analysis: NOCS**

Seawater was collected for the analysis/determinations of dissolved inorganic nutrients, DO, Barium,  $\delta^{18}\text{O}$ , and salinity. Samples were taken from 44 CTD casts out of the total 72 sampling stations (**Figure I.6.5.1**). Samples were either analysed on board or stored for later analysis. On average, seawater samples from 11-13 depths were taken for dissolved inorganic nutrients, Barium, and  $\delta^{18}\text{O}$ , from 6 depths for DO, and from 2-3 depths for salinity analyses. DO and salinity samples were taken for calibration purposes. Samples were stored for later processing

---

<sup>1</sup> e. g., see [http://nsidc.org/news/press/2007\\\_seaiceminimum/20070810\\\_index.html](http://nsidc.org/news/press/2007\_seaiceminimum/20070810\_index.html)

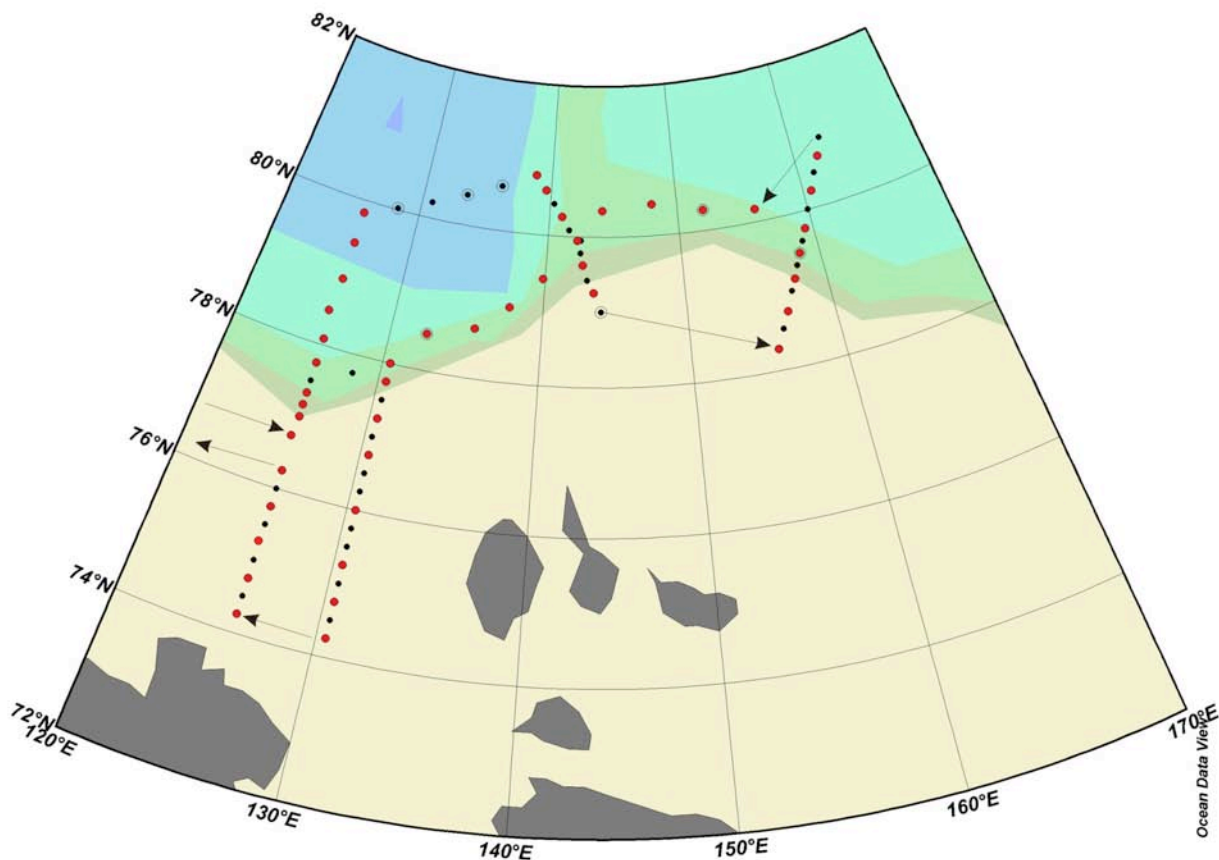


**Figure I.6.5.1.** Map showing the VB07 cruise track.. Gray and red dots show station positions. Red dots show hydrochemical sampling stations.

**Barium:** Water samples were collected into 15 mL Nalgene bottles after rinsing each bottle three times with sampled water. Bottles were filled up to the bottle neck in order to avoid leakage due to expansion during warming of cold water. All samples were stored and transported back to the UK for later analysis. All bottle lids were checked for tightness before transport. The BAS will send these samples to Dr. Kelly Falkner (Oregon State University, USA) for processing.

**$\delta^{18}\text{O}$ :** Water samples were collected in 100 mL glass bottles after rinsing each bottle three times with sampled water. A small air gap was left and the bottles were then closed using rubber lids and tin caps secured with a clamp. All samples were stored and transported back to the UK for later analysis. BAS will send these samples to Dr. M. Leng of the UK NERC Geoscience Isotope Laboratory (British Geological Survey, Keyworth) for processing.

**Salinity:** Samples were collected in 200 mL glass salinity bottles after rinsing each bottle three times with sampled water. Bottles were filled up to the neck and then sealed with plastic stoppers (inserts). The bottles were then wiped to remove seawater droplets in order to keep the bottle neck free of sea salt crystals and were finally closed with screw caps. Samples were stored and transported back to the UK for later determination of salinity at the NOCS.

#### **I.6.5.5 Samples analyzed on board**

**Dissolved inorganic nutrients:** Seawater samples were collected in 30 mL plastic pots for the analysis of nitrate and nitrite ( $\text{NO}_3^- + \text{NO}_2^-$ ), phosphate ( $\text{PO}_4^{3-}$ ), and silicate ( $\text{Si}(\text{OH})_4$ ). Pots were

rinsed three times with seawater before collection. Analyses were carried out within 30 minutes of sample collection using a segmented continuous-flow Skalar San<sup>plus</sup> autoanalyser set up for analysis and data logging with the Flow Access Software version 1.3.11. The analysis was calibrated using the set of standards shown in **Table 1.6.5.1**. Five mM stock standard solutions prepared in Milli-Q water were used to produce working standards. In turn, working standards were prepared in a saline solution (40 g NaCl/L of Milli-Q water) which was also used as a diluent for the analysis. Analysis runs consisted of a set of calibration standards, wash and drift cups, certified low-nutrient seawater (in order to test for contamination of the saline solution), and samples. Given the ship's lack of a Milli-Q system, 350 L of ultra pure (Milli-Q) water for general lab use was brought from the NOCS (UK) in 25 L acid-washed (15% HCl) carboys. Dry chemicals and wet reagents were either pre-weighed or previously prepared at NOCS.

**Table 1.6.5.1.** Set of calibration standards (*Std*) used for dissolved inorganic nutrient analysis. Concentration units are  $\mu\text{mol L}^{-1}$ .

	$\text{NO}_3^-$	$\text{PO}_4^{3-}$	$\text{Si(OH)}_4$
<i>Std 1</i>	20	2	20
<i>Std 2</i>	10	1	10
<i>Std 3</i>	5	0.5	5
<i>Std 4</i>	1	0.25	1
<i>Std 5</i>	0.5	0.1	0.5

The precision of the method was analyzed by examining variations in the complete set of standards measured throughout the cruise. Results of 84 total measurements of each of 5 different standards are summarized in **Table 1.6.5.2** and shown in **Figure 1.6.5.2**. Replicate measurements of randomly selected samples were carried out in order to test for reproducibility and showed that replicates varied by <3.5% from mean concentrations.

**Table 1.6.5.2.** Mean and variation of all standards measured, and precision of the analysis at each concentration ( $\mu\text{mol L}^{-1}$ ).

	$\text{NO}_3^-$	Prec.	$\text{PO}_4^{3-}$	Prec.	$\text{Si(OH)}_4$	Prec.
<i>Std 1</i>	$20.0 \pm 0.5$	2.3%	$2.01 \pm 0.01$	0.7%	$20.1 \pm 0.3$	1.7%
<i>Std 2</i>	$10.0 \pm 0.3$	2.5%	$1.00 \pm 0.01$	1.1%	$10.1 \pm 0.2$	2.3%
<i>Std 3</i>	$5.0 \pm 0.2$	3.4%	$0.50 \pm 0.01$	1.6%	$5.0 \pm 0.1$	2.7%
<i>Std 4</i>	$1.1 \pm 0.1$	8.1%	$0.25 \pm 0.01$	3.8%	$1.0 \pm 0.1$	9.0%
<i>Std 5</i>	$0.5 \pm 0.1$	13.8%	$0.10 \pm 0.01$	10.4%	$0.5 \pm 0.1$	21.5%

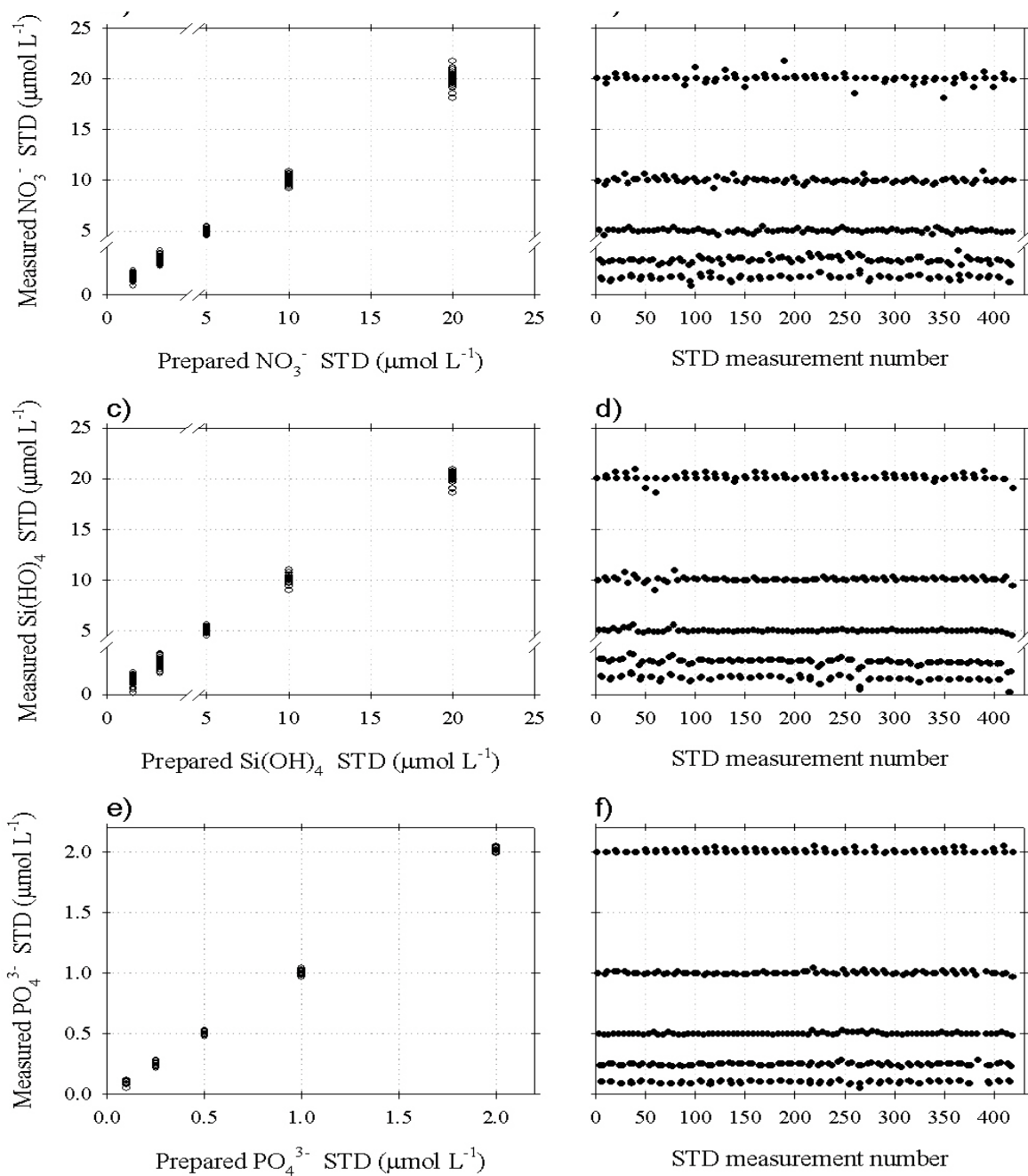


**Figure I.6.5.2.** Complete set of ‘measured’ standards plotted against the ‘prepared or intended’ concentration (a, b, and c). ‘Measured’ standards plotted against respective analysis number (d, e, and f). Y-axis on left side panels are the same as Y-axis on the right side panels. Note breaks on panels a to d.

In general the method worked very well, although noise in all three nutrient signals and baselines was observed at all times from the moment the ship entered open waters. This kind of noise has been previously observed to occur onboard larger ships when stormy weather is experienced. It is believed the rocking and vibrations of the ship interfere with the signal detection within the autoanalyser system. The noise, however, was always much lower than the signals of the three nutrients measured when detectable. The limits of detection of this method during VB07 were 0.03, 0.2, and 0.3  $\mu\text{mol L}^{-1}$  for  $\text{PO}_4^{3-}$ ,  $\text{NO}_3^-$ , and  $\text{Si}(\text{OH})_4$  respectively.

Results show typical nutrient profiles, with concentrations increasing at depth (**Figure I.6.5.3**). However, while phosphate and silicate exhibit a wide range of surface (<50 m) concentrations, nitrate appears to be depleted. Measured concentrations ranged as follows: nitrate, from nondetectable (nd) values to  $16.65 \mu\text{mol L}^{-1}$ ; silicate, nd to  $23.11 \mu\text{mol L}^{-1}$ ; and phosphate, 0.07 to  $1.35 \mu\text{mol L}^{-1}$ . Maximum surface phosphate and silicate concentrations were observed over the eastern continental slope of the Laptev Sea (**Figure I.6.5.5**). Maximum nitrate concentrations were observed in the bottom layers of the Laptev Sea (not shown). Dissolved nutrient concentrations measured during this cruise are similar to or within the range of concentrations reported in the literature for the Arctic Ocean; for instance, 0-20  $\mu\text{mol L}^{-1}$  nitrate, 0-0.8  $\mu\text{mol L}^{-1}$  phosphate, and 0-110  $\mu\text{mol L}^{-1}$  silicate [Dittmar and Kattner, 2003].

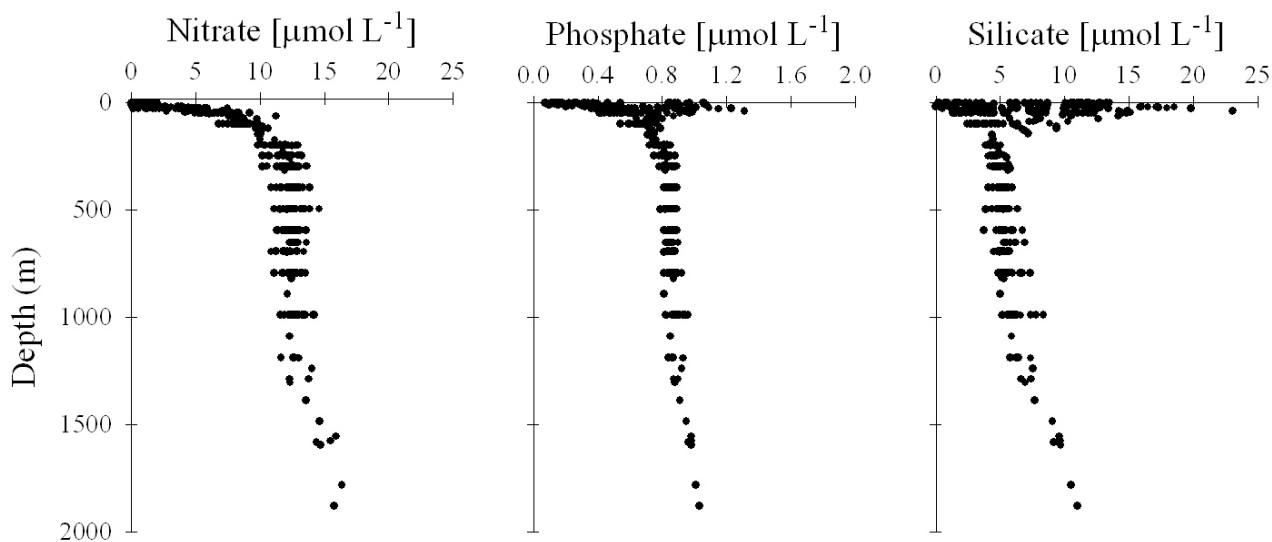


**Figure I.6.5.3** Nutrient profiles.

Dissolved oxygen: Seawater samples for DO determinations (**Figure I.6.5.4**) were collected directly into pre-calibrated glass bottles using a silicon tube. Before the sample was drawn, bottles were flushed with seawater for several seconds (about 2-3 times the volume of the bottle). Care was taken to avoid bubbles inside the sampling tube. The fixing reagents (i.e., manganese chloride and sodium hydroxide/sodium iodide solutions) were added just after the temperature of the sample was recorded. Samples were thoroughly mixed following the addition of reagents and were then kept in a dark plastic crate for 30-40 min to allow the precipitate to settle down to  $\geq 50\%$  the volume of the bottle. Once the precipitate had settled down, all samples were thoroughly mixed for a second time in order to maximize the efficiency of the reaction. Titrations were carried out within 2 h of sample collection. Sampling for DO was done before any other sample was taken.

DO determinations were made using a Winkler  $\Omega$ -Metrohm titration unit (794 DMS Titrino) with an amperometric system to determine the end point of the titration [Culbertson and Huang, 1987]. Chemical reagents were previously prepared at NOCS following the procedures described by Dickson [1994]. Recommendations given by Dickson [1994] and by Holley and Hydes [1994] were adopted. Thiosulphate calibrations were carried out every 5-6 days and overall consisted of the analysis of 5 blanks and 5 standards. Blanks were prepared by pipetting 1 mL of a 1.667 mM certified OSIL iodate standard into approximately 70 ml of Milli-Q water. The analytical standard was prepared by pipetting 10 ml of the 1.667 mM certified OSIL iodate standard into  $\sim 70$  ml of Milli-Q water. Averaged blank and standard titration volumes from every calibration were recorded

and used for computing oxygen concentrations. Calculation of oxygen concentrations were facilitated by the use of an Excel spreadsheet provided by Dr. Richard Sanders (NOCS). As with the analyses of nutrients, replicate measurements of randomly-selected samples were also carried out in order to test for reproducibility. Results showed that variability of replicate measurements was  $\leq 0.3 \mu\text{mol O}_2 \text{ L}^{-1}$ .

A wide range of DO concentrations was measured in surface and shallow waters, from 240 up to 395  $\mu\text{mol L}^{-1}$ . Maximum concentrations were found between 500 and 1500 m depth (**Figure I.6.5.4**). Highest surface concentrations were observed over the northern parts of the Laptev Sea and East Siberian Sea transects, while the lowest surface concentrations were observed towards the coast of the Laptev Sea (**Figure I.6.5.5**).

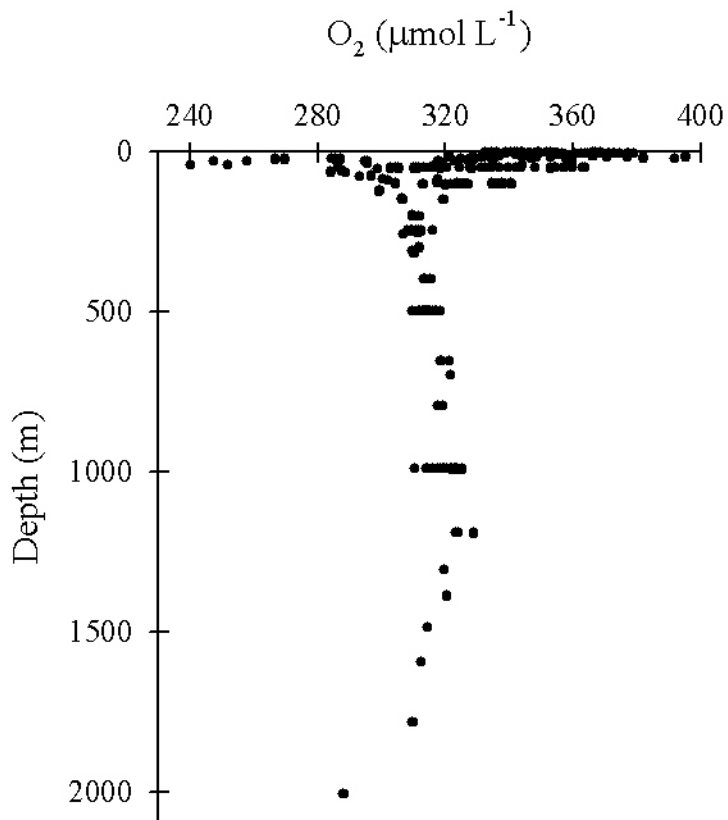


**Figure I.6.5.4.** Dissolved oxygen plotted against depth.

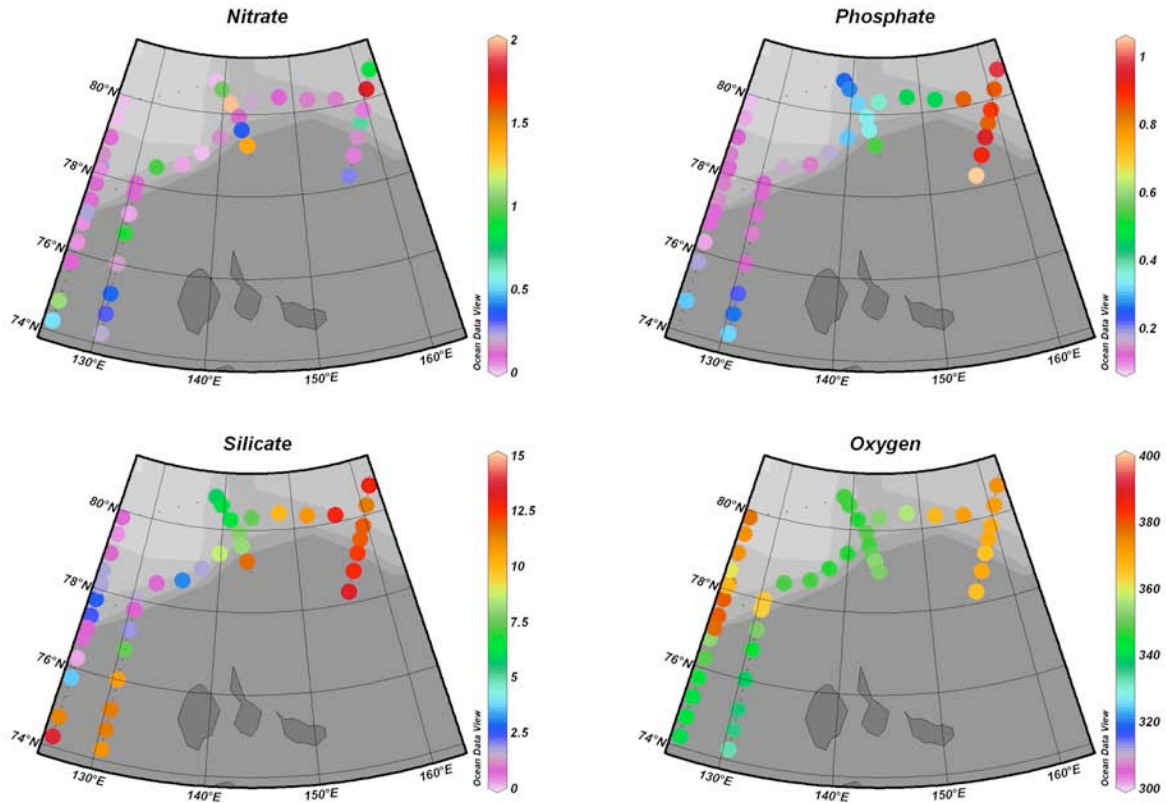


**Figure I.6.5.5.** Surface nutrients and dissolved oxygen concentrations along the *Viktor Buynitsky* cruise track (concentration units are  $\mu\text{mol L}^{-1}$ ).

## I.6.6. BIOLOGICAL OBSERVATIONS (*C. Bouchard, L. Fortier, M.-È. Garneau, C. Lalande, C. Lovejoy, J.-É. Tremblay; LU*)

### I.6.6.1. Arctic Cod (*Boreogadus saida*) ecology (*C. Bouchard, L. Fortier*)

#### I.6.6.1.1. Objectives

The Arctic cod (*Boreogadus saida*) is a key species in the Arctic and is intimately adapted to life under sea ice. Depending on the region, the species displays two distinct hatching patterns: 1) a short hatching season centered around the ice break-up where there is no river input, and 2) an early, long hatching season during which higher water temperatures due to freshwater input allow larvae to hatch and survive in winter [*Bouchard and Fortier, in press*]. In light of this dichotomy in reproduction strategy, the degree of connectivity between Arctic cods from different regions is unknown: do they constitute a panmictic population or several smaller populations? The key to this question lies in the study of genetic differentiation among Arctic cod across the Arctic; elucidating these genetics constitutes a primary objective of our future research. In the Laptev Sea, Arctic cod larvae that hatch in January-February survive because the open water in winter polynyas provides the light necessary for prey perception and capture [*Bouchard and Fortier, in press*]. Hence, one response of this key species to a predicted future lighter ice regime in the Laptev Sea could be better larval survival due to more frequent winter and spring polynyas, leading to enhanced recruitment,

and potentially larger populations. However, a long-term study of survival and recruitment is needed to confirm this hypothesis.

### I.6.6.1.2. Methods

The same type of sampler as in previous years was used to catch zooplankton along with juvenile Arctic cod (two zooplankton nets, 500 and 750  $\mu$  m mesh, 1 m<sup>2</sup> mouth aperture each, mounted side by side on a metal frame equipped with TSK flowmeters and deployed horizontally to ca. 75 m). Fish sampled by the net tow were individually measured and photographed before being preserved in 95% ethanol. Zooplankton samples were preserved in 4% buffered formalin solution. In future laboratory studies the age and daily growth of Arctic cod will be estimated by otolith microstructure analyses and the results compared with other years and regions. Also, juvenile Arctic cods from the Laptev Sea will be used in a circumpolar study of the species' genetics.

### I.6.6.1.3. Preliminary results

In 2007, we successfully deployed the zooplankton/fish sampler at 47 stations (**Table I.6.6.1**). At 36 of those stations, between 1 and 22 juvenile Arctic cods were caught (for a total of 169) along with 18 juvenile fish belonging to other species (**Table I.6.6.1**). The number of Arctic cod caught in 2007 is relatively low compared with 2003 (n=169) and 2005 (n=427) considering the sampling effort (15 stations sampled in 2003 and 30 in 2005). However, the juveniles were larger in 2007 (from 18 to 63 mm with a mean of 40.8 mm) than in 2003 (17 and 55 mm with a mean of 26.4) and 2005 (from 14 to 59 mm with a mean of 36.1 mm, **Figure I.6.6.1**), perhaps indicating low survival among the larval population but rapid growth and/or a long growth season for the survivors.

**Table I.6.6.1.** List of stations sampled with the horizontal net and number of juvenile Arctic cod (*Boreogadus saida*) and other juvenile fish collected.

Station	# of Arctic cod	# of other fish	Station	# of Arctic cod	# of other fish
VB0507	1	0	VB3807	1	0
VB0607	3	0	VB3907	0	0
VB0707	5	0	VB4007	1	0
VB0807	2	0	VB4107	1	0
VB0907	1	0	VB4207	6	0
VB1007	15	0	VB4307	3	0
VB1107	3	0	VB4607	1	0
VB1607	2	0	VB4707	2	0
VB1707	0	0	VB4807	5	0
VB2007	2	0	VB4907	1	0
VB2107	9	1	VB5007	0	0
VB2207	14	0	VB5107	0	0
VB2307	1	0	VB5507	8	1
VB2407	0	0	VB5607	2	1
VB2507	0	0	VB5807	0	1
VB2707	0	0	VB6107	4	1
VB2807	1	0	VB6307	14	5
VB2907	0	0	VB6407	8	5
VB3007	1	1	VB6707	0	0
VB3307	4	1	VB6907	2	0
VB3407	2	0	VB7107	15	1
VB3507	1	0	VB7307	22	0
VB3607	1	0	VB7507	0	0
VB3707	5	0			
<b>Total = 47</b>				<b>169</b>	<b>18</b>

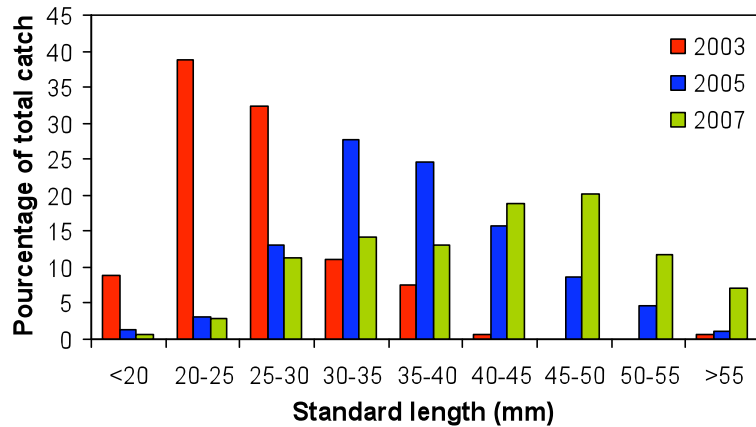


**Figure I.6.6.1.** Size distribution of juvenile arctic cod (*Boreogadus saida*) captured during NABOS 2003, 2005, and 2007.

### I.6.6.2. Vertical export flux of biogenic matter (*C. Lalande, L. Fortier*)

Despite considerable efforts devoted to assessing vertical fluxes of particulate carbon in different oceanic provinces, few annual investigations of these fluxes have been performed on the Arctic shelves due to the complexity and cost of long-term sampling in these areas. As a result of this data scarcity we have only partial knowledge of the physical and biological processes driving the production and export of particulate carbon on the Arctic shelves. The need for comparable and extended datasets is therefore critical if we are to improve our capacity to understand and model feedbacks linking environmental changes and carbon cycling in the Arctic shelf system. The ArcticNet Observatory Program composed of mooring lines equipped with automated sediment traps aims to provide such long-term time series. Moorings deployed in the Laptev Sea represent one ArcticNet observatory, and complement sampling conducted in the Beaufort Sea, Northern Baffin Bay, and Hudson Bay in the Canadian Arctic.

#### I.6.6.2.1 Objectives

- 1) To monitor vertical particle fluxes and identify physical and biological processes driving those fluxes; and
- 2) To compare export fluxes from the Laptev Sea with results obtained by similar sampling programs conducted in the Canadian Arctic.

#### I.6.6.2.2 Methods

Both sediment traps (Technicap PPS 3/3, 12 cups per trap) deployed on the M3 line (180m and 850m) were recovered and indicated a successful collection of sinking particles for a complete 12-month period from September 2006 to August 2007. These sediment traps were redeployed at a new location on the M10 line, while six additional sediment traps (Technicap PPS 3/3, 24 cups per trap) were deployed at the M3 line location (100m, 200m, 400m, 600m, 1000m, and 1300m). Analyses currently performed on the 2006-2007 sediment trap samples focus on the biogenic components of the vertical flux: particulate organic carbon (POC), particulate organic nitrogen (PON), planktonic organisms (swimmers), and biochemical composition of the sinking particles (stable isotope  $\delta^{13}\text{C}$ ). These results will be compared to the CTD record from M3 to verify whether the particles collected in sediment traps present characteristics supporting the hypothesis that the disappearance of the AW layer during almost two months in winter can be explained by the advection of water originating from the western Laptev Sea polynya.

### I.6.6.2.3 Preliminary results

Vertical POC fluxes and C:N ratios of sinking particles obtained at 175 m and 840 m in 2005-2006 are presented in **Figure I.6.6.2**. The annual POC flux obtained at 175 m in the Laptev Sea was lower than the annual POC flux obtained at a similar depth in the North Water polynya, but higher than in the Beaufort Sea, with an annual POC flux of  $3.8 \text{ g C m}^{-2} \text{ y}^{-1}$ . POC fluxes at 175 m and 840 m were relatively high from January to March ( $>10 \text{ g C m}^{-2} \text{ d}^{-1}$ ). POC fluxes were higher in summer at 175 m than at 840 m, reflecting the export of freshly-produced biogenic matter from the surface. C:N ratios indicate that sinking particles collected at 175 m were mostly labile, while particles collected at 840 m were more refractory.

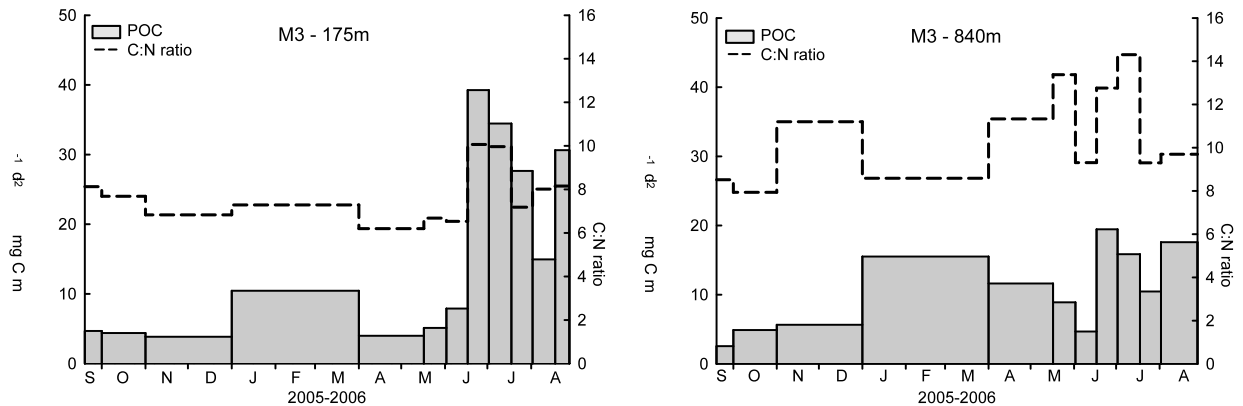


**Figure I.6.6.2** POC fluxes and C:N ratios of sinking particles collected at two levels of mooring M3 in 2005-2006.

### I.6.6.3. Nutrient concentrations (*C. Lalonde, J.-É. Tremblay*)

#### I.6.6.3.1 Objectives

The main objective of this project is to assess the impacts of reduced sea-ice cover, increased sea temperatures, and altered ocean circulation on nutrient loading and biological productivity in the Laptev Sea. More precisely, nitrate, nitrite, phosphate, and silicate will be measured to determine nutrient concentrations and origins in relation to water masses in the Laptev Sea.

#### I.6.6.3.2 Methods

Samples were taken at each depth of almost every rosette cast for nutrient measurements (59 stations). Seawater was filtered through a swinnex with a  $5.0 \mu\text{m}$  polycarbonate filter and 14 ml was collected from each depth in tubes that were stored in 10% HCl until sampling [Kattner, 1999]. A mercuric chloride solution ( $50 \mu\text{l}$ ) was added to each sample for preservation until analysis in laboratory in 2008.

### I.6.6.4. Microbial Ecology (*M.-È. Garneau, C. Lovejoy*)

#### I.6.6.4.1. Objectives

The microbial ecology subprogram intends (1) to study the microbial biodiversity using DNA samples and fluorescence *in situ* hybridization (FISH) to identify microbial and eukaryotic cells, and (2) to relate microbial communities to the Atlantic and Pacific water masses entering the Arctic Ocean, particularly deep water masses, and to the water from the Lena River plume in the Laptev Sea.

Surface water samples were collected along a transect at 126°00 E in the Lena River plume where strong gradients in salinity, temperature, and particulate material (organic and inorganic) loads are likely to affect the microbial assemblage distribution. The interpretation of the data collected will possibly contribute to one of the major objectives of the NABOS project: *“to estimate the rate of exchange between the arctic shelves and the interior in order to clarify mechanisms of the arctic halocline formation.”*

Samples were also collected at several depths at offshore stations, i.e. in the upper and lower Atlantic layers, in the Pacific layer whenever present, and at bottom depth. Elucidating the vertical distribution of microbial diversity might contribute to a second NABOS objective: *“to quantify the structure and variability of the circulation in the upper, intermediate, and lower layers of the Eurasian and Canadian Basins.”*

#### **I.6.6.4.2. Methodology**

Microbial abundance and diversity were measured in the surface mixed layer (10-m depth) at coastal stations in the Lena River plume. At offshore stations, several depths were sampled, i.e. in the upper and lower Atlantic layers, in the Pacific layer whenever present, and at the bottom depth. Along with microbial variables, surface CDOM (coloured dissolved organic matter) and chlorophyll *a* concentration were measured at every station.

**Table I.6.6.2.** Summary of the methods for microbial sampling during NABOS 2007

<b>Parameter</b>	<b>Methods</b>
CDOM (coloured dissolved organic matter)	Filtration on 0.2- $\mu\text{m}$ syringe filter
Chlorophyll <i>a</i> (chl <i>a</i> )	Filtration on GF/F membrane, porosity 0.7 $\mu\text{m}$
Bacteria (bact) and eukaryote (euk) abundance	Glutaraldehyde fixation, filtration on 0.2- $\mu\text{m}$ (bact) and 0.8- $\mu\text{m}$ (euk) black filters and DNA staining with DAPI; filters were mounted on microscopic slides with aquapolymount
DNA	Filtration on 0.2 sterivex filters and 3- $\mu\text{m}$ membranes for later determination of clone libraries of greater than and less than 3 $\mu\text{m}$ fractions
Fluorescence in situ hybridization (FISH)	Formalin fixation, filtration on polycarbonate 0.2 $\mu\text{m}$ filters for further analysis with rRNA-targeted oligonucleotide probes

#### **I.6.6.4.3. Future work**

The first step is the microscopic evaluation of microbial abundance, which will be done in the next months. The abundance distribution will be related to the physico-chemical environment to give an overview of the bacterial distribution. The dataset will be a useful tool for determining the most interesting samples and will be used to set up the priorities for DNA analysis and the clone libraries.

**Table I.6.4.3.** List of NABOS 2007 microbial samples. M: mooring; surf: surface; Atl: Atlantic

Date	Station	Type	Lat. °N	Long. °E	Depth layer	#niskin m	
17-Sep-07	VB0107	Transect 1	76°44.13	125°55.18	surf	5	5
	VB0207	Transect 1	77°00	126°00	surf	5	5
18-Sep-07	VB0607	Transect 1	77°45	126°00	surf	5	3
		Transect 1	77°45	126°00	Atl top layer	250	13
		Transect 1	77°45	126°00	Atl lower layer	700	20
		Transect 1	77°45	126°00	deep	1000	24
	VB0807	transect 1 - M1	78°27.99	125°44.95	surf	5	3
19-Sep-07	VB1007	profile 2	79°25	126°00	surf	5	3
		profile 2	79°25	126°00	Atl top layer	250	13
		profile 2	79°25	126°00	Atl lower layer	700	20
		profile 2	79°25	126°00	deep	1000	24
20-Sep-07	VB1607	deep profile 3 - M8	80°47	138°44	surf	5	3
		deep profile 3 - M8	80°47	138°44	Atl top layer	300	9
		deep profile 3 - M8	80°47	138°44	Atl lower layer	900	20
		deep profile 3 - M8	80°47	138°44	bottom	2030	24
21-Sep-07	VB2107	deep profile 4 -transect 2	79°56.60	142°23.66	surf	5	1-2-3
		deep profile 4 -transect 2	79°56.60	142°23.66	Atl top layer	250	9
		deep profile 4 -transect 2	79°56.60	142°23.66	Atl lower layer	1200	20
		deep profile 4 -transect 2	79°56.60	142°23.66	bottom	1330	22-23
22-Sep-07	VB2407	transect 2	79°25	143°00	surf	5	3
	VB2507	transect 2	79°15.420	143°30	surf	5	3
	VB2607	transect 2	79°00	144°00.6	surf	5	3
24-Sep-07	VB3807	profile 5 -M9	80°27	161°15	surf	5	3
		profile 5 -M9	80°27	161°15	Pacific	100	9
		profile 5 -M9	80°27	161°15	Atl top layer	250	13
		profile 5 -M9	80°27	161°15	Atl lower layer	700	20
		profile 5 -M9	80°27	161°15	deep	1000	24
26-Sep-07	VB4507	M3	79°25.00	139°50.00	surf	5	3
		M3	79°25.00	139°50.00	Atl top layer	250	13
		M3	79°25.00	139°50.00	Atl lower layer	750	20
		M3	79°25.00	139°50.00	Atl lower layer	1000	24
30-Sep-07	VB6707	transect 1 (continued)	74.15°00	126°00	surf	4	3
	VB6907	transect 1 (continued)	74.45°00	126°00	surf	4	3
	VB7007	transect 1 (continued)	75°00	126°00	surf	4	3
	VB7207	transect 1 (continued)	75°30,10' N	126°00	surf	4	3
	VB7307	transect 1 (continued)	75°45,03' N	126°00	surf	4	3
	VB7507	transect 1 (continued)	76°15,04' N	126°00	surf	4	3

## **I.6.7. BIOGEOCHEMICAL STUDIES: CONTRIBUTION FROM THE SIBERIAN SHELF STUDY PROJECT**

*(I. Semiletov, N. Shakhova, IARC; O. Dudarev, A. Salyuk, .I. Pipko, .N. Savelieva, POC; I. Repina, IAF; O. Gustaffson, USS; Bart van Dongen, SEAES; M. Elmquist, USS; A. Charkin, D. Kosmach and E. Spivak, POI)*



### **I.6.7.1. Introduction**

The Arctic is linked to the rest of globe biogeochemically via carbon and fresh water exchanges [SEARCH, 2005]. Since the effects of arctic change on the global radiation balance and the carbon cycle are central to the Arctic's role in the broader earth system, we focus our study on exploration of carbon cycling in the Arctic atmosphere-land-shelf system in connection with environmental variability. A major constraint on our ability to understand linkages between the Arctic Ocean and the global climate system is the scarcity of observational data in the Siberian marginal seas where major freshwater (FW) input and terrestrial carbon-nitrogen-phosphorus (CNP) fluxes exist. The role of the Siberian Shelf in transport and fate of FW and terrestrial organic carbon (terrOC) has not been discussed sufficiently. Thus we focus our attention on the Russian part of the Pacific sector of the Arctic (which remains the most under-sampled area in the Arctic Ocean), where processes of interaction between the local shelf waters (influenced strongly by fluvial and coastal erosion input) and Atlantic- and Pacific-derived waters are most pronounced. Four joint Russian-US cruises in the East-Siberian and Laptev seas plus one joint expedition along the Lena River stream were accomplished within the framework of the Siberian Shelf study (SSS) project in the 2003-2006 summers to study the key biogeochemical and FW fluxes with an emphasis on lateral and vertical methane (CH<sub>4</sub>) and carbon dioxide (CO<sub>2</sub>) transfer. In the summer of 2007 the US-Russian SSS biogeochemical group joined the NABOS cruise, extending the study area to the outer shelf.

The main objectives were:

- 1) Estimate the geographic variability of the main carbon cycle components, including partial pressure of CO<sub>2</sub> (pCO<sub>2</sub>), colored dissolved organic matter (CDOM), and dissolved organic carbon/particulate organic carbon (DOC/POC), and water mass parameters including currents, water temperature and salinity, pH, total alkalinity, oxygen, turbidity, and stable oxygen isotopes.
- 2) Investigate the connection between seasonal anomalies of CO<sub>2</sub> and CH<sub>4</sub> in shelf water and dynamics of the water mass in connection with Lena River runoff (lateral fluxes).
- 3) Identify the particular sources of CH<sub>4</sub> and CO<sub>2</sub> within the shelf area, and the factors that affect sea surface-atmosphere CH<sub>4</sub> and CO<sub>2</sub> exchange (vertical fluxes).
- 4) Provide a benchmark of the composition and provenance, and elucidate the extent of degradation of the terrOC currently being exported by coastal erosion and river runoff onto the extensive Siberian Arctic shelf.
- 5) Examine the transport and fate of terrestrial POC vs. marine OC

#### **I.6.7.1.2. Expedition itinerary**

The US scientific party (International Arctic Research Center, University of Alaska Fairbanks, IARC-UAF; USA) joined the main Russian party (Pacific Oceanological Institute, POI; Russia) on the RV *Victor Buinitsky* at the port of Kirkenes. A second Russian group took an air-freighter (AN-12) from Vladivostok (Russian Far East) to Tiksi (Laptev Sea) where they chartered the small vessel *TB-0012* with the specific goal of collecting data and samples in the near-shore zone (<20 m).

Thus, during the 2007 expedition two research platforms were used to accomplish field work: the ice-strengthened research vessel *Victor Buinitsky*, and the small commercial vessel *TB 0012* (**Figure I.6.7.1**).



**Figure I.6.7.1.** Research platforms for the 2007 research cruise: left- *Victor Buinitsky*; right – *TB-0012*.

The expedition onboard *Victor Buinitsky* got under way on September 9; a few days later continuous meteorological and greenhouse gases flux measurements were begun, accompanied by semi-continuous measurements of temperature, salinity, CDOM, turbidity, and pCO<sub>2</sub> in the surface layer.

Discrete surface water samples were collected to measure dissolved CH<sub>4</sub>, pH, and concentration of particulate material, PM (on filters). *Group 1* conducted these measurements onboard *Victor Buinitsky* until October 14, conducting the same measurements and water collections

at complex oceanographic stations (75 stations in total, at depths from ~20 m to ~2,000 m). *Group 2* worked onboard *TB-0012* from October 7<sup>th</sup> to October 12<sup>th</sup> when work was stopped by strong winds, a drastic temperature drop, and icing. *Group 2* collected water and sediment samples at 25 stations east and northeast of the Lena River delta for further onshore lab studies (including isotopic and molecular OC composition), measured hydrological parameters and dissolved CH<sub>4</sub>, and tested a new seismo-acoustical technique over shallow water of mean depth ≈10 m

### **I.6.7.3. Methods and measurements**

The overarching goal of the 2007 field program was almost identical to that of the previous expedition of 2006: to link the marine and terrestrial carbon cycles by elucidating the fate of terrestrial carbon that enters the sea in different forms including DOC, dissolved inorganic carbon (DIC), POC, and CDOM, and to measure products of carbon transformation (CO<sub>2</sub> and CH<sub>4</sub>) within the coastal and shelf/slope areas. Another goal was measurement of gas exchange (CO<sub>2</sub> and CH<sub>4</sub>) in the form of turbulent fluxes between the sea surface and overlaying atmosphere. Measurements of *in situ* oceanographic parameters (such as temperature, conductivity [salinity], turbidity, and photosynthetically active radiation [PAR]) and “in lab” oceanographic parameters (such as total alkalinity) were also of interest. In addition, we sampled POC retained on filters and in sediment to provide a benchmark of the composition and provenance, and to elucidate the extent of degradation of the terrOC currently being exported by coastal erosion and river transport onto the extensive Siberian Arctic shelf. Meteorological and air-sea CH<sub>4</sub> and CO<sub>2</sub> flux studies were performed continuously along the ~5,000 miles of ship tracks. Temperature, salinity/conductivity, and CDOM in the surface water were measured along the ship’s route each minute using a group of sensors installed on the conductivity-temperature-depth (CTD) Seabird 19+ meter deployed in a 150 liter barrel into which flowing sea water was pumped at a rate of ≈80-100 liters per minute. All these parameters were validated at oceanographic stations. Surface dissolved CH<sub>4</sub> was sampled each 3-4 hours and measured using the head-space gas chromatographic technique described elsewhere [Shakhova et al., 2005], while the pCO<sub>2</sub> value was measured each 15 minutes using an autonomous SAMI-CO<sub>2</sub> (#33) sensor deployed in the same barrel with the CTD. This approach was successfully used in joint USA-Russian SSS cruises since the summer of 2003 [Semiletov, 2005; Semiletov and Pipko, 2007]. The full suit of physical and hydrochemical measurements was conducted at each of the 75 stations (see details below).

A CTD-rosette system equipped with a deep WETLabs ECO CDOM fluorometer was used for measurements on the Siberian shelf and the Eurasian continental margin as an extension of the SSS 2003-2006 experiments in the Laptev and East Siberian seas and along the Northern Sea Route. The SAMI-CO<sub>2</sub> sensor was deployed at one NABOS mooring in summer 2006; this sensor was recovered in fall 2007. It will be deployed again for another year (2008/09) to obtain a longer record over the Laptev Sea shelf slope.

**I.6.7.3.1. Methane (and non-methane hydrocarbons) dissolved in water.** At each station, water sampling was carried out with Niskin bottles at 3 basic levels (surface, pycnocline, and bottom) and at additional horizons (up to 12) depending upon station depth. The total sampling time was 1 hour or less. The samples were processed in the ship’s laboratory within 2-3 hours after collection. Water samples were analyzed for CH<sub>4</sub> with a MicroTech-8160 gas chromatograph equipped with a flame ionization detector. The headspace technique for equilibrating between the dissolved and gaseous phases was applied [Semiletov et al., 1996; Shakhova et al., 2005]. The concentration of dissolved CH<sub>4</sub> in the water samples was calculated with the Bunsen adsorption coefficient for CH<sub>4</sub> [Wiesenburg and Guinasso, 1979] at the appropriate equilibration temperature. In total, 573 CH<sub>4</sub> samples were taken at stations (double-sampled at each of stations). In addition, about 120 surface water samples were collected along the way.

**1.6.7.3.2. Carbonate system parameters.** On these cruises we measured  $\text{pH}_{\text{sws}}$  at  $25 \pm 0.1^\circ\text{C}$  with an ORION 8103 Ross electrode on the SWS-scale, using tris-buffer prepared according to Goyet and Dickson [DOE, 1994], with a precision of  $\pm 0.002$  pH unit. Total alkalinity ( $A_T$ ) data were obtained by direct indicator titration in an open cell using a 665-Dosimat system with a precision of  $\pm 0.1\%$ . Values of  $\text{pCO}_2$  and total inorganic carbon concentrations ( $C_T$ ) will be calculated using values of  $A_T$ , pH, temperature (T), and salinity (S), following a scheme and constants advocated respectively by *Millero* [1995] and Goyet and Dickson (DOE, 1994). This technique has traditionally been used since 1996 on our cruises in the Arctic seas [*Pipko et al.*, 2002; *Semiletov et al.*, 2007].

Related information was obtained by the hydrological group and not funded through this project. Using the ship's Seabird CTD meter, continuous profiles of conductivity, temperature, pressure, light transmission, *in situ* fluorescence (from CDOM, which regionally is strongly correlated with DOC), turbidity, and oxygen were made on the downcast with data averaged over 1 dbar intervals. Water samples were taken using Niskin bottles. An Autosal salinometer referenced against IAPSO standard sea water will be used to test the CTD salinity data. The autonomous SAMI- $\text{CO}_2$  device described in [www.sunburstensors.com](http://www.sunburstensors.com) [*De Grandpre et al.*, 1999] was used for *in situ*  $\text{pCO}_2$  measurement..

**1.6.7.3.3  $\text{CO}_2$  and  $\text{CH}_4$  fluxes.**  $\text{CO}_2$  and  $\text{CH}_4$  fluxes were measured using either micrometeorological or enclosure methods, or both, as we did above the sea ice surface in June of 2002 [*Semiletov et al.*, 2004b). In our  $\text{CO}_2$  and  $\text{CH}_4$  exchange study setup, momentum and the fluxes of sensible and latent heat will be measured using the eddy correlation (EC) technique, which is the most direct micrometeorological method [*Fairal et al.*, 1997; *Edson et al.*, 1998; *Fairal et al.*, 2000; *Baldocchi*, 2003]. In this technique the vertical flux of a scalar constituent is obtained as

$$F = \overline{w'c'}$$

where  $w$  is the vertical wind speed and  $c$  is the quantity of interest (e.g., temperature, humidity, or gas concentration). An over-bar denotes the time average, and a prime denotes the fluctuation of an instantaneous value from this average, e.g.,

$$w' = \overline{w} - w$$

Fluxes of  $\text{CO}_2$  ( $F_{\text{CO}_2}$ ), water vapor ( $L_E$ ), and heat ( $H_E$ ) will be calculated using EC technique equations described elsewhere [*Baldocchi*, 2003]:

$$\tau_0 = -\rho_0 \left[ \overline{u'w'^2} + \overline{v'w'^2} \right]^{1/2} = \rho_0 u_*^2$$

$$H_E = c_p \rho_0 \overline{w'T'}$$

$$L_E = \rho_0 \overline{w'q'L_s}$$

$$F_{\text{CO}_2} = \overline{w'c'}$$

where  $\rho_0$  is the air density ( $\text{kg m}^{-3}$ ),  $c_p$  is the specific heat ( $\text{J kg}^{-1} \text{ } ^\circ\text{C}^{-1}$ ),  $L_s$  is the latent heat of vaporization for water ( $\text{J kg}^{-1}$ ),  $\tau$  is the momentum flux ( $\text{N m}^{-2}$ ), and  $u_*$  is the frictional wind velocity ( $\text{m s}^{-1}$ ).  $w'$ ,  $u'$  and  $v'$  are the turbulent fluctuations in vertical and two components of horizontal velocities.  $T'$  is the turbulent fluctuation in air temperature, and  $q'$  and  $c'$  are turbulent fluctuations in the specific humidity and  $\text{CO}_2$  concentration. Vertical and horizontal wind speed and temperature fluctuations were measured at 10-20 Hz using a three-dimensional sonic anemometer-thermometer aligned with the mean wind direction.  $\text{CO}_2$  and water vapor fluctuations were measured at 10-20 Hz with a fast-response open-path infrared Li-Cor 7500 gas analyzer. The 2007 cruise data are still being processed; some previous results and details of EC measurements (vs chamber and/or

calculated fluxes) may be found elsewhere [Semiletov *et al.*, 2004b; Repina *et al.*, 2007; Semiletov *et al.*, 2007; Pipko *et al.*, accepted].



**Figure I.6.7.2** Shipboard micrometeorological equipment.

**I.6.7.3.4 Methane in the air.** The concentration of CH<sub>4</sub> in air was measured with a High-Accuracy Fast Methane Analyzer, HAFMA (response time <0.05 seconds; accuracy better than 1% of reading; concentration range 10ppb-25ppmv; [www.lgrinc.com](http://www.lgrinc.com)) which includes a dry scroll vacuum pump, and is designed to suit many applications including conducting EC flux measurements using established micrometeorological techniques [Fairal *et al.*, 1997; Edson *et al.*, 1998; Fairal *et al.*, 2000; Baldocchi, 2003]. We plan to use the data measured with HAFMA for CH<sub>4</sub> turbulent flux estimates. We plan also to compare the turbulent and calculated CH<sub>4</sub> fluxes with the turbulent and calculated CO<sub>2</sub> fluxes which have been measured on our cruises since 2005 [Semiletov *et al.*, 2007]. We will also apply the EC and chamber techniques to evaluate the CO<sub>2</sub> and CH<sub>4</sub> fluxes across the fast ice in the winter-spring season as we did earlier in the Chukchi Sea [Semiletov *et al.*, 2004b]. The flux package consisted of:

- HAFMA and CSAT-3 sonic anemometer (Campbell Scientific Inc.) measuring the 3D wind vector and sonic temperature;
- Li-Cor 1400 meteorological station measuring the wind speed, direction, moisture and temperature;
- Li-Cor 7500 open path infrared gas analyzer, measuring H<sub>2</sub>O and CO<sub>2</sub>.

The flux package was mounted at a height of ~12m above mean sea level on a meteorological mast used during the 2002 IARC expedition on the fast ice of the Chukchi Sea and beyond [Semiletov *et al.*, 2004b].

**I.6.7.3.5. Freshwater components (runoff vs melt water)** will be distinguished using an already-described technique [Cooper *et al.*, 1993; Macdonald *et al.*, 1995]. Salinity will be analyzed with a precision of  $\pm 0.003$  psu using a Guideline Autoasl (model 8400A) instrument. Samples will be standardized against Standard Sea Water (Standard Seawater Service, Institute of Oceanography, Wormley, UK). Oxygen isotopic composition will be measured by a mass spectrometer connected to a CO<sub>2</sub>-H<sub>2</sub>O equilibration unit with precision of  $\pm 0.003$  through a subcontract with the Institute of Marine Sciences, UAF.

**I.6.7.3.6. C and H isotope signatures of CH<sub>4</sub>** are frequently adequate to reliably characterize natural gas type as bacterial or thermogenic [Whiticar, 1999]. In certain situations, such as mixing of different natural gases or where extreme substrate depletion and consumption occur, ambiguous CH<sub>4</sub>

isotope signals could be produced. In these cases, the C- and H-isotopes of CH<sub>4</sub>, in concert with coexisting isotope information about CO<sub>2</sub> and H<sub>2</sub>O, are excellent tracers of bacterial formation and consumption processes. The isotopes will be measured in gas extracted from water/sediment by isotope-ratio mass spectrometry [Whiticar, 1999; Whiticar and Faber, 1999; Lorenson et al., 2005]. The gas samples will be sent to the University California Irvine (B. Reeburgh's laboratory)

#### I.6.7.3.7. Establishing a new methodical approach to monitoring environmental changes over the East Siberian Shelf

Empirical regional relationships ( $r^2 > 0.9$ ) between concentration of DOC and CDOM, PM and turbidity, and salinity and DIC have been established for the East Siberian Arctic Shelf (ESAS). These relationships may be used for validating satellite data, restoring DOC/DIC, river plume, and PM dynamics over the last three decades, and developing biogeochemical models. A new empirical algorithm to predict riverine DOC from satellite- and *in situ*-measured CDOM, turbidity (and chlorophyll a), and sea surface temperature (SST) may be developed using the data obtained during the 2003-2007 East-Siberian and Laptev seas cruises.

Concomitant dynamics of the shelf environment were studied using the integrated values of different carbon compounds obtained by vertical and horizontal interpolation between available data points. This simple approach offers an opportunity for quantitatively evaluating environmental changes on the ESAS, an area which is most strongly impacted by global warming

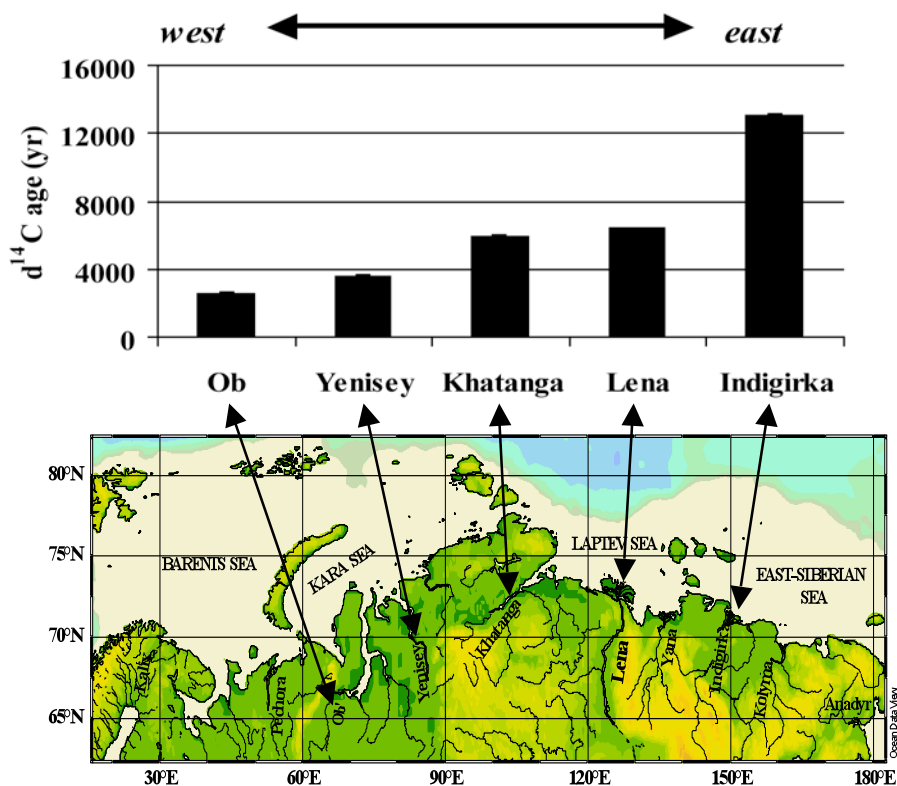


**Figure I.6.7.3** The average age of bulk organic carbon in surface sediments collected from the mouths of Russian Arctic rivers along the entire continental margin [after Guo et al., 2004]

**I.6.7.3.8. Other measurements** include advanced chemical analyses to constrain the sources

and degradation of terrestrial organic matter, including compound –specific radiocarbon analyses of terrestrial biomarkers. Initial results reveal both bulk radiocarbon (**Figure I.6.7.3**) and molecular-level variations in organic matter composition of exported terrOC that are consistent with continent-scale trends in climate and vegetation [Guo et al., 2004; van Dongen et al., 2008]. It was also reported that the river export of CH<sub>4</sub> increases from west to east; this may be related to the west-to-east freshness of terrOC in the watersheds of the great Siberian rivers [Shakhova et al., 2007a]. Note that river export of CH<sub>4</sub> plays a minor role in the regional marine CH<sub>4</sub> balance compared with seabed sources [Shakhova and Semiletov, 2007; Shakhova et al., submitted].

Measurement of total nitrogen (TN), OC, C/N molar ratio, C-14, biomarkers, mineralogy, elemental composition, and stable isotopic composition data will be obtained from sediments sampled by Van-Veen grab. Basic techniques were described in Guo et al. [2004] and Semiletov et al. [2005]. Advanced chemical analyses to constrain the sources and degradation of terrestrial organic matter, including compound –specific radiocarbon analyses of terrestrial biomarkers, will be mostly performed using the Stockholm University facilities using an approach developed in our previous collaborations [Guo et al., 2004; van Dongen et al., 2008; Elmquist et al., 2008].

#### I.6.7.4. Preliminary look at the data

Most of the data are still being processed. Therefore we present here only initial results with an emphasis on the spatial distribution and dynamics of dissolved CH<sub>4</sub> and the carbonate system in connection with environmental conditions.

##### I.6.7.4.1 Methane in the water

Based on the data obtained by previous Russian-US cruises in the Laptev and East-Siberian seas (2003-2006) and the winter/spring expedition of 2007, we found that, during the open-water season, CH<sub>4</sub> input to the shallow Laptev Sea water column might be a result of biogenic production within bottom sediments or the decay of shallow gas hydrates, and subsequent gas movement upwards; on the other hand, it is also possible for CH<sub>4</sub> to be introduced by riverine discharge, and to spread onto the shelf via lateral fluxes. However, our previous results show a minor role for river export compared with CH<sub>4</sub> release from the seabed [Shakhova and Semiletov, 2007; Shakhova et al., submitted].

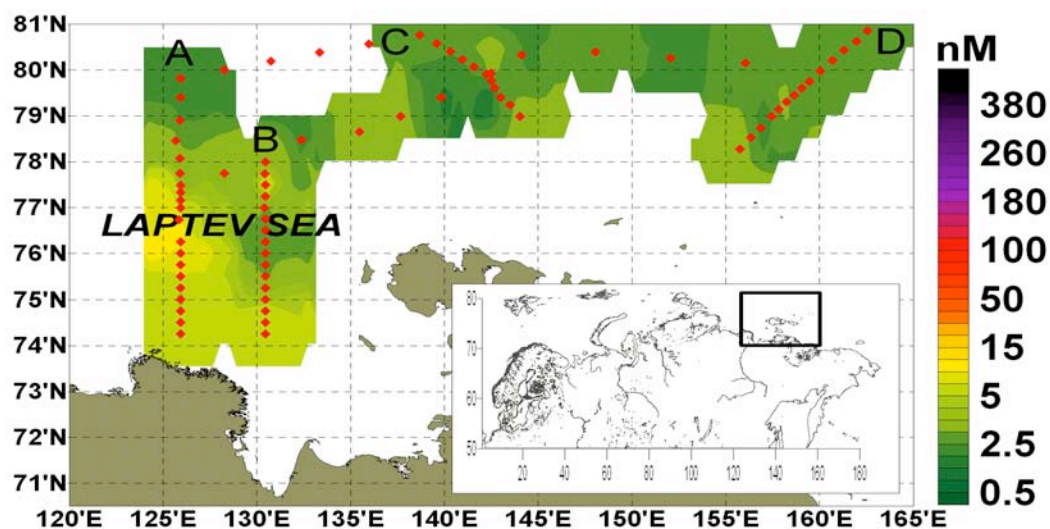


**Figure I.6.7.4.** Distribution of dissolved methane in the surface water in the Laptev and East-Siberian seas.

The surface CH<sub>4</sub> values obtained in the second half of September 2007 are significantly lower than those obtained in early September during 2003-2005 [Shakhova and Semiletov, 2007; **Figure I.6.7.4**]. That is because CH<sub>4</sub> escapes into the atmosphere during the fall water convection which starts in that area around 10 September.

Cross shelf transects (shown in **Figure I.6.7.5**) show that seabed in the shelf slope and the shallow area north of the Lena Delta are sources of CH<sub>4</sub> which are associated with degradation of the Arctic shallow hydrates [Shakhova et al., 2008, submitted]; a gas flare was detected along 130E which may indicate this type of CH<sub>4</sub> release [Shakhova et al., submitted] The subsurface maximum of dissolved CH<sub>4</sub> is spatially correlated with the position of the pycnocline core/bottom which may trap small rising CH<sub>4</sub> bubbles.

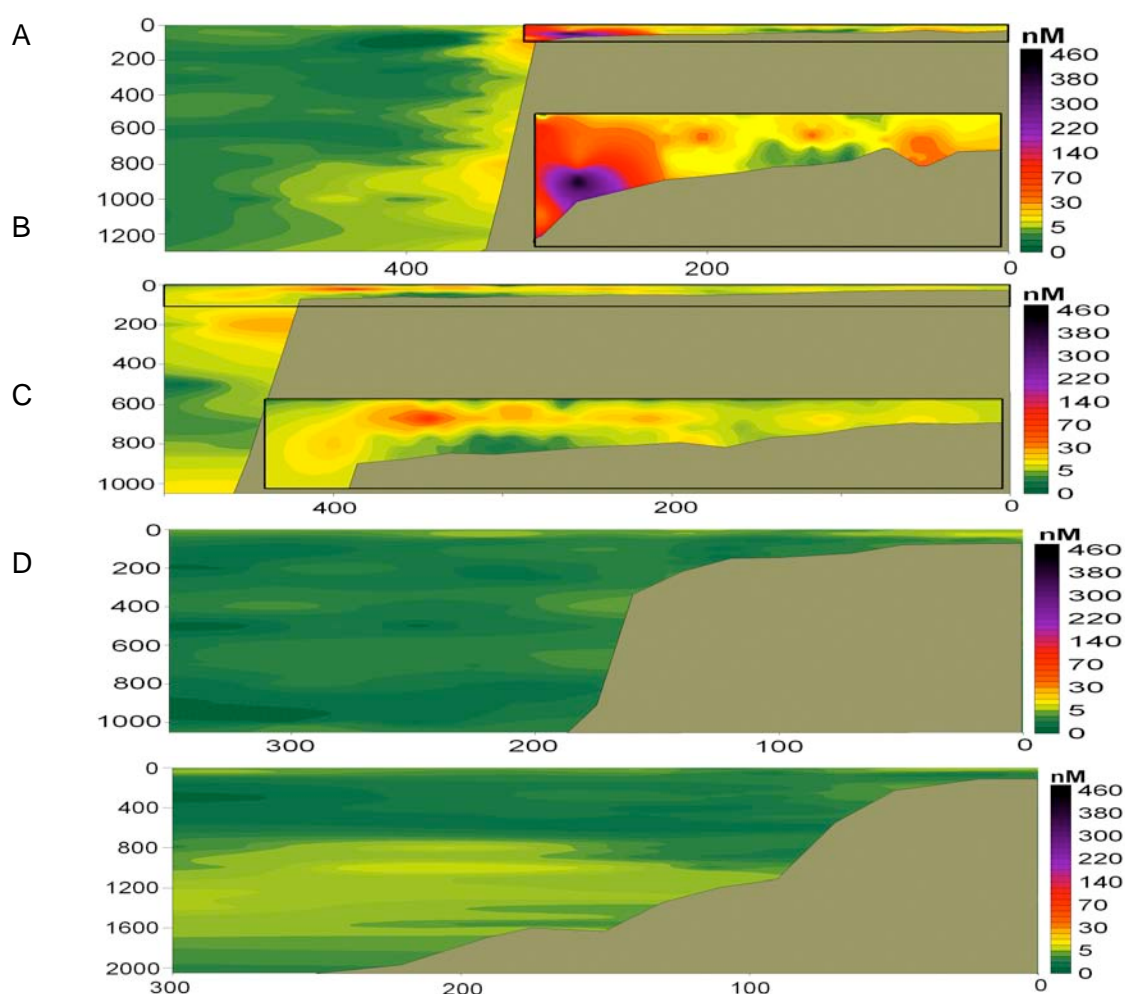


**Figure I.6.7.5.** Dissolved methane distribution along the transects A, B, C, D (shown in **Figure I.6.7.4**.)

#### I.6.7.4.2. Carbonate system.

Ship observations have revealed differences in intensity and direction of gas exchange, which depend on the characteristics of the underlying water masses. Coastal areas, strongly influenced by coastal erosion and the river input of terrestrial carbon (suspended and dissolved), are the sources of CO<sub>2</sub> into the atmosphere. Emission of CO<sub>2</sub> from the Arctic coastal zone is influenced by coastal erosion and river runoff water, which is generally low in transparency and productivity; erosion and runoff may increase as global warming continues [Semiletov et al., 2007].

Surface data obtained in 2007 along the Eurasian Arctic continent (Figures I.6.7.4.6 and I.6.7.4.7) using the SAMI-CO<sub>2</sub> sensor (almost 100 *in situ* measurements per day) show that in autumn the ocean was a sink rather than a source of atmospheric CO<sub>2</sub>; this result agrees with the data obtained in 2006 onboard the ice-breaker *Kapitan Dranytsin*, and is the result of water cooling and, consequently, photosynthesis ceasing as we move from west to east [Pipko et al., 2002; Semiletov et al., 2007]. Minimal values of pCO<sub>2</sub> (down to 230 ppm) were found in the Barents and Kara seas where the biological pump is much stronger than in the low-productivity Laptev and East-Siberian seas. However, in our case, the pCO<sub>2</sub> decrease from 350 ppm down to 230 ppm as we moved eastward from ~ 10 E to ~ 40E can be explained by the temperature factor alone: the water cooled from 4.8°C to -1 °C. The highest pCO<sub>2</sub> values (up to 470 ppm) were obtained along the 126E and 130E tracks where the Lena River plume is well-traced by the high values of CDOM/DOC distribution (not shown here), silicates (~ 12 μM), and normalized (vs 35 psu) total alkalinity (up to 2.660 mM), Figure I.6.7.4.8.

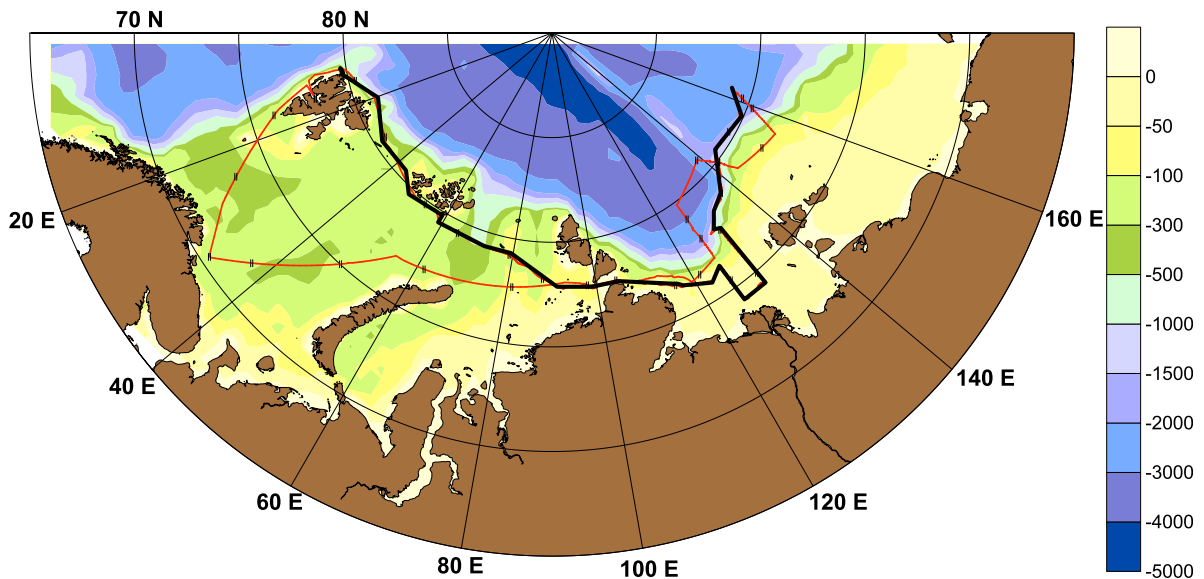
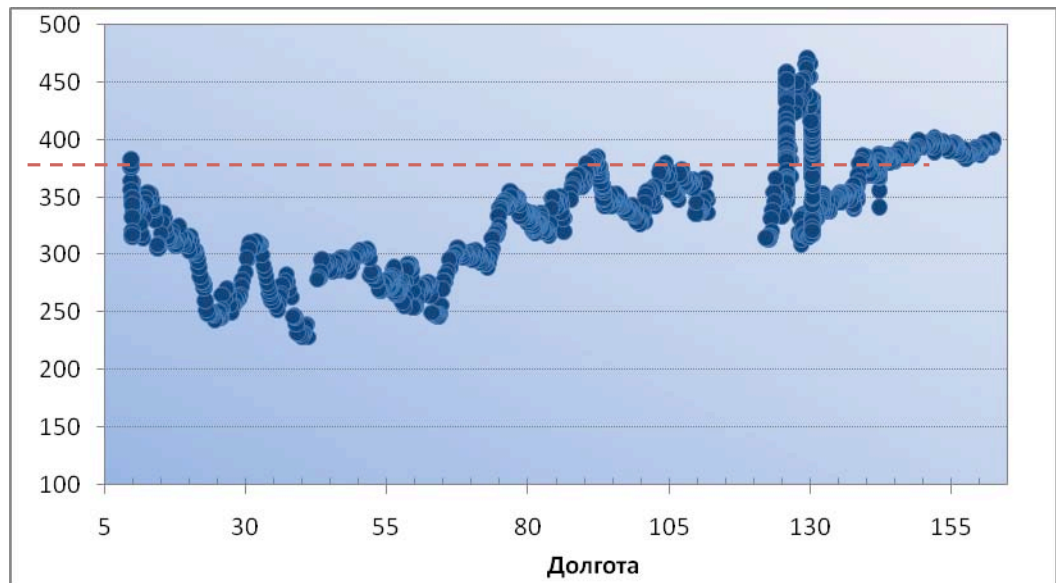
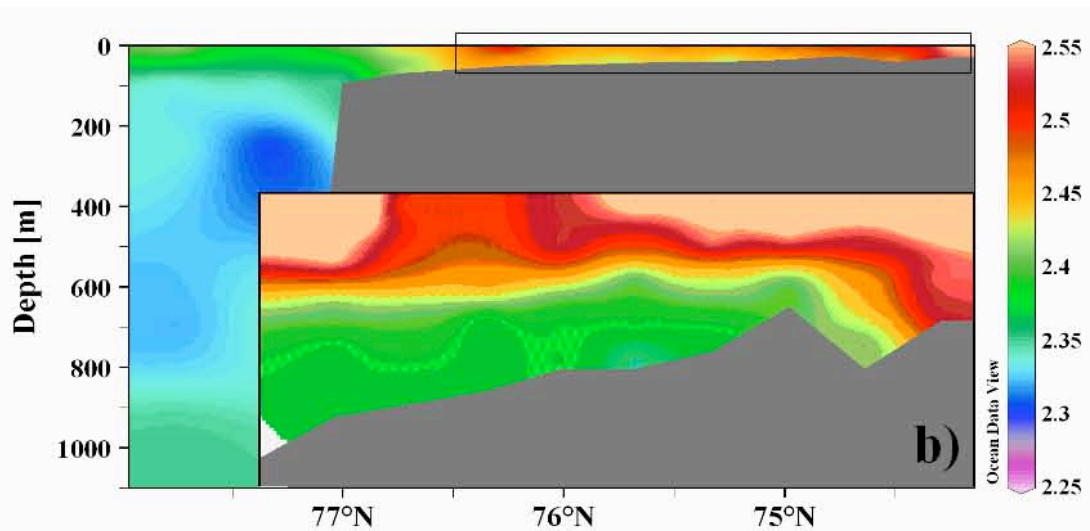


Figure I.6.7.4.6. Ship's tracks accompanied by pCO<sub>2</sub> measurements in the surface water.



**Figure I.6.7.4.7.** Measured  $p\text{CO}_2$  distribution from west to east, ppm



**Figure I.6.7.4.8.** The south-north distribution of the normalized total alkalinity, mM, along transect (A)

Surprisingly low values of  $p\text{CO}_2$  were found in the core (at depth  $\sim 285\text{m}$ ) of the Atlantic intermediate water (AIW) at mooring No. 3 (M3):  $p\text{CO}_2$  decreased from 310-300 ppm in late August-September, 2006 to  $\sim 230$  ppm in December, 2006 (**Figure I.6.7.9**). On this cruise we detected such a low  $p\text{CO}_2$  only on the surface of the highly productive Barents Sea, though in the fall decreasing  $p\text{CO}_2$  may be determined by cooling, as we earlier found in the highly productive Chukchi Sea [Pipko et al., 2002]. We may assume therefore that the measured  $p\text{CO}_2$  decrease might be related somehow to enhanced inflow of the Barents branch of AIW. Additional study is required to elucidate the mechanism by which different AIW modifications affect the carbonate chemistry regime along the pan-Arctic shelf margin.

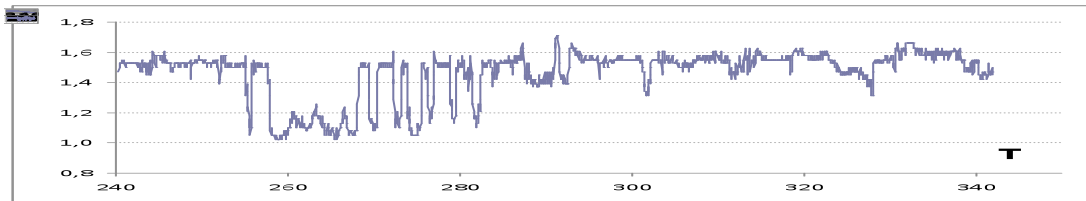


**Figure I.6.7.4.9.** Mooring-based record of temperature (T), pCO<sub>2</sub>, and salinity (S) in the AIW core from September-December, 2006.

#### **I.6.7.5 Preliminary conclusions**

Ship observations have revealed differences in intensity and direction of gas exchange, which depend on the characteristics of the underlying water masses, and on sea bottom morphological settings. The knowledge gained will be essential for understanding sources and sinks, transport and fate of fresh water, organic and inorganic carbon, sediments, particulate material, trace elements, and pollutants delivered to the Siberian shelf and Arctic Ocean by the great Siberian Arctic rivers and coastal erosion.





## SECTION II

# CABOS-07 Expedition to the Beaufort Sea aboard the Canadian Coast Guard Icebreaker *Louis S. St-Laurent* (September 2007)

Sarah Zimmerman<sup>1</sup>, Eddy Carmack<sup>1</sup>, Mike Dempsey<sup>2</sup>, and Igor Polyakov<sup>3</sup>

1 - Institute of Ocean Sciences, Sidney, British Columbia, Canada

2 - Oceanetic Measurement Ltd., Sidney, BC, Canada

3 - International Arctic Research Center, University of Alaska Fairbanks  
Fairbanks, Alaska, USA

## II.1. INTRODUCTORY NOTE

The Canadian Basin Observation System (CABOS) mooring (**Figure II.1**) has been deployed on Institute of Ocean Sciences (IOS) Arctic cruises on behalf of IARC since 2003. The location of the mooring has varied due to ice conditions but has been continuously placed to monitor the flow of AW around the southeast slope of the Canada Basin. The mooring is part of a string of moorings deployed by IARC to observe the movement of AW through the Arctic and measure the heat flux to upper waters. The NABOS consists of a series of MMP and conventional moorings located around the self break of the Laptev Sea. The CABOS mooring provides complementary data in the Canada Basin for the NABOS array. In 2007 it was decided to recover but not re-deploy the CABOS mooring in order to concentrate equipment resources in the Laptev Sea.

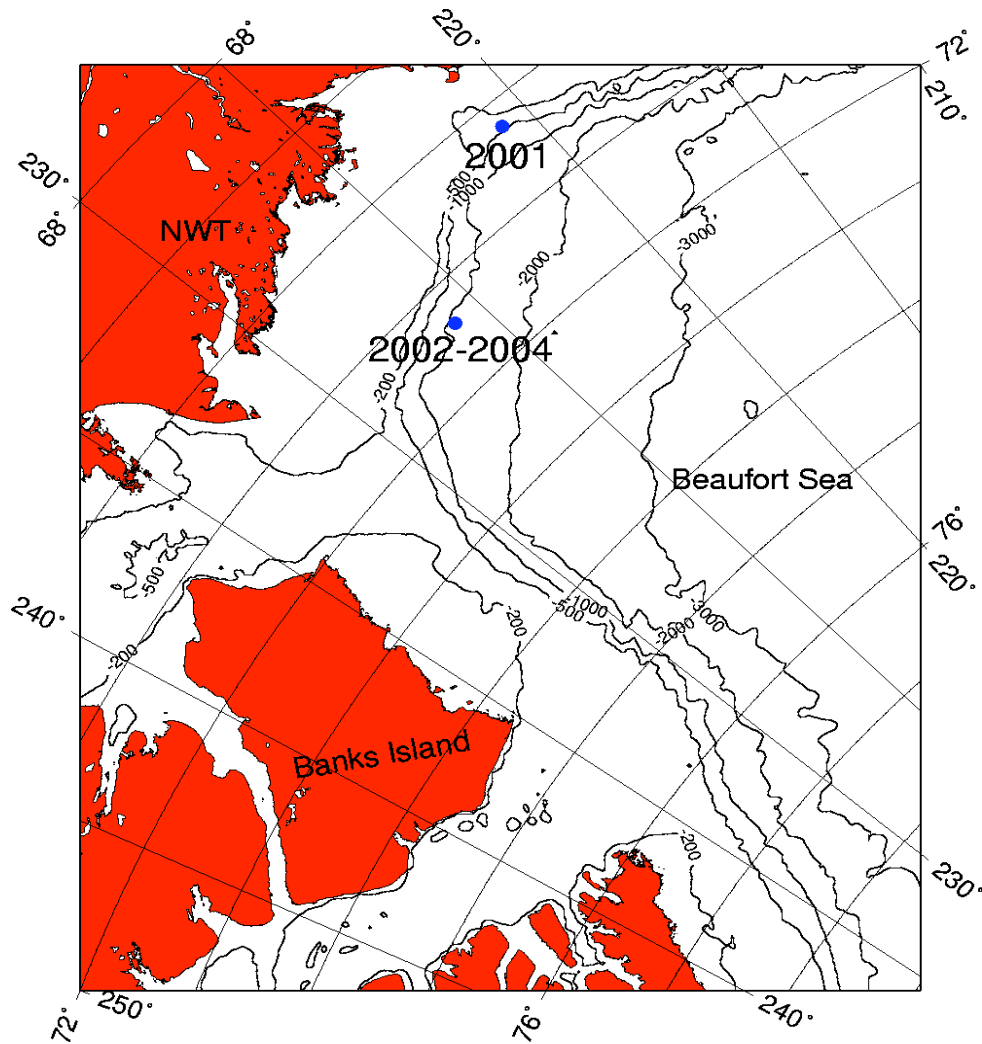


**Figure II.1.** Map with CABOS mooring location

## II.2. RESEARCH VESSEL

A brief description of the ship used for CABOS mooring deployment and recovery is taken from the web page [http://www.ccg-gcc.gc.ca/vessels-navires/details\\_e.asp?id=A-1](http://www.ccg-gcc.gc.ca/vessels-navires/details_e.asp?id=A-1) and shown in **Table II.1**.

**Table II.1.** Canadian Coast Guard (CCGS) *LOUIS S. ST-LAURENT*

Official No:	328095			
Type:	Heavy Gulf Icebreaker			
Port of Registry:	Ottawa			
Region:	Maritimes			
Home Port:	Dartmouth,	Nova Scotia,	Canada	
Call Sign:	CGBN			
When Built:	1969			
Builder:	Canadian Vickers, Montreal, Québec, Canada			
Modernized:	1988 - 1993 - Halifax Shipyard & 2000 new props			
<b>Certificates</b>	<b>Complement</b>			
Class of Voyage:	Home Trade I	Officers:	13	
Ice Class:	100 A	Crew:	33	
MARPOL:	Yes	Total:	46	
IMO:	6705937	Crewing Regime:	Lay Day	
		Available Berths:	53	

The program for the extended cruise of the Canadian icebreaker in 2007 included several mooring deployments and recoveries for several scientific programs and a CTD survey, including CABOS mooring recovery and deployment (see **Figure II.I** for mooring location).

## II.3 MOORING RECOVERY AND DEPLOYMENT

### II.3.1 CHRONOLOGY OF THE MOORING RECOVERY (*M. Dempsey, O.M.*)

**2007/08/28**

**1710:** CTD – Approaching 2006 deploy position. 2/10-4/10 ice cover with some old ridges. Last year's sound speed  $1483\text{ms}^{-1}$

**1715:** On station near 2006 deploy location. Sent command “220475” to EdgeTech 8242XS acoustic release #29336. Release enabled. Ranges on deck unit 1213, 1214, and 1212 m. Operations carried out from forward lab using Edgetech 8011A deck unit and ship's Knudsen transducer.

**1719:** Ping top EdgeTech transponder (interrogate 11 kHz, reply 14 kHz). Range 496, 492, and 486 m.

**1721:** Change control of deck unit from manual to serial control via WHOI ARCTASS s/w.

**1726:** 71° 49.572'N and 131° 45.036'E. Plot 2 ranges for surface transponder at 1<sup>st</sup> site. 2 way acoustic travel time 0.6034 s.

**1730:** Two rings near fit 17 m from drop position. Move ship to next site.

**1745:** On 2<sup>nd</sup> site - 71° 49.372'N, 131° 46.386'E. Two-way travel time 0.7062 s.

**1755:** On 3<sup>rd</sup> site - 71° 49.914'N, 131° 45.624'E. Two-way acoustic travel time 0.6144 s. Best estimate of top transponder z=45 m.

**1805:** Moved ship over transponder position. Top steel sphere seen on Skipper sounder. ~4/10ths ice over top of mooring. Ship spends some time pushing the smaller bits out of the way.

**1819:** Sent release command "242578". Repeated twice. Did not appear to release. Sent enable command 376614 to 8242XS s/n 28388. Enabled. Disabled other unit.. Did not appear to release. Multiple pings received but did not appear to be proper response. Moved 150m off to get better range for navigation program.

**1832:** Sent release command 354547 to 28388 1093 slant range. Appears to be off bottom(?) Mooring thought to be released and trapped under ice. Range on top transponder and move in.

**1839:** Top sphere spotted on surface 25 m off of port beam in 3/10ths ice.

**1918:** Difficulty in hooking top bale. Finally hook onto top sphere and lift up to A frame.

**1925:** Take weight on stopper chain in A frame. Remove top 37" sphere, SBE37 Microcat s/n 2368, EdgeTech transponder, two glass spheres and top MMP bumper. Transfer bull rope on Lebus winch to take load on Nilspin mooring line.

**1932:** Start pulling in mooring line. Sent enable code 376614 to release 28388.

**1955:** Pull up MMP s/n 11474 out of water on bottom bumper. Stop off at chain between glass balls. Remove MMP from wire.

**2005:** All on deck. 71° 49.736'N and 131° 47.565'E. All secured. Proceed to Kugluktuk.

The two acoustic releases were checked to see which one actually released. Contrary to what was originally suspected, the mooring was released by the first unit. However, release #28388 was hung up on a small burr on the release toggle and with a little effort on deck it dropped the link. After the deck and equipment were cleaned up, the MMP #11474 was connected to a PC and the data checked; 350 record sets of similar size indicated that the profiler had worked for the whole period. The MMP clock was compared to GPS time and was found to be 26 minutes 42 seconds fast. (MMP clocks typically are 20-30 minutes fast over a year-long deployment.) Once the profiler was opened and the PCMCIA memory card copied, it was verified that the profiler appeared to work well even during the recovery (last record 1846 local time). Later analysis by Rick Krishfield of Woods Hole Oceanographic Institute (WHOI) checked the whole data record using WHOI's MatLab tools.

The SBE37 Microcat #2368 was also connected to a PC and the memory checked. The Microcat clock was 3 minutes 7 seconds fast compared to GPS time, and 33538 records had been recorded. An attempt was made to upload the data using the upload command in the SeaTerm GUI. There was an "unable to read status" message; the data were not recoverable using the proper method, but were captured in SeaTerm after sending a two-letter upload command. The data are ASCII and human readable, but cannot be used directly with Seabird processing software. Another attempt will be made on shore (at Seabird) to recover the original complete data file.

**Table II.2.** 2007 Operations, CABOS mooring

Investigator	Recovery	Recovery	Recovery	Deployment
	Depth (m)	Location	Time	Depth (m)

UAF/IARC	1111	71°49.688'N	29 Aug 07	Not
I. Polyakov		131°45.624'W	1522(UTC)	redeployed

### **II.3.2 CHRONOLOGY OF THE MOORING DEPLOYMENT** (*M. Dempsey, O.M.*)

### **II.4. MOORING DESCRIPTION**

## Canadian CABOS (F) As Deployed 2006

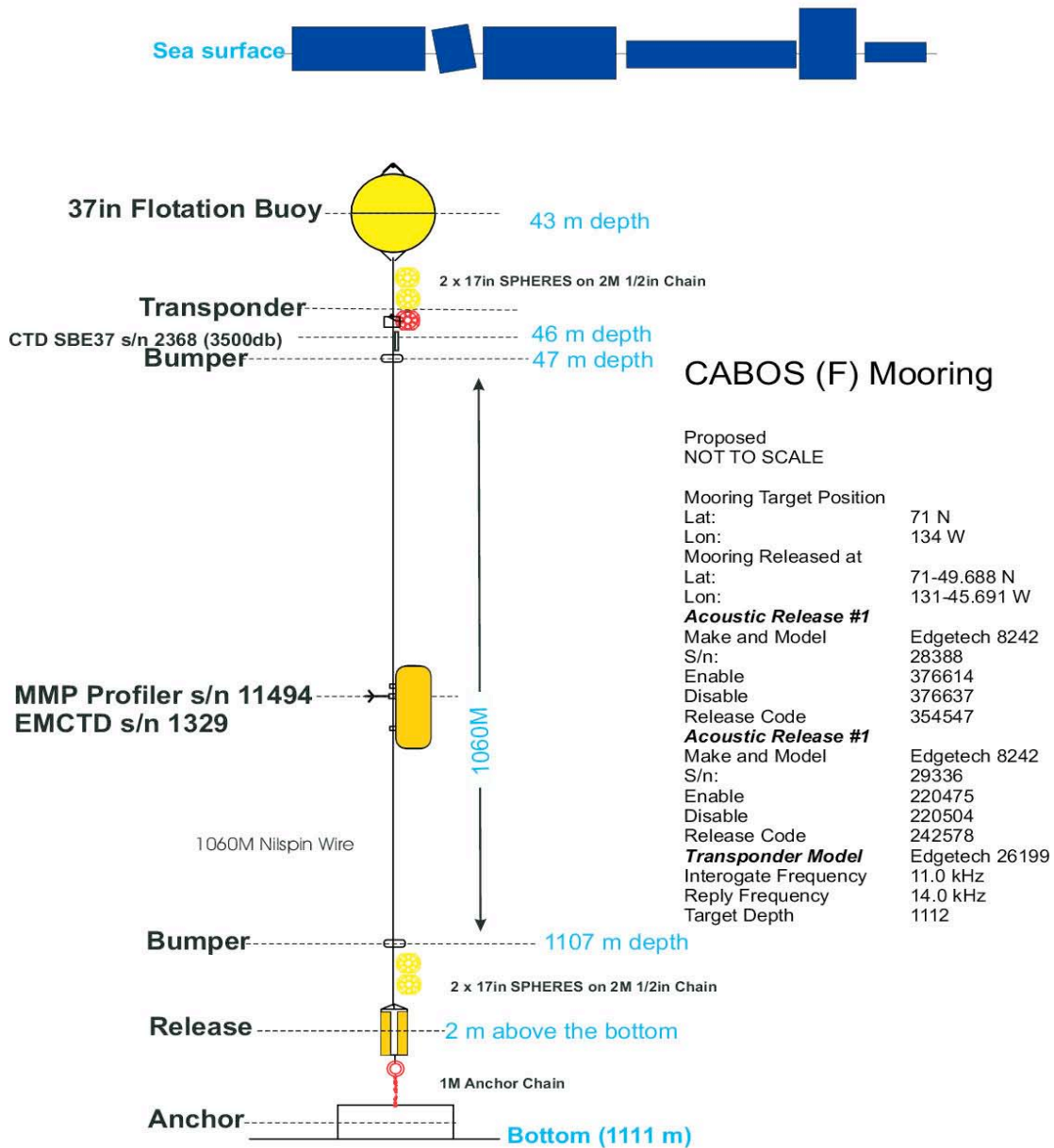


**Figure II.2.** Recovered (2006-07) CABOS mooring design and equipment.

### II.5. PRELIMINARY LOOK AT MOORING DATA

The MMP appeared to be almost perfectly ballasted and apart from a couple of profiles during which the profiler was momentarily stuck, all the records appear good (see **Figs. II.3** and **II.4**).

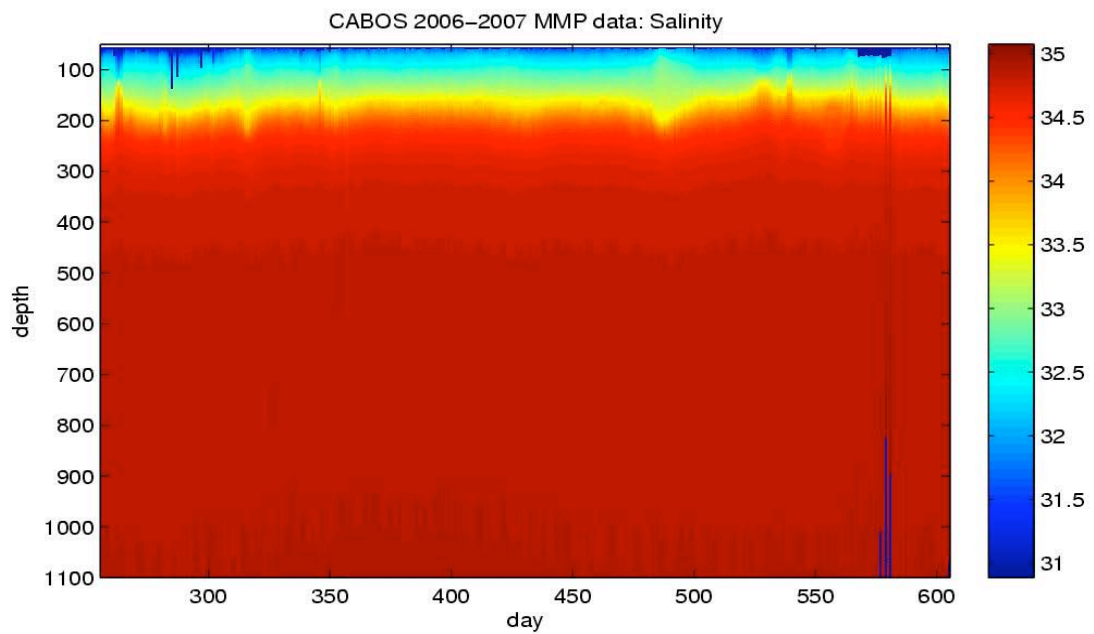
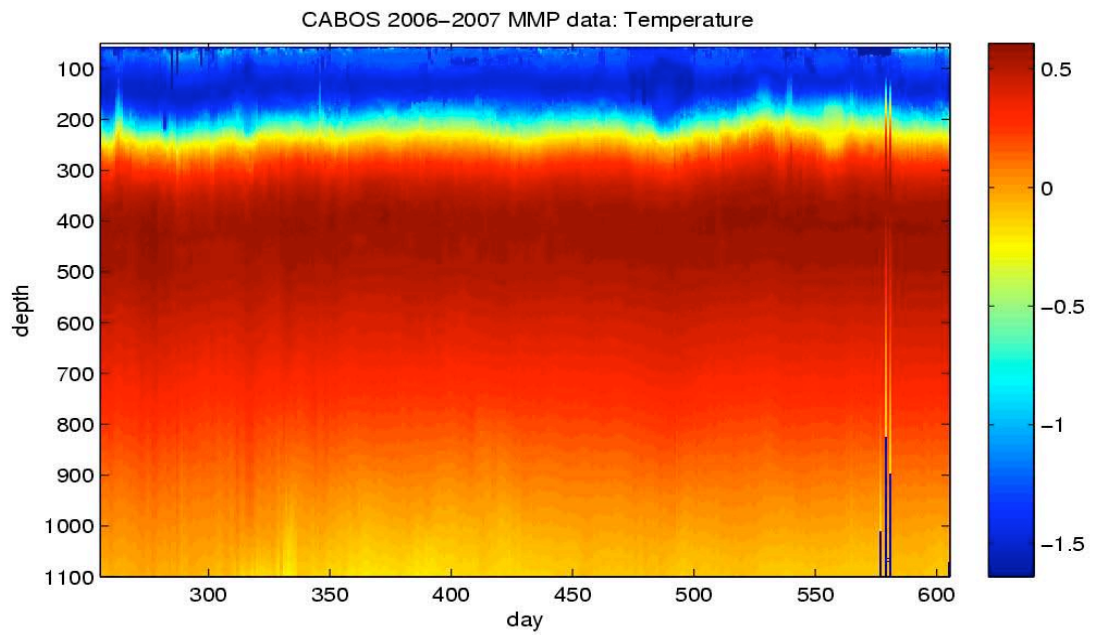


**Figure II.3.** Water temperature and salinity from the CABOS McLane Mooring Profiler (MMP) in 2006-07.

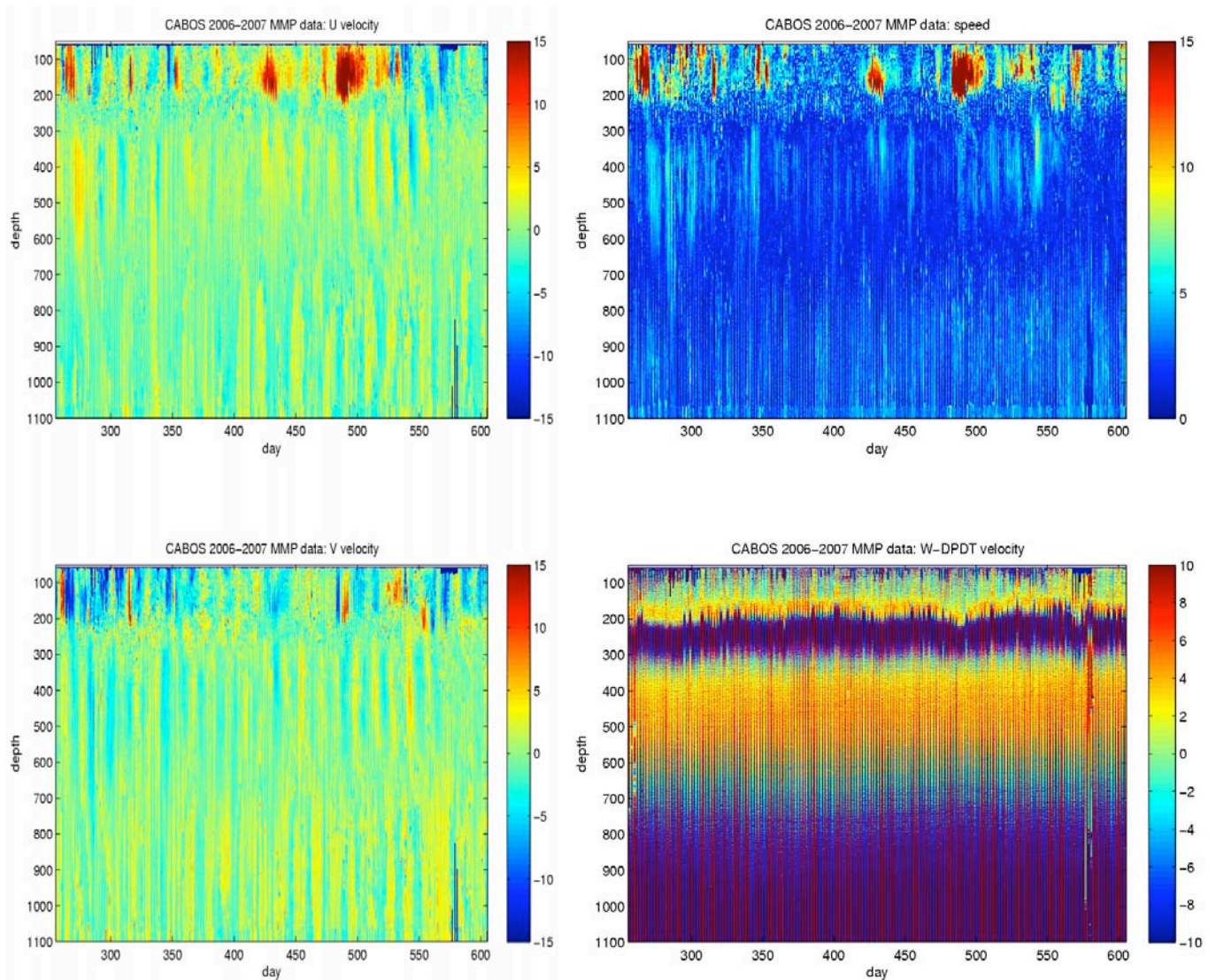


**Figure II.4.** Currents from the CABOS McLane Mooring Profiler (MMP) in 2006-07.

An example of the MMP record obtained from September 2006 – September 2007 from the Canada Basin is shown in **Figure II.3** and **II.4**. Water temperatures in the AW layer are about 0.4-0.6°C, close to typical climatic values (**Figure II.3**), while salinity is increased from ~31 psu in the upper part of the record to ~35 psu near the bottom. Problems with data centered at ~575 Julian day in the deep part may be clearly seen in the record. Several eddy-like structures may be seen in the records of temperature, salinity, and currents (**Figures II.3, II.4**). Temperature, salinity, and current profiles are shown in **Figure II.5**. The plots show near-freezing temperatures closer to the surface, a subsurface potential temperature maximum at ~400 m, and a surface salinity minimum with salinity increasing rapidly with depth to ~34.9-35 psu. A great deal of variability is apparent from the profiles of currents – in the upper part of the record the current speed varies from 0 to 20-30 cm/s with a maximum reached at 180-200 m depth. Much weaker currents not exceeding 5-7 cm/s are found at deeper parts of the profiles. Interestingly, the record shows some increase of current speed from ~600m down to the bottom.

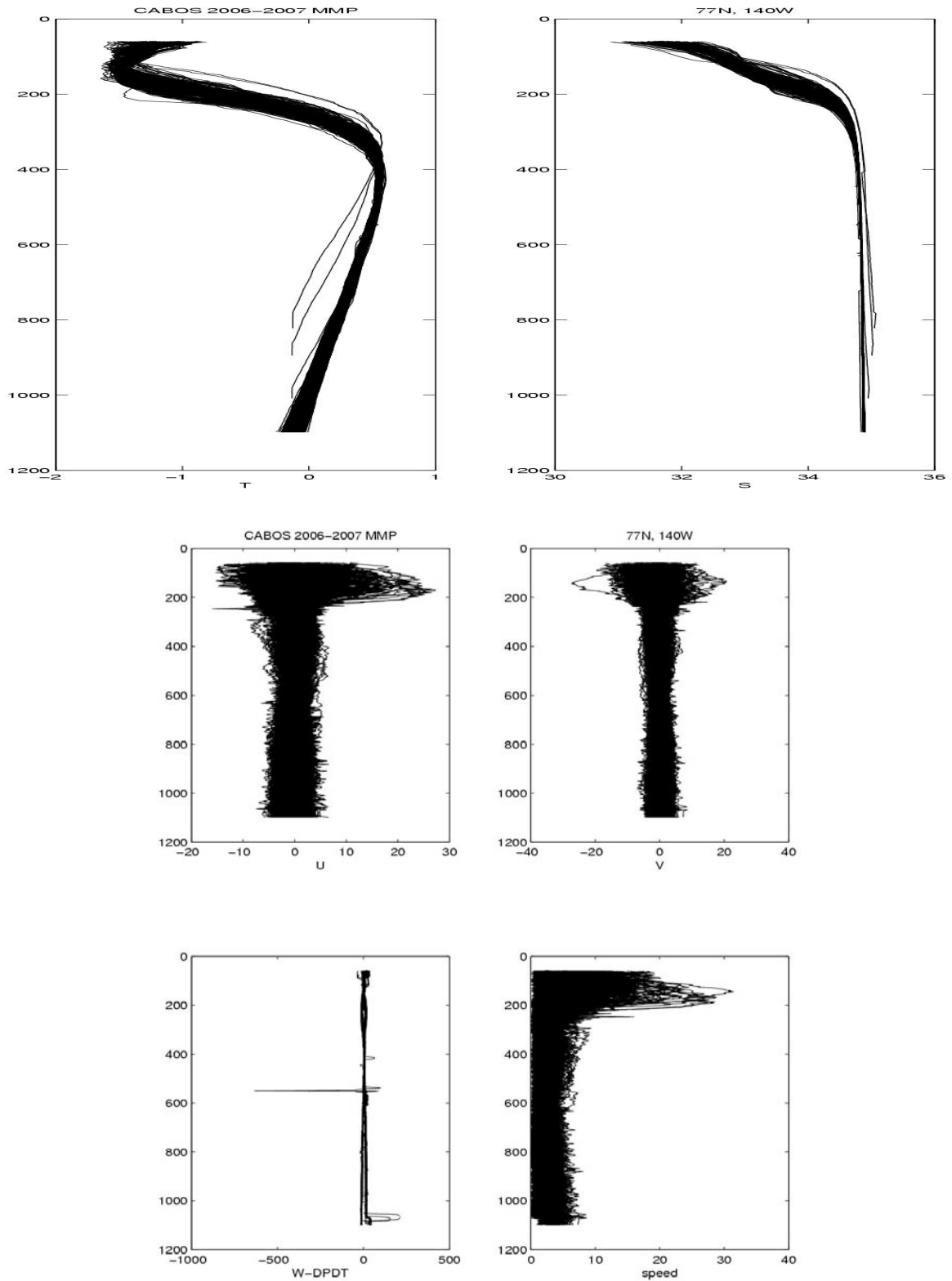


**Figure II.5.** Profiles of water temperature and salinity (top) and currents (middle and bottom) from the CABOS MMP in 2006-07.

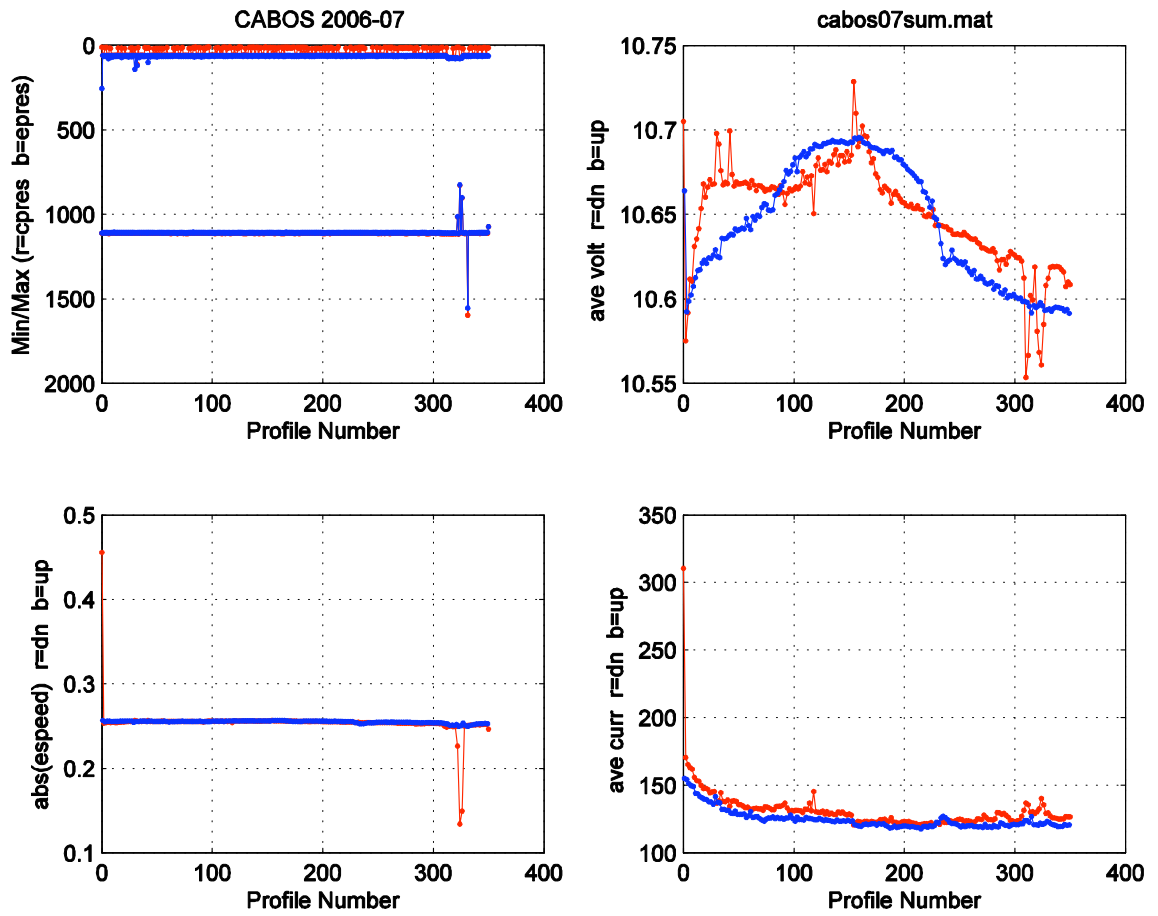


Figure II.6. MMP engineering information.

## REFERENCES

- Aagaard, K., and E. C. Carmack (1989), The role of sea ice and other freshwater in the arctic circulation, *Journal of Geophysical Research*, 94 (C10), 14485-14498.
- Bareiss, J., and K. Gorgen (2005), Spatial and temporal variability of sea ice in the Laptev Sea: Analysis and review of passive microwave data and model results, 1979 to 2002, *Global and Planetary Change*, 48, 28-54.
- Bouchard, C. and L. Fortier (in press), Impact of polynyas on the hatching season, early growth and survival of polar cod (*Boreogadus saida*) in the Laptev Sea, *Marine Ecology Prog. Series*.
- Cherny, I.V., and V. Yu. Raizer (1998), Passive microwave remote sensing of ocean. Wiley, UK, 300 p.
- Coachman, L. K., and C. A. Barnes (1963), The movement of Atlantic Water in the Arctic Ocean, *Arctic*, 16, 8-16.
- Culberson, C. H. and S. Huang (1987), Automated amperometric oxygen titration, *Deep Sea Research*, 34875-34880.
- Dickson, A. G. (1994), Determination of dissolved oxygen in seawater by Winkler titration, Tech. rep., WOCE operations manual, WOCE report 68/91 Revision 1 November 1994.
- Dittmar, T. and G. Kattner (2003), The biogeochemistry of the river and shelf ecosystem of the Arctic Ocean: A review. *Marine Chemistry*, 83, 103–120.
- Dmitrenko, I.A., D. Bauch, S.A. Kirillov, N. Koldunov, V.V. Ivanov, J. A. Höleman and L.A. Timokhov (submitted), Barents Sea upstream events impact the interannual variability of Atlantic water inflow into the Arctic Ocean through the northern Kara Sea: Evidence from 2005-2006 downstream observations, submitted to *Deep Sea Res.*
- Dmitrenko, I.A., S.A. Kirillov, V.V. Ivanov, and R.A. Woodgate (2008), Mesoscale Atlantic Water eddy off the Laptev Sea continental slope carries the signature of upstream interaction, *J. Geophys. Res.*, doi:10.1029/2007JC004491, in press.
- Edson, J. B., A.A. Hinton, K.E. Prada, J.E. Hare and C.W. Fairall (1998), Direct covariance flux estimates from mobile platforms at sea, *J. Atmos. Oceanic Technol.*, 15, 547-562.
- Elmqvist, M., I. Semiletov, L. Guo and Ö. Gustafsson (2008), Pan-Arctic patterns in black carbon sources and fluvial discharges deduced from radiocarbon and PAH source apportionment markers in estuarine surface sediments, *Global Biogeochemical Cycles*, in press.
- French, J.R., W.M. Drennan, Z.A. Zhang and P.G. Black (2007), Turbulent fluxes in the hurricane boundary layer. Part I: Momentum flux. *Journal of Atmospheric Science*, 64, 1089-1102.
- Grachev, A.A., C.W. Fairall and S.E. Larsen (1998), On the determination of the neutral drag coefficient in the convective boundary layer. *Boundary Layer Meteorology* 86, 257-278.
- Holland, M. M., C. M. Bitz and B. Tremblay (2006), Future abrupt reductions in the summer Arctic sea ice. *Geophysical Research Letters*, 33:doi:10.1029/2006GL028024.
- Holley, S. E. and D. J. Hydes (1994), Procedures for the determination of dissolved oxygen in seawater. Tech. rep., James Rennell Centre for Ocean Circulation.
- Ivanov, V.V. (2002), Atlantic Water in the western Arctic, Experience of structured oceanographic investigations in the Arctic Ocean, Lisitzin, A.P., M.E. Vinogradov and E.A. Romankevich (Eds.), Moscow, Nauchny Mir, 76-91 (in Russian).
- Ivanov V.V. and P.N. Golovin (2007), Observations and modeling of dense water cascading from the Laptev Sea shelf, *J. Geophys. Res.*, 112, C09003, doi:10.1029/2006JC003882
- Ivanov V.V., I.V. Polyakov, I.A. Dmitrenko, E. Hansen, I.A. Repina, S.S. Kirillov, C. Mauritzen, H. Simmons, and L.A. Timokhov (Submitted), Seasonal Variability in Atlantic Water off Spitsbergen, submitted to *Deep Sea Res.*

- Ivanov, V.V., I.A. Repina, V.A. Alexeev, I.V. Polyakov and I.A. Dmitrenko (2008), Propagation of seasonal signal in the Atlantic Water layer in the Arctic Ocean, ASLO Conference, Orlando FL, USA, March 2-8, 2008.
- Jones, E.P. (2001), Circulation in the Arctic Ocean, *Polar Research*, 29(2), 139-146.
- Kattner, G. (1999), Storage of dissolved inorganic nutrients in seawater: Poisoning with mercuric chloride. *Marine Chemistry* 67, 61-66.
- Kudryavtsev V.N. (2006), On the effect of sea drops on the atmospheric boundary layer, *J. Geophys. Res.*, 111, C07020.
- Nikiforov, Ye. G., and A. O. Shpaikher (1980), Features of the formation of hydrological regime large-scale variations in the Arctic Ocean, Gydrometeoizdat, Leningrad, 269 pp (in Russian).
- Osborn, T.R. (1980), Estimates of the local rate of vertical diffusion from dissipation measurements, *J. Phys. Oceanogr.*, 10(1), 83-89.
- Pfirman, S.L., D. Bauch, and T.Gammelsrod (1994), The northern Barents Sea: Water mass distribution and modification. In: *The Polar Oceans and Their Role in Shaping the Global Environment*, 77-94.
- Polyakov, I. V., A. Beszczynska, E. C. Carmack, I. A. Dmitrenko, E. Fahrbach, I. E. Frolov, R. Gerdes, E. Hansen, J. Holfort, V. V. Ivanov, M. A. Johnson, M. Karcher, F. Kauker, J. Morison, K. A. Orvik, U. Schauer, H. L. Simmons, Ø. Skagseth, V. T. Sokolov, M. Steele, L. A. Timokhov, D. Walsh and J. E. Walsh (2005), One more step toward a warmer Arctic, *Geophysical Research Letters*, 32:doi:10.1029/2005GL023740
- Polyakov, I. V., D. Walsh, I. A. Dmitrenko, R. L. Colony, and L. A. Timokhov (2003), Arctic Ocean variability derived from historical observations, *Geophys. Res. Lett.*, 30(6), 1298-1291, [doi:10.1029/2002GL016441](https://doi.org/10.1029/2002GL016441)[2003](https://doi.org/10.1029/2003GL018341).
- Quadfasel, D., A. Sy, and B. Rudels (1993), A ship of opportunity section to the North Pole: Upper ocean temperature observations, *Deep-Sea Res.*, 40, 777-789.
- Repina, I.A., I. Semiletov, and A.S. Smirnov (2007), Direct measurement of CO<sub>2</sub> fluxes in the Laptev Sea in summer, *Transactions of Russian Academy of Sciences*, 413 (5), (translated into English by Springer).
- Rigor, I. G., J. M. Wallace, and R. L. Colony (2002), Response of sea ice to the Arctic Oscillation, *J. Climate*, 15, 2648–2663.
- Rudels, B., E. P. Jones, L. G. Anderson, and G. Kattner (1994), On the intermediate depth waters of the Arctic Ocean, In: *The Polar Oceans and Their Role in Shaping the Global Environment: The Nansen Centennial Volume*, Geophys. Monogr. Ser. vol. 85, Johannessen, O.M., R. D. Muench, and J. E. Overland (Eds.), pp. 33-46, AGU, Washington, D.C.
- Rudels, B., R.D. Muench, J. Gunn, U. Schauer and H.J. Friedrich (2000), Evolution of the Arctic Ocean boundary current north of the Siberian shelves, *J. Marine Syst.*, 25 (2000), 77-99.
- Schauer, U., R. D. Muench, B. Rudels, and L. Timokhov (1997), Impact of eastern Arctic shelf waters on the Nansen Basin intermediate layers, *J. Geophys. Res.*, 102(C2), 3371-3382.
- Schauer, U., B. Rudels, E.P. Jones, L.G. Anderson, R.D. Muench, G. Björk, J.H. Swift, V. Ivanov and A.-M. Larsson (2002), Confluence and redistribution of Atlantic water in the Nansen, Amundsen and Makarov basins, *Annales Geophysicae*, 20 (2), 257 – 273.
- Semiletov, I.P. and I.I. Pipko (2007), Sinks and sources of carbon dioxide in the Arctic Ocean, *Transactions of Russian Academy of Sciences*, 414 (3), (translated into English by Springer).
- Semiletov, I.P., I.I. Pipko, I.A. Repina, and N. Shakhova (2007), Carbonate dynamics and carbon dioxide fluxes across the atmosphere-ice-water interfaces in the Arctic Ocean Pacific sector of the Arctic, *Journal of Marine Systems*, 66 (1-4), 204-226.
- Shakhova, N. and I. Semiletov (2007), Methane release and coastal environment in the East Siberian Arctic shelf, *Journal of Marine Systems*, 66 (1-4), 227-243.

- Shakhova, N., I. Semiletov, A. Salyuk, N. Belcheva, and D. Kosmach (2007a), Anomalies of methane in air above the sea surface in the East-Siberian Arctic shelf, *Transactions of Russian Academy of Sciences*, 414 (6), (translated into English by Springer).
- Shakhova, N., I. Semiletov, and N. Belcheva (2007b), The Great Siberian Rivers as a source of methane on the Russian Arctic shelf, *Transactions of Russian Academy of Sciences*, 414 (5), (translated into English by Springer).
- Spren, G., L. Kaleschke, and G. Heygster (2007), Sea ice remote sensing using AMSR-E 89 GHz channels, *J. Geophys. Res.*, in press.
- Timofeev, V. T., (1960), *Vodniye Massy Arkticheskogo Basseina* (Water masses of the Arctic Basin), GydrometeoIzdat, Leningrad.
- Van Dongen, B.E., I.P. Semiletov, J.W.H. Weijers, and Ö. Gustafsson (2008), Contrasting lipid biomarker composition of terrestrial organic matter exported from across the Eurasian Arctic by the five Great Russian Arctic Rivers, *Global Biogeochemical Cycles*, 22, GB1011, doi:10.1029/2007GB002974.
- Vetrov, A.A., I.P. Semiletov, O.V. Dudarev, V.I. Peresipkin, and A.N. Charkin (2007), Study of composition and origin of organic matter in the East-Siberian Sea bottom sediments, *Geokhimiya (Geochemistry)*, 3 (translated into English).
- Vetrov, A.A., I.P. Semiletov, O.V. Dudarev, V.I. Peresipkin, and A.N. Charkin (2008), Study of composition and origin of organic matter in the East-Siberian Sea bottom sediments, *Geokhimiya (Geochemistry)*, in press.
- Woodgate, R. A., K. Aagaard, R. D. Muench, J. Gunn, G. Bjork, B. Rudels, A. T. Roach, and U. Schauer (2001), The Arctic Ocean boundary current along the Eurasian slope and the adjacent Lomonosov Ridge: Water mass properties, transports and transformations from moored instruments, *Deep-Sea Research*, Part 1, 48, 1757-1792.
- Zakharov, V.F. (1996), *Sea Ice in the Climate System*. St.Petersburg, Hydrometeoizdat, 213 pp. (in Russian)

### ***Acknowledgments***

This work was supported by the International Arctic Research Center of the University of Alaska Fairbanks (by the Cooperative Institute for Arctic Research through NOAA Cooperative Agreement NA17RJ1224), the Far-Eastern Branch of the Russian Academy of Sciences, RAS, and the Russian Foundation for Basic Research (grants Nos. 07-05-00050a, 08-05-00184a, 08-05-00191a).

Recovery of the CABOS 2006-07 mooring was accomplished quickly with the help of many others. The assistance of a trained and motivated LSSL deck crew and bosun Bob Taylor was much appreciated. Also crew did an excellent job of keeping the ship very accurately on station during recovery and deployment. Many thanks to Rick Krishfield, Kris Newhall, and Jim Dunne of WHOI for their help on deck and for the use of their Lebus dual capstan traction winch. Also, many thanks to Rick Krishfield for downloading the instruments and conducting the preliminary data analysis.

Participation in the cruise was supported by the NSF (ARC0743972).

Elena and Sinhue are very grateful to Elizaveta Bodrova and Ekaterina Chernyavskaya for their help in collecting samples for nutrient analysis. Very much appreciated!

**APPENDIX: NABOS-07 Station List** (I.A. Dmitrenko, S.A. Kirillov)

Station Number: VB0107 Data: 17/09/07 Time of beginning: 18:35  
 dd/mm/yy hh:mm (GMT)  
 Latitude: 76° 43,89' N Longitude: 125° 53,73' E Depth: 69 m Ice: 0

#	Research Activity	Time, GMT		GPS Position		Comments 1	Comments 2
		beginning	end	beginning	end		
1	CTD/Rosette	18:40	18:50	$\varphi=76^{\circ}44,25'$ $\lambda=125^{\circ}54,32'$	$\varphi=76^{\circ}44,6'$ $\lambda=125^{\circ}54,4'$		Sampling levels: 2, 3, 5, 5, 7, 8, 9, 10, 10, 12, 15, 17, 20, 21, 23, 31, 32, 41, 42, 50, 52, 60, 61, 61
2	Tow	19:35	20:00	$\varphi=76^{\circ}48,82'$ $\lambda=125^{\circ}51,71'$	$\varphi=76^{\circ}48,91'$ $\lambda=125^{\circ}51,86'$		
3	Microstructure	18:50	19:05	$\varphi=76^{\circ}44,6'$ $\lambda=125^{\circ}54,4'$	$\varphi=76^{\circ}43,51'$ $\lambda=125^{\circ}51,86'$		

Station Number: VB0207 Data: 17/09/07 Time of beginning: 21:50  
 dd/mm/yy hh:mm (GMT)  
 Latitude: 77° 00,84' N Longitude: 125° 59,71' E Depth: 93 m Ice: 0

#	Research Activity	Time, GMT		GPS Position		Comments 1	Comments 2
		beginning	end	beginning	end		
1	CTD/Rosette	21:55	22:06	$\varphi=77^{\circ}00,0'$ $\lambda=125^{\circ}59,7'$	$\varphi=77^{\circ}00,0'$ $\lambda=125^{\circ}59,6'$		Sampling levels: 5, 6, 7, 10, 11, 15, 16, 17, 20, 22, 24, 50, 52, 75, 78, 85, 86, 87, 90, 90, 90, 90, 90, 90
2	Microstructure	22:07	22:18	$\varphi=77^{\circ}00,1'$ $\lambda=125^{\circ}59,58'$	$\varphi=76^{\circ}59,94'$ $\lambda=125^{\circ}59,5'$		

Station Number: VB0307 Data: 17/09/07 Time of beginning: 23:45  
 dd/mm/yy hh:mm (GMT)  
 Latitude: 77° 69,99' N Longitude: 125° 59,46' E Depth: 925 m Ice: 0

#	Research Activity	Time, GMT		GPS Position		Comments 1	Comments 2
		beginning	end	beginning	end		
1	CTD/Rosette	23:48	00:24	$\varphi=77^{\circ}09,94'$ $\lambda=125^{\circ}59,35'$	$\varphi=77^{\circ}09,52'$ $\lambda=125^{\circ}59,52'$		Sampling levels: 5,6,6,30,32,50,52,100, 102,200, 248, 250, 252, 300, 399, 498, 597, 654, 696, 698, 794, 795, 795, 796
2	Microstructure	00:27	00:57	$\varphi=77^{\circ}09,52'$ $\lambda=125^{\circ}59,52'$	$\varphi=77^{\circ}09,08'$ $\lambda=125^{\circ}59,27'$		

Station Number: VB0407 Data: 18/09/07 Time of beginning: 02:17  
 dd/mm/yy hh:mm (GMT)  
 Latitude: 77° 19,97' N Longitude: 126° 00,03' E Depth: 1278 m Ice: 0

#	Research Activity	Time, GMT		GPS Position		Comments 1	Comments 2
		beginning	end	beginning	end		
1	CTD/Rosette	02:20	03:13	$\varphi=77^{\circ}19,97'$ $\lambda=126^{\circ}00,03'$	$\varphi=77^{\circ}19,37'$ $\lambda=125^{\circ}59,84'$		Sampling levels: 5, 7, 8, 30, 32, 50, 52, 100, 102, 200, 248, 250, 252, 299, 399, 498, 597, 655, 696, 993, 1191, 1193, 1241, 1242
2	Microstructure	03:13	03:45	$\varphi=77^{\circ}19,37'$ $\lambda=125^{\circ}59,84'$	$\varphi=77^{\circ}18,93'$ $\lambda=125^{\circ}59,11'$		

Station Number: VB0507 Data: 18/09/07 Time of beginning: 05:07  
 dd/mm/yy hh:mm (GMT)  
 Latitude: 77° 30,11' N Longitude: 125° 59,77' E Depth: 1500 m Ice: 0

#	Research Activity	Time, GMT		GPS Position		Comments 1	Comments 2
		beginning	end	beginning	end		
1	CTD/Rosette	05:19	06:26	$\varphi=77^{\circ}29,63'$ $\lambda=125^{\circ}59,37'$	$\varphi=77^{\circ}29,15'$ $\lambda=125^{\circ}58,91'$		Sampling levels:
2	Tow	07:05	07:30	$\varphi=77^{\circ}28,87'$ $\lambda=125^{\circ}58,35'$	$\varphi=77^{\circ}29,47'$ $\lambda=125^{\circ}59,98'$		
3	Microstructure	06:28	06:53	$\varphi=77^{\circ}29,15'$ $\lambda=125^{\circ}58,91'$	$\varphi=77^{\circ}28,87'$ $\lambda=125^{\circ}58,35'$		

Station Number: VB0607 Data: 18/09/07 Time of beginning: 09:15  
 dd/mm/yy hh:mm (GMT)  
 Latitude: 77° 44,95' N Longitude: 125° 59,07' E Depth: >2000 m Ice: 0

#	Research Activity	Time, GMT		GPS Position		Comments 1	Comments 2
		beginning	end	beginning	end		
1	CTD/Rosette	09:25	10:15	$\varphi=77^{\circ}44,95'$ $\lambda=125^{\circ}59,05'$	$\varphi=77^{\circ}43,95'$ $\lambda=125^{\circ}57,13'$		Sampling levels: 5,6,6,30,32,51,53,100 102,201,247,250,252, 300,398,498,598,655, 697, 698, 796,992, 995, 996
2	Tow	10:50	11:05	$\varphi=77^{\circ}43,96'$ $\lambda=125^{\circ}57,15'$	$\varphi=77^{\circ}44,44'$ $\lambda=125^{\circ}58,88'$		
3	Microstructure	10:15	10:45	$\varphi=77^{\circ}43,95'$ $\lambda=125^{\circ}57,13'$	$\varphi=77^{\circ}43,93'$ $\lambda=125^{\circ}57,10'$		

Station Number: VB0707 Data: 18/09/07 Time of beginning: 13:30  
 dd/mm/yy hh:mm (GMT)  
 Latitude: 78° 04,83' N Longitude: 125° 58,85' E Depth: >2000 m Ice: 0

#	Research Activity	Time, GMT		GPS Position		Comments 1	Comments 2
		beginning	end	beginning	end		
1	CTD/Rosette	13:45	14:40	$\varphi=78^{\circ}04,83'$ $\lambda=125^{\circ}58,85'$	$\varphi=78^{\circ}04,27'$ $\lambda=125^{\circ}57,60'$		Sampling levels: 4, 6, 7, 30, 31, 50, 52, 100, 102, 200, 247, 250, 253, 300, 399, 498, 598, 655, 696, 699, 795, 991, 993, 994
2	Tow	15:15	15:30	$\varphi=78^{\circ}04,03'$ $\lambda=125^{\circ}56,92'$	$\varphi=78^{\circ}04,45'$ $\lambda=125^{\circ}57,66'$		
3	Microstructure	14:40	15:05	$\varphi=78^{\circ}04,27'$ $\lambda=125^{\circ}57,60'$	$\varphi=78^{\circ}04,03'$ $\lambda=125^{\circ}56,92'$		

Station Number: VB0807 Data: 18/09/07 Time of beginning: 18:22  
 dd/mm/yy hh:mm (GMT)  
 Latitude: 78° 27,99' N Longitude: 125° 43,79' E Depth: >2000 m Ice: 0

#	Research Activity	Time, GMT		GPS Position		Comments 1	Comments 2
		beginning	end	beginning	end		
1	CTD/Rosette	18:22	19:10	$\varphi=78^{\circ}27,99'$ $\lambda=125^{\circ}43,79'$	$\varphi=78^{\circ}27,27'$ $\lambda=125^{\circ}43,60'$		Sampling levels: 5, 6, 8, 31, 33, 50, 52, 100, 101, 201, 248, 250, 251, 300, 399, 497, 597, 655, 697, 698, 796, 992, 994, 995
2	Mooring deployment	03:09	05:50	$\varphi=78^{\circ}28,80'$ $\lambda=125^{\circ}43,68'$	$\varphi=78^{\circ}29,58'$ $\lambda=125^{\circ}49,09'$		
3	Tow	20:00	20:16	$\varphi=78^{\circ}26,72'$ $\lambda=125^{\circ}43,19'$	$\varphi=78^{\circ}27,16'$ $\lambda=125^{\circ}44,81'$		
4	Mooring recovering	20:30		$\varphi=78^{\circ}24,56'$ $\lambda=125^{\circ}40,19'$			
5	Microstructure	19:10	19:50	$\varphi=78^{\circ}27,27'$ $\lambda=125^{\circ}43,60'$	$\varphi=78^{\circ}26,76'$ $\lambda=125^{\circ}42,34'$		

Station Number: VB0907 Data: 19/09/07 Time of beginning: 09:30  
 dd/mm/yy hh:mm (GMT)  
 Latitude: 78° 55,03' N Longitude: 125° 58,89' E Depth: >2000 m Ice: 0

#	Research Activity	Time, GMT		GPS Position		Comments 1	Comments 2
		beginning	end	beginning	end		
1	CTD/Rosette	09:40	10:30	$\varphi=78^{\circ}55,05'$ $\lambda=125^{\circ}58,90'$	$\varphi=78^{\circ}54,62'$ $\lambda=125^{\circ}57,45'$		Sampling levels: 5, 6, 7, 30, 33, 50, 52, 100, 102, 200, 248, 251, 252, 299, 399, 498, 596, 655, 696, 698, 796, 991, 993, 996
2	Tow	10:58	11:19	$\varphi=78^{\circ}54,43'$ $\lambda=125^{\circ}57,31'$	$\varphi=78^{\circ}54,98'$ $\lambda=125^{\circ}58,80'$		
3	Microstructure	10:25	10:55	$\varphi=78^{\circ}54,62'$ $\lambda=125^{\circ}57,45'$	$\varphi=78^{\circ}54,45'$ $\lambda=125^{\circ}56,68'$		

Station Number: VB1007 Data: 19/09/07 Time of beginning: 14:33  
 dd/mm/yy hh:mm (GMT)  
 Latitude: 79° 24,99' N Longitude: 126° 00,09' E Depth: >2000 m Ice: 0

#	Research Activity	Time, GMT		GPS Position		Comments 1	Comments 2
		beginning	end	beginning	end		
1	CTD/Rosette	14:47	15:37	$\varphi=79^{\circ}24,99'$ $\lambda=125^{\circ}59,45'$	$\varphi=79^{\circ}24,82'$ $\lambda=125^{\circ}59,29'$		Sampling levels: 5, 6, 7, 30, 33, 50, 52, 100, 102, 200, 248, 250, 251, 300, 399, 498, 597, 655, 696, 699, 796, 991, 994, 995
2	Tow	15:53	16:15	$\varphi=79^{\circ}24,68'$ $\lambda=126^{\circ}00,13'$	$\varphi=79^{\circ}25,36'$ $\lambda=126^{\circ}01,12'$		
3	Microstructure	15:30	15:45	$\varphi=79^{\circ}24,82'$ $\lambda=125^{\circ}59,29'$	$\varphi=79^{\circ}24,76'$ $\lambda=125^{\circ}59,36'$		

Station Number: VB1107 Data: 19/09/07 Time of beginning: 18:51  
 dd/mm/yy hh:mm (GMT)  
 Latitude: 79° 50,06' N Longitude: 125° 59,54' E Depth: >2000 m Ice: 0

#	Research	Time, GMT	GPS Position	Com-
---	----------	-----------	--------------	------

#	Activity	Time, GMT		GPS Position		ments 1	Comments 2
		beginning	end	beginning	end		
1	CTD/Rosette	19:03	19:54	$\varphi=79^{\circ}50,06'$ $\lambda=125^{\circ}59,54'$	$\varphi=79^{\circ}49,84'$ $\lambda=125^{\circ}58,57'$		Sampling levels: 5, 6, 7, 30, 32, 50, 52, 100, 102, 200, 248, 250, 252, 299, 398, 498, 598, 655, 696, 698, 796, 991, 993, 996
2	Tow	20:14	20:31	$\varphi=79^{\circ}49,55'$ $\lambda=125^{\circ}58,71'$	$\varphi=79^{\circ}49,76'$ $\lambda=125^{\circ}59,72'$		
3	Microstructure	19:50	20:13	$\varphi=79^{\circ}49,84'$ $\lambda=125^{\circ}58,57'$	$\varphi=79^{\circ}49,55'$ $\lambda=125^{\circ}58,71'$		

Station Number: VB1207 Data: 20/09/07 Time of beginning: 23:32  
dd/mm/yy hh:mm (GMT)  
Latitude: 80° 01,09' N Longitude: 128° 20,42' E Depth: >2000 m Ice: 0

#	Research Activity	Time, GMT		GPS Position		Com- ments 1	Comments 2
		beginning	end	beginning	end		
1	XCTD	23:32	23:37	$\varphi=80^{\circ}01,09'$ $\lambda=128^{\circ}20,42'$	$\varphi=80^{\circ}01,17'$ $\lambda=128^{\circ}19,31'$		

Station Number: VB1307 Data: 20/09/07 Time of beginning: 02:23  
dd/mm/yy hh:mm (GMT)  
Latitude: 80° 12,39' N Longitude: 130° 47,28' E Depth: >2000 m Ice: 0

#	Research Activity	Time, GMT		GPS Position		Com- ments 1	Comments 2
		beginning	end	beginning	end		
1	XCTD	02:23	02:28	$\varphi=80^{\circ}12,39'$ $\lambda=130^{\circ}47,28'$	$\varphi=80^{\circ}12,50'$ $\lambda=130^{\circ}46,18'$		

Station Number: VB1407 Data: 20/09/07 Time of beginning: 05:15  
dd/mm/yy hh:mm (GMT)  
Latitude: 80° 23,95' N Longitude: 133° 23,04' E Depth: >2000 m Ice: 0

#	Research Activity	Time, GMT		GPS Position		Com- ments 1	Comments 2
		beginning	end	beginning	end		
1	XCTD	05:15	05:20	$\varphi=80^{\circ}23,95'$ $\lambda=133^{\circ}23,04'$	$\varphi=80^{\circ}24,62'$ $\lambda=133^{\circ}22,15'$		

Station Number: VB1507 Data: 20/09/07 Time of beginning: 08:08  
dd/mm/yy hh:mm (GMT)  
Latitude: 80° 35,29' N Longitude: 136° 00,95' E Depth: >2000 m Ice: 0

#	Research	Time, GMT	GPS Position	Com-
---	----------	-----------	--------------	------

#	Activity	Time, GMT		GPS Position		ments 1	Comments 2
		beginning	end	beginning	end		
1	XCTD	08:08	08:13	$\varphi=80^{\circ}35,29'$ $\lambda=136^{\circ}00,95'$	$\varphi=80^{\circ}35,70'$ $\lambda=136^{\circ}00,01'$		

Station Number: VB1607 Data: 20/09/07 Time of beginning: 11:10  
dd/mm/yy hh:mm (GMT)  
Latitude: 80° 47,07' N Longitude: 138° 42,54' E Depth: 2050 m Ice: 0

#	Research Activity	Time, GMT		GPS Position		Comments 1	Comments 2
		beginning	end	beginning	end		
1	CTD/Rosette	11:23	12:56	$\varphi=80^{\circ}47,07'$ $\lambda=138^{\circ}42,57'$	$\varphi=80^{\circ}47,27'$ $\lambda=138^{\circ}38,35'$		Sampling levels: 5, 7, 8, 50, 52, 53, 100, 102, 298, 300, 498, 696, 795, 993, 1191, 1389, 1586, 1784, 1881, 1883, 1885, 2009, 2011, 2011
2	Mooring deployment	14:40	17:44	$\varphi=80^{\circ}46,93'$ $\lambda=138^{\circ}47,95'$	$\varphi=80^{\circ}47,03'$ $\lambda=138^{\circ}47,23'$		
3	Tow	17:51	18:14	$\varphi=80^{\circ}47,02'$ $\lambda=138^{\circ}47,08'$	$\varphi=80^{\circ}46,97'$ $\lambda=138^{\circ}50,71'$		
4	Microstructure	13:12	14:00	$\varphi=80^{\circ}47,27'$ $\lambda=138^{\circ}38,35'$	$\varphi=80^{\circ}46,90'$ $\lambda=138^{\circ}38,95'$		

Station Number: VB1707 Data: 20/09/07 Time of beginning: 19:53  
dd/mm/yy hh:mm (GMT)  
Latitude: 80° 35,49' N Longitude: 139° 36,39' E Depth: >2000 m Ice: 0

#	Research Activity	Time, GMT		GPS Position		Comments 1	Comments 2
		beginning	end	beginning	end		
1	CTD/Rosette	20:01	20:41	$\varphi=80^{\circ}35,68'$ $\lambda=139^{\circ}36,30'$	$\varphi=80^{\circ}36,10'$ $\lambda=139^{\circ}35,78'$		Sampling levels: 5, 6, 7, 30, 33, 50, 52, 100, 102, 200, 247, 250, 253, 300, 399, 497, 598, 654, 696, 698, 796, 991, 994, 996
2	Tow	21:12	21:35	$\varphi=80^{\circ}36,10'$ $\lambda=139^{\circ}35,80'$	$\varphi=80^{\circ}36,15'$ $\lambda=139^{\circ}38,94'$		
3	Microstructure	20:40	21:11	$\varphi=80^{\circ}36,10'$ $\lambda=139^{\circ}35,78'$	$\varphi=80^{\circ}36,10'$ $\lambda=139^{\circ}35,80'$		

Station Number: VB1807 Data: 20/09/07 Time of beginning: 23:08  
dd/mm/yy hh:mm (GMT)  
Latitude: 80° 25,16' N Longitude: 140° 19,27' E Depth: 1700 m Ice: 0

#	Research Activity	Time, GMT		GPS Position		Comments 1	Comments 2
		beginning	end	beginning	end		
1	CTD/Rosette	23:09	23:47	$\varphi=80^{\circ}25,16'$ $\lambda=140^{\circ}19,27'$	$\varphi=80^{\circ}25,41'$ $\lambda=140^{\circ}18,18'$		Sampling levels: 5, 6, 7, 30, 32, 50, 52, 100, 103, 200, 248, 250, 252, 300, 399, 499, 597, 655, 696, 698, 796, 991, 993, 996
2	Microstructure	23:45	00:20	$\varphi=80^{\circ}25,41'$ $\lambda=140^{\circ}18,18'$	$\varphi=80^{\circ}25,49'$ $\lambda=140^{\circ}17,17'$		

Station Number: VB1907 Data: 21/09/07 Time of beginning: 02:00  
dd/mm/yy hh:mm (GMT)  
Latitude: 80° 15,11' N Longitude: 140° 58,90' E Depth: 1614 m Ice: 0

#	Research Activity	Time, GMT		GPS Position		Comments 1	Comments 2
		beginning	end	beginning	end		
1	CTD/Rosette	02:02	03:05	$\varphi=80^{\circ}15,11'$ $\lambda=140^{\circ}58,83'$	$\varphi=80^{\circ}14,85'$ $\lambda=140^{\circ}53,96'$		Sampling levels: 5, 7, 51, 53, 100, 102, 201, 203, 300, 399, 498, 500, 795, 993, 1092, 1191, 1290, 1488, 1557, 1558, 1576, 1578, 1596, 1597
2	Microstructure	03:04	03:28	$\varphi=80^{\circ}14,85'$ $\lambda=140^{\circ}53,96'$	$\varphi=80^{\circ}14,80'$ $\lambda=140^{\circ}52,06'$		

Station Number: VB2007 Data: 21/09/07 Time of beginning: 05:00  
dd/mm/yy hh:mm (GMT)  
Latitude: 80° 04,99' N Longitude: 141° 34,33' E Depth: >2000 m Ice: 0

#	Research	Time, GMT	GPS Position	Com-
---	----------	-----------	--------------	------

#	Activity	Time, GMT		GPS Position		ments 1	Comments 2
		beginning	end	beginning	end		
1	CTD/Rosette	05:02	05:49	$\varphi=80^{\circ}04,99'$ $\lambda=141^{\circ}34,33'$	$\varphi=80^{\circ}05,15'$ $\lambda=141^{\circ}32,80'$		Sampling levels: 5, 6, 7, 30, 33, 50, 52, 100, 102, 200, 248, 250, 252, 300, 399, 498, 598, 654, 697, 699, 796, 991, 994, 995
2	Tow	06:05	06:29	$\varphi=80^{\circ}05,29'$ $\lambda=141^{\circ}32,02'$	$\varphi=80^{\circ}05,46'$ $\lambda=141^{\circ}35,87'$		
3	Microstructure	05:47	06:05	$\varphi=80^{\circ}05,15'$ $\lambda=141^{\circ}32,80'$	$\varphi=80^{\circ}05,29'$ $\lambda=141^{\circ}32,02'$		

Station Number: VB2107 Data: 21/09/07 Time of beginning: 08:00  
dd/mm/yy hh:mm (GMT)  
Latitude: 79°56,23' N Longitude: 142°18,65' E Depth: 1347 m Ice: 0

#	Research Activity	Time, GMT		GPS Position		Com-ments 1	Comments 2
		beginning	end	beginning	end		
1	CTD/Rosette	11:26	12:34	$\varphi=79^{\circ}55,84'$ $\lambda=142^{\circ}14,71'$	$\varphi=79^{\circ}55,78'$ $\lambda=142^{\circ}11,42'$		Sampling levels: 5, 7, 9, 30, 51, 101, 200, 250, 252, 299, 399, 498, 597, 696, 698, 796, 894, 994, 1092, 1191, 1290, 1307, 1309, 1310
2	Tow	12:55	13:22	$\varphi=79^{\circ}55,61'$ $\lambda=142^{\circ}10,99'$	$\varphi=79^{\circ}55,30'$ $\lambda=142^{\circ}11,44'$		
3	Mooring recovering	08:15	10:40	$\varphi=79^{\circ}56,23'$ $\lambda=142^{\circ}18,65'$	$\varphi=79^{\circ}55,84'$ $\lambda=142^{\circ}14,64'$		
4	Microstructure	12:29	12:55	$\varphi=79^{\circ}55,78'$ $\lambda=142^{\circ}11,39'$	$\varphi=79^{\circ}57,29'$ $\lambda=142^{\circ}12,02'$		

Station Number: VB2207 Data: 21/09/07 Time of beginning: 14:20  
dd/mm/yy hh:mm (GMT)  
Latitude: 79°46,96' N Longitude: 142°30,19' E Depth: 1200 m Ice: 0

#	Research	Time, GMT	GPS Position	Com-
---	----------	-----------	--------------	------

#	Activity	Time, GMT		GPS Position		ments 1	Comments 2
		beginning	end	Beginning	end		
1	CTD/Rosette	14:24	15:16	$\varphi=79^{\circ}46,96'$ $\lambda=142^{\circ}30,19'$	$\varphi=79^{\circ}47,33'$ $\lambda=142^{\circ}28,19'$		Sampling levels: 5, 7, 9, 30, 32, 50, 52, 100, 103, 200, 247, 250, 252, 299, 399, 498, 597, 654, 696, 699, 795, 991, 994, 995
2	Tow	15:57	16:17	$\varphi=79^{\circ}47,76'$ $\lambda=142^{\circ}27,63'$	$\varphi=79^{\circ}47,40'$ $\lambda=142^{\circ}29,40'$		
3	Microstructure	15:16	15:51	$\varphi=79^{\circ}47,33'$ $\lambda=142^{\circ}28,19'$	$\varphi=79^{\circ}47,76'$ $\lambda=142^{\circ}27,63'$		

Station Number: VB2307 Data: 21/09/07 Time of beginning: 17:35  
dd/mm/yy hh:mm (GMT)  
Latitude: 79° 37,17' N Longitude: 142° 41,22' E Depth: 1120 m Ice: 0

#	Research Activity	Time, GMT		GPS Position		Comments 1	Comments 2
		beginning	end	Beginning	end		
1	CTD/Rosette	17:47	18:40	$\varphi=79^{\circ}37,17'$ $\lambda=142^{\circ}41,22'$	$\varphi=79^{\circ}37,92'$ $\lambda=142^{\circ}42,22'$		Sampling levels: 5, 6, 9, 31, 51, 101, 200, 249, 251, 299, 399, 497, 597, 599, 696, 698, 795, 796, 993, 994, 994, 994, 995
2	Tow	19:08	19:24	$\varphi=79^{\circ}37,97'$ $\lambda=142^{\circ}43,55'$	$\varphi=79^{\circ}37,68'$ $\lambda=142^{\circ}45,62'$		
3	Microstructure	18:35	19:00	$\varphi=79^{\circ}37,92'$ $\lambda=142^{\circ}42,22'$	$\varphi=79^{\circ}37,98'$ $\lambda=142^{\circ}43,54'$		

Station Number: VB2407 Data: 21/09/07 Time of beginning: 20:58  
dd/mm/yy hh:mm (GMT)  
Latitude: 79° 25,03' N Longitude: 143° 00,48' E Depth: 563 m Ice: 0

#	Research	Time, GMT	GPS Position	Com-
---	----------	-----------	--------------	------

#	Activity	Time, GMT		GPS Position		ments 1	Comments 2
		beginning	end	Beginning	end		
1	CTD/Rosette	21:00	21:24	$\varphi=79^{\circ}25,03'$ $\lambda=143^{\circ}00,48'$	$\varphi=79^{\circ}25,17'$ $\lambda=143^{\circ}00,22'$		Sampling levels: 4, 5, 6, 30, 32, 50, 52, 100, 102, 200, 248, 250, 252, 300, 399, 497, 497, 497, 498, 498, 498, 499, 499, 499
2	Tow	21:53	22:13	$\varphi=79^{\circ}25,22'$ $\lambda=142^{\circ}59,47'$	$\varphi=79^{\circ}24,71'$ $\lambda=143^{\circ}00,84'$		
3	Microstructure	21:25	21:49	$\varphi=79^{\circ}25,17'$ $\lambda=143^{\circ}00,22'$	$\varphi=79^{\circ}25,31'$ $\lambda=142^{\circ}59,83'$		

Station Number: VB2507 Data: 21/09/07 Time of beginning: 23:38  
dd/mm/yy hh:mm (GMT)  
Latitude: 79° 15,07' N Longitude: 143° 30,64' E Depth: 214 m Ice: 0

#	Research Activity	Time, GMT		GPS Position		Comments 1	Comments 2
		beginning	end	Beginning	end		
1	CTD/Rosette	23:38	23:48	$\varphi=79^{\circ}15,07'$ $\lambda=143^{\circ}30,64'$	$\varphi=79^{\circ}15,16'$ $\lambda=143^{\circ}30,77'$		Sampling levels: 4, 6, 7, 11, 12, 16, 17, 19, 20, 23, 25, 51, 52, 76, 79, 100, 102, 151, 153, 175, 200, 201, 205, 206
2	Tow	00:14	00:32	$\varphi=79^{\circ}15,42'$ $\lambda=143^{\circ}29,30'$	$\varphi=79^{\circ}15,04'$ $\lambda=143^{\circ}30,26'$		
3	Microstructure	23:48	00:13	$\varphi=79^{\circ}15,16'$ $\lambda=143^{\circ}30,77'$	$\varphi=79^{\circ}15,42'$ $\lambda=143^{\circ}29,30'$		

Station Number: VB2607 Data: 22/09/07 Time of beginning: 02:22  
dd/mm/yy hh:mm (GMT)  
Latitude: 79° 00,05' N Longitude: 144° 00,83' E Depth: 100 m Ice: 0

#	Research Activity	Time, GMT		GPS Position		Comments 1	Comments 2
		beginning	end	Beginning	end		

1	CTD/Rosette	02:24	02:33	$\varphi=79^{\circ}00,06'$ $\lambda=144^{\circ}00,84'$	$\varphi=79^{\circ}00,21'$ $\lambda=144^{\circ}00,68'$		Sampling levels: 2, 3, 4, 5, 6, 7, 9, 10, 11, 12, 17, 19, 21, 24, 31, 41, 51, 61, 71, 72, 85, 87, 95, 96
2	Microstructure	02:30	02:53	$\varphi=79^{\circ}00,21'$ $\lambda=144^{\circ}00,68'$	$\varphi=79^{\circ}00,42'$ $\lambda=144^{\circ}00,30'$		

Station Number: VB2707 Data: 22/09/07 Time of beginning: 17:55  
dd/mm/yy hh:mm (GMT)  
Latitude: 78° 16,99' N Longitude: 155° 43,10' E Depth: 78 m Ice: 0

#	Research Activity	Time, GMT		GPS Position		Comments 1	Comments 2
		beginning	end	Beginning	end		
1	CTD/Rosette	18:04	18:19	$\varphi=78^{\circ}16,99'$ $\lambda=155^{\circ}43,10'$	$\varphi=78^{\circ}17,25'$ $\lambda=155^{\circ}43,46'$		Sampling levels: 2, 4, 5, 7, 9, 11, 11, 12, 12, 12, 12, 16, 17, 21, 31, 32, 41, 43, 50, 51, 64, 65, 72, 73
2	Tow	18:21	18:45	$\varphi=78^{\circ}17,26'$ $\lambda=155^{\circ}43,25'$	$\varphi=78^{\circ}16,65'$ $\lambda=155^{\circ}43,26'$		

Station Number: VB2807 Data: 22/09/07 Time of beginning: 20:40  
dd/mm/yy hh:mm (GMT)  
Latitude: 78° 32,08' N Longitude: 156° 16,60' E Depth: 85 m Ice: 0

#	Research Activity	Time, GMT		GPS Position		Comments 1	Comments 2
		beginning	end	Beginning	end		
1	CTD/Rosette	20:46	20:51	$\varphi=78^{\circ}32,08'$ $\lambda=156^{\circ}16,60'$	$\varphi=78^{\circ}32,18'$ $\lambda=156^{\circ}16,82'$		Sampling levels: 3, 4, 5, 6, 6, 7, 8, 10, 11, 12, 14, 16, 18, 22, 30, 32, 41, 52, 61, 63, 76, 76, 80, 81
2	Tow	21:02	21:15	$\varphi=78^{\circ}32,03'$ $\lambda=156^{\circ}16,65'$	$\varphi=78^{\circ}31,60'$ $\lambda=156^{\circ}17,02'$		

Station Number: VB2907 Data: 22/09/07 Time of beginning: 22:55  
dd/mm/yy hh:mm (GMT)  
Latitude: 78° 45,01' N Longitude: 156° 49,99' E Depth: 128 m Ice: 0

#	Research	Time, GMT	GPS Position	Com-
---	----------	-----------	--------------	------

#	Activity	Time, GMT		GPS Position		ments 1	Comments 2
		beginning	end	Beginning	end		
1	CTD/Rosette	22:58	23:06	$\varphi=78^{\circ}45,01'$ $\lambda=156^{\circ}50,00'$	$\varphi=78^{\circ}45,04'$ $\lambda=156^{\circ}50,09'$		Sampling levels: 5, 5, 6, 10, 13, 15, 16, 18, 21, 22, 23, 50, 53, 75, 77, 91, 100, 103, 111, 113, 121, 122, 123, 125
2	Tow	23:14	23:29	$\varphi=78^{\circ}44,89'$ $\lambda=156^{\circ}49,98'$	$\varphi=78^{\circ}44,46'$ $\lambda=156^{\circ}50,47'$		

Station Number: VB3007 Data: 23/09/07 Time of beginning: 01:25  
dd/mm/yy hh:mm (GMT)  
Latitude: 79°00,12' N Longitude: 157°23,98' E Depth: 155 m Ice: 0

#	Research Activity	Time, GMT		GPS Position		Com-ments 1	Comments 2
		beginning	end	Beginning	end		
1	CTD/Rosette	01:27	01:37	$\varphi=79^{\circ}00,12'$ $\lambda=157^{\circ}23,98'$	$\varphi=79^{\circ}00,14'$ $\lambda=157^{\circ}24,24'$		Sampling levels: 5, 6, 11, 31, 33, 51, 53, 76, 78, 100, 102, 111, 113, 121, 123, 131, 133, 140, 141, 145, 146, 148, 150, 151
2	Tow	01:44	02:02	$\varphi=79^{\circ}00,09'$ $\lambda=157^{\circ}23,78'$	$\varphi=78^{\circ}59,47'$ $\lambda=157^{\circ}24,23'$		

Station Number: VB3107 Data: 23/09/07 Time of beginning: 03:16  
dd/mm/yy hh:mm (GMT)  
Latitude: 79°09,06' N Longitude: 157°47,10' E Depth: 160 m Ice: 0

#	Research Activity	Time, GMT		GPS Position		Com-ments 1	Comments 2
		beginning	end	Beginning	end		

1	CTD/Rosette	03:18	03:25	$\phi = 79^{\circ} 09,06'$ $\lambda = 157^{\circ} 47,10'$	$\phi = 79^{\circ} 08,99'$ $\lambda = 157^{\circ} 47,12'$		Sampling levels: 6, 7, 12, 31, 33, 51, 53, 76, 78, 101, 103, 111, 112, 121, 124, 131, 133, 140, 143, 145, 147, 149, 150, 150
---	-------------	-------	-------	--	--	--	---

Station Number: VB3207 Data: 23/09/07 Time of beginning: 04:45  
dd/mm/yy hh:mm (GMT)  
Latitude: 79° 18,98' N Longitude: 158° 10,62' E Depth: 225 m Ice: 0

#	Research Activity	Time, GMT		GPS Position		Comments 1	Comments 2
		beginning	end	Beginning	end		
1	CTD/Rosette	04:50	05:00	$\phi = 79^{\circ} 18,99'$ $\lambda = 158^{\circ} 10,62'$	$\phi = 79^{\circ} 18,99'$ $\lambda = 158^{\circ} 11,08'$		Sampling levels: 4, 6, 8, 10, 13, 15, 16, 18, 20, 22, 22, 50, 52, 75, 77, 101, 103, 150, 152, 175, 177, 199, 200, 202

Station Number: VB3307 Data: 23/09/07 Time of beginning: 06:10  
dd/mm/yy hh:mm (GMT)  
Latitude: 79° 28,08' N Longitude: 158° 35,08' E Depth: 348 m Ice: 0

#	Research Activity	Time, GMT		GPS Position		Comments 1	Comments 2
		beginning	end	Beginning	end		
1	CTD/Rosette	06:13	06:26	$\phi = 79^{\circ} 28,08'$ $\lambda = 158^{\circ} 35,08'$	$\phi = 79^{\circ} 28,10'$ $\lambda = 158^{\circ} 35,40'$		Sampling levels: 5, 6, 10, 11, 31, 51, 53, 101, 104, 151, 153, 174, 201, 203, 230, 233, 259, 260, 289, 292, 310, 312, 319, 321
2	Tow	06:51	07:10	$\phi = 79^{\circ} 28,30'$ $\lambda = 158^{\circ} 35,36'$	$\phi = 79^{\circ} 27,85'$ $\lambda = 158^{\circ} 33,67'$		
3	Microstructure	06:28	06:47	$\phi = 79^{\circ} 28,10'$ $\lambda = 158^{\circ} 35,40'$	$\phi = 79^{\circ} 28,21'$ $\lambda = 158^{\circ} 35,72'$		

Station Number: VB3407 Data: 23/09/07 Time of beginning: 08:33  
dd/mm/yy hh:mm (GMT)  
Latitude: 79° 36,93' N Longitude: 158° 59,23' E Depth: 950 m Ice: 0

#	Research Activity	Time, GMT		GPS Position		Comments 1	Comments 2
		beginning	end	Beginning	end		

1	CTD/Rosette	08:40	09:29	$\phi = 79^{\circ} 36,93'$ $\lambda = 158^{\circ} 59,23'$	$\phi = 79^{\circ} 37,15'$ $\lambda = 159^{\circ} 01,39'$		Sampling levels: 6, 8, 9, 30, 31, 50, 52, 100, 102, 201, 248, 249, 251, 300, 399, 499, 598, 695, 698, 699, 795, 893, 894, 895
2	Tow	09:53	10:14	$\phi = 79^{\circ} 37,17'$ $\lambda = 159^{\circ} 00,71'$	$\phi = 79^{\circ} 36,93'$ $\lambda = 158^{\circ} 59,84'$		
3	Microstructure	09:25	09:48	$\phi = 79^{\circ} 37,14'$ $\lambda = 159^{\circ} 01,38'$	$\phi = 79^{\circ} 37,27'$ $\lambda = 159^{\circ} 02,14'$		

Station Number: VB3507 Data: 23/09/07 Time of beginning: 11:34  
dd/mm/yy hh:mm (GMT)  
Latitude: 79° 46,02' N Longitude: 159° 24,40' E Depth: 1511 m Ice: 0

#	Research Activity	Time, GMT		GPS Position		Comments 1	Comments 2
		beginning	end	Beginning	end		
1	CTD/Rosette	11:58	12:48	$\phi = 79^{\circ} 46,12'$ $\lambda = 159^{\circ} 24,75'$	$\phi = 79^{\circ} 46,32'$ $\lambda = 159^{\circ} 25,10'$		Sampling levels: 4, 6, 7, 29, 32, 50, 53, 100, 102, 200, 249, 251, 252, 300, 399, 498, 598, 696, 698, 699, 795, 992, 994, 995
2	Mooring deployment	13:40	16:30	$\phi = 79^{\circ} 46,25'$ $\lambda = 159^{\circ} 24,78'$	$\phi = 79^{\circ} 45,41'$ $\lambda = 159^{\circ} 20,01'$		
3	Tow	17:14	17:33	$\phi = 79^{\circ} 45,40'$ $\lambda = 159^{\circ} 18,56'$	$\phi = 79^{\circ} 44,98'$ $\lambda = 159^{\circ} 19,12'$		
4	Microstructure	11:40 12:48 16:30	11:58 13:20 17:00	$\phi = 79^{\circ} 46,19'$ $\lambda = 159^{\circ} 24,71'$	$\phi = 79^{\circ} 46,20'$ $\lambda = 159^{\circ} 24,70'$		

Station Number: VB3607 Data: 23/09/07 Time of beginning: 19:20  
dd/mm/yy hh:mm (GMT)  
Latitude: 80° 00,07' N Longitude: 159° 59,33' E Depth: >1000 m Ice: 0

#	Research Activity	Time, GMT		GPS Position		Comments 1	Comments 2
		beginning	end	Beginning	end		

1	CTD/Rosette	19:48	20:30	$\varphi=80^{\circ}00,14'$ $\lambda=159^{\circ}58,31'$	$\varphi=80^{\circ}00,27'$ $\lambda=159^{\circ}56,77'$		Sampling levels: 5, 7, 9, 30, 31, 50, 52, 100, 103, 201, 249, 252, 252, 300, 398, 497, 597, 696, 696, 696, 796, 992, 994, 995
2	Tow	21:12	21:30	$\varphi=80^{\circ}00,34'$ $\lambda=159^{\circ}54,66'$	$\varphi=80^{\circ}00,11'$ $\lambda=159^{\circ}56,93'$		
3	Microstructure	19:20 20:35	19:40 21:05	$\varphi=80^{\circ}00,00'$ $\lambda=159^{\circ}56,34'$	$\varphi=80^{\circ}00,42'$ $\lambda=159^{\circ}54,89'$		

Station Number: VB3707 Data: 23/09/07 Time of beginning: 23:10  
dd/mm/yy hh:mm (GMT)  
Latitude: 80° 13,59' N Longitude: 160° 37,50' E Depth: >2000 m Ice: 0

#	Research Activity	Time, GMT		GPS Position		Comments 1	Comments 2
		beginning	end	Beginning	end		
1	CTD/Rosette	23:14	23:53	$\varphi=80^{\circ}13,59'$ $\lambda=160^{\circ}37,50'$	$\varphi=80^{\circ}13,84'$ $\lambda=160^{\circ}36,26'$		Sampling levels: 5, 6, 6, 30, 33, 50, 53, 99, 100, 201, 249, 250, 252, 300, 399, 497, 598, 696, 697, 698, 796, 991, 993, 994
2	Tow	00:02	00:22	$\varphi=80^{\circ}13,79'$ $\lambda=160^{\circ}30,23'$	$\varphi=80^{\circ}14,15'$ $\lambda=160^{\circ}40,14'$		

Station Number: VB3807 Data: 24/09/07 Time of beginning: 01:58  
dd/mm/yy hh:mm (GMT)  
Latitude: 80° 26,99' N Longitude: 161° 14,59' E Depth: >2000 m Ice: 0

#	Research Activity	Time, GMT		GPS Position		Comments 1	Comments 2
		beginning	end	Beginning	end		

1	CTD/Rosette	02:00	02:40	$\varphi=80^{\circ}26,99'$ $\lambda=161^{\circ}14,59'$	$\varphi=80^{\circ}26,74'$ $\lambda=161^{\circ}13,73'$		Sampling levels: 5, 7, 6, 30, 33, 51, 53, 100, 103, 201, 249, 250, 252, 299, 399, 498, 598, 695, 697, 700, 795, 992, 993, 995
2	Mooring deployment	03:15	11:38	$\varphi=80^{\circ}26,47'$ $\lambda=161^{\circ}12,23'$	$\varphi=80^{\circ}20,93'$ $\lambda=161^{\circ}15,76'$		
3	Tow	11:53	12:11	$\varphi=80^{\circ}21,69'$ $\lambda=161^{\circ}07,24'$	$\varphi=80^{\circ}21,98'$ $\lambda=161^{\circ}06,16'$		
4	Microstructure	02:40	03:09	$\varphi=80^{\circ}26,52'$ $\lambda=161^{\circ}12,95'$	$\varphi=80^{\circ}26,52'$ $\lambda=161^{\circ}12,95'$		

Station Number: VB3907 Data: 24/09/07 Time of beginning: 14:50  
dd/mm/yy hh:mm (GMT)  
Latitude: 80° 39,90' N Longitude: 161° 52,65' E Depth: >1000 m Ice: 0

#	Research Activity	Time, GMT		GPS Position		Comments 1	Comments 2
		beginning	end	Beginning	end		
1	CTD/Rosette	15:01	15:50	$\varphi=80^{\circ}39,79'$ $\lambda=161^{\circ}53,83'$	$\varphi=80^{\circ}39,44'$ $\lambda=161^{\circ}58,57'$		Sampling levels: 5, 6, 7, 30, 31, 50, 51, 100, 102, 199, 248, 250, 252, 299, 399, 498, 598, 697, 698, 795, 991, 992, 994
2	Tow	16:24	16:42	$\varphi=80^{\circ}39,40'$ $\lambda=161^{\circ}59,92'$	$\varphi=80^{\circ}39,44'$ $\lambda=161^{\circ}57,36'$		
3	Microstructure	15:45	16:18	$\varphi=80^{\circ}39,43'$ $\lambda=161^{\circ}58,63'$	$\varphi=80^{\circ}39,52'$ $\lambda=161^{\circ}58,75'$		

Station Number: VB4007 Data: 24/09/07 Time of beginning: 18:20  
dd/mm/yy hh:mm (GMT)  
Latitude: 80° 52,81' N Longitude: 162° 28,75' E Depth: >2000 m Ice: 0

#	Research Activity	Time, GMT		GPS Position		Comments 1	Comments 2
		beginning	end	Beginning	end		

1	CTD/Rosette	18:33	19:23	$\varphi=80^{\circ}52,71'$ $\lambda=162^{\circ}29,36'$	$\varphi=80^{\circ}52,50'$ $\lambda=162^{\circ}31,91'$		Sampling levels: 5, 6, 7, 30, 32, 50, 53, 100, 101, 199, 248, 250, 252, 299, 399, 498, 597, 696, 698, 699, 796, 991, 993, 995
2	Tow	19:49	20:02	$\varphi=80^{\circ}52,63'$ $\lambda=162^{\circ}32,58'$	$\varphi=80^{\circ}52,73'$ $\lambda=162^{\circ}30,12'$		
3	Microstructure	19:18	19:42	$\varphi=80^{\circ}52,50'$ $\lambda=162^{\circ}31,88'$	$\varphi=80^{\circ}52,55'$ $\lambda=162^{\circ}31,90'$		

Station Number: VB4107 Data: 25/09/07 Time of beginning: 04:04  
dd/mm/yy hh:mm (GMT)  
Latitude: 80° 09,97' N Longitude: 156° 00,37' E Depth: 1000 m Ice: 0

#	Research Activity	Time, GMT		GPS Position		Comments 1	Comments 2
		beginning	end	Beginning	end		
1	CTD/Rosette	04:04	04:40	$\varphi=80^{\circ}09,97'$ $\lambda=156^{\circ}00,37'$	$\varphi=80^{\circ}10,39'$ $\lambda=156^{\circ}01,17'$		Sampling levels: 5, 7, 7, 30, 31, 50, 51, 100, 102, 200, 249, 250, 252, 300, 399, 498, 598, 695, 697, 699, 795, 991, 993, 995
2	Tow	04:41	05:09	$\varphi=80^{\circ}10,39'$ $\lambda=156^{\circ}01,17'$	$\varphi=80^{\circ}09,87'$ $\lambda=156^{\circ}00,90'$		

Station Number: VB4207 Data: 25/09/07 Time of beginning: 09:28  
dd/mm/yy hh:mm (GMT)  
Latitude: 80° 16,24' N Longitude: 152° 00,56' E Depth: 1680 m Ice: 0

#	Research Activity	Time, GMT		GPS Position		Comments 1	Comments 2
		beginning	end	Beginning	end		

1	CTD/Rosette	09:42	10:29	$\varphi=80^{\circ}16,43'$ $\lambda=152^{\circ}00,76'$	$\varphi=80^{\circ}17,39'$ $\lambda=152^{\circ}01,14'$		Sampling levels: 5, 6, 8, 30, 32, 50, 53, 100, 102, 200, 249, 251, 253, 300, 399, 498, 597, 695, 696, 698, 795, 990, 990, 990
2	Tow	10:32	10:52	$\varphi=80^{\circ}17,39'$ $\lambda=152^{\circ}00,70'$	$\varphi=80^{\circ}17,16'$ $\lambda=151^{\circ}58,21'$		

Station Number: VB4307 Data: 25/09/07 Time of beginning: 15:14  
dd/mm/yy hh:mm (GMT)  
Latitude: 80°24,08' N Longitude: 148°00,66' E Depth: 1800 m Ice: 0

#	Research Activity	Time, GMT		GPS Position		Comments 1	Comments 2
		beginning	end	Beginning	end		
1	CTD/Rosette	15:47	16:38	$\varphi=80^{\circ}24,70'$ $\lambda=148^{\circ}02,20'$	$\varphi=80^{\circ}25,68'$ $\lambda=148^{\circ}05,04'$		Sampling levels: 5, 7, 8, 30, 32, 50, 52, 99, 101, 200, 248, 250, 252, 300, 399, 498, 597, 695, 696, 698, 796, 991, 993, 994
2	Tow	16:40	17:09	$\varphi=80^{\circ}25,71'$ $\lambda=148^{\circ}04,89'$	$\varphi=80^{\circ}25,34'$ $\lambda=148^{\circ}01,59'$		
3	Microstructure	16:40	17:09	$\varphi=80^{\circ}24,20'$ $\lambda=148^{\circ}01,01'$	$\varphi=80^{\circ}24,69'$ $\lambda=148^{\circ}02,17'$		

Station Number: VB4407 Data: 25/09/07 Time of beginning: 22:18  
dd/mm/yy hh:mm (GMT)  
Latitude: 80°18,84' N Longitude: 144°01,42' E Depth: 1500 m Ice: 0

#	Research Activity	Time, GMT		GPS Position		Comments 1	Comments 2
		beginning	end	Beginning	end		

1	CTD/Rosette	01:13	01:55	$\varphi = 80^{\circ} 20,57'$ $\lambda = 144^{\circ} 07,43'$	$\varphi = 80^{\circ} 21,04'$ $\lambda = 144^{\circ} 08,61'$		Sampling levels: 5, 7, 8, 30, 32, 50, 52, 99, 101, 200, 248, 250, 252, 300, 399, 498, 597, 695, 696, 698, 699, 796, 991, 993, 994
2	Microstructure	22:18 23:00	22:50 23:35	$\varphi = 80^{\circ} 18,84'$ $\lambda = 144^{\circ} 01,44'$	$\varphi = 80^{\circ} 19,56'$ $\lambda = 144^{\circ} 04,52'$		

Station Number: VB4507 Data: 26/09/07 Time of beginning: 06:10  
dd/mm/yy hh:mm (GMT)  
Latitude: 79° 56,56' N Longitude: 142° 24,92' E Depth: >1000 m Ice: 0

#	Research Activity	Time, GMT		GPS Position		Comments 1	Comments 2
		beginning	end	Beginning	end		
1	CTD/Rosette	06:45	07:38	$\varphi = 79^{\circ} 56,96'$ $\lambda = 142^{\circ} 29,21'$	$\varphi = 79^{\circ} 57,57'$ $\lambda = 142^{\circ} 34,53'$		Sampling levels: 5, 6, 7, 29, 31, 50, 51, 100, 102, 200, 249, 250, 252, 300, 399, 498, 598, 695, 697, 699, 795, 991, 992, 994
2	Mooring deployment	13:00	19:27	$\varphi = 79^{\circ} 56,60'$ $\lambda = 142^{\circ} 20,21'$	$\varphi = 79^{\circ} 56,11'$ $\lambda = 142^{\circ} 19,32'$		
3	Microstructure	06:10 07:40 19:30	06:42 08:15 20:02	$\varphi = 79^{\circ} 56,56'$ $\lambda = 142^{\circ} 24,94'$	$\varphi = 79^{\circ} 56,96'$ $\lambda = 142^{\circ} 29,21'$		

Station Number: VB4607 Data: 27/09/07 Time of beginning: 02:10  
dd/mm/yy hh:mm (GMT)  
Latitude: 79° 25,04' N Longitude: 139° 50,91' E Depth: >1000 m Ice: 0

#	Research Activity	Time, GMT		GPS Position		Comments 1	Comments 2
		beginning	end	Beginning	end		

1	CTD/Rosette	02:13	03:03	$\varphi=79^{\circ}25,04'$ $\lambda=139^{\circ}50,91'$	$\varphi=79^{\circ}25,81'$ $\lambda=139^{\circ}55,62'$		Sampling levels: 5, 5, 7, 30, 32, 50, 52, 100, 102, 200, 249, 250, 251, 299, 399, 498, 597, 695, 697, 698, 795, 991, 993, 994
2	Tow	03:13	03:34	$\varphi=79^{\circ}25,84'$ $\lambda=139^{\circ}56,74'$	$\varphi=79^{\circ}25,69'$ $\lambda=140^{\circ}00,30'$		

Station Number: VB4707 Data: 27/09/07 Time of beginning: 08:35  
dd/mm/yy hh:mm (GMT)  
Latitude: 79° 00,25' N Longitude: 137° 40,64' E Depth: >1000 m Ice: 0

#	Research Activity	Time, GMT		GPS Position		Comments 1	Comments 2
		beginning	end	Beginning	end		
1	CTD/Rosette	08:42	09:29	$\varphi=79^{\circ}00,26'$ $\lambda=137^{\circ}40,64'$	$\varphi=79^{\circ}00,88'$ $\lambda=137^{\circ}41,35'$		Sampling levels: 5, 7, 9, 30, 32, 50, 52, 100, 101, 201, 249, 251, 253, 300, 399, 498, 597, 695, 697, 699, 796, 991, 993, 995
2	Tow	09:56	10:18	$\varphi=79^{\circ}01,22'$ $\lambda=137^{\circ}42,32'$	$\varphi=79^{\circ}01,24'$ $\lambda=137^{\circ}40,35'$		
3	Microstructure	09:25	09:51	$\varphi=79^{\circ}00,88'$ $\lambda=137^{\circ}41,35'$	$\varphi=79^{\circ}01,26'$ $\lambda=137^{\circ}41,72'$		

Station Number: VB4807 Data: 27/09/07 Time of beginning: 14:00  
dd/mm/yy hh:mm (GMT)  
Latitude: 78° 39,88' N Longitude: 135° 30,95' E Depth: 1500 m Ice: 0

#	Research Activity	Time, GMT		GPS Position		Comments 1	Comments 2
		beginning	end	Beginning	end		

1	CTD/Rosette	14:08	14:56	$\varphi=78^{\circ} 39,89'$ $\lambda=135^{\circ} 30,97'$	$\varphi=78^{\circ} 39,85'$ $\lambda=135^{\circ} 32,43'$		Sampling levels: 5, 7, 9, 30, 33, 49, 51, 99, 101, 200, 249, 251, 253, 300, 398, 498, 597, 695, 697, 699, 795, 992, 992, 995
2	Tow	15:18	15:37	$\varphi=78^{\circ} 39,82'$ $\lambda=135^{\circ} 33,40'$	$\varphi=78^{\circ} 39,44'$ $\lambda=135^{\circ} 34,03'$		
3	Microstructure	14:56	15:15	$\varphi=78^{\circ} 39,84'$ $\lambda=135^{\circ} 32,45'$	$\varphi=78^{\circ} 39,82'$ $\lambda=135^{\circ} 32,46'$		

Station Number: VB4907 Data: 27/09/07 Time of beginning: 19:37  
dd/mm/yy hh:mm (GMT)  
Latitude: 78° 29,15' N Longitude: 132° 25,80' E Depth: 2050 m Ice: 0

#	Research Activity	Time, GMT		GPS Position		Comments 1	Comments 2
		beginning	end	Beginning	end		
1	CTD/Rosette	19:47	20:30	$\varphi=78^{\circ} 29,08'$ $\lambda=132^{\circ} 25,03'$	$\varphi=78^{\circ} 28,33'$ $\lambda=133^{\circ} 22,69'$		Sampling levels: 5, 7, 9, 30, 31, 50, 52, 100, 101, 199, 249, 251, 252, 299, 399, 498, 597, 695, 696, 699, 795, 992, 993, 995
2	Tow	21:06	21:22	$\varphi=78^{\circ} 27,91'$ $\lambda=132^{\circ} 20,72'$	$\varphi=78^{\circ} 28,18'$ $\lambda=132^{\circ} 18,46'$		
3	Microstructure	20:28	21:02	$\varphi=78^{\circ} 28,33'$ $\lambda=133^{\circ} 22,69'$	$\varphi=78^{\circ} 27,89'$ $\lambda=132^{\circ} 21,23'$		

Station Number: VB5007 Data: 28/09/07 Time of beginning: 01:00  
dd/mm/yy hh:mm (GMT)  
Latitude: 77° 59,98' N Longitude: 130° 29,64' E Depth: >1000 m Ice: 0

#	Research Activity	Time, GMT		GPS Position		Comments 1	Comments 2
		beginning	end	Beginning	end		

1	CTD/Rosette	01:03	01:44	$\varphi=77^{\circ}59,99'$ $\lambda=130^{\circ}29,64'$	$\varphi=77^{\circ}59,61'$ $\lambda=130^{\circ}27,97'$		Sampling levels: 5, 5, 7, 30, 32, 50, 52, 100, 101, 201, 249, 251, 252, 299, 399, 498, 598, 695, 697, 699, 796, 992, 993, 995
2	Tow	02:15	02:33	$\varphi=77^{\circ}59,45'$ $\lambda=130^{\circ}26,26'$	$\varphi=77^{\circ}59,71'$ $\lambda=130^{\circ}24,03'$		
3	Microstructure	01:45	02:12	$\varphi=77^{\circ}59,61'$ $\lambda=130^{\circ}27,97'$	$\varphi=77^{\circ}59,45'$ $\lambda=130^{\circ}26,26'$		

Station Number: VB5107 Data: 28/09/07 Time of beginning: 05:40  
dd/mm/yy hh:mm (GMT)  
Latitude: 77° 44,38' N Longitude: 128° 20,01' E Depth: >1000 m Ice: 0

#	Research Activity	Time, GMT		GPS Position		Comments 1	Comments 2
		beginning	end	Beginning	End		
1	CTD/Rosette	05:40	06:21	$\varphi=77^{\circ}44,98'$ $\lambda=128^{\circ}20,00'$	$\varphi=77^{\circ}44,76'$ $\lambda=128^{\circ}20,35'$		Sampling levels: 4, 6, 8, 30, 31, 50, 52, 100, 102, 201, 249, 251, 252, 300, 399, 497, 597, 695, 697, 699, 795
2	Tow	06:49	07:09	$\varphi=77^{\circ}44,56'$ $\lambda=128^{\circ}20,21'$	$\varphi=77^{\circ}44,52'$ $\lambda=128^{\circ}21,44'$		
3	Microstructure	06:22	06:45	$\varphi=77^{\circ}44,76'$ $\lambda=128^{\circ}20,35'$	$\varphi=77^{\circ}44,56'$ $\lambda=128^{\circ}20,21'$		

Station Number: VB5207 Data: 28/09/07 Time of beginning: 10:00  
dd/mm/yy hh:mm (GMT)  
Latitude: 77° 45,03' N Longitude: 130° 29,96' E Depth: 1500 m Ice: 0

#	Research Activity	Time, GMT		GPS Position		Comments 1	Comments 2
		beginning	end	Beginning	End		

1	CTD/Rosette	10:37	11:20	$\varphi=77^{\circ} 44,80'$ $\lambda=130^{\circ} 29,32'$	$\varphi=77^{\circ} 44,28'$ $\lambda=128^{\circ} 28,35'$		Sampling levels: 5, 7, 9, 30, 32, 50, 52, 100, 102, 200, 249, 251, 300, 399, 499, 597, 696, 795, 796, 819, 820, 824, 825, 826
2	Microstructure	10:00	10:35	$\varphi=77^{\circ} 45,01'$ $\lambda=130^{\circ} 29,49'$	$\varphi=77^{\circ} 44,80'$ $\lambda=130^{\circ} 29,32'$		

Station Number: VB5307 Data: 28/09/07 Time of beginning: 12:50  
dd/mm/yy hh:mm (GMT)  
Latitude: 77° 29,99' N Longitude: 130° 30,45' E Depth: 72 m Ice: 0

#	Research Activity	Time, GMT		GPS Position		Comments 1	Comments 2
		beginning	end	Beginning	End		
1	CTD/Rosette	12:50	13:12	$\varphi=77^{\circ} 29,83'$ $\lambda=130^{\circ} 29,95'$	$\varphi=77^{\circ} 29,85'$ $\lambda=130^{\circ} 29,95'$		Sampling levels: 1, 4, 6, 7, 7, 7, 9, 10, 11, 12, 15, 16, 22, 31, 41, 51, 55, 56, 59, 60, 61, 64, 65, 66
2	Microstructure	13:07	13:27	$\varphi=77^{\circ} 29,85'$ $\lambda=130^{\circ} 29,95'$	$\varphi=77^{\circ} 29,85'$ $\lambda=130^{\circ} 29,59'$		

Station Number: VB5407 Data: 28/09/07 Time of beginning: 15:00  
dd/mm/yy hh:mm (GMT)  
Latitude: 77° 14,98' N Longitude: 130° 30,81' E Depth: 67 m Ice: 0

#	Research Activity	Time, GMT		GPS Position		Comments 1	Comments 2
		beginning	end	Beginning	End		
1	CTD/Rosette	15:00	15:15	$\varphi=77^{\circ} 14,95'$ $\lambda=130^{\circ} 29,99'$	$\varphi=77^{\circ} 14,81'$ $\lambda=130^{\circ} 24,40'$		Sampling levels: 2, 4, 5, 7, 8, 11, 12, 13, 20, 22, 30, 32, 40, 42, 50, 51, 54, 55, 59, 60, 61, 63, 64
2	Microstructure	15:13	15:29	$\varphi=77^{\circ} 14,81'$ $\lambda=130^{\circ} 24,40'$	$\varphi=77^{\circ} 14,63'$ $\lambda=130^{\circ} 28,59'$		

Station Number: VB5507 Data: 28/09/07 Time of beginning: 17:20  
dd/mm/yy hh:mm (GMT)  
Latitude: 76° 59,87' N Longitude: 130° 27,76' E Depth: 60 m Ice: 0

#	Research Activity	Time, GMT		GPS Position		Comments 1	Comments 2
		beginning	end	Beginning	End		

1	CTD/Rosette	17:28	17:41	$\varphi=76^{\circ}59,87'$ $\lambda=130^{\circ}27,71'$	$\varphi=76^{\circ}59,77'$ $\lambda=130^{\circ}26,38'$		Sampling levels: 3, 4, 5, 6, 6, 8, 9, 10, 10, 11, 15, 17, 20, 24, 30, 33, 41, 43, 50, 52, 54, 55, 56
2	Tow	17:55	18:10	$\varphi=77^{\circ}59,78'$ $\lambda=130^{\circ}25,40'$	$\varphi=76^{\circ}59,84'$ $\lambda=130^{\circ}24,98'$		
3	Microstructure	17:36	17:52	$\varphi=76^{\circ}59,80'$ $\lambda=130^{\circ}26,20'$	$\varphi=77^{\circ}59,78'$ $\lambda=130^{\circ}25,40'$		

Station Number: VB5607 Data: 28/09/07 Time of beginning: 20:00  
dd/mm/yy hh:mm (GMT)  
Latitude: 76° 45,18' N Longitude: 130° 29,65' E Depth: 62 m Ice: 0

#	Research Activity	Time, GMT		GPS Position		Comments 1	Comments 2
		beginning	end	Beginning	End		
1	CTD/Rosette	20:04	20:15	$\varphi=76^{\circ}45,18'$ $\lambda=130^{\circ}29,65'$	$\varphi=76^{\circ}45,26'$ $\lambda=130^{\circ}29,10'$		Sampling levels: 2, 3, 5, 5, 7, 8, 9, 10, 12, 12, 15, 17, 20, 21, 22, 30, 31, 41, 42, 51, 51, 54, 55, 56
2	Tow	20:33	20:45	$\varphi=76^{\circ}45,49'$ $\lambda=130^{\circ}28,21'$	$\varphi=76^{\circ}45,90'$ $\lambda=130^{\circ}28,36'$		
3	Microstructure	20:10	20:30	$\varphi=76^{\circ}45,26'$ $\lambda=130^{\circ}29,10'$	$\varphi=76^{\circ}45,49'$ $\lambda=130^{\circ}28,21'$		

Station Number: VB5707 Data: 28/09/07 Time of beginning: 23:30  
dd/mm/yy hh:mm (GMT)  
Latitude: 76° 30,14' N Longitude: 130° 30,01' E Depth: 58 m Ice: 0

#	Research Activity	Time, GMT		GPS Position		Comments 1	Comments 2
		beginning	end	Beginning	End		
1	CTD/Rosette	22:32	22:38	$\varphi=76^{\circ}30,14'$ $\lambda=130^{\circ}30,01'$	$\varphi=76^{\circ}30,23'$ $\lambda=130^{\circ}29,66'$		Sampling levels: 2, 4, 5, 5, 6, 8, 9, 10, 11, 12, 15, 16, 20, 21, 22, 29, 31, 40, 41, 50, 51, 51, 51, 51
2	Microstructure	22:37	22:58	$\varphi=76^{\circ}30,23'$ $\lambda=130^{\circ}29,66'$	$\varphi=77^{\circ}30,46'$ $\lambda=130^{\circ}28,56'$		

Station Number: VB5807 Data: 29/09/07 Time of beginning: 00:45  
dd/mm/yy hh:mm (GMT)  
Latitude: 76° 15,10' N Longitude: 130° 30,29' E Depth: 53 m Ice: 0

#	Research Activity	Time, GMT		GPS Position		Comments 1	Comments 2
		beginning	end	Beginning	End		

1	CTD/Rosette	00:47	00:50	$\varphi=76^{\circ}15,10'$ $\lambda=130^{\circ}30,28'$	$\varphi=76^{\circ}15,18'$ $\lambda=130^{\circ}30,05'$		Sampling levels: 2, 3, 5, 6, 7, 8, 9, 10, 11, 12, 13, 15, 16, 20, 21, 22, 30, 31, 41, 42, 46, 47, 48, 49, 50
2	Tow	01:09	01:22	$\varphi=76^{\circ}15,35'$ $\lambda=130^{\circ}29,76'$	$\varphi=76^{\circ}15,74'$ $\lambda=130^{\circ}30,04'$		
3	Microstructure	00:50	01:09	$\varphi=76^{\circ}15,18'$ $\lambda=130^{\circ}30,05'$	$\varphi=76^{\circ}15,35'$ $\lambda=130^{\circ}29,76'$		

Station Number: VB5907 Data: 29/09/07 Time of beginning: 03:07  
dd/mm/yy hh:mm (GMT)  
Latitude: 76° 00,04' N Longitude: 130° 30,31' E Depth: 51 m Ice: 0

#	Research Activity	Time, GMT		GPS Position		Comments 1	Comments 2
		beginning	end	Beginning	End		
1	CTD/Rosette	03:09	03:14	$\varphi=76^{\circ}00,05'$ $\lambda=130^{\circ}30,32'$	$\varphi=76^{\circ}00,07'$ $\lambda=130^{\circ}30,47'$		Sampling levels: 3, 3, 5, 6, 7, 8, 10, 11, 13, 14, 16, 18, 20, 21, 23, 30, 31, 41, 42, 46, 47, 48, 48, 48

Station Number: VB6007 Data: 29/09/07 Time of beginning: 04:45  
dd/mm/yy hh:mm (GMT)  
Latitude: 75° 44,92' N Longitude: 130° 30,14' E Depth: 48 m Ice: 0

#	Research Activity	Time, GMT		GPS Position		Comments 1	Comments 2
		beginning	end	Beginning	End		
1	CTD/Rosette	04:49	04:55	$\varphi=75^{\circ}44,93'$ $\lambda=130^{\circ}30,15'$	$\varphi=75^{\circ}44,91'$ $\lambda=130^{\circ}29,58'$		Sampling levels: 2, 3, 5, 6, 8, 9, 11, 13, 14, 15, 17, 18, 20, 22, 22, 30, 31, 40, 42, 46, 46, 46, 46, 46

Station Number: VB6107 Data: 29/09/07 Time of beginning: 06:30  
dd/mm/yy hh:mm (GMT)  
Latitude: 75° 29,95' N Longitude: 130° 29,85' E Depth: 53 m Ice: 0

#	Research Activity	Time, GMT		GPS Position		Comments 1	Comments 2
		beginning	end	Beginning	End		

1	CTD/Rosette	06:32	06:40	$\varphi=75^{\circ}29,96'$ $\lambda=130^{\circ}29,86'$	$\varphi=75^{\circ}30,15'$ $\lambda=130^{\circ}29,14'$		Sampling levels: 2, 4, 5, 6, 7, 9, 10, 11, 13, 14, 15, 17, 20, 21, 22, 29, 31, 41, 41, 46, 47, 48, 49, 50
2	Tow	06:43	06:57	$\varphi=75^{\circ}30,15'$ $\lambda=130^{\circ}29,14'$	$\varphi=75^{\circ}30,23'$ $\lambda=130^{\circ}29,67'$		

Station Number: VB6207 Data: 29/09/07 Time of beginning: 08:38  
dd/mm/yy hh:mm (GMT)  
Latitude: 75° 15,13' N Longitude: 130° 30,17' E Depth: 43 m Ice: 0

#	Research Activity	Time, GMT		GPS Position		Comments 1	Comments 2
		beginning	end	Beginning	End		
1	CTD/Rosette	08:48	08:55	$\varphi=75^{\circ}15,24'$ $\lambda=130^{\circ}29,76'$	$\varphi=75^{\circ}17,29'$ $\lambda=130^{\circ}29,39'$		Sampling levels: 3, 4, 5, 7, 9, 10, 11, 11, 11, 12, 15, 17, 20, 22, 23, 30, 31, 39, 40, 41, 41, 41, 41, 41, 41
2	Microstructure	08:53	09:10	$\varphi=75^{\circ}17,29'$ $\lambda=130^{\circ}29,39'$	$\varphi=75^{\circ}19,40'$ $\lambda=130^{\circ}29,15'$		

Station Number: VB6307 Data: 29/09/07 Time of beginning: 10:56  
dd/mm/yy hh:mm (GMT)  
Latitude: 75° 00,05' N Longitude: 130° 30,52' E Depth: 38,5 m Ice: 0

#	Research Activity	Time, GMT		GPS Position		Comments 1	Comments 2
		beginning	end	Beginning	End		
1	CTD/Rosette	11:00	11:12	$\varphi=75^{\circ}00,05'$ $\lambda=130^{\circ}30,52'$	$\varphi=75^{\circ}00,19'$ $\lambda=130^{\circ}30,65'$		Sampling levels: 3, 5, 10, 11,16, 18, 21, 23, 26, 28, 31, 31, 32, 33, 34, 35, 36, 36, 36, 36, 36, 36, 36, 36
2	Tow	11:23	11:35	$\varphi=75^{\circ}00,27'$ $\lambda=130^{\circ}31,20'$	$\varphi=74^{\circ}59,95'$ $\lambda=130^{\circ}31,31'$		
3	Microstructure	11:05	11:18	$\varphi=75^{\circ}00,19'$ $\lambda=130^{\circ}30,65'$	$\varphi=75^{\circ}00,23'$ $\lambda=130^{\circ}30,63'$		

Station Number: VB6407 Data: 29/09/07 Time of beginning: 13:12  
dd/mm/yy hh:mm (GMT)  
Latitude: 74° 45,04' N Longitude: 130° 30,53' E Depth: 30 m Ice: 0

#	Research Activity	Time, GMT		GPS Position		Comments 1	Comments 2
		beginning	end	Beginning	end		

1	CTD/Rosette	13:19	13:31	$\varphi=74^{\circ}45,12'$ $\lambda=130^{\circ}30,73'$	$\varphi=74^{\circ}45,25'$ $\lambda=130^{\circ}30,99'$		Sampling levels: 3, 5, 10,12,16, 18, 20, 22,23, 24, 24, 25, 25, 26, 26, 26, 27, 28, 29,29, 29, 29, 29, 29
2	Tow	13:40	13:55	$\varphi=74^{\circ}45,35'$ $\lambda=130^{\circ}31,60'$	$\varphi=74^{\circ}45,28'$ $\lambda=130^{\circ}32,09'$		
3	Microstructure	13:28	13:38	$\varphi=74^{\circ}45,26'$ $\lambda=130^{\circ}31,01'$	$\varphi=74^{\circ}45,35'$ $\lambda=130^{\circ}31,58'$		

Station Number: VB6507 Data: 29/09/07 Time of beginning: 15:31  
dd/mm/yy hh:mm (GMT)  
Latitude: 74° 30,05' N Longitude: 130° 30,10' E Depth: 26 m Ice: 0

#	Research Activity	Time, GMT		GPS Position		Comments 1	Comments 2
		beginning	end	Beginning	End		
1	CTD/Rosette	15:37	15:44	$\varphi=74^{\circ}30,07'$ $\lambda=130^{\circ}30,11'$	$\varphi=74^{\circ}30,09'$ $\lambda=130^{\circ}29,99'$		Sampling levels: 3, 4, 6, 8, 10, 11, 14, 15, 17, 18, 20, 21, 21, 21, 21, 22, 23, 24, 25, 25, 25, 25, 25, 25
2	Microstructure	15:45	15:53	$\varphi=74^{\circ}30,09'$ $\lambda=130^{\circ}29,99'$	$\varphi=74^{\circ}30,10'$ $\lambda=130^{\circ}29,69'$		

Station Number: VB6607 Data: 29/09/07 Time of beginning: 17:28  
dd/mm/yy hh:mm (GMT)  
Latitude: 74° 15,07' N Longitude: 130° 30,12' E Depth: 27 m Ice: 0

#	Research Activity	Time, GMT		GPS Position		Comments 1	Comments 2
		beginning	end	Beginning	End		
1	CTD/Rosette	15:37	15:44	$\varphi=74^{\circ}30,07'$ $\lambda=130^{\circ}30,11'$	$\varphi=74^{\circ}30,09'$ $\lambda=130^{\circ}29,99'$		Sampling levels: 3, 4, 6, 8, 11, 13, 13, 15, 17, 19, 20, 22, 23, 23, 24, 24, 24, 24, 24, 24, 24, 25, 25, 25
2	Microstructure	17:34	17:50	$\varphi=74^{\circ}30,07'$ $\lambda=130^{\circ}30,10'$	$\varphi=74^{\circ}15,05'$ $\lambda=130^{\circ}29,82'$		

Station Number: VB6707 Data: 30/09/07 Time of beginning: 02:20  
dd/mm/yy hh:mm (GMT)  
Latitude: 74° 15,06' N Longitude: 126° 60,15' E Depth: 29 m Ice: 0

#	Research Activity	Time, GMT		GPS Position		Comments 1	Comments 2
		beginning	End	Beginning	End		

1	CTD/Rosette	02:21	02:24	$\varphi=74^{\circ}15,07'$ $\lambda=126^{\circ}00,16'$	$\varphi=74^{\circ}15,24'$ $\lambda=126^{\circ}00,31'$		Sampling levels: 2, 4, 5, 6, 10, 12, 12, 14, 15,16, 17, 17 18, 19, 20, 21, 22, 23, 24, 25, 26, 26, 26, 26
2	Tow	02:30	02:45	$\varphi=74^{\circ}15,24'$ $\lambda=126^{\circ}00,31'$	$\varphi=74^{\circ}15,52'$ $\lambda=126^{\circ}01,84'$		

Station Number: VB6807 Data: 30/09/07 Time of beginning: 04:10  
dd/mm/yy hh:mm (GMT)  
Latitude: 74° 30,06' N Longitude: 125° 59,92' E Depth: 40 m Ice: 0

#	Research Activity	Time, GMT		GPS Position		Comments 1	Comments 2
		beginning	End	Beginning	End		
1	CTD/Rosette	04:16	04:20	$\varphi=74^{\circ}30,07'$ $\lambda=125^{\circ}59,92'$	$\varphi=74^{\circ}30,05'$ $\lambda=125^{\circ}59,73'$		Sampling levels: 2, 4, 11, 12, 16, 17, 21, 22, 26, 27, 31, 32, 33, 34, 34, 35, 36, 37, 38, 39, 39, 39, 39
2	Microstructure	04:24	04:34	$\varphi=74^{\circ}30,05'$ $\lambda=125^{\circ}59,73'$	$\varphi=74^{\circ}29,90'$ $\lambda=125^{\circ}59,26'$		

Station Number: VB6907 Data: 30/09/07 Time of beginning: 06:09  
dd/mm/yy hh:mm (GMT)  
Latitude: 74° 44,99' N Longitude: 125° 59,88' E Depth: 26 m Ice: 0

#	Research Activity	Time, GMT		GPS Position		Comments 1	Comments 2
		beginning	end	Beginning	End		
1	CTD/Rosette	06:09	06:22	$\varphi=74^{\circ}44,99'$ $\lambda=125^{\circ}59,88'$	$\varphi=74^{\circ}45,00'$ $\lambda=125^{\circ}59,57'$		Sampling levels: 2, 3, 4, 5, 6, 8, 8, 9, 10, 11, 13, 14, 14, 15, 16, 17, 18, 19, 21, 21, 22, 23, 24, 25
2	Tow	06:30	06:42	$\varphi=74^{\circ}45,11'$ $\lambda=125^{\circ}59,41'$	$\varphi=74^{\circ}45,02'$ $\lambda=126^{\circ}00,19'$		
3	Microstructure	06:22	06:28	$\varphi=74^{\circ}45,00'$ $\lambda=125^{\circ}59,57'$	$\varphi=74^{\circ}45,11'$ $\lambda=125^{\circ}59,41'$		

Station Number: VB7007 Data: 30/09/07 Time of beginning: 08:23  
dd/mm/yy hh:mm (GMT)  
Latitude: 75° 00,22' N Longitude: 125° 59,73' E Depth: 36 m Ice: 0

#	Research Activity	Time, GMT		GPS Position		Comments 1	Comments 2
		beginning	End	Beginning	End		

1	CTD/Rosette	08:39	08:44	$\varphi=75^{\circ}00,22'$ $\lambda=125^{\circ}59,26'$	$\varphi=75^{\circ}00,23'$ $\lambda=125^{\circ}59,05'$		Sampling levels: 2, 3, 4, 6, 7, 11, 12, 16, 17, 20, 21, 22, 24, 25, 26, 27, 29, 30,31, 33, 33, 34, 35, 35
2	Tow	08:26	08:38	$\varphi=75^{\circ}00,23'$ $\lambda=125^{\circ}59,05'$	$\varphi=75^{\circ}00,22'$ $\lambda=125^{\circ}59,28'$		

Station Number: VB7107 Data: 30/09/07 Time of beginning: 10:20  
dd/mm/yy hh:mm (GMT)  
Latitude: 75° 15,10' N Longitude: 126° 00,08' E Depth: 40 m Ice: 0

#	Research Activity	Time, GMT		GPS Position		Comments 1	Comments 2
		beginning	end	Beginning	End		
1	CTD/Rosette	10:45	10:57	$\varphi=75^{\circ}15,40'$ $\lambda=126^{\circ}00,69'$	$\varphi=75^{\circ}15,47'$ $\lambda=125^{\circ}59,87'$		Sampling levels: 2, 4, 5, 7, 8, 11, 12, 16, 17, 20, 21, 22, 25, 26, 27, 29, 30, 32, 35, 36, 37, 37, 38, 38
2	Tow	11:00	11:18	$\varphi=75^{\circ}15,62'$ $\lambda=125^{\circ}59,84'$	$\varphi=75^{\circ}16,18'$ $\lambda=126^{\circ}00,64'$		
3	Microstructure	10:25	10:45	$\varphi=75^{\circ}15,16'$ $\lambda=126^{\circ}00,07'$	$\varphi=75^{\circ}15,40'$ $\lambda=126^{\circ}00,69'$		

Station Number: VB7207 Data: 30/09/07 Time of beginning: 12:45  
dd/mm/yy hh:mm (GMT)  
Latitude: 75° 30,10' N Longitude: 126° 00,14' E Depth: 40 m Ice: 0

#	Research Activity	Time, GMT		GPS Position		Comments 1	Comments 2
		beginning	end	Beginning	End		
1	CTD/Rosette	12:51	12:58	$\varphi=75^{\circ}30,11'$ $\lambda=126^{\circ}00,15'$	$\varphi=75^{\circ}30,15'$ $\lambda=126^{\circ}00,14'$		Sampling levels: 3, 4, 5, 7, 9 11, 11, 16, 17, 20, 21, 23, 25, 26, 28, 30, 31, 31, 334, 35, 36, 38, 39, 39
2	Microstructure	12:56	13:09	$\varphi=75^{\circ}30,15'$ $\lambda=126^{\circ}00,14'$	$\varphi=75^{\circ}30,16'$ $\lambda=126^{\circ}00,12'$		

Station Number: VB7307 Data: 30/09/07 Time of beginning: 14:40  
dd/mm/yy hh:mm (GMT)  
Latitude: 75° 45,03' N Longitude: 126° 00,13' E Depth: 45 m Ice: 0

#	Research Activity	Time, GMT		GPS Position		Comments 1	Comments 2
		beginning	end	Beginning	End		

1	CTD/Rosette	14:46	14:58	$\varphi=75^{\circ} 45,03'$ $\lambda=126^{\circ} 00,13'$	$\varphi=75^{\circ} 45,01'$ $\lambda=126^{\circ} 00,08'$		Sampling levels: 3, 5, 6, 7, 9, 11, 11, 16, 18, 20, 22, 24, 26, 27, 29, 29,30, 31, 34, 35, 36, 42, 43, 43
2	Tow	15:09	15:28	$\varphi=75^{\circ} 45,17'$ $\lambda=125^{\circ} 59,94'$	$\varphi=75^{\circ} 45,23'$ $\lambda=126^{\circ} 02,19'$		
3	Microstructure	14:54	15:04	$\varphi=75^{\circ} 45,03'$ $\lambda=126^{\circ} 00,13'$	$\varphi=75^{\circ} 44,99'$ $\lambda=126^{\circ} 00,04'$		

Station Number: VB7407 Data: 30/09/07 Time of beginning: 17:11  
dd/mm/yy hh:mm (GMT)  
Latitude: 75° 59,96' N Longitude: 125° 59,89' E Depth: 48 m Ice: 0

#	Research Activity	Time, GMT		GPS Position		Comments 1	Comments 2
		beginning	end	Beginning	End		
1	CTD/Rosette	17:17	17:26	$\varphi=75^{\circ} 59,87'$ $\lambda=125^{\circ} 59,68'$	$\varphi=75^{\circ} 59,74'$ $\lambda=125^{\circ} 59,37'$		Sampling levels: 3, 4, 6, 8, 10, 12, 15, 18, 20, 22, 26, 31, 36, 41,43, 44, 44, 45, 45, 46, 47, 47, 47, 47
2	Microstructure	17:20	17:36	$\varphi=75^{\circ} 59,74'$ $\lambda=125^{\circ} 59,37'$	$\varphi=75^{\circ} 59,69'$ $\lambda=125^{\circ} 59,70'$		

Station Number: VB7507 Data: 30/09/07 Time of beginning: 19:24  
dd/mm/yy hh:mm (GMT)  
Latitude: 76° 15,04' N Longitude: 125° 59,61' E Depth: 51 m Ice: 0

#	Research Activity	Time, GMT		GPS Position		Comments 1	Comments 2
		beginning	end	Beginning	End		
1	CTD/Rosette	19:27	19:38	$\varphi=76^{\circ} 15,03'$ $\lambda=125^{\circ} 59,57'$	$\varphi=76^{\circ} 14,93'$ $\lambda=125^{\circ} 58,87'$		Sampling levels: 3, 4, 5, 7, 10, 11, 12, 15, 17, 20, 22, 26, 31, 36, 41, 42, 42, 43, 44, 45, 46, 47, 48, 49, 49
2	Tow	19:52	20:10	$\varphi=76^{\circ} 14,85'$ $\lambda=125^{\circ} 58,17'$	$\varphi=76^{\circ} 15,09'$ $\lambda=125^{\circ} 58,10'$		
3	Microstructure	19:33	19:49	$\varphi=76^{\circ} 14,93'$ $\lambda=125^{\circ} 58,87'$	$\varphi=76^{\circ} 14,85'$ $\lambda=125^{\circ} 58,17'$		

Station Number: VB7607 Data: 7/10/07 Time of beginning: 11:20  
dd/mm/yy hh:mm (GMT)  
Latitude: 80° 33,52' N Longitude: 32° 37,41' E Depth: 91 m Ice: 0

#	Research Activity	Time, GMT		GPS Position		Comments 1	Comments 2
		beginning	end	Beginning	end		
1	XBT	11:20	11:22	$\varphi=80^{\circ} 33,52'$ $\lambda=32^{\circ} 37,41'$	-----		

Station Number: VB7707 Data: 7/10/07 Time of beginning: 13:07  
 dd/mm/yy hh:mm (GMT)  
 Latitude: 80° 38,22' N Longitude: 30° 44,58' E Depth: 199 m Ice: 0

#	Research Activity	Time, GMT		GPS Position		Comments 1	Comments 2
		beginning	end	Beginning	end		
1	XCTD	13:07	13:10	$\varphi= 80^{\circ} 38,22'$ $\lambda=30^{\circ} 44,58'$	-----		

Station Number: VB7807 Data: 7/10/07 Time of beginning: 13:24  
 dd/mm/yy hh:mm (GMT)  
 Latitude: 80° 38,56' N Longitude: 30° 26,01' E Depth: 225 m Ice: 0

#	Research Activity	Time, GMT		GPS Position		Comments 1	Comments 2
		beginning	end	Beginning	end		
1	XCTD	13:24	13:26	-----	-----		

Station Number: VB7907 Data: 7/10/07 Time of beginning: 13:30  
 dd/mm/yy hh:mm (GMT)  
 Latitude: 80° 39,10' N Longitude: 30° 19,27' E Depth: 264 m Ice: 0

#	Research Activity	Time, GMT		GPS Position		Comments 1	Comments 2
		beginning	end	Beginning	end		
1	XBT	13:30	13:32	-----	-----		

Station Number: VB8007 Data: 7/10/07 Time of beginning: 13:34  
 dd/mm/yy hh:mm (GMT)  
 Latitude: 80° 39,20' N Longitude: 30° 15,04' E Depth: 294 m Ice: 0

#	Research Activity	Time, GMT		GPS Position		Comments 1	Comments 2
		beginning	end	Beginning	end		
1	XCTD	13:34	13:36	-----	-----		

Station Number: VB8107 Data: 7/10/07 Time of beginning: 13:42  
 dd/mm/yy hh:mm (GMT)  
 Latitude: 80° 39,31' N Longitude: 30° 06,06' E Depth: 346 m Ice: 0

#	Research Activity	Time, GMT		GPS Position		Comments 1	Comments 2
		beginning	end	Beginning	end		
1	XBT	13:42	13:44	-----	-----		

Station Number: VB8207 Data: 7/10/07 Time of beginning: 13:52  
 dd/mm/yy hh:mm (GMT)  
 Latitude: 80° 39,48' N Longitude: 29° 57,39' E Depth: 312 m Ice: 0

#	Research Activity	Time, GMT		GPS Position		Comments 1	Comments 2
		beginning	end	Beginning	end		
1	XCTD	13:52	13:54	-----	-----		

Station Number: VB8307 Data: 7/10/07 Time of beginning: 14:13  
 dd/mm/yy hh:mm (GMT)  
 Latitude: 80° 40,36' N Longitude: 29° 31,43' E Depth: 369 m Ice: 0

#	Research Activity	Time, GMT		GPS Position		Comments 1	Comments 2
		beginning	end	Beginning	end		
1	XBT	14:13	14:15	-----	-----		

Station Number: VB8407 Data: 7/10/07 Time of beginning: 14:30  
 dd/mm/yy hh:mm (GMT)  
 Latitude: 80° 41,10' N Longitude: 29° 12,39' E Depth: 494 m Ice: 0

#	Research Activity	Time, GMT		GPS Position		Comments 1	Comments 2
		beginning	end	Beginning	end		
1	XCTD	14:30	14:32	-----	-----		

Station Number: VB8507 Data: 7/10/07 Time of beginning: 14:36  
 dd/mm/yy hh:mm (GMT)  
 Latitude: 80° 41,25' N Longitude: 29° 05,55' E Depth: 557 m Ice: 0

#	Research Activity	Time, GMT		GPS Position		Comments 1	Comments 2
		beginning	end	Beginning	end		
1	XBT	14:36	14:38	-----	-----		

Station Number: VB8607 Data: 7/10/07 Time of beginning: 14:50  
 dd/mm/yy hh:mm (GMT)  
 Latitude: 80° 41,49' N Longitude: 28° 51,37' E Depth: 541 m Ice: 0

#	Research Activity	Time, GMT		GPS Position		Comments 1	Comments 2
		beginning	end	Beginning	end		
1	XCTD	14:50	14:52	-----	-----		

Station Number: VB8707 Data: 7/10/07 Time of beginning: 14:56  
 dd/mm/yy hh:mm (GMT)

Latitude: 80° 41,48' N Longitude: 28° 45,31' E Depth: 446 m Ice: 0

#	Research Activity	Time, GMT		GPS Position		Comments 1	Comments 2
		beginning	end	Beginning	end		
1	XBT	14:56	14:58	-----	-----		

Station Number: VB8807 Data: 7/10/07 Time of beginning: 15:00  
 dd/mm/yy hh:mm (GMT)  
 Latitude: 80° 41,48' N Longitude: 28° 41,17' E Depth: 426 m Ice: 0

#	Research Activity	Time, GMT		GPS Position		Comments 1	Comments 2
		beginning	end	Beginning	end		
1	XCTD	15:00	15:02	-----	-----		

Station Number: VB8907 Data: 7/10/07 Time of beginning: 15:05  
 dd/mm/yy hh:mm (GMT)  
 Latitude: 80° 42,04' N Longitude: 28° 36,13' E Depth: 346 m Ice: 0

#	Research Activity	Time, GMT		GPS Position		Comments 1	Comments 2
		beginning	end	Beginning	end		
1	XBT	15:05	15:07	-----	-----		

Station Number: VB9007 Data: 7/10/07 Time of beginning: 15:08  
 dd/mm/yy hh:mm (GMT)  
 Latitude: 80° 42,10' N Longitude: 28° 32,54' E Depth: 154 m Ice: 0

#	Research Activity	Time, GMT		GPS Position		Comments 1	Comments 2
		beginning	end	Beginning	end		
1	XBT	15:08	15:10	-----	-----		

Station Number: VB9107 Data: 7/10/07 Time of beginning: 15:11  
 dd/mm/yy hh:mm (GMT)  
 Latitude: 80° 42,04' N Longitude: 28° 29,37' E Depth: 79 m Ice: 0

#	Research Activity	Time, GMT		GPS Position		Comments 1	Comments 2
		beginning	end	Beginning	end		
1	XBT	15:11	15:13	-----	-----		